(12) STANDARD PATENT (11) Application No. **AU 2020281012 B1**
(19) AUSTRALIAN PATENT OFFICE

(54) Title
Apparatuses Based on Jet-Effect and Thermoelectric Effect

(51) International Patent Classification(s)
H01L 35/00 (2006.01) ***G01N 29/32*** (2006.01)
F15D 1/12 (2006.01) ***H01L 35/28*** (2006.01)

(21) Application No: **2020281012** (22) Date of Filing: **2020.12.01**

(43) Publication Date: **2021.06.17**
(43) Publication Journal Date: **2021.06.17**
(44) Accepted Journal Date: **2021.06.17**

(71) Applicant(s)
SOLITON HOLDINGS CORPORATION, DELAWARE CORPORATION

(72) Inventor(s)
Abramov, Yuri

(74) Agent / Attorney
Yuri Abramov, 24 Sagan Dr, Cranbourne North VIC, VIC, 3977, AU

(56) Related Art
WO 2011/028287 A2

ABSTRACT OF THE DISCLOSURE

The invention discloses a method and modified aerodynamic apparatuses: fluid pushers-off and fluid motion-sensors, making enable efficient implementation and use of a controllable enhanced jet-effect, either the waving jet-effect, the Coanda jet-effect, the lift-effect, the effect of thrust, the Venturi effect, and/or the de Laval jet-effect, all are controllable using the Peltier effect and/or the Seebeck effect. The modified aerodynamic apparatuses are geometrically shaped and supplied with built-in thermoelectric devices, wherein the presence of the thermoelectric devices provides for new functional properties of the modified aerodynamic apparatuses. The method solves the problem of effective control of the operation of modified aerodynamic apparatuses such as airfoil wings of a flying vehicle, convergent-divergent nozzles, loudspeakers, and detectors of acoustic waves, all of a highly-efficient functionality.

Apparatuses Based on Jet-Effect and Thermoelectric Effect

FIELD OF THE INVENTION

The invention relates generally to the use of a jet-effect in combination with a thermoelectric effect destined for controlling both the jet-effect and the laminarity of a headway moving fluid flow, and, more particularly, to a method for designing an aerodynamic apparatus controllably pulling-in and pushing-off a portion of fluid; the apparatus comprises a matrix of thermoelectric elements which are controllable to trigger origination of desired temperature differences and, thereby, to suppress the concomitant turbulence in the accelerated fluid portion.

BACKGROUND OF THE INVENTION

The following issued patents and publications provide potentially relevant background material, and are all incorporated by reference in their entirety:

- GB2546834 by Abramov, further indicated by **A01,**
- US 20190280561 by Abramov, further indicated by **A02,**
- AU 2018204546 by Abramov, further indicated by **A03,**
- EP1215936 (A2) by YOSHIKAWA TAKAMASA, further indicated by **A04**;
- EP2061098 (A1) by MIYACHI MAMORU, further indicated by **A05**;
- WO2019207578 (A1) by CUKUREL BENI, further indicated by **A06**;
- US5367890 (A) by DOKE MICHAEL J, further indicated by **A07**;
- **the paper** "*Thermoelectric Materials: Principles, Structure, Properties, and Applications*" by T.M. Tritt [**book**: "Encyclopedia of Materials: Science and Technology (Second Edition)" ELSEVIER-2002, Pages 1-11] further indicated by **D01**;
- **the paper "Thermoelectric Materials: Principles, Structure, Properties, and Applications"** by I.Terasaki [**"Reference Module in Materials Science and Material** Engineering" ELSEVIER-2016], further indicated by **D02**;
- **the paper "Thermo-Electric Cooler: Peltier Device Characteristics" by Jeethendra** Kumar P.K. and Ajeya PadmaJeeth, KamalJeeth Instrumentation & Service Unit, Tata Nagar, Bengaluru-560092, Karnataka, India, further indicated by **D03**;
- US20090272417 A1 by Jurgen Schulz-Harder, further indicated by **D04**,
- NASA EP-89, 1971, p. 68, further indicated by **D05**,
- NASA TN-1384, 1947, further indicated by **D06**,
- US Patent 6,981,366 by Sharpe, further indicated by **D07**,

- US 2008/0061559 A1 by Hirshberg, further indicated by **D08**,
- US 8,268,030 by Abramov, further indicated by **D09**,
- US 8,221,514 by Abramov, further indicated by **D10**,
- US 8,601,787 by Bulman, further indicated by **D11**,
- Patent **FR577087 "Pile électrique" by Karpen**, further indicated by **D12**;
- **Bernd Heinrich, "Thermoregulation in Endothermic Insects"** -- Science, New Series, Vol. 185, No. 4153. (Aug. 30, 1974), pp. 747-756, further indicated by **D13**;
- **Jose Eduardo Bicudo,** "Control and Regulatory Mechanisms Associated with Thermogenesis in Flying Insects and Birds" -- DOI: 10.1007/s10540-005-2883-8, further indicated by **D14**; and
- Ono, M.; **Okada, I.; Sasaki, M. (1987), "Heat production by balling in the Japanese** honeybee, Apis cerana japonica as a defensive behavior against the hornet, Vespa **simillima xanthoptera (Hymenoptera: Vespidae)", Cellular and Molecular Life** Sciences, 43 (9): 1031-1034, doi: 10.1007/BF01952231, further indicated by **D15**.

Preamble and Terminology

The prior art applications **A01, A02,** and **A03** disclose a nozzle with a through-hole tunnel having a specific shape, in general, configured as either converging, or divergent, or convergent-divergent, or two-stage convergent-divergent, optimized such that, when the nozzle is exposed to laminar flow of a certain fluid moving with a certain velocity, the fluid flow becomes accelerated and remains laminar as moving within and along the through-hole tunnel. As well, when the fluid flows around a body, an airfoil corpus of the body plays the role of such a nozzle while a boundary layer originated around the corpus is interpreted as a flow portion moving through an imaginary tunnel optimized to have the mentioned specific shape. In this relation, the introduced **term "actually-airfoil" applied to** the corpus should be understood as characterizing such a geometrical configuration of the corpus having a smooth curvature and optionally having a fluid-repellent (for instance, hydrophobic) surface that provides for the fluid flow remaining laminar when moving around as well as downstream behind the corpus.

In **THE BACKGROUND OF THE INVENTION**, a portion of descriptions of the prior art applications, which comprises aspects introducing to the claims of the present patent application, is repeated and amended. In particular, the inventor points out again to the feature that:

- a portion of a molecular fluid moving within a through-hole tunnel,
- a portion of a molecular fluid flowing around a body, for instance, an airfoil wing, and

- an elastic wave in a molecular fluid as a kind of motion of a portion of the molecular fluid around another portion of the molecular fluid,

all are accompanied by changes in thermodynamic parameters of portions of the molecular fluid, i.e., in other words, each of them comprises a fluid stream subjected to the jet-effect at least one of headway-accelerating and waving.

For the purposes of the present patent application, the introduced term "molecular fluid" should be understood as a fluid substance composed of randomly moving and interacting molecules, according to the kinetic theory of matter. In this relation:

- symbols a, b should be understood as the van der Waals parameters;
- symbol γ should be understood as the effective adiabatic compressibility parameter of the fluid, which (the γ) is defined such that, for a hypothetically ideal gas, it becomes equal to adiabatic compressibility-constant j, in turn, specified as equal to $1 + 2/n$, where n is the number of degrees of freedom per molecule of the hypothetical ideal gas wherein n depends on a configuration of the hypothetical ideal gas molecules; for instance, for air having dominantly bi-atomic molecules, $n = 5$, and $j = 7/5$ that is a good approximation for the generalized adiabatic compressibility parameter γ;
- **the terms** "partial pressure-a P_a", "partial pressure-b P_b", **and** "partial pressure-c P_c", description of which is in **A01**, **A02**, and **A03** and is not narrated herein for brevity, should be understood as characterizing fluid state subjected to different kinds of action; wherein: (a) a partial deep-stagnation pressure-a δP_a is characterized by varying δa in the van der Waals parameter a; (b) a partial stagnation pressure-b δP_b is interrelated with a change of a **moving portion's** volume V and, thereby, of the compression ratio r defined as $V/(V - b)$, while retaining the same inter-molecular forces defined by van der Waals parameter a; and (c) a partial pressure-c δP_c, associated with the Coanda-effect, is a measure of the cumulative aligning-impact of the fluid molecules on the imaginary boundaries of a fluid portion moving in the imaginary boundary layer adjacent to stationary walls of a body; and
- the symbol a_w should be understood as the van der Waals parameter of attraction between, on the one hand, molecules of a solid wall, and, on the other hand, molecules of adjacent fluid.

The well-known and widely-used jet-effect provides for the effect of gas extension and thereby acceleration. Accelerated flow is widely applied to push-off some kinds of vehicles

having jet-engines usually supplied by either converging or convergent-divergent nozzles, to which the term "jet-nozzle" is also applied to emphasize the jet-effect importance.

In **D07**, numerous modifications of the jet-effect implementation are overviewed.

In **D08**, the author points out that the jet-effect is accompanied by decreasing static pressure and temperature, and suggests applying the phenomenon as a trigger for vapor-to-water condensation.

In **D09** and **D10**, the author points out that a long cascade of streamlined nozzles provides a convergence of a wider front of fluid flow, and provides for an adaptation of the jet-effect use for big-scale devices.

In **the present patent application**, a diversity of embodiments, in which additional degrees of freedom allowing to control thermodynamic parameters of moving fluid are utilized to solve aerodynamic problems of controlling the moving fluid, is disclosed. The diversity includes:

- an improved acoustic device,
- an actually-airfoil convergent-divergent jet-nozzle,
- an actually-airfoil wing similar to a wing of a warm-blooded bird,
- a jet-nozzle applied to boost a sound, and
- a levitating capsule.

In relation to the molecular fluid, to analyze the equation of the molecular fluid motion, for the purposes of the present patent application, the term "jet-effect" is used in a wide sense as the effect of fluid flow portion convective acceleration at the expense of fluid portion heat. In particular, the jet-effect occurs when the fluid portion moves adjacent to configured walls and is subjected to the walls accelerating action, as seemingly "negative drag". For example, the fluid is gas and the walls are configured to form a converging or convergent-divergent nozzle. In particular, the term "jet-effect" is applied to the well-known and widely-used effect of convective acceleration of a wind-portion, which is flowing over a convex upper-side surface of an airplane wing and is thereby being subjected to the varying of flow front cross-section in an imaginary convergent-divergent nozzle. Another example is a case, wherein the fluid is water and the configured walls have a hydrophobic surface. Thus, the term "jet-effect", used here in a wide sense, assumes that the process of fluid extension may be insignificant or latent.

The jet-effect is the nature of the well-known Coanda-effect, defined as a tendency of a fluid jetstream to be attracted to and aligned with a nearby airfoil surface, i.e. to be specifically accelerated at the expense of the fluid warmth. For the purposes of the present patent application, to emphasize the jet-effect nature of the Coanda-effect, the term "Coanda-jet-

effect" is also applied as equivalent to the commonly known term "Coanda-effect". As the Coanda-effect assumes a laminar flow, **looking ahead, the term "airfoil" will be specified as "actually-airfoil" in contrast to "seemingly-airfoil".**

For the purposes of the present patent application, further terms are specified as follows:

- **the term "imaginary wall", applied to a flowing fluid's streamlines, should be understood as a material (but not virtual) wall, formed by the fluid's matter, forcedly**-bordering a portion of the flowing fluid. I.e. the material but optionally invisible by the human eye and thereby imaginary wall acts on adjoining fluid portions, enforcing the fluid portions to move along the streamlines, i.e. in alignment with the imaginary wall. When flowing plasma is subjected to an action of a magnetic field, **"imaginary walls" are formed by the magnetic field's force**-lines defining the streamlines of the flowing plasma;
- **the term "fluid pusher-off" should be understood in a broad sense as a device** interacting with a portion of the ambient fluid, gaseous or liquid, to cause pulling-in and/or pushing-off the fluid portion resulting in motion of the fluid portion relative to the device corpus;
- **the term "fluid motion-sensor" should be understood in a b**road sense as a device interacting with a portion of the ambient fluid, gaseous or liquid, to detect motions of the fluid portion relative to the device corpus;
- the term "velocity of a flying body" should be understood as the body motion velocity relative to a stationary fluid; and vice-versa, the term "flow velocity" should be understood as the fluid flow velocity relative to the considered body submerged in the fluid stream. These two terms are interrelated according to Galilean relativity;
- the term "M-velocity" should be understood as the fluid velocity measured in Mach numbers or velocity normalized to the temperature-dependent velocity of sound in the fluid;
- the term "specific M-velocity" is as introduced and specified in detail in **A01**, **A02**, and **A03** to **separate the terms "low M-velocities", associated with M**-velocities lower than the specific M-velocity indicated by M_*, **and "high M-velocities", associated with M**-velocities higher than the specific M-velocity M_*. Namely, the value of specific M-velocity is quantified via the effective adiabatic compressibility parameter of the fluid γ as $M_* = \sqrt{(\gamma - 1)/\gamma}$; for air as a diatomic molecular gas, the generalized adiabatic compressibility parameter γ equals $\gamma = 7/5 = 1.4$, and $M_* = \sqrt{(\gamma - 1)/\gamma} \approx 0.5345\ Mach$; and
- the well-**known terms "low-subsonic", "high-subsonic", "transonic", "supersonic", and "hypersonic" are used to specify the flow velocity ranges as the following:**

(a) the low-subsonic velocity range is defined as the M-velocity range comprising M-velocities lower than $0.3\ Mach$;

(b) the high-subsonic velocity range is defined as the M-velocity range comprising M-velocities higher than $0.3\ Mach$ and lower than $0.8\ Mach$;

(c) the transonic velocity range is defined as the M-velocity range comprising M-velocities higher than $0.8\ Mach$ and lower than $1.2\ Mach$;

(d) the supersonic velocity range is defined as the M-velocity range comprising M-velocities higher than $1\ Mach$ and lower than $5\ Mach$; and

(e) the hypersonic velocity range is defined as the M-velocity range comprising M-velocities higher than $5\ Mach$.

- the well-known terms "audible sound" and "ultrasound" are used to specify frequency ranges of acoustic waves as follows:

  (a) the audible frequency range is defined as including frequencies from $20\ Hertz$ to $20\ kHertz$; and

  (b) the ultrasound frequencies are defined as frequencies higher than $20\ kHertz$ and further specified as lower than $1\ gigaHertz$.

and

- the well-known terms "direct current (DC)" and "alternating current (AC)" should be understood in a broader sense:

  (a) the direct current (DC) should be understood as a current, value of which can vary but remaining either positive or negative; and

  (b) the alternating current (AC) should be understood as a current, value of which changes in a sign during a considered time.

Referring to the defined term "molecular fluid", the earlier defined term "flow velocity" is further specified as a measure of the molecular fluid's molecules motion in a prevalent direction in addition to the random Brownian motion. For instance, the air is considered as a molecular fluid, and the wind is considered as a natural process, bringing fresh portions of air, storing at least both: the heat energy of molecules Brownian random motion and the kinetic energy of the wind motion. Normally, in nature, when the wind is of $10\ m/sec$, the proportion is such that 99.96% is the heat energy [i.e. warmth] and only 0.04% is the kinetic energy of the wind motion as a whole. A phenomenon of a transformation of warmth into hurricane power is well-known; however, the warmth of ambient natural air remains largely unused in the world industry. Possession of a

technology to control the transformation of the surrounding air and/or water warmth into a directional motion of the fluid could provide a renewable cycle, comprising:

- transformation of the flowing fluid heat-power into acquired kinetic-power of an arisen jetstream (and/or into acquired wave power of an arisen wave);
- conversion of the jetstream kinetic-power into useful electric power; and
- consumption of the electric power, in the final analysis, inevitably dissipating back into the warmth of the surrounding matter.

There is, therefore, a need in the art for a method and apparatus to provide a proper optimal design of a system, implementing a controllable jet-effect appropriate for use in industry.

Venturi Effect

Reference is now made to prior art **Fig. 1b**. **Fig. 1b** is a schematic illustration of an airfoil-shaped convergent-divergent nozzle **102**, pipe-section in a sagittal plane. The shape can be described as comprising an inlet part **103** constricting into a narrow throat **104,** further followed by a divergent outlet part **105**. When a fluid **106** flows slowly through convergent-divergent nozzle **102**, a jet-effect is observed in an adiabatic process, i.e. velocity increases in narrow throat **104** at the expense of the static pressure in fluid **106**. Speedometers **1071**, **1072**, **1073,** and barometers **1081**, **1082**, **1083** illustrate the interrelated behavior of the velocity and static pressure. This jet-effect is known also as the Venturi effect. Thus, the Venturi acceleration effect is observed in the case of a slow and converging flow, and the Venturi retarding effect is observed in the case of slow and divergent flow.

The inventor points out and emphasizes that the phenomenon of the Venturi effect is the self-acceleration and self-retarding of an airflow portion, i.e. is the airflow velocity self-oscillation, at the expense of the air portion's warmth. I.e., in other words, the Venturi effect of the airflow velocity self-oscillation (as well as the Coanda-jet-effect) has the jet-effect nature.

When observing a freely falling water jetstream, one explains a conic constriction of the water jetstream by the Venturi effect, where the accelerated jetstream becomes accompanied by a decrease of the cross-sectional area.

De Laval Effect

Reference is now made to prior art **Figs. 1c** and **1d**. **Fig. 1c** shows schematically pipe **100** referred to the de Laval nozzle that, in principle, is similar to pipe **102** shown in **Fig. 1b**, but now the incoming fluid-flow **101** is sufficiently fast such that fluid **101** becomes substantially compressible-expandable. In this case, in an adiabatic process, the de Laval effect is observed. This is the effect of the extension of fluid **101** in the divergent outlet part **142** resulting in a

further decrease of the static pressure and temperature and a correlated increase of the flow velocity.

Fig. 1d illustrates schematically graphics of distributions of the fluid-flow **101's** (**Fig. 1c**) three mutually-scaled parameters: headway velocity **150,** static pressure **160**, and temperature **170**, each along the length of nozzle **100**. A standard rocket convergent-divergent jet-nozzle **100** can be modeled as a cylinder **140** that leads to a constriction **141**, known as the "throat", which leads into a widening "exhaust bell" **142** open at the end. The location of the narrowest cross-section of **the throat is called the "critical condition" point 180**. High speed and therefore compressible-expandable hot fluid **101** flows through throat **141**, where the velocity picks up as a jump **151** and the pressure and temperature suddenly fall, **161** and **171**, correspondingly. Hot fluid **101** exits throat **141** and enters the widening exhaust bell **142.** It expands rapidly, and this expansion drives the velocity up **152**, while the pressure and temperature continue to fall, **162** and **172** correspondingly. This jet-effect phenomenon of fluid **101** extra-acceleration at the expense of the fluid **101** heat energy, defined by the static pressure, absolute temperature, and mass density, is applied to jet-engines, particularly, to accelerate a rocket. A sharp slope of the static pressure, observed in throat **141**, results in pressure waves, called Mach waves. An undesired influence of the Mach waves in the de Laval nozzle is described, in particular, in **D11** -- US Patent 8,601,787 **"Rocket nozzles for unconventional vehicles" by Bulman.**

In **A01, A02,** and **A03**, the enhanced implementations of jet-effects: the Venturi effect, the de Laval jet-effect, and the de Laval retarding-effect, are suggested, wherein the essence of the improvement is in stationary geometrical configurations of a Venturi pipe and a de Laval jet-nozzle, correspondingly, such that the stationary geometrical configurations are passively adapted to certainly-given velocity and thermodynamic parameters of an incoming fluid flow to provide for laminar flow. Namely, the prior art improved passively adapted stationary geometrical configuration of a de Laval jet-nozzle is such that the varying cross-sectional area characterized by a passively adapted cross-sectional area profile function $A_0(x)$ given by an equation expressed as:

$$A_0(x) = \frac{A_*}{M(x)}\left(\frac{\gamma-1}{\gamma}\right)^{\frac{1}{2}}\left(\frac{2+\gamma(M(x))^2}{\gamma+1}\right)^{\frac{\gamma+1}{2(\gamma-1)}} \quad \text{Eq. (1.a),}$$

where A_* is the minimal cross-sectional area of a narrow throat, γ is an adiabatic compressibility parameter of the fluid flow, and $M(x)$ is a gradually-smoothed monotonic function of x representing a profile of an M-velocity of the fluid flow moving within and through the nozzle. In particular, to accelerate a certain gas flow characterized by a specific gas

constant R, entering the open inlet of the improved passively adapted stationary geometrical configuration of a de Laval jet-nozzle with an initial velocity u_{in} and temperature T_{in}, and to result in the enhanced de Laval jet-effect, the stationary geometrical configuration of the de Laval jet-nozzle must have the ratio A_{in}/A_* of the cross-sectional area of the open inlet to the minimal cross-sectional area of a narrow throat strictly quantified as

$$\frac{A_{in}}{A_*} = \frac{1}{u_{in}}\sqrt{(\gamma-1)RT_{in}}\left(\frac{2+u_{in}^2/(RT_{in})}{\gamma+1}\right)^{\frac{\gamma+1}{2(\gamma-1)}} \quad \text{Eq. (1.b).}$$

However, the prior art stationary geometrical configuration remains not optimized for arbitrary velocity and thermodynamic parameters of the incoming fluid flow that makes the prior art solution not universal for practical use in industry.

For the purposes of the present patent application:

- the term "de Laval effect" should be understood in a wide sense as comprising both: the de Laval jet-effect, defined as an effect of flow extra-acceleration, and the de Laval retarding-effect, defined as an effect of flow extra-slowing; thus, the de Laval jet-effect is a particular case of the de Laval effect; also,
- the term "de Laval-like jet-effect" should be understood in a wider sense including a case when an enhanced jet-effect occurs in an open space imaginarily bordered by the flow streamlines, wherein the imaginary borders constitute a convergent-divergent shape, i.e. similar to a de Laval nozzle.

The Phenomenon of Convective Self-Acceleration

Fig. 1f is a prior art schematic drawing of a body **1f.0** blown by an initially laminar airflow having portion **1f.2** enveloping body **1f.0**. It is assumed that the velocity of the airflow motion is much lower than **0.5** $Mach$, for instance, $1\ m/sec$. For simplicity and without loss of reasoning, consider a case when the body **1f.0** corpus has at least partially airfoil shape providing for that ambient-adjoining sub-portions **1f.5** and **1f.6** of airflow portion **1f.2** remain laminar at least upstream afore a frontal plane, crossing the body **1f.0** corpus. Here:

- such a frontal plane is marked with the dotted line having numeral **1f.1**;
- dashed lines **1f.3** and **1f.4** are imaginary streamlines bordering airflow portion **1f.2** as a whole and being sufficiently far from body **1f.0** that allows ignoring the airflow streamlines minor curving when bordering ambient-adjoining sub-portions **1f.5** and **1f.6**; and
- arrow **1f.7** symbolizes a portion of downstream airflow, not obligatorily laminar.

When flowing around body **1f.0**, ambient-adjoining sub-portions **1f.5** and **1f.6** of airflow portion **1f.2** become subjected to reshaping and can be considered as moving through an imaginary tunnel, which is characterized by varying cross-sectional area. According to the mass conservation law, called also the equation of continuity: $A\rho u = Const$, where ρ is the mass density of flux; u is the flux velocity, and A is the flux cross-sectional area, the ambient-adjoining sub-portions: **1f.5** and **1f.6**, both move faster than yet to be reshaped airflow portion **1f.2** because the air mass density changes are minor at low airflow velocities and the sub-portions have the cumulative cross-sectional area smaller than the cross-sectional area of yet to be reshaped airflow portion **1f.2**. Therefore, the cumulative kinetic energy of ambient-adjoining sub-portions: **1f.5** and **1f.6**, together, is higher than the kinetic energy of oncoming airflow portion **1f.2** yet to be subjected to the reshaping.

One of the key questions about the origin of flowing fluid portion acceleration is the following. At the expense of what kind of energy, the sub-portions became accelerated, if the case is adiabatic? The answer to the question is the self-acceleration occurs at the expense of the internal heat energy of the flowing fluid portion itself, wherein the initial velocity of the **flowing fluid portion plays a role of a "trigger-catalyst" defining** the intensity of the self-acceleration, namely, a higher velocity results in a greater self-acceleration. The answer shows that the phenomenon of convective self-acceleration is inevitable for fluid flowing around a body with relatively low velocities in an adiabatic process, i.e. upon conditions usually provided in the actual practice.

The inventor points out and emphasizes that a portion of the flowing fluid can play the role of a body subjected to blowing by another portion of the flowing fluid – this situation occurs, for instance, in acoustic waves.

Airfoil Wing (definition of attack angle)

Fig. 1g comprises five parts: **Case (A), Case (B)**, **Graph (C)**, **Graph (D)**, and **Scheme (E)**.

Fig. 1g Case (A) is a prior art schematic drawing of a classic airfoil profile of an airplane wing **10.A** oriented horizontally in a sagittal plane. The wing profile is recognizable by a rounded leading edge, a convex profile contour, having smoothly curved, elongated sides: more convex and lesser convex, and a sharp trailing end.

To move the wing **10.A** with the velocity u_0 through a real fluid (for instance, air), an engine **"ENGINE-A"**, which is not shown here, consumes power to overcome a certain resistance of the ambient fluid. The certain resistance (sometimes, called a drag in a wide sense) against the headway motion is defined as the cumulative resistance including:

- drag in the direct sense against a cross-sectional area; the drag is determined by the **wing's cross**-sectional area and shape;
- skin-friction determined by the chemical composition of the air and shell of the wing and manifested as the fluid viscosity and stickiness between the fluid and the wing **10.A**; and
- the additional resistance, determined by turbulence (as the turbulent portions draw other portions of the fluid thereby further increasing the drag and inter-air friction).

Again, the consumed power (for instance, the energy of burned fuel) goes to overcome the certain drag in the wide sense.

A horizontal oncoming airstream **10.0** runs on the rounded leading edge and flows around wing **10.A**, thereby being divided into two dominantly-laminarly moving portions: upper-side air portion B_1 **10.1** forming an upper-side air flux **10.3** (called also an upper-side boundary layer) and lower-side air portion B_2 **10.2** forming a lower-side air flux **10.4** (called also a lower-side boundary layer), both going off from the sharp trailing end.

For the purposes of the present patent application, the introduced terms "upper-side" and "lower-side" applied to an object should be understood as indicating the location of the object: adjacently above an upper side and adjacently under a lower side, correspondingly.

The axis **10.C** of wing **10.A** is codirectional with a so-called chord of the wing, which (the chord of the wing), sometimes, is defined relatively arbitrary, based on a side-view profile of the wing. Since a wing can have a twist, a chord line of the whole wing may not be definable, so an alternate reference line is simply defined. Often, the chord line of the so-**called "root of the wing" is chosen as the reference line. Another choice is to use a horizontal line on the** fuselage as the reference line (and also as the longitudinal axis) **10.H**. Axis **10.C** of wing **10.A** and the axis **10.H** constitute an angle of the wing asymmetry **13**. **To define "an angle of attack", s**ome authors use a so-**called "zero lift axis" where, by** the specific definition, "a zero angle of attack" corresponds to zero coefficient of lift. In contrast, for the purposes of the present patent application, taking into account the dual nature of lift-force **10.F**: by impact and by the Coanda-**effect, an "attack angle" or "angle of attack" should be understood as an angle between the** horizontal direction of oncoming airstream **10.0** and the longitudinal axis **10.H**, while the chord of the wing **10.C** is conditionally defined as separating the upper-side and lower-side fluxes. In other words, the attack angle is defined relative to the zero attack angle that, in turn, is specified by a manifestation such that the zero attack angle provides for minimized impact by the oncoming flow and, thereby, for the lift-force **10.F** generation due to the Coanda-jet-effect only or at least dominantly. The more convex upper side provides a slippery surface, and the

lesser convex lower side, exposed to oncoming air stream **10.0** with the attack angle (zero or non-zero positive) and so subjected to friction and impact by lower air flux **10.4**, has thereby more frictional-dragging surface. Thereby, the shown profile of wing **10.A** oriented horizontally is defined as a profile of wing exposed to the oncoming wind **10.0** at the zero attack angle and subjected to the minimum drag and a certain lift originated due to the Conada-effect.

Lift-Force Mechanism

The well-known lift-effect of an airplane wing **10.A** arises due to the non-symmetrical profile of wing **10.A** when the upper side is more convex determining the angle of the wing asymmetry **13**. Firstly, a lift-force **10.F** is defined by the attack angle, which redirects the flowing wind. Secondly, when the attack angle is equal to zero, wing **10.A**, having an ideally streamlined contour, provides that the sliding upper-side air flux **10.3** and the impacting lower-side air flux **10.4**, both subjected to the Coanda-jet-effect operation, meet behind wing **10.A**. Sliding upper-side air flux **10.3** and impacting lower-side air flux **10.4**, flowing around wing **10.A**, incur changes in their cross-sectional areas and are accelerated convectively according to the mass conservation law. Considering relatively low velocities, the varying cross-sectional areas result in that the sliding upper-side air flux **10.3** runs faster than the impacting lower-side flux **10.4**. According to Bernoulli's principle, this results in less so-called static pressure on wing **10.A** from sliding upper-side flux **10.3** than the static pressure from the impacting lower-side flux **10.4**. If upper-side flux **10.3** and lower-side flux **10.4** flow around wing **10.A** laminarly, the difference between the static pressures is defined as $\Delta P_L = C_L \rho u_0^2/2$, where ΔP_L is the static pressure difference defining the lift-force **10.F**, C_L is the coefficient of lift depending on wing **10.A**'s non-symmetrical profile shape and orientation, ρ is the mass density of the air, and u_0 is the velocity of the ambient airflow relative to wing **10.A**.

Fig. 1g Graph (C) illustrates the dependence of the coefficient of lift C_L for the classic airplane wing **10.A** on the attack angle, wherein the marked range **10.L** of the coefficient of lift C_L corresponds to the attack angles close to zero. **In practice, "the zero attack angle" has a** tolerance $\delta\varphi$ of several degrees [for instance, it is well-known for an airplane pilot that, when Boing 777 is flying strictly horizontally, the orientation of fuselage is at a positive $\delta\varphi$]. In this case, the lift-force is substantial and the drag is minimal.

Thus, quintessentially, a frequently cited explanation of a mechanism of the lift-force origination is that the static pressure in a shaped boundary layer above the upper side of the wing **10.A** is lower than the static pressure in a shaped boundary layer under the lower side of the wing **10.A**. In addition, for the purpose of the present patent application, to introduce to

claimed method and devices, a more detailed explanation of the mechanism of the lift-force origination is expounded hereinafter in the sub-**paragraph** "Boundary-Layer". In particular, it will be emphasized that the two portions of air: B_1 **10.1** and B_2 **10.2** (which originally being portions of the oncoming airstream **10.0** characterized by the ambient static pressure), when becoming portions of the upper-side and lower-side shaped boundary layers **10.3** and **10.4**, both are subjected to just-sudden changes in the static pressures: ΔP_{B1} and ΔP_{B2}, correspondingly, and the coefficient of lift C_L **is determined by the interrelated wing's shape and** suddenness of pressure changes. A wing, having an elaborated airfoil profile, provides for an unbroken, **gradual variation of the airflow static pressure along the profile's smoothly** curved contour that, when flying with a certain velocity, results in an unbroken distribution of the airflow velocities **along the profile's smoothly curved contour,** i.e. satisfies a condition preventing an origination of turbulences. Consider an air portion flowing around wing **10.A**, referring to the Clapeyron-Mendeleev law concerning a so-called hypothetical ideal gas state: $P = \rho R_0 T/\mu$, where P is the gas static pressure, ρ is the gas mass density, T is the absolute temperature of the gas, μ is the gas molar mass, and R_0 is the universal gas constant. One could apply rough and more exact explanations for changes in the gas state parameters of the air portion flowing around wing **10.A**.

Roughly, for the sake of estimation of a relatively slow wind tendency only, considering the flowing air as substantially incompressible gas, Gay-Lussac's law for an isochoric process interrelates the static pressure P and absolute temperature T by the equation $\Delta P/P = \Delta T/T$, i.e. the reducing static pressure is accompanied by the decreasing absolute temperature.

More exactly, for the wind at low speeds as well as at higher speeds running, in general, at a non-zero attack angle, the air (being compressible-extendable as an ideal or van der Walls gas), when flowing around wing **10.A**, is subjected to an adiabatic process rather than to an isochoric process. An adiabatic process in gas is described by the condition $P/\rho^{\gamma} = Const$ or $P/T^{\gamma/(\gamma-1)} = Const$ or the equivalent thermodynamic differential equations interrelating changes in absolute temperature T, mass density, and static pressure P of gas as follows:

$$\begin{cases} \dfrac{d\rho}{\rho} = \dfrac{1}{\gamma}\dfrac{dP}{P} & Eq.\ (1.1a) \\ \dfrac{dT}{T} = \dfrac{\gamma-1}{\gamma}\dfrac{dP}{P} & Eq.\ (1.1b) \end{cases}$$

Boundary-Layer

In general, when a portion of air flows nearby a solid surface, attraction forces between the air molecules differ from the attraction forces between, on the one hand, molecules of the air

and, on the other hand, molecules of the solid surface. Normally, the effect of stiction of the flowing air to the solid surface is observed.

Fig. 1g Graph (D) is a prior art schematic drawing extracted from **D05** showing a flow velocity profile $u(z)$ **1G.0** in height within a flat boundary layer nearby a solid surface **1G.1**, when the ambient velocity u_0 **1G.32** above the dashed line **1G.2** is in the low-subsonic velocity range. The dashed line **1G.2** indicates an imaginary boundary between the flat boundary layer characterized by the effective thickness δ **1G.3** and an outer ambient portion of the flow moving substantially free. The velocity profile $u(z)$ **1G.0** is shown as a function of the x-component (projection to the axis **X**) of velocity-dependent on **Z**-coordinate, where the axis **Z** shows the distance from the solid surface **1G.1**. It is well-known that, normally, solid surface **1G.1** is sticky for a real flow (in particular, airflow) such that an airflow portion adjacent to the solid surface **1G.1** moves slower than a portion moving farther from the solid surface **1G.1**. The stickiness, in particular, says that the effective thickness δ **1G.3** of the flat boundary layer is specified as a thickness, for simulation of which a spatial temperature distribution and heat exchange between the flow and the solid surface **1G.1** should be taken into account. The ambient velocity u_0 **1G.32** above the dashed line **1G.2** is much higher than the velocity $u(z \ll \delta)$ **1G.31** near the solid surface **1G.1**, wherein there are extremely low velocities $u(z \ll \delta)$ in close proximity above the solid surface **1G.1**. Moreover, normally, the condition $u(0) \to 0$ of the zero velocity at the zero height above the solid surface **1G.1** is satisfied for much higher ambient velocities, including the supersonic velocity range. The velocity profile $u(z)$ **1G.0** and the effective thickness δ **1G.3**, both are velocity-dependent: the higher the ambient velocity u_0 **1G.32**, the thinner the boundary layer. In frames of the aerodynamics, one estimates the thickness δ **1G.3** of a boundary layer, dependent on both a so-called **"characteristic size"** L_* and the so-called Reynolds Number Re, as, for example, approximation by Prandtl: $\delta = 0.37 \times L_*/Re^{0.2}$, where L_* has the sense of a chord of an airfoil wing **10.A**. As well, the thickness δ **1G.3** of the boundary layer can be specified experimentally for a kind of body corpus. Looking ahead, it will be pointed out that, if the temperature of the solid surface is maintained forcibly; on the one hand, a tiny portion of airflow moving adjacent to the solid surface can be heated or cooled by the solid surface and get the temperature of the solid surface and, on the other hand, a big portion of the airflow moving farther from the solid surface is capable of removing or, vice-versa, reverting an increased or, vice-versa, a reduced portion of the heat, correspondingly, thereby, providing for the two useful

tendencies: on the one hand, the faster airflow the faster heat removing and/or reverting, and, on the other hand, the tiny portion always tends to have the temperature of the solid surface.

According to the Bernoulli theorem, the distributed velocity $u(z)$ is interrelated with the distributed static pressure $\overline{P_B}(z)$ and mass density $\rho(z)$ of the air within the flat boundary layers as follows:

$$\frac{\overline{P_B}(z)}{\rho(z)} - \frac{\overline{P_B}(0)}{\rho(0)} = \frac{u(0)^2}{2} - \frac{u(z)^2}{2} \qquad \text{Eq. (1.1c)}$$

A common convention is that $u(0)$ is extremely low and for low velocities the assumption $\rho(z) \cong const$ is a good approximation, so the equation Eq. (1.1c) can be rewritten as

$$\overline{\Delta P}_B(z) \approx -\rho_0 \frac{u(z)^2}{2} \qquad \text{Eq. (1.1d)}$$

where $\overline{\Delta P}_B(z)$ is a change in static pressure within the flat boundary layer and ρ_0 is the mass density of the ambient airflow. Thus, the effective change $\overline{\Delta P}_B$ in the static pressure of the flat boundary layer due to the effect of stiction relative to the ambient static pressure is positive because the velocities $u(z)$ within the flat boundary layer are lower than the ambient velocity u_0. When considering convexly curved surfaces of wing **10.A**, in addition to the effect of stiction, the Coanda-effect is observed. The Coanda-effect makes the boundary layers shaped; in other words, the motion of airflow within the shaped boundary layers is accompanied by changes in the cross-sectional area of the airflow. I.e. the air portions, B_1 **10.1** and B_2 **10.2**, both become subjected to acceleration interrelated with the cross-sectional area convergence and divergence due to the Venturi effect. The partial static pressures, indicated by $\widetilde{\Delta P}_{B1}$ and $\widetilde{\Delta P}_{B2}$, originated due to the convective accelerations of the Coanda-effect plus the Venturi effect and contributed to the resulting changes ΔP_{B1} and ΔP_{B2} of the static pressures of the shaped boundary layers, are interrelated with the resulting effective velocities, indicated by u_1 and u_2, of the upper-side and lower-side shaped boundary layers, correspondingly. The resulting changes ΔP_{B1} and ΔP_{B2} of the static pressures of the shaped boundary layers are specified as:

$$\Delta P_{B1} = \overline{\Delta P}_B + \widetilde{\Delta P}_{B1} \qquad \text{Eq. (1.1e)}$$

$$\Delta P_{B2} = \overline{\Delta P}_B + \widetilde{\Delta P}_{B2} \qquad \text{Eq. (1.1f)}$$

and, according to the Bernoulli theorem:

$$\Delta P_{B1} \approx \rho_0 \frac{u_0^2 - u_1^2}{2} \qquad \text{Eq.(1.1g)}$$

$$\Delta P_{B2} \approx \rho_0 \frac{u_0^2 - u_2^2}{2} \qquad \text{Eq. (1.1h)}$$

wherein, again, the symbol of approximate equality, '≈', is used as the mass density is approximated by the constant ρ_0. Thereby, the resulting static pressure difference $(\Delta P_{B1} - \Delta P_{B2})$ is approximated by:

$$(\Delta P_{B1} - \Delta P_{B2}) \approx \rho_0 \frac{u_2^2 - u_1^2}{2} \qquad \text{Eq. (1.1i).}$$

As the curvature of the upper side is more convex than the curvature of the lower side of the wing **10.A**, then, for the relatively low ambient velocity u_0, the condition $(\Delta P_{B1} - \Delta P_{B2}) < 0$ is satisfied, wherein:

- the resulting changes ΔP_{B1} and ΔP_{B2} of the static pressures, both are positive, if the contribution of the effective change $\overline{\Delta P}_B$ is dominant relative to $\widetilde{\Delta P}_{B1}$ and $\widetilde{\Delta P}_{B2}$;
- the resulting changes ΔP_{B1} and ΔP_{B2} of the static pressures, both are negative, if the contributions $\widetilde{\Delta P}_{B1}$ and $\widetilde{\Delta P}_{B2}$ are dominant and the effective change $\overline{\Delta P}_B$ is minor; and
- the resulting change ΔP_{B1} is negative and the resulting change ΔP_{B2} is positive, if the condition $|\widetilde{\Delta P}_{B1}| > |\overline{\Delta P}_B| > |\widetilde{\Delta P}_{B2}|$ is satisfied.

For the sake of concretization and without loss of generality, consider the case when $\Delta P_{B1} < 0$ and $\Delta P_{B2} > 0$. When, on the one hand, the portion B_1 **10.1** becoming the upper-side shaped boundary layer **10.3** is subjected to a sudden decrease in the resulting static pressure ΔP_{B1}, it pulls-in both an upper-side portion **10.5** of the ambient air and the wing **10.A** into the upper-side boundary layer **10.3**, and, on the other hand, the portion B_2 **10.2** becoming the lower-side shaped boundary layer **10.4** is subjected to a sudden increase in the resulting static pressure ΔP_2, it pushes-off both a lower-side portion **10.6** of the ambient air and the wing **10.A** away from the lower-side shaped boundary layer **10.4**. The resulting action on wing **10.A** in unison is manifested as the lift effect characterized by the lift-force F_L **10.F**. In the assumption that the air portions B_1 **10.1** and B_2 **10.2** suddenly become the shaped boundary layers **10.3** and **10.4**, correspondingly, wherein the shaped boundary layers are extremely thin, **completely laminar, and ideally aligned with the wing sides' curvatures, as the pulling**-in and pushing-off act to both the wing **10.A** and ambient air in the same extent, i.e. not more than a half the difference $(\Delta P_{B1} - \Delta P_{B2})$ contributes to the lift, the lift-force F_L **10.F** acting on the wing **10.A** is limited by the value

$$\left[-\frac{1}{2} \times (\Delta P_{B1} - \Delta P_{B2})\right] \times A_{WING},$$

where A_{WING} is the area of a projection of wing **10.A** on a horizontal plane. The actual value of the lift-force F_L **10.F** is determined by the suddenness of the transformation of the air portions B_1 **10.1** and B_2 **10.2** into the upper-side and lower-side thin boundary layers **10.3** and **10.4**,

correspondingly. The suddenness is specified by the suddenness factor C_S. Namely, as the interaction between, on the one hand, the wing **10.A** and, on the other hand, the refreshed and suddenly compressed or decompressed air portions within the shaped boundary layers **10.3** and **10.4** is relevant for the lift force F_L **10.F** origination, then, in the case when the relatively thin shaped boundary layers **10.3** and **10.4** (the thickness of which is velocity-dependent) are strictly-aligned to the relatively big airfoil surfaces of the wing **10.A**, the velocity-dependent suddenness factor C_S tends to 1 ($C_S \to 1$), and, the slower-refreshed and so thicker the boundary layers **10.3** and **10.4** and the weaker the alignment, the smaller the velocity-dependent suddenness factor C_S. Assuming an airfoil corpus moving with the velocity u_0, which remains lower than a critical velocity u_* such when the lift-force F_L **10.F** is yet upward-directed, a simplified approximation for the velocity-dependent suddenness factor C_S is given by the expression:

$$C_S = \frac{M}{M_*}\ ,\ \ M \leq M_* \quad \text{Eq. (1.1j),}$$

where M is M-velocity specified as the velocity measured in Mach numbers and M_* is the specific M-velocity specified as equal to $\sqrt{(\gamma-1)/\gamma}$, where γ is the adiabatic compressibility parameter of the air (again, $\gamma = 7/5$ is a good approximation for the air composed of diatomic molecules dominantly). Taking into account the suddenness factor C_S, the lift-force F_L **10.F** is specified as:

$$F_L = \left[-\frac{1}{2}C_S(\Delta P_{B1} - \Delta P_{B2})\right] \times A_{WING} \quad \text{Eq. (1.1k).}$$

The expression in the squired brackets in the right part of the equation Eq. (1.1k) has the physical sense of the effective pressure difference ΔP_L providing the lift-force F_L **10.F**, i.e.

$$F_L = \Delta P_L \times A_{WING} \qquad \text{Eq. (1.1l),}$$

wherein the effective pressure difference ΔP_L is commonly written in the form:

$$\Delta P_L \approx C_L \times \rho_0 \frac{u_0^2}{2} \qquad \text{Eq. (1.1m)}$$

where C_L is a so-called coefficient of lift that depends on the wing geometry and Reynolds Number. (For instance, for the classic asymmetric wing **10.A** exposed to airflow at the zero attack angle, when the associated Reynolds Number is in the range between 5×10^6 and 10×10^6, the value 0.52 is an acceptable approximation of the coefficient of lift C_L.) Comparing the equations Eq. (1.1i), Eq. (1.1k), and Eq. (1.1m), the lift coefficient C_L is interrelated with the suddenness factor C_S as follows:

$$C_L = \frac{1}{2}C_S\frac{u_1^2 - u_2^2}{u_0^2} \qquad \text{Eq. (1.1n),}$$

wherein the geometry-dependence is performed by the values of the boundary layers velocities u_1 and u_2, which, also depend on the suddenness factor C_S.

Fig. 1g Case (B) is a prior art schematic drawing of a geometrically symmetric airfoil profile of an airplane wing **10.B**, symmetric relative to a horizontal plane when oriented horizontally in a sagittal plane. Comparison between the classic asymmetric airfoil profile of the airplane wing **10.A** and geometrically symmetric airfoil profile of the airplane wing **10.B** is further analyzed to clarify a contribution to the lift-force **10.F** generated due to the Coanda-effect.

To move the wing **10.B** with the mentioned certain relatively-low velocity u_0, an engine **"ENGINE-B"**, which is not shown here, consumes a certain power to overcome the mentioned certain resistance of the ambient fluid. The two wing configurations: **10.A** and **10.B**, characterized by equal cross-sectional areas and chords, are subjected to the same resistance against the headway motion. So, to move the wings **10.A** and **10.B** with the same velocity u_0, the engines: **"ENGINE-A"** and **"ENGINE-B"**, correspondingly, consume the same power, burning the same amount of fuel. However, while wing **10.B** is not subjected to a lift-force, wing **10.A** is subjected to the lift-force, seemingly, given free of charge. Actually, the lift-force **10.F** acting on wing **10.A** is given due to the Coanda-effect at the expense of the heat energy of the ambient fluid, and so, from the point of view of the burned fuel, the lift-force **10.F** is given free of charge **indeed. Note that the phrase "given free of charge" does not mean "given from nothing". It is** the well-known principle of commonly used airplanes. So (for the sake of simplicity, considering the zero attack angle), a very heavy airplane flies using a relatively economical engine providing for a headway motion and thereby triggering the Coanda-jet-effect originating the lift-force **10.F** working at the expense of the heat energy of the ambient fluid.

Airfoil Wing is not a Perpetuum Mobile

Meanwhile, on the one hand, the above-expounded analysis, made from the point of view of the Energy Conservation Law, says **that the term "given free of charge" does not mean "given from nothing" and so** proves that the airfoil wing **10.A** is not a Perpetuum Mobile of the first kind; on the other hand, it remains the frequently asked question if the airfoil wing **10.A** is a Perpetuum Mobile of the second kind contravening to the Second Law of Thermodynamics because the heat energy of the ambient fluid becomes transformed into the useful lift-force without any additional contribution of energy as soon as we compare the wings **10.A** of **Case (A)** and **10.B** of **Case (B)**.

For this matter, the applicant points out that:

1. The case of a wing, moving in a fluid, is the same as the case of moving fluid, flowing around the wing, according to Galilean relativity; and
2. Any portion of the moving fluid cannot be considered as an isolated system, at least because the moving portion of fluid inherently contacts with both: an adjacent upstream portion and an adjacent downstream portion of the ambient fluid, i.e. it is not an isolated system by definition.

Hence, the Second Law of Thermodynamics is not applicable to the moving portion of the fluid flowing around the wing, because the moving portion of the fluid is an open system from the point of view of the thermodynamics by definition, and so, the wing **10.A** of **Case (A)** cannot be defined as the Perpetuum Mobile of the second kind as well.

When the attack angle is zero, an aircraft consumes power for headway forwarding against the frictional-dragging only, and the lift-force F_L **10.F** working for the keeping a height of flight (i.e. for the upward motion against the gravity) is originated at the expense of the ambient warmth due to the Coanda-jet-effect; the use of this phenomenon is one of the primary features of claimed embodiments of the present patent application;

Broken Boundary Layer

Fig. 1g Scheme (E) is a prior art schematic drawing extracted from **D06** showing a widening boundary layer **1G.40** bordered, on the one side, by a seemingly-airfoil solid surface **1G.41** of a wing and, on the other side, by a streamline **1G.42**. Portions of streamlines within the boundary layer **1G.40** are indicated by a set of arrows **1G.43**. The dashed line **1G.44** divides the boundary layer **1G.40** between two portions: upstream, where the boundary layer is yet laminar, and downstream, where the turbulent vortex **1G.45** takes place. The separation point **1G.46** is the point on the upper side, where the boundary layer is completely separated from the surface, reducing lift drastically. This is known as stalling. There are broken or jumping all: the headway velocity, the static pressure, the absolute temperature, and the mass density nearby the separation point **1G.46**.

Two prior art methods of boundary layer control are: first, Prandtl developed mechanisms to suck the boundary layer along the upper side of wings, thus maintaining the laminar flow and preventing separation and, second, others studied ways of blowing air into the boundary layer near the leading edge, to energize the boundary layer and prevent separation. One of the difficulties to implement the controlled sucking portions from and/or blowing portions into the boundary layer is that the boundary layer structure depends on the airflow velocity.

Further Features Of Airfoil Wing

The inventor points out that:

- To control a lift-force of an airfoil wing, one uses wings supplied with moving flaps that, as well as a non-zero attack angle, undesirably boosts turbulence and drag;
- A well-known phenomenon of upper-side flux **10.3** adiabatic cooling at low-subsonic velocities is observed. Natural air is humid, and the local cooling, accompanied by the pressure reduction, acts, in particular, as a water condensation trigger. If the wind flows around a wing with an M-velocity equal to or higher than the Mach number (i.e. the speed of sound), a well-known phenomenon of shock sound-wave emission takes place. This shock sound-wave is not caused by wing vibration, but arises when a myriad of acoustic waves become in-phase superposed thereby forming the resonance resulting in the shock sound-wave; moreover, it becomes evident that the shock sound-wave is originated at the expense of the internal heat energy of air and so is accompanied by the air temperature shock decrease, provoking the process of vapor condensation into water-aerosols;
- One could note that the effect of considerable amounts of water-vapor condensation into water-aerosols and sublimate into micro-flakes-of-snow, which are observed behind the high-speed aircraft's wings, occurs at flow speeds substantially lower than the Mach number, i.e. it is not triggered by the mentioned phenomenon of shock sound-wave emission. In contrast to the prediction of the extra-decrease of static pressure and temperature at transonic and supersonic velocities only, on the one hand, an explanation of this phenomenon and, on the other hand, the phenomenon that air-fluxes flowing nearby around a body, when the body flies in air-environment with transonic, supersonic, and/or hypersonic velocities become warmer and extra-warmed, both are is expounded, for example, in **A01**, **A02**, and **A03**;
- When flying with transonic and supersonic velocities, the warmed and extra-warmed portion of flow moving above a wing, having the classic airfoil profile **10.A** oriented horizontally, results in a negative lift-force and so a non-zero attack angle undesirably boosting a drag is required to fly horizontally; and
- It is also well-known that, when flying with transonic and supersonic velocities, a wing, having the classic airfoil profile **10.A** oriented horizontally but knocked-over to have a convexity on the lower side of the wing, results in a positive lift-force.

Had one possessed a technique to control the flow velocity and static pressure within the boundary layer without inertia and without moving parts, it would become possible to suppress the undesired concomitant turbulence and, thereby, to improve the functionality of the wing

substantially. The present patent application proposes a method for providing the laminarity within a boundary layer resulting in an increased lift-force and proposes solutions to overcome the problematic occurrence of turbulence and negative lift-force.

Point of Sail

The term "point of sail" is used to describe a sailing boat orientation relative to a prevalent direction of the ambient wind.

Prior art **Fig. 1i** is a schematic illustration of points of sail. A sailboat exposed to ambient headwind **18.0** in positions and orientations: **18.1**, **18.3**, **18.5**, **18.6**, **18.7**, **18.9**, **18.11**, and **18.12** relative to the prevalent direction of ambient headwind **18.0** is shown schematically. The positions and orientations of the sailboat, i.e. the points of sail, are classified by groups, indicated by symbols "A", "B", "C", "D", and "E". Group "A" is the so-called "in irons" (into the wind) or "no-go zone", group "B" is so-called "close-hauled", group "C" is so-called "beam reach", group "D" is so-called "broad reach", and group "E" is so-called "running".

The sailboat is a well-known example, showing that a passive sail, playing a role of a trivial nozzle, enables to move the sailboat at least partially in the upstream direction against ambient headwind **18.0**, for instance along a zigzag path. In other words, the passive sail exposed to ambient headwind **18.0** produces "a net jet-thrust" against the ambient headwind **18.0**. In simple words, in fact, the ambient headwind **18.0** sucks the passive sail but not pushes off it. Shaded sector **18.2** corresponds to the "no-go zone", where the single passive sail, being in position and orientation **18.12** belonging to point of sail group "A", does not provide a net jet-thrust in the upstream direction against the ambient headwind **18.0**.

Point of sail "B", called also "B"-point of sail, having the sailboat position and orientation **18.1**, is shown also in enlarged view **18**. Streamlines **18.13** show a windward wind flow aligned with the concave side of sail; streamlines **18.14** show a leeward wind flow subjected to the Coanda-effect and so moving along a curved trajectory adjoining the convex side of the elastic sail, self-adapted to pressures of the wind flows; a multiplicity of arrows **18.15** indicate "lift-forces", in this case, directed horizontally, caused by the difference between static pressures at the concave and convex sides of sail; and arrow **18.16** indicates a portion of wind accelerated convectively, i.e. at the expense of the internal heat energy of wind. The convectively accelerated wind portion **18.16** acts on the sailboat by reactive force **18.17** according to Newton's Third Law. Reactive force **18.17** is vectored in the upstream direction. While lift-forces **18.15** become compensated dominantly by a stabilizing reaction of the sailboat's keel, which is not shown here, the reactive force **18.17** defines the sailboat headway motion

primarily. The effect of net jet-thrust against the ambient wind is a kind of jet-effect; i.e. it is the effect of convective acceleration of a wind portion flowing along a curved trajectory adjoining **the convex side of passive sail in point of sail "B" due to the Co**anda-jet-effect, and in turn, the accelerated wind portion causes the net jet-**thrust, according to Newton's Third Law. To** move against the wind, the sail, characterized by the point of sail **"B" and orientation 18.1**, must extract from the air the internal heat power, associated with the arisen reactive force **18.17**, higher than the mechanical power of the oncoming headwind **18.0** blowing the sail downstream away. In this case, one observes that the drag in the wide sense, determined by the cumulative resistance of the sailboat to the oncoming airflow due to: the sailboat non-zero frontal cross-sectional area plus the effect of so-called skin-friction and plus the effect of turbulence, is **weaker than the seemingly "negative drag", determined by the jet**-thrust.

The inventor takes note that, when tracing after a wind portion relative to a system of coordinates linked with the wind portion yet to be accelerated due to the Coanda-jet-effect operation, one interprets the mentioned wind portion local acceleration as a peculiar shock-like wave propagating downstream, backward relative to the headway motion of the sailboat.

For the purposes of the present patent application, **the introduced term "peculiar shock**-like **wave" or "peculiar wave" should be understood as a fluid reaction originated by a fluid portion local acceleration in a prevalent direction, in contrast to the term** "forced wave" **that should be** understood as fluid oscillation originated and determined by an action of an external periodically-alternating force.

In view of the foregoing description referring to prior art **Fig. 1i**, it will be evident to a person skilled in the art that two sailboats, both being positioned in **"B"**-point of sail, wherein one of the sailboats has the position and orientation **18.1** and the other sailboat has the position and orientation **18.11**, when consolidated together and thereby aggregated as a whole, provide a condition for a resultant net jet-thrust applied to the aggregation, directed straight against the ambient headwind **18.0**. In this case, the ambient headwind **18.0** just sucks the passive pair of sailboats.

The inventor points out and emphasizes that the phenomenon of net jet-thrust of sail in **point of sail "B"** occurs due to the self-acceleration of an airflow portion at the expense of the **air portion's warmth. I.e., in other words, the net jet**-thrust of sail **in point of sail "B"** occurs due to the Coanda-jet-effect.

In spite of the fact that the effect of net jet-thrust against the ambient wind is widely used in cruising on the water, the effect remains unused in the world industry.

There is, therefore, a need in the art for a method and apparatus to provide proper analysis and optimal design of a system, implementing the kind of jet-effect providing the net thrust in the upstream direction, for a controllable use in industry.

Flying Bird

For the purposes of the present patent application, the inventor points out to a flying bird, to take note that the jet-effect is not so exotic, to emphasize the jet-effect potential efficiency, and to make clear that the Coanda-jet-effect is one of the primary and quintessential aspects of the present patent application. The inventor points out that a flying bird makes waving motions rather than rowing or pushing-off motions by its wings. The waving can be interpreted as a booster of the Coanda-jet-effect as well as a source of forced elastic waves. The inventor points out to a flying bird, the wings waving of which is not so frequent but-nevertheless is enviably efficient. In particular for a pigeon, while the wings waving velocity relative to the bird body is between 1 and 2 m/sec only, the bird flying-acceleration in a horizontal direction up to seemingly-paradoxical high velocities, higher than 10 m/sec (actually, higher than 30 m/sec and even 40 m/sec), becomes reachable; – it confirms that the primary mechanism of the flying-acceleration is at least not the pushing-off in the direct sense.

For comparison, a flying relatively large bird, for instance, a golden eagle, and a running cheetah, both overcome the air drag and support the upward and downward mobility (wherein **the cheetah's vertical mobility is defined by a ground relief and small jumps of the cheetah's** center of mass only). For simplicity of the comparison, ignore the sidelong (leftward and rightward) mobility. The flying golden-eagle, **"pushing-off" gaseous air** (take note, the **"pushing-off" is not intensively**-frequent), overcomes the air drag and supports the upward and downward mobility much easier and moves in the horizontal direction much faster, than the running cheetah **pushing-off a stationary surface**, wherein pushing-off substantially more intensive-**frequently providing for a velocity of paws relative to cheetah's body being equal to** the velocity of a cheetah. At first glance, this fact looks like a confusingly-paradoxical mystery. However, it becomes easily-explainable, if not to ignore the triggered Coanda-jet-effect as for the lift-force as well as for the forward motion acceleration (analogously as the net jet-thrust in the aforementioned example with the sailboat in **"B"**-point of sail described with the reference to **Fig. 1i**). I.e. it becomes easily-explainable if the wing of a bird is interpreted as a sail oriented horizontally as **"B"**-point of sail to provide an upward-and-forward jet-thrust as seemingly **"negative drag"**. **As further examples**:

- a flying snowy owl is extremely noiseless, i.e. it has an actually-airfoil wing and body as a whole to provide for the suppression of turbulences, and
- a bird-swift is capable of non-stop flying for a long time, measured in months and years, wherein the bird-swift, flying under its own power and wherein not-frequently waving, is capable of reaching a horizontal velocity of 47 m/sec (169 km/h).

In spite of the fact, that the efficiency of net jet-thrust of the flying bird is attractively high, the phenomenon remains unused in the world industry.

Furthermore, the style of a flock of cranes flying is well-known. The style combines the waving of wings when the flying is accelerating and the wings gliding when the flying is stabilized. This style prompts that:

- on the one hand, there are no turbulent vortices behind the gliding wings of the flying cranes, i.e. the wings of a crane are actually-airfoil, and so the previous gliding crane does not hinder but even helps the next gliding crane in a lift and jet-thrust; and
- on the other hand, there is an interference of omnidirectional waves generated by the waving wings of the cranes of the flock, thus, it is self-suggested the assumption that the flying cranes use constructive interference thereby helping each other in the waving-itself.

In spite of the fact that the cranes apply the cascaded multi-stage repeating and thereby reinforcing the Coanda-jet-effect for originating both: the lift-force and the net jet-thrust, over a long time, this technique remains unused in the world industry.

There is, therefore, a need in the art for a method and apparatus to provide proper analysis and optimal design of a system implementing the repeatedly reinforced Coanda-jet-effect of laminar moving fluid as well as the repeatedly reinforced constructive interference of waves in the fluid, both providing the scalable and controllable use of the acquired power in the industry.

The inventor also points out the capability of taking-off, for example, a pigeon, having a mass of $\mathbf{0.3}\,\boldsymbol{kG}$ and span of wings of $\mathbf{0.5}\,\boldsymbol{m}$, when waving with the wings waving velocity relative to the bird body of between $\mathbf{1}$ and $\mathbf{2}\,\boldsymbol{m/sec}$ only, can rise dominantly-vertically faster than $\mathbf{2}$ meters per second. The "pushing-off" from the gaseous air more efficiently than the pushing-off from a hypothetical "fixed ladder" already looks like a confusingly-paradoxical mystery. Moreover, the inventor points out that:

- to raise the mass of the pigeon, the lift-force $\boldsymbol{F_L}$ of wings must be greater than $\mathbf{3}\boldsymbol{N}$, i.e. $\boldsymbol{F_L > 3N}$;

- the lift-force of wings F_L is interrelated with the wings area A_{WINGS} given approximately as $0.08\,m^2$ and a difference in static and/or stagnation pressures ΔP_L in the air portions under and above the wings by the expression $F_L = A_{WINGS} \times \Delta P_L$;
- taking into account a classic specification of the ΔP_L, the equation for the lift-force is: $F_L = 0.5 \times A_{WINGS} \times C_L \times \rho \times u_W^2$, where ρ is the air mass density given as $\rho \approx 1.2\,kG/m^3$, u_W is the velocity of an air portion relative to the wings, and C_L is the coefficient of lift, which at most can reach the value **1.75** in the extremal case of airflow impacting a classic wing **10.A** at the attack angle of 16^0 as illustrated in **Fig. 1g Graph (C)** and a value between **2.0** and **3.0** when it becomes a coefficient of drag in the extremal case of airflow striking a hemispherical concave surface (the value **1.75** is used for the coefficient of drag of a parachute). So, to reach the value for F_L of $3N$, a pigeon must accelerate an air portion up to the velocity $u_W = \sqrt{2F_L/(A_{WINGS} \times C_L \times \rho)}$ estimated as at least $5\,m/sec$; it is much higher than the reachable velocity of the wings waving.

It looks like a mystery if not to take into account the thermoregulation of the warm-blooded bird providing for that the fuzz at the lower side of the **bird's** wing keeps air warmer than the air kept in the fuzz at the **wing's upper** side (because both dominant warming muscles: pectoralis and supracoracoideus, are located **lower than the bird's wings)** and that the frequent waving results in the origination of air boundary layers around the wings, wherein the fuzz also smooths surges in pressure gradients.

As the mechanism of the taking-off effect of warm-blooded birds is directly related to claims of the present patent application, a detailed explanation of the mechanism is expounded hereinafter in the sub-**paragraph** "Taking-off Of A Warm-blooded Bird".

Taking-off Of A Warm-blooded Bird

When considering a wing of a bird, for the sake of simplicity and without loss of reasonability, reference is made again to the schematic profile of classic wing **10.A** (**Fig. 1g**).

The thermodynamic equation Eq. (1.1b), when applied to the boundary layers around a wing of a bird, in particular, says that, in contrast to a **"cold-blooded" wing of an airplane** acting on the convergent-**divergently shaped boundary layers by "passive" heating and cooling due to** either: the effect of skin-friction, and/or the Coanda-effect, and/or the Venturi effect; the warm-blooded wing of bird causes active heating of the convergent-divergently shaped boundary **layers in addition to the mentioned "passive" heating and cooling**. In particular, as the **wing's** lower side is warmer **than the wing's upper side**, while the upper-side shaped boundary layer is

subjected to the "passive" warming and cooling dominantly, the lower-side shaped boundary layer is kept heated by the warmed fuzz. This means that the lower portion of the airflow is subjected to forced sudden warming ΔT_F resulting in additional forced sudden compression ΔP_F. The additional forced sudden compression ΔP_F is added to the mentioned difference ΔP_{B2}, thereby, increasing the difference $|\Delta P_{B1} - \Delta P_{B2}|$ and, in turn, increasing the lift-force F_L. To estimate, how much the added forced sudden compression ΔP_F can contribute to the effect of taking-off of a pigeon, consider:

- the normal ambient air conditions: $T \approx 300K$, $P \approx 100{,}000Pa$, and $\gamma = 7/5$;
- the wings of the pigeon having a chord of $16\,cm$ and a total span of $50\,cm$; i.e. $A_{WING} = 0.08\,m^2$;
- the effective velocity u_W of wings waving is given by $2\,m/sec$ that corresponds to about 5 swayings per second; i.e. the suddenness factor is $C_S \approx 0.01$, and
- an exemplary value of the additional to ambient temperature difference: ΔT_F of $(-9C)$, is taken for the estimation, noting that ΔT_F is interrelated with the suddenly originated effective additional static pressure difference ΔP_F according to the equation Eq. (1.1b).

So, the ratio $|\Delta T_F|/T \approx 0.03$, the ratio $|\Delta P_F|/P \approx 0.03 \times (7/5)/(2/5) = 0.1$, the contribution to the suddenly originated additional static pressure difference is $|\Delta P_F| \approx 0.1 \times 10^5 Pa$, and the contribution to the lift-force is specified as

$$\Delta F_L = \frac{1}{2} \times C_S \times A_{WING} \times |\Delta P_F| \quad \text{Eq.(1.1o)}$$

and estimated as approximately $4N$; it is sufficient to lift the mass $0.3\,kG$ of the pigeon in the vertical direction with the acceleration of up to $3.3\,m/sec^2$. Thereby, the estimation shows that the forced sudden warming ΔT_F plays a decisive role in the taking-off of the pigeon.

Now, to estimate the efficiency of the temperature regulation of a warm-blooded wing to contribute to the effect of thrust, further consider as follows:

- the frontal cross-sectional area of a pigeon including both the relatively thin wings and approximately elliptical body is $A_{FR} \approx 0.0025\,m^2$;
- the overall surface area of the pigeon including two sides of wings and the approximately elliptical body is $A_{OV} \approx 0.45\,m^2$;
- considering the warm-blooded bird capability of thermoregulation, an exemplary value of the additional temperature difference ΔT_{TH} between the "head" and rear part of the bird's body and wings is taken as $(-5C)$; i.e. the temperature is distributed such that the head of the bird is colder than the bird's rear part of the body; and

- the value of the forced sudden compression ΔP_{TH} caused by the additional temperature difference ΔT_{TH}, estimated using the interrelation Eq. (1.1b) is:

$$\Delta P_{TH} = \left(\frac{-5}{300}\right) \times \left(\frac{7}{2}\right) \times 10^5 \approx -6{,}000\ Pa.$$

So, the contribution to the thrust ΔF_{TH} specified as

$$\Delta F_{TH} = \frac{1}{2} \times C_S \times A_{FR} \times |\Delta P_{TH}| \qquad \text{Eq.(1.1p)}$$

is estimated as $1.5\ N$. The contribution to the thrust of $1.5\ N$ is sufficient to accelerate the mass of the pigeon in the horizontal direction with the acceleration of up to $5\ m/sec^2$ and to overcome a velocity-dependent drag in the air when moving with the headway velocity u_0 of at least $33\ m/sec$ that follows from the interrelation derived from the well-known equation for drag and skin-friction, namely $u_0 = \{|\Delta F_{TH}|/[0.5\rho_0(C_d A_{FR} + C_f A_{OV})]\}^{1/2}$, where:

C_f is the skin-friction coefficient, normally, given as about 0.045 for an airfoil wing that can be interpreted as the worst-case approximation for the body and wings of the pigeon,

C_d is the drag coefficient, normally, given as about 0.5 for a frontal convexly-rounded configuration of an airfoil body that, again, can be interpreted as the worst-case approximation for the body and wings of the pigeon.

The estimation of $u_0 \geq 33 m/sec$ was done assuming the minimal value of the suddenness factor C_S estimated for waving wings, although the suddenness factor C_S is higher when the bird moves with a higher velocity.

Flying Insects

Fig. 1j is an illustration of a honeybee **1J.0** as an exemplary insect capable of flying. In **contrast to the bird's wings, the insect's wings are neither profiled nor warm**-blooded. It is a well-known frequently asked question in relation to the possibility of insects flying. One pays **attention that the size of the insect's wings 1J.1** and the **velocity of the insect's wings motion** are far from sufficient for active lifting the mass of the insects. However, this becomes explainable if to take into account that, on the one hand, **the insect's wings function as a ventilator blowing the insect's** hairy corpus and, on the other hand, the phenomenon of in-flight and pre-flight thermoregulation **of the insect's corpus**, as described, in particular, in **D13** and **D14**. For instance, Japanese honeybee is capable of increasing their body temperature above $46^0 C$, as described in **D15**.

In particular, consider the honeybee **1J.0** having an ellipsoidal-like hairy corpus having a mass of $0.1\ g$, length **1J.3** of $15\ mm$, cross-sectional diameter **1J.2** of $5\ mm$, and cross-sectional area in a frontal plane of about $20\ mm^2$. The honeybee **1J.0**, having a pair of blade-

like wings **1J.4**, each of which is $10\ mm$ in length **1J.1** and up to $2.5\ mm$ in width such that the area A_{WINGS} of a pair of wings is at most of $25\ mm^2$, is capable of waving at a rate up to **250** blows per second, corresponding to the effective velocity $\overline{u_B}$ of the blade-like wings of approximately $2.5\ m/sec$, mystery-providing a much higher flying velocity u_0 up to $18\ m/sec$ ($65\ km/h$). Moreover, to provide the lift-force $F_{L,INSECT} \approx 0.001N$ for taking-off, the blade-like wings, seemingly, **must blow the honeybee's body with the velocity** u_B (i.e. must move with the velocity u_B) defined as $\sqrt{2F_{L,INSECT}/(\rho C_L A_{WINGS})}$ and estimated as at least $6\ m/sec$; it is confusingly higher than the reachable effective velocity $\overline{u_B}$ of the wings waving.

The insects use their neither profiled nor warm-blooded wings as blades to blow their hairy corpus which (the corpus), in turn, plays the role of a thermoregulated wing proving the lift-force. Thus, when referring to equation Eq. (1.1o), the area A_{WINGS} has the sense of an area A_{INSECT} **of the insect's corpus** projection on a horizontal plane. For the considered case, the area A_{INSECT} is estimated as $75\ mm^2$ and the effective velocity $\overline{u_B}$ of the blade-like wings of approximately $2.5m/sec$ determines the suddenness factor C_S of approximately **0.013**. Considering the exemplary honeybee and referring to the equation Eq. (1.1o), but now using the value $A_{INSECT} = 75\ mm^2$ and taking into account the capability of pre-flight thermoregulation, the lift-force is specified as:

$$\Delta F_{L,INSECT} = \frac{1}{2} \times C_S \times A_{INSECT} \times |\Delta P_{INSECT}| \quad \text{Eq. (1.1q)}$$

It can be derived from the equation Eq. (1.1q) that, to provide the lift-force $F_{L,INSECT} \approx 0.001N$ for taking-off using the actual blade-like wings waving with the effective velocity of $2.5m/sec$, the insect must provide the static pressure difference $|\Delta P_{INSECT}|$ of approximately $2\ kPa$ due to the temperature difference of about 1.7^0C; this and much bigger temperature differences correspond to **the capability of the honeybee's thermoregulation**.

It follows from the foregoing sub-**paragraphs** "Flying Bird" **and** "Flying Insects" that there is a need in the art for a method and apparatus to provide a design of a system implementing an increased lift-force allowing for controllable use of the increased lift-force in the industry.

The use of the controllable temperature difference between boundary layers to contribute to the lift-force is suggested in the present patent application.

Fig. 1k is a prior art schematic illustration of a wind turbine **17.1** built-in into cylinder **17.2** having real sidewalls and open butt-ends. A widened description of **Fig. 1k** may be referred to **AU03**, which (the widened description) is not narrated herein for brevity. Instead, the inventor points out that the sub-portion **17.41** of the fluid stream enters cylinder **17.2** with a certain

headway-motion velocity, indicated by u_{41}, which is lower than the headway-motion velocity of sub-portion **17.42**, indicated by u_{42}, which flows outside cylinder **17.2**. The reason for the negative difference $(u_{41} - u_{42})$ is explained by the drag of blades of wind turbine **17.1**, namely, as the blades are subjected to impact of flow **17.41**, the blades retard the flow **17.41** by the same drag according to **Newton's Third Law of motion. In such an application, the effect of** flow retarding is undesired. There is, therefore, a need in the art for a method and apparatus to provide a design of an improved wind turbine where the undesired effect of flow retarding would be reduced and the desired effect of producing electric power would be boosted.

Sound as Complicated Movement in Molecular Fluid

In physics, an acoustic (elastic) wave is an oscillation accompanied by a transfer of energy that travels through a medium (for instance, the ambient fluid). Waves consist of oscillations or vibrations of particles (molecules), around almost fixed locations.

A forcedly accelerated membrane is a trivial aerodynamic device – a fluid pusher-off, capable of originating an elastic wave propagating in the ambient fluid. Wave motion transfers energy from one point to another, displacing particles of the transmission medium with little or no associated mass transport. From the point of view of the energy consumption by a source of the acoustic wave, the energy transmission is given free of charge; it is given at the expense of the heat energy of the ambient fluid as a result of the triggered waving jet-effect as described in **A02** and **A03**. The wave-front propagates in accordance with the **Huygens-Fresnel principle** saying that every point, which a wave-front disturbance reaches, becomes a source of a secondary spherical wave, wherein the interference superposition of these secondary waves determines the form of the wave at any subsequent time.

In physics, sound (acoustic wave) in a fluid is interpreted as an oscillating change of the **fluid's thermodynamic parameters**, namely, the oscillating change of the static pressure P, mass density ρ, and absolute temperature T, wherein the thermodynamic parameters are interrelated according to the van der Waals law of fluid state in an adiabatic process. Wherein, the oscillating changes in the fluid's thermodynamic parameters are such to result in triggering of the jet-effect manifested as fluid motion in the form of the propagating acoustic wave.

For the sake of concretization and without loss of generality, consider:

- the air as a particular case of the fluid, and
- the sound propagating in the air as a particular case of the acoustic wave propagating in the fluid.

The associated with sound oscillating changes of the fluid's thermodynamic parameters along an axis x collinear with the direction of the sound propagation is expressed as:

$$\begin{cases} \delta P = \Delta P \times e^{-i(\omega t - \kappa x)} & Eq.(1.2a) \\ \delta \rho = \Delta \rho \times e^{-i(\omega t - \kappa x)} & Eq.(1.2b) \\ \delta T = \Delta T \times e^{-i(\omega t - \kappa x)} & Eq.(1.2c) \end{cases}$$

where:

δP, $\delta \rho$, δT are the oscillating changes of the static pressure, the mass density, and the absolute temperature, correspondingly;

ΔP, $\Delta \rho$, ΔT are amplitudes of the oscillating change of the static pressure, the mass density, and the absolute temperature, correspondingly;

ω is the cyclic frequency of the oscillating change;

κ is the wavenumber interrelated with the cyclic frequency ω of the acoustic wave as $\kappa = \omega / u_s$, where u_s is the phase velocity of the sound propagation in the fluid.

Taking into account the interrelations between the thermodynamic parameters in an adiabatic process described hereinabove in the sub-paragraph "Lift-Force Mechanism" referring to Fig. 1g Graph (C) by the equations *Eqs. (1.1a) and (1.1b)*, the equations *Eqs. (1.2a), (1.2b),* and *(1.2c)* describing the oscillating changes of the fluid's thermodynamic parameters associated with the sound are rewritten as a system of equivalent equations as follows:

$$\begin{cases} \dfrac{\delta P}{P} = \dfrac{\Delta P}{P} \times \exp[-i(\omega t - \kappa x)] & Eq.(1.3a) \\ \dfrac{\delta \rho}{\rho} = \dfrac{1}{\gamma} \dfrac{\Delta P}{P} \times \exp[-i(\omega t - \kappa x)] & Eq.(1.3b) \\ \dfrac{\delta T}{T} = \dfrac{\gamma - 1}{\gamma} \dfrac{\Delta P}{P} \times \exp[-i(\omega t - \kappa x)] & Eq.(1.3c) \end{cases}$$

A human-hearer perceives the oscillating changes of the air static pressure as sound loudness; the air static pressure, absolute temperature, and mass density are measured by the so-called "SPL" (sound pressure level), "STL" (sound temperature level), and "SDL" (sound density level), correspondingly; and the sound loudness is measured also by "SIL" (sound intensity level) or "SWL" sound power level.

The SPL is measured in decibels (dB). It is equal to $20 \times log_{10}$ of the ratio of the route mean square (RMS) of sound pressure to the reference of sound pressure that (the reference sound pressure) in the air is $2 \times 10^{-5} N/m^2$ or $0.0002\ Pa$, in turn, corresponding to the reference acoustic wave power (the loudness as power) estimated approximately as $10^{-12} W$. The characteristic SPL of speakers is defined for the distance of $1\ m$ from the speaker.

Normally, a range of the characteristic SPL for a speaker is between 0 to $80\,dB$ that corresponds to changes in the static pressure in the range from $0.0002\,Pa$ to $2\,Pa$ and changes in the acoustic wave power in the range from $10^{-12}W$ to $10^{-4}W$. Using the equation Eq. (1.3c), the reference sound temperature in the air is estimated as $5.4 \times 10^{-10}K$ and the range of temperature changes for the speaker is estimated from $5.4 \times 10^{-10}K$ to $5.4 \times 10^{-6}K$.

Sound (acoustic wave) is considered as a complicated movement of a molecular fluid, wherein the complicated movement is composed of:

- The Brownian motion of the air molecules with the Brownian velocity, indicated by $u_{Brownian}$, which interrelates with the velocity of sound u_{sound} as $u_{Brownian} = \sqrt{3/\gamma} \times u_{sound}$; $u_{sound} \approx 345\,m/sec$ and $u_{Brownian} \approx 500\,m/sec$.
- The oscillating motion of molecules with so-called "particle velocity", the amplitude of which is indicated by $u_{particle}$ and interrelated with the sound loudness; normally, in the air,
    - near an oscillating membrane which is a source of the sound, the particle velocity amplitude $u_{particle}$ is predetermined by the velocity of the oscillating membrane and is between $0.1\,m/sec$ and $10\,m/sec$, while
    - far from the oscillating membrane, where the sound front becomes substantially widened, the particle velocity amplitude $u_{particle}$ is very low: between $5 \times 10^{-8}\,m/sec$ and $5 \times 10^{-4}\,m/sec$;

  wherein the particle velocity relates to the mass of the oscillating air as a whole; note that, considering a local slow flow moving with the particle velocity, a widening of a frontal cross-sectional area is accompanied by a decrease in the amplitude of the particle velocity, according to the equation of continuity;
- The specific conveying motion that is interrelated with the cascaded oscillating motion of particles moving with the "particle velocity" that [the "particle velocity"], in turn, is interrelated with the acoustic wave amplitude manifested as the sound loudness. The specific conveying motion is a kind of movement, which (in contrast to the oscillating motion of the air as a whole) is interpreted as a directional motion of a tiny portion of fluid mass that [the tiny portion of mass] determines the air mass density oscillating change only. The specific conveying motion can be interpreted as composed of two complementary alternating movements of positive and negative changes of air mass density, wherein both alternating movements are in the same direction (that is the direction of sound propagation) and, when in open space, with the M-velocity of $1\,Mach$. The so-called Umov-vector is a measure of the specific conveying motion of the tiny portion of the fluid mass. The SPL, characterizing

the sound loudness, is interrelated with the so-called: "SVL" (sound particle velocity level). Thus, the oscillating (positive and negative) change in mass density along the direction of the wave propagation (again, which is interrelated with the sound loudness) is considered as the directional motion of the tiny mass, wherein the motion is with the mass density change conveying velocity u_{convey} that is the same as the velocity of sound u_{sound}, i.e., when propagating in open space, M-velocity of 1 $Mach$; and

- The concomitant turbulent motion, as dis-laminarity of the mentioned oscillating and conveying components of the complicated movement of air, depends on both the shape of a horn and the acoustic wave amplitude (sound loudness);

wherein,

in contrast to acoustic waves in open space where the turbulent component of fluid motion, inherently-accompanying the acoustic waves, causes the inevitable dissipation of the propagating acoustic waves manifested as a decrease of sound loudness,

the turbulent component of fluid motion within a horn is pre-determined by restricted degrees of freedom, so, the horn, if elaborated, can provide for reduced concomitant turbulence accompanied by increased intensity of sound. In other words, the elaborated horn plays the role of a fluid pusher-off capable of transforming the kinetic power of the concomitant turbulence into the wave power accompanied by increased both the particle velocity amplitude $u_{particle}$ and the conveying velocity u_{convey}.

For the purposes of the present patent application, the term "heat energy in a broad sense" should be understood as the cumulative kinetic energy of both the Brownian motion of the air molecules and the concomitant turbulent motion.

When a sound is originated by an oscillating membrane of a classic source of acoustic waves rated by a power supplier, the net-efficiency, defined for the classic source of acoustic waves as the ratio of the power of sound to the supplied power, normally, is between 0.1% and 2%. The mentioned originated concomitant turbulence, originated due to sudden jumping changes of thermodynamic parameters and velocity of adjacent fluid portions, especially, near the edges of the moving membrane, is the dominant reason for:

- such a low net-efficiency of sound launching and, vice-versa, detection (the introduced term "sound detection" should be understood as registration and/or recording the electric voltage and/or current induced in the electrical circuit due to sound impact); and

- that, when the sound is propagating in open space, the sound loudness measured in SPL is further decreasing exponentially with the propagation path increase; wherein the exponential decrease in SPL is stronger for the sound of higher frequencies.

I.e., in other words, 98% to 99.9% of the power consumed by a classic source of acoustic waves goes for the kinetic power of the undesired turbulent motion of the ambient fluid.

One way to reduce the undesired concomitant turbulence accompanying the originated sound is to reduce the ratio of the amplitude of motion to the area of an oscillating membrane and, thereby, to reduce the contribution of the sudden jumping changes of thermodynamic parameters and velocity of adjacent fluid portions to the concomitant turbulence. For example, it is the commonly used piezo-effect manifested as small deformations of a piezo plate originating an ultrasound. However, taking into account that the power of sound is proportional to squared both amplitude and frequency of oscillation, the way can provide for the audible sound of unpractically ultra-low power and has a practical sense to launch and detect the ultrasound only.

There is, therefore, a need in the art for a method and apparatus to provide an improved design of a source and detector of acoustic waves; wherein, in particular, a net-efficiency would be increased by suppression of originated concomitant turbulence in the ambient fluid.

Horn as Sound-Booster

To reduce the kinetic power of the concomitant turbulence and thereby to increase the net-efficiency of sound launching, one uses an elaborated nozzle as an aerodynamic apparatus capable of transforming the kinetic energy, in general, of fluid particles, and, in particular, of the concomitant turbulence into the wave power of the sound.

Fig. 1n, a prior art illustration of horns playing the role of a sound booster, is divided into three schematic drawings: case **(A)**, case **(B)**, and case **(C)** as follows:

- **Case (A)**, illustrating a megaphone-A **1n.A** comprising a movable membrane **1n.A1**, capable of a controlled oscillating motion originating a sound, and an exponentially-divergent horn **1n.A2** having an outlet area **1n.AA**;
- **Case (B)**, illustrating a megaphone-B **1n.B** comprising a movable membrane **1n.B1**, capable of a controlled oscillating motion originating a sound, and a triple-folded exponentially-divergent horn formed by three cascaded sequentially scaled parts: **1n.B2, 1n.B3,** and **1n.B4.** The triple-folded exponentially-divergent horn as a whole has an outlet area **1n.BA** which is the same as the outlet area **1n.AA**; in another view, megaphone-B **1n.B** differs from megaphone-A **1n.A** by the triple-folded cumulative length of the

exponentially-divergent nozzle. It is found that, while megaphone-A **1n.A** increases the intensity of the originated sound on $10\,dB$, the megaphone-B **1n.B** increases the intensity of the originated sound on $20\,dB$; and

- **Case (C)**, illustrating a gramophone **1n.C** supplied by an exponentially-divergent nozzle **1n.C1** playing the role of the acoustic waveguide. Diameter D_{ou} **1n.C2** of sound-outlet of the exponentially-divergent nozzle **1n.C1** is greater than the diameter D_{in} of a narrow sound-inlet throat **1n.C3** by the factor F_D that is much greater than 1, in some implementation, the factor F_D is equal to **60**. The factor F_D equal to **60** corresponds to the area-variation ratio of the sound frontal-outlet cross-sectional area to the sound frontal-inlet cross-sectional area of **3,600**. The exponentially-divergent nozzle **1n.C1** is destined to solve the problem to widen the frontal cross-sectional area of sound rather than to contribute, in general, to the heat in a broad sense, and, in particular, to the concomitant turbulence of fluid. When a sound is established, in addition to the mentioned complicated movement of fluid, a portion of air, that takes a place within the exponentially-divergent nozzle **1n.C1**, is subjected to forward-and-backward oscillating longitudinal motion accompanied by substantial deformations and accelerations of the air portion. If to ignore the de Laval jet-effect, it is expected that the area-variation ratio of **3,600** is accompanied by the air velocity inverse ratio of the same order of value. When considering the fluid motion component moving with the conveying velocity u_{convey}, a change in cross-sectional area of longitudinally-moving change in fluid mass density triggers the de Laval jet-effect, as soon as the velocity u_{convey} measured in Mach numbers is higher than the specific M-velocity, and, when considering the fluid motion component moving with the particle velocity $u_{particle}$, a local change in the cross-sectional area of forward-and-backward oscillating longitudinally moving fluid triggers the local Venturi effect. In any case for an elaborated horn, the jet-effect of a transformation of both:
    - the fluid heat energy, and
    - the energy of the concomitant turbulence,

  into the energy of the fluid oscillating motion is manifested as sound boosting.

On the one hand, the advantage of the use of an elaborated horn as a sound booster self-suggests finding an optimal geometrical configuration of the elaborated horn, and, on the other hand, a disadvantage of the use of any horn as a sound booster is that a source of acoustic waves supplied by such a horn occupies an increased space.

The inventor points out that the set of equations *Eqs. (1.3a), (1.3b)*, and *(1.3c)*, described hereinabove in the subparagraph "Sound as Complicated Movement in Molecular Fluid", in fact, says that a sound can be generated by a forced inertialess varying of the temperature of a portion of the ambient fluid, and, as a result, the static pressure and mass density of the fluid portion will become varied as a derivation according to the interrelations *Eqs. (1.3a)*, *(1.3b)*, and *(1.3c)*. I.e., in other words, the mentioned subparagraph says that, hypothetically, it is possible to manipulate the temperature of a portion of fluid such that to result in triggering of the jet-effect manifested as the fluid motion in the form of the propagating acoustic wave. Had one possessed a technique to change the temperature of the ambient fluid potion without inertia and without moving parts, it would become possible to create sound with no creation of the undesired concomitant turbulence and, thereby, to increase the efficiency of a source of sound substantially. On the other hand, had one possessed a technique to detect the temperature changes of the ambient fluid potion without inertia and without moving parts, it would become possible to avoid undesired concomitant turbulence and so to increase the efficiency of a sound detector substantially.

There is, therefore, a need in the art for a method and apparatus to provide an improved design of a compact source and detector of acoustic waves; wherein, in particular, a net-efficiency would be increased by suppression of originated concomitant turbulence in the ambient fluid.

External Ear as Sound Booster

Fig. 1L comprises a schematic drawing of a sectional profile of a human ear in a sagittal plane. External ear **1L.0** of humans comprises a pinna and ear canal. The pinna, destined to be exposed to an incoming sound, comprises a funnel characterized by an outer-inlet cross-section **1L.1,** and the ear canal, destined for conveying the sound to eardrum **1L.6**, comprises an ear canal inlet cross-section **1L.2** such that the pinna funnel outer-inlet cross-sectional area is greater than the ear canal inlet cross-sectional area by the factor F_{12} of, approximately, **5.5**. The ear canal is a tunnel for sound, further characterized by:

- an after-inlet widened cross-section **1L.3**, the cross-sectional area of that is greater than the cross-sectional area of the ear canal inlet cross-section **1L.2** by the factor F_{32} of at least 1.1,
- a narrow throat cross-section **1L.4**, the cross-sectional area of that is smaller than the cross-sectional area of the ear canal after-inlet widened cross-section **1L.3** by the factor F_{34} of, approximately, **3**; moreover, the cross-sectional area of the ear canal

inlet cross-section **1L.2** is greater than the cross-sectional area of the narrow throat cross-section **1L.4** by the factor F_{14} of approximately **2.7**; and

- a wide outlet cross-section **1L.5** adjacent to the eardrum **1L.6**, the cross-sectional area of that [**1L.5** or **1L.6**] is greater than the cross-sectional area of the ear canal narrow throat cross-section **1L.4** by the factor F_{54} of, approximately, **5.5**.

The inventor points out the primary set of conditions satisfied for the shape of external ear **1L.1** as follows:

- the factor $F_{12} \approx 5.5$ is much greater than the ratio of $1\ Mach$ to the specific M-velocity, i.e. $F_{12} > 1/M_*$,
- $F_{32} > 1$,
- $F_{34} > F_{32}$,
- $F_{14} > 1$, and
- $F_{54} > 1/M_*$;

which (the set of conditions) will be further commented hereinbelow in sub-**paragraph** "Two-Stage Convergent-Divergent Jet-Nozzle" **referring to Fig. 6c** and in sub-paragraph "Phonendoscope and Sound Booster" **referring to Fig. 7a cases (B) and (C)**, where it will be shown that the external ear, shaped to provide the mentioned set of satisfied conditions, functions as an aerodynamic apparatus pulling-in and pushing-off portions of fluid (i.e. a fluid pusher-off) which is capable of sound loudness boosting wherein the aerodynamic apparatus – the fluid pusher-off can be further amended.

There is, therefore, a need in the art for a method and apparatus to provide proper analysis and optimal design of a convergent-divergent nozzle to implement applications appropriate for use in industry for efficient boosting the sound based on enhanced jet-effects accompanied, in general, with reduced heat energy in a broad sense, and, in particular, with suppressed concomitant turbulence.

Thermoelectric Devices

A well-known thermoelectric effect is an aspect of claims of the present patent application.

Fig. 1o is a prior art schematic illustration of a thermocouple **1o.0.** The thermocouple **1o.0** is an electrical device consisting of two dissimilar electrical conductors: **1o.1** (for instance, Niquel-Cromo) and **1o.2** (for instance, Aluminio-Cromo), forming an electrical junction **1o.3**. When the junction **1o.3** is submerged in an ambient fluid having a certain temperature (for instance, the absolute temperature of $573K$ or $300C$), the thermocouple **1o.0** produces a temperature-dependent voltage **V 1o.4** (for instance, $12.2mV$) between the two dissimilar

electrical conductors **1o.1** and **1o.2**. Thus, the thermocouple **1o.0** inertialessly originates a self-transformation of the absolute temperature into the electrical voltage **V 1o.4**. In **D12**, the author (Karpen), testing several systems providing the thermocouple effect: the voltage self-generation solely due to the presence of contacting mutually-repelling materials, points out that there is no any chemical reaction between the phases in contact, i.e. there is no process which would be stopped in the future. At the first glance, a system, comprising the thermocouple **1o.0** and an electrical circuit powered by the induced voltage, seems like a closed system, where one seemingly confusingly-paradoxically observes a local decrease in entropy, i.e. that the charging of the electrical circuit occurs at the expense of own temperature, but not a temperature difference. However, in reality, the system is inherently characterized by the junction **1o.3** of mutually-repelling materials contacting with the ambient fluid (i.e. the system is open from the point of view of thermodynamics), and the electric power is acquired at the expense of the ambient heat that is allowed for an open system. Thereby, the system, open from the point of view of thermodynamics, is neither a Perpetuum Mobile of the first kind nor a Perpetuum Mobile of the second kind. The thermocouple is an inherent attribute of a thermoelectric element providing for either Seebeck effect or the Peltier effect, both assuming an amplifying the thermocouple effect accompanied with acquired useful energy when either a temperature gradient between the ends of two dissimilar mutually-repelling electrical conductors is provided to induce an electromotive force (**emf**) or, vice-versa, forcedly established **emf** results in temperature separation, correspondingly, as described hereinafter.

For the purpose of the present patent application the terms "thermocouple" and "thermoelectric (TE) couple" and are reserved for the thermocouple **1o.0** that, in contrast to a TE element **1.0** described hereinafter referring to **Fig. 1p**, provides inertialess interrelation between the absolute temperature of the junction **1o.3** [but not a temperature difference] and the temperature-dependent voltage **1o.4** (or a derivative current in a closed electric circuit).

The term "thermoelectric device" should be understood in a broad sense including (a) an electric heater consuming electric power and radiating Jole heat which (the electric heater) is interpreted as a trivial thermoelectric device wherein the temperature increase due to the Joule heating effect is time-dependent (the longer the time, the higher the temperature), (b) a thermocouple which, in addition to the capability to radiate the Jole heat, is capable of inertialessly-inducing a temperature-dependent voltage bias and so is capable of functioning as a detector of temperature changes, and (c) a thermoelectric (TE) element described hereinbelow referring to **Fig. 1p**, which (the TE element) is further capable of transmitting heat

from one side to another side of the device and so is capable of inertialessly-controlling of a temperature difference between the two sides of the device.

Fig. 1p, divided into three parts:

Case (A) REFRIGERATION MODE,

Case (A) TIME CHARACTERISTIC, and

Case (B) POWER GENERATION MODE,

is a prior art illustration of a **THERMOELECTRIC ELEMENT 1.0**, called also a thermoelectric (TE) module, and its **exemplary time characteristic, where numerals, which have the letter "A",** belong to **Case (A) and numerals, which have the letter "B", belong to Case (B)**.

The TE module **1.0**, as in particular described in **D01**, comprises a TE element **1.0A** or **1.0B**, in turn, composed of:

- an n-type (negative thermopower and electron carriers) **1.1A** or **1.1B** semiconductor material, and
- a p-type (positive thermopower and hole carriers) **1.2A** or **1.2B** semiconductor material,

both inter-connected through highly electro-conductive (normally, made from copper) contact pads, on the one hand, **1.3A** or **1.3B,** and, on the other hand, a pair of pads: **1.41A and 1.42A,** or **1.41B and 1.42B**. Ceramic buses, on the one hand, **1.7A** and **1.7B**, or, on the other hand, **15A**, and **15.B** are usually made of aluminum oxide.

Fig. 1p Case (A) REFRIGERATION MODE illustrates the Peltier effect, which is the basis for many modern-day thermoelectric refrigeration devices, and **Fig. 1p Case (B) POWER GENERATION MODE** illustrates the Seebeck effect, which is the basis for TE power generation devices; both devices are with no moving parts. The refrigeration and power generation, both can be accomplished using the same TE module **1.0**.

In **Case (A) REFRIGERATION MODE**, thermoelectric energy conversion utilizes the heat using the Peltier-Seebeck Thermoelectric Element **1.0A**, wherein, due to the Peltier effect, when an electric current, generated by a source **1.6A** of direct current (DC) electromotive force (**emf**), circulates through the Peltier-Seebeck Thermoelectric Element **1.0A** where the DC direction is indicated by arrow **1.8A**, the temperature difference between the bus **ACTIVE COOLING 1.7A** and the bus **HEAT REJECTOR 1.5A** is originated such that the bus **ACTIVE COOLING 1.7A** becomes colder than the bus **HEAT REJECTOR 1.5A** and so the ambient heat, first, becomes absorbed on the cold side **1.7A** (i.e. on the bus **ACTIVE COOLING**), then, transferred through (or pumped by) the thermoelectric materials **1.1A** and **1.2A** to the bus **HEAT REJECTOR 1.5A**, and, further,

rejected at the sink (the bus **HEAT REJECTOR**) **1.5A**. Thereby, the cold side **1.7A** providing a refrigeration capability. In other words, the cold side **1.7A**, when becoming colder than the ambient fluid, extracts additional heat **1.91** from the ambient fluid and the TE element conveys and contributes the additional heat to the rejected heat **1.92A**. In practice, to function efficiently, a powerful ventilator **1.9A** is used to provide that the heat, accumulated at the bus **HEAT REJECTOR 1.5A**, transmitting away from the bus **HEAT REJECTOR 1.5A** for thermostating the bus **HEAT REJECTOR 1.5A** and so providing for cooling the bus **ACTIVE COOLING** making it colder than the ambient fluid. Normally, an airflow made by the powerful ventilator is slower than $10\,m/sec$. The presence of the ventilator **1.9A** reduces the advantage of the absence of moving parts. If, instead of the source **1.6A** of DC **emf**, to use a source of the DC **emf** of opposite polarity originating a DC in the opposite direction relative to the DC direction **1.8A**, the heat transfer becomes in the opposite direction as well.

In **Case (B) POWER GENERATION MODE**, the thermoelectric energy conversion occurs due to a passive Peltier-Seebeck thermoelectric element **1.0B** that utilizes the temperature difference ΔT between a heat source **1.7B** and heat sink **1.5B**. Namely, a DC **emf** is generated due to the Seebeck effect when the passive Peltier-Seebeck thermoelectric element **1.0B** utilizes the overabundant heat **1.92B** entrapped by a heat source **1.7B** (for instance, the heat source is powered by sunlight) while the heat passes through a thermoelectric materials **1.1B** and **1.2B**, and, further, is dissipated at the heat sink **1.5B** being colder than the heat source **1.7B**; the DC **emf** is manifested as a voltage bias induced at the pair of pads **1.41B** and **1.42B** and applied to an electrical load **1.6B** accompanied by DC the direction of which is indicated by arrow **1.8B**. If the load resistor **1.6B** is replaced with a voltmeter, the circuit functions as a temperature-sensing thermocouple. The advantages of TE solid-state energy conversion are compactness, quietness (no moving parts), and localized heating or cooling. However, speaking stricter, in practice, to function efficiently, a powerful ventilator **1.9B** is used to provide that the heat, accumulated at the bus **HEAT SINK 1.5B**, transmitting away from the bus **HEAT SINK 1.5B** for thermostating the bus **HEAT SINK 1.5B** and so making the bus **HEAT SOURCE** as functioning for absorbing the ambient heat. The presence of ventilator **1.9B** reduces the advantage of the absence of moving parts. If to use a source of coldness instead of the heat source **1.7B** and to use a cold sink instead of the heat sink **1.5B**, the originated DC **emf** will be manifested as a DC in the opposite direction relative to the DC direction **1.8B**.

Considering a thermoelectric element, the phenomena of:

- the Seebeck effect triggered by the temperature difference resulting in:

- the expected heat transfer from a hotter side to a colder side, and
- the seemingly-unexpected origination of electric current bringing electric power given free of charge in a certain sense, i.e. at the expense of the ambient heat,

and

- the Peltier effect triggered by the electric current resulting in:
  - the expected consumption of electric power, for instance, for Joule heating, and
  - the seemingly-unexpected decrease in entropy manifested as heat transfer from one side becoming colder to another side becoming hotter, wherein the decrease in entropy is given free of charge in a certain sense, i.e., again, at the expense of the ambient heat,

both are the property of thermoelectric materials contacted with the ambient fluid.

The basic interrelations between the physical characteristics of the Seebeck effect and the Peltier effect are expounded in **D02**. In particular, the current density $\boldsymbol{J}$ is directly-proportional to the temperature difference $\boldsymbol{\Delta T}$ between conductive contacts, on the one hand, **1.3A** or **1.3B**, and, on the one hand, the pads: **1.41A** and **1.42A** or the pads: **1.41B** and **1.42B**, correspondingly. Namely, the Seebeck effect generates an electromotive force, leading to the equation:

$$\boldsymbol{J = \sigma(-\Delta V - S\Delta T)} \qquad \boldsymbol{Eq.(1.4a),}$$

where: $\boldsymbol{\sigma}$ is the effective electric conductivity of the thermoelectric module as a whole;

$\boldsymbol{\Delta V}$ is the voltage bias between the pads **1.41B** and **1.42B**;

$\boldsymbol{\Delta T}$ is the mentioned temperature difference; and

$\boldsymbol{S}$ is the Seebeck coefficient, a property of the used material.

Peltier elements are thermoelectric components capable of pumping heat from one end of the device to the other end based on the direction of current, wherein the originated temperature is interrelated with the current according to the equation Eq. (1.4a) just rewritten as:

$$\boldsymbol{\Delta T = \frac{(-\Delta V - J/\sigma)}{S}} \qquad \boldsymbol{Eq.(1.4b).}$$

The interrelations *Eqs. (1.4a)* and *(1.4b)*, both being forms of the Joule law for an electric circuit comprising **emf**, quantify the phenomena of the Seebeck effect and the Peltier effect, correspondingly, in the assumption of a hypothetically ideal contact with the ambient fluid providing for accumulated heat removing away inertialessly, where the value $\boldsymbol{(-S\Delta T)}$ determines the **emf** of the electric circuit. In the case of the Seebeck effect described by the equation *Eq. (1.4a)*, when the two sides of the TE element are subjected to a forced temperature difference, the heat transfer from the hot side to the cold side accompanied by the

origination of the acquired DC **emf** looks seemingly contradicting to both the Energy Conservation Law and the Second Law of Thermodynamics, if to ignore that the DC **emf** of the TE element, as an open thermodynamic system, is triggered by the temperature difference and acquired at the expense of the ambient heat, i.e., from the point of view of the forced temperature difference, the DC **emf** is given free of charge (i.e. at the expense of the ambient heat) or, speaking stricter, is given due to the heat entering via a cold side and removing away from a hot side. In the case of the Peltier effect described by the equation *Eq. (1.4b)*, when the two sides of the TE element are subjected to a forced DC **emf**, a Joule heat dissipation, in particular, seemingly-confusingly accompanied by the temperature separation and so in the decrease in the entropy of a nearby fluid portion, looks like contradicting to both the Energy Conservation Law and the Second Law of Thermodynamics, if to ignore that the work for the temperature separation around the TE element (which is an open thermodynamic system) is triggered by the electric current and acquired at the expense of the ambient heat, i.e., from the point of view of the forced DC **emf**, the temperature separation is given free of charge (i.e. at the expense of the ambient heat) or, speaking stricter, is given due to the heat entering via the cold side and removing away from the hot side.

The thermoelectric element is neither:

- a Perpetuum Mobile of the first kind as the energy balance is satisfied when either:
  - the acquired DC **emf** is from the ambient heat; it is triggered by the temperature difference, or
  - the acquired temperature separation is at the expense of the ambient heat; it is triggered by DC **emf**,

  nor
- a Perpetuum Mobile of the second kind when is capable of decreasing the local entropy when either:
  - the heat transfer is triggered by the temperature difference and accompanied by the acquired DC **emf** manifested as the origination of the Joule heating effect, or
  - the acquired temperature separation triggered by the DC **emf** and accompanied by the work of DC **emf** manifested as the origination of the Joule heating effect,

as it is an open (but not isolated) system as the system inherently contacting with the ambient fluid wherein it is inherently assumed that the heat removing away.

In relation to the time-invariance, the interrelation *Eq. (1.4a)* between the temperature difference $\boldsymbol{\Delta T}$ as a reason and the current density $\boldsymbol{J}$ as an originated effect as well as the

interrelation *Eq. (1.4b)* between the current density $\boldsymbol{J}$ as a reason and the temperature difference $\boldsymbol{\Delta T}$ as an originated effect, both are time-invariant, i.e. the equations *Eqs. (1.4a)* and *(1.4b)* are equations of state interrelating the temperature difference and the current density at any time moment. In practice, the time-invariance of the equations *Eqs. (1.4a)* and *(1.4b)* is restricted by thermo-conductivity and thickness of the used thermo-conductive buses and an inertial ventilator functioning for the heat removing away. The inertial ventilator, in particular, results in another parasitic effect determined by that the temperature difference triggers the inertial heat transfer from the hot side to the cold side through the thermoelectric material that reduces the efficiency of both the Seebeck effect and the Peltier effect. The combination of all the effects results in that, in reality, the Peltier effect is manifested not as a suddenly arisen temperature difference $\boldsymbol{\Delta T}$ but as a growing temperature difference gradually reaching the value $\boldsymbol{\Delta T}$ of saturation after a certain time. The lower the inertness of the desired heat removing away, the higher the efficiency of the TE element.

Case (A) TIME CHARACTERISTIC comprises a graph **1.80A** extracted from **D03**. The graph **1.80A** illustrates a time characteristic of an exemplary single-stage thermoelectric cooler. The exemplary thermoelectric cooler produces a maximal temperature difference of about 51°C between its hot and cold sides [Typically, the reachable temperature difference $\boldsymbol{\Delta T}$, dependent on a value of DC **1.8A** and a quality of heat rejector **1.5A**, is 70°C]. An issue with performance is a direct consequence of one of their advantages: being small. The TE modules can be constructed ranging in size from approximately 2.5 to 50 mm with square shape and, if using either the so-called direct copper bond technology or the so-called active solder process, 2.5 – 5 mm in height, and if using Nano-technologies, 0.5 – 1 mm in height as described, for example, in **D04**. This means that:

- the hot side and the cool side will be very close to each other (a few millimeters away), making it easier for the heat to go back to the cool side, and harder to insulate the hot and cool side from each other; and
- a common 40 mm x 40 mm can generate 60 W or more, that is, 4W/cm² or more, requiring a powerful radiator to move the heat away.

The net-efficiency of the TE element depends on used thermoelectric material, a relevant property of which is characterized by the Seebeck coefficient and on the functionality of the powerful ventilator to remove the parasitic heat away from the cold side. From the point of view of the energy:

- the Peltier effect and the Seebeck effect, both given free of charge in a certain sense (if to exclude the power consumption by the powerful ventilator) due to a non-zero value $\boldsymbol{\sigma} \times \boldsymbol{S}$, and
- the energy consumption, in particular, goes for the parasitic Joule heating occurring due to the limited value $\boldsymbol{\sigma}$.

In real refrigeration applications, thermoelectric junctions have about 10-15% net-efficiency, because between 85% and 90% of the consumed energy goes to originate the Joule heating effect, which, normally, is unwanted and so the redundant heat must be removed using a ventilator. Due to this low efficiency, thermoelectric cooling is generally used in environments where the solid-state nature (no moving parts), low maintenance, compact size, and orientation insensitivity outweigh pure efficiency.

Had one possess a technology to implement and use the Seebeck-Peltier effect without a powerful ventilator, the net-efficiency would depend on the values $\boldsymbol{\sigma}$ and $\boldsymbol{S}$ characterizing the used thermoelectric material only, and a higher net-efficiency as the ratio of the power provided due to the Seebeck-Peltier effect given free of charge in the certain sense to the power consumed to trigger the Seebeck-Peltier. There is, therefore, a need in the art for a method and apparatus, when applied to a system appropriate for use in industry, to provide such an embodiment of the Peltier effect and/or the Seebeck effect that, on the one hand, would not require powerful ventilation and, on the other hand, would provide for a high net-efficiency and explicit relevance of all the mentioned possible advantages.

The curve **1.81A** shows that the temperature difference ΔT of 48^0C is reached in $240\ sec$, i.e. the average temperature rate is $0.2\ C/sec$. However, considering the first 20 seconds, the local temperature rate is $0.25\ C/sec$ which is indicated by the dotted line **1.82A**. Further, referring to the mentioned in **D04** TE modules made using Nano-technologies, the estimated local temperature rate is $1.25\ C/sec$ which is indicated by the dashed line **1.83A**. This, in particular, means that a very small temperature change, for instance, ranged from $5.4 \times 10^{-10}K$ to $5.4 \times 10^{-6}K$ can be reached for a short time ranged from $4.4 \times 10^{-6}sec$ to $4.4 \times 10^{-10}sec$, correspondingly. This estimation takes into account the parasitic inertia due to a normally used ventilator for transmitting the accumulated heat away. Looking ahead, for disclosed systems related to acoustic waves such that there will neither significant temperature differences nor accumulated heat in the disclosed systems, this estimation will be used as a reference for the worst-case estimations with a spare reserve. The fact that a small

temperature change can be reached for an extremely short time is one of the primary features that is used in the present patent application.

Furthermore, assuming a hypothetic possibility of extra-fast removing the accumulated heat away, the local temperature rate becomes dependent on the used material for the thermoconductive buses **1.3A** and **1.5A** in **Case (A)**, and **1.3B** and **1.5B** in **Case (B)**. For example, the thermoconductivity of aluminum oxide is between 28 and 35 $Wm^{-1}K^{-1}$, the thermoconductivity of copper is 384.1 $Wm^{-1}K^{-1}$, and the thermoconductivity of natural diamond is yet higher between 895 and 1350 $Wm^{-1}K^{-1}$. Referring to the commonly used copper pads **1.3A** and **1.41A** and aluminum oxide buses **1.7A** and **1.5A**, the estimated local temperature rate is about $3 \times 10^4\ C/sec$, i.e. the buses **1.7A, 1.3A, 1.41A,** and **1.5A**, each of 0.5 mm thickness, are almost inertialess indeed. Looking ahead, this estimation will be a reference for the estimation of applications related to extra-fast cooled surfaces. The possibility to reduce the reaction time of the TE module would allow for a specific use of the TE module to control a local temperature immediately without a significant delay, however, if the necessity of a powerful ventilator is avoided. The present patent application discloses such use of a TE module.

An advanced Peltier device comprises a multiplicity of TE elements which are electrically connected by conductive (for instance, copper) bridges in series as shown hereinafter in **Figs. 1q** and **1r**. Ceramic plates, usually made of aluminum oxide, are used to thermally bond the conductive bridges which are electrically separated each from other.

Reference is now made to **Fig. 1q**, divided between two parts: **Case (A)** and **Case (B)**, illustrating schematically a prior art TE multi-module device **1Q.0** comprising an array of TE elements; **wherein the numerals, which have the letter "A", belong to Case (A)** and the **numerals, which have the letter "B", belong to Case (B)**. The TE multi-module device **1Q.0** is built up of an array of the TE elements **1Q.0A1** or **1Q.0B1**, which are arranged electrically in series and thermally in parallel to manifest thermal properties in unison. From the point of view of functioning, the use of TE multi-module device **1Q.0** is considered in two cases:

- **Case (A)** where the TE multi-module device **1Q.0A** comprises a source **1Q.6A** of DC **emf** and an in-line cascade of several TE elements **1Q.0A1 [shown three]** that, from the electric point of view, are connected into a sequential electrical circuit and, from the constructive point of view, have a common bus of **ACTIVE COOLING** becoming colder and a common bus of **HEAT REJECTOR** becoming warmer when the source **1Q.6A** of DC **emf**

originates a voltage bias applied to the end pads: **1Q.41A** and **1Q.42A**, and an electric **CURRENT** indicated by arrow **1Q.8A;**

- **Case (B)** where the TE multi-module device **1Q.0B** comprises an electrical load **1Q.6B** and an in-line cascade of several TE elements **1Q.0B1 [shown three]** that, from the electric point of view, are connected into a sequential electrical circuit and, from the constructive point of view, have a common bus of **HEAT SOURCE** exposed to the overabundant ambient warmth and a common bus of **HEAT SINK** being colder than the bus of **HEAT SOURCE**; wherein, as a result, the sequentially connected TE elements **1Q.0B** provide for the cumulative electromotive force (**emf**) manifested as:
  - a voltage bias induced between the end pads: **1.41B** and **1.42B**, and applied to the electrical load **1Q.6B**, and
  - an induced electric **CURRENT** indicated by arrow **1Q.8B.**

Fig. 1r is a prior art schematic illustration of an exemplary planar arrangement **1R.0A** of a multiplicity of thermoelectric elements (modules) **1R.0A1** that (the planar arrangement **1R.0A**) is a quintessential component of a multi-layer TE multi-module device. Again, from the electric point of view, the TE elements **1R.0A1** are connected each to another in a boustrophedon trajectory, thereby, forming a sequential electrical circuit and, from the constructive point of view, the TE elements **1R.0A1** have contacts pads **1R.3A** at the cold side and contacts pads **1R.4A** at the warm side. There is but not shown both:

- a common bus of **ACTIVE COOLING** above the contacts pads **1R.3A**, and
- a common bus of **HEAT REJECTOR** under the contacts pads **1R.4A.**

When the source **1R.6A** of DC **emf** originates both:

- a voltage bias applied to the end pads: **1R.41A** and **1R.42A**, and
- an electric **CURRENT** indicated by arrow **1R.8A**,

the common bus of **ACTIVE COOLING** (again, that is not shown here) becomes colder and the common bus of **HEAT REJECTOR** (that is not shown here) becomes warmer.

Reference is now made to **Fig. 1t**, divided between two parts: **Case (A)** and **Case (B)**, illustrating schematically a prior art multi-layer TE multi-module device **1t.0** comprising a matrix of TE elements aggregated in layers one above another multi-stage repeatedly; wherein the **numerals having the letter "A" belong to Case (A) and the numerals having the letter "B"** belong to **Case (B)**. The multi-layer TE multi-module device **1t.0** is built up of a matrix of the elements **1t.0A1 or 1t.0B1**, which are arranged, on the one hand, electrically in series along a

boustrophedon trajectory and, on the other hand, in layers spatially cascaded one above another to cascade manifestations of the thermal properties multi-stage repeatedly in unison.

From the point of view of functioning, the use of multi-layer TE multi-module device **1t.0** is considered in two cases:

- **Case (A)** where the multi-layer TE multi-module device **1t.0A** comprises a source **1t.6A** of DC **emf** and a matrix of several TE elements **1t.0A1 [shown 9]**. When the source **1t.6A** of DC **emf** originates a voltage bias applied to the end pads: **1t.41A** and **1t.42A**, and an electric **CURRENT** indicated by arrow **1t.8A**, the TE elements **1t.0A1**:
  - from the electric point of view, are connected into a sequential electrical circuit along a boustrophedon trajectory, and,
  - from the constructive point of view, have common **EXTERNAL AND INTERNAL ACTIVE COOLING BUSES** becoming colder and common **EXTERNAL AND INTERNAL HEAT REJECTION BUSES** becoming warmer, wherein the common **INTERNAL ACTIVE COOLING BUSES** and the common **INTERNAL HEAT REJECTION BUSES** are arranged adjacently, thereby, in the final analysis, to transmit the warmth from the common **EXTERNAL ACTIVE COOLING BUS** to the common **EXTERNAL HEAT REJECTION BUS;**

  and
- **Case (B)** where the multi-layer TE multi-module device **1t.0B** comprises an electrical load **1t.6B** and a matrix of several TE elements **1t.0B1 [shown 9]**. From the electric point of view, the TE elements **1t.0B1** are connected into a sequential electrical circuit along a boustrophedon trajectory. From the constructive point of view, the TE elements **1t.0B1** have:
  - a common **EXTERNAL HEAT SOURCE BUS** exposed to the overabundant ambient warmth,
  - adjacently arranged **INTERNAL HEAT SINK BUSES** and **INTERNAL HEAT SOURCE BUSES**, and
  - a common **EXTERNAL HEAT SINK BUS** being colder than the common **EXTERNAL HEAT SOURCE BUS**.

  As a result, the multi-layer matrix **1t.0B** of TE elements **1t.0B1** provides for the cumulative electromotive force (**emf**) manifested as:
  - a voltage bias induced between the end pads: **1t.41B** and **1t.42B**, and applied to the electrical load **1t.6B**, and
  - an induced electric **CURRENT** indicated by arrow **1t.8B.**

As a sound propagating in the fluid is accompanied by oscillating changes: δP, $\delta \rho$, and δT, of thermodynamic parameters: the static pressure, mass density, and absolute temperature, correspondingly, of the fluid portions wherein the interrelation between the changes is inertialess, a controller of a source of the sound should be if not inertialess then at least almost inertialess to provide the desired frequency of oscillating changes. A thermoelectric device: either a thermocouple or a thermoelectric (TE) element, but rather than an electric heater, provides the desired requirement. For instance:

- in prior art document **A04**, a speaker based on the Joule heating effect is suggested; however, as the heating does not provide cooling in the direct sense, disadvantages of the use of an electric heater capable of varying heating at least are that the device is subjected to permanent heating, thereby, unwantedly changing the reference temperature value and unjustifiably exceeding consumption of the electric power,
- in prior art document **A05**, a Peltier element is used for sound or ultrasound generation, wherein:
    - as on the one hand, the Peltier element operation is accompanied by the unwanted Joule heating effect, the device is subjected to permanent heating, thereby, unwantedly changing the reference temperature value and unjustifiably exceeding consumption of the electric power,
    - as on the other hand, the Peltier element operation is accompanied by the unwanted Seebeck inverse-effect, the device is subjected to reduced efficiency of operation, again, unjustifiably exceeding consumption of the electric power, and
    - would the technology of the prior art be applied to sound detection using the Seebeck effect (it is not suggested in A05), the accompanying unwanted Peltier inverse-effect would reduce the net-efficiency of operation.

  Thereby, a device, which would combine all the Joule heating effect, the Peltier effect, and the Seebeck effect as to control a laminarity of fluid flow within a boundary layer near a curved surface as well as to boost a sound or ultrasound at the expense of ambient heat, were not disclosed;
- in prior art document **A06**, a suppressor comprising a pair of devices: a (classic) microphone plus an electric heater, is suggested, wherein neither a device based on the Peltier effect nor a device based on the Seebeck effect to use at least partially the ambient heat is disclosed for the purpose; moreover, the used two devices:

microphone and electric heater, can be located near each other but not at the same place that would be preferred for the claimed purpose, and alike, the Joule heating effect requires changing the reference temperature value; and

- in prior art document **A07**, an improved controller of hot and cold sides is suggested, wherein the improvement is achieved due to improvement of a heat-transfer within a thermoelectric element, however, a method for efficient removing of the unwantedly-accumulated heat was not disclosed.

Thus, the prior art documents **A04**, **A05**, **A06**, and **A07**, on the one hand, confirm the possibility of the use of thermoelectric devices to control the thermodynamic parameters of a portion of the ambient fluid, and, on the other hand, do not disclose further features that reduce the mentioned disadvantages and/or provide additional useful properties.

SUMMARY OF THE INVENTION

Unity and novelty of the invention

The unity and novelty of the invention are in a method and modified aerodynamic apparatuses: fluid pushers-off and/or fluid motion-sensors, which are geometrically shaped and supplied with built-in thermoelectric devices having sensor-controllers; wherein the thermoelectric devices are controlled by the sensor-controllers to provide for the spatial distribution of the temperature-dependent static pressure in ambient fluid around the modified aerodynamic apparatuses to result in pulling-in and/or pushing-off and/or motion detection of a portion of the ambient fluid; furthermore, the modified aerodynamic apparatuses are designed to operate in such a way as to exclude the necessity of a powerful ventilator, wherein the presence of the thermoelectric devices provides for improved and new functional properties of the fluid pushers-off and fluid motion-sensors.

Primary basic features of the present invention

The claims define the invention.

One of the primary features of the present invention is a method for:

- extra-fast removing of accumulated heat from a space adjacent to a thermoelectric device without a powerful ventilator,
- using thermoelectric elements, inertialess manipulation of the temperature difference between components of the modified aerodynamic apparatus – the fluid pusher-off;

- using thermoelectric elements, inertialess detection of a temperature difference between portions of ambient fluid moving adjacent to the modified aerodynamic apparatus – the fluid motion-sensor; and
- providing the improved and new functional properties of the modified aerodynamic apparatuses such that the modified aerodynamic apparatuses supplied with thermoelectric elements becoming functioning either as:
  - a highly-efficient source of acoustic waves (a fluid pusher-off as a motionless loudspeaker),
  - a highly-efficient detector of acoustic waves (a fluid motion-sensor as a motionless microphone),
  - a wireless charger based on ultrasound,
  - a modified convergent-divergent nozzle adapted to an acceleration of laminar flow,
  - a modified convergent-divergent nozzle adapted to an acceleration of a tiny portion of the fluid and thereby to boost a sound,
  - an airfoil wing capable of controlling a lift-force and thrust; and
  - an airfoil corpus which, when blown, contributes to lift-force and thrust.

In particular:

- In the matter of the modified convergent-divergent nozzle supplied with built-in a multiplicity of thermoelectric elements, the thermoelectric elements aggregated into a surface matrix a side of which has a thermoconductive bus aligned with a smoothly shaped tunnel to provide for triggering the Joule heating effect, the Seebeck effect, and the Peltier effect altogether allowing for controllably distributed temperature along the tunnel such to adapt a geometrical configuration of the tunnel to a velocity of fluid flow entering the tunnel, wherein the tunnel having a varying cross-sectional area characterized by a cross-sectional area profile function $A(x)$ of x interrelated with functions $u(x)$ and $T(x)$ of x representing profiles of the fluid flow's headway velocity and absolute temperature, correspondingly, along the tunnel length, wherein the multiplicity of the thermoelectric elements providing for a degree of freedom to interrelate the functions $A(x)$, $u(x)$, and $T(x)$ by the condition of flow continuity *Eq. (6.0)* expressed as:

$$A(x) = \frac{A_* \sqrt{(\gamma-1)RT(x)}}{u(x)} \left(\frac{2RT(x)+u^2(x)}{(\gamma+1)RT(x)} \right)^{\frac{\gamma+1}{2(\gamma-1)}} ,$$

where A_* is a constant, γ is an adiabatic compressibility parameter of the fluid flow, and R is a specific gas constant characterizing the fluid, wherein the functions $u(x)$ and $T(x)$ both are gradually-smoothed monotonic, wherein:

- the gradually-smoothed monotonic function of the absolute temperature $T(x)$ is determined by:
  - an absolute temperature T_{in} of the fluid flow at the open inlet,
  - temperature change $\delta T_0(x)$ interrelated with adiabatic compression-expansion occurred due to an adiabatic action of the Coanda-jet-effect, and/or the Venturi effect, and/or the de Laval jet-effect, all, in turn, determined by a curvature of the stationary geometrical configuration of the tunnel, and
  - forcedly established temperature contribution $\delta T_1(x)$ to the absolute temperature $T(x)$ along the boundary layers subjected to controllable heating and/or cooling action of the thermoelectric device, such that

$$T(x) = T_{in} + \delta T_0(x) + \delta T_1(x),$$

and

- the gradually-smoothed monotonic function of the headway velocity $u(x)$ is determined by the velocity u_{in} of the fluid flow at the open inlet, convective acceleration resulting in a velocity gradient along the tunnel length as the fluid flow is subjected to the adiabatic Coanda-jet-effect, and/or the Venturi effect, and/or the de Laval jet-effect, and controllable acceleration occurred due to controllable heating and/or cooling action of the thermoelectric devices.

thereby, the modified convergent-divergent nozzle is applicable to convey:

- in general, laminar flow to solve the problem of originated turbulence, and
- in particular, tiny portions of the fluid associated with the propagation of an acoustic wave to solve the problem of sound power dissipation;

note that:

- the degree of freedom $\delta T_1(x)$ to manipulate with the function $T(x)$ allows to adapt a tunnel having a smooth shape to a wide range of velocities of incoming fluid flow entering the tunnel; and
- the relatively fast fluid flow provides for conditions allowing to exclude using a powerful ventilator;

■ In the matter of a thermoelectric device functioning as the highly-efficient source of the acoustic waves (loudspeaker), on the one hand, the controlled temperature difference

between two opposite sides of the thermoelectric device and, on the other hand, the controlled temperature distribution along a divergent horn of the loudspeaker, both allow for efficient generation of acoustic waves accompanied by suppressed concomitant turbulence in the ambient fluid nearby the source of the acoustic waves; wherein the generation of acoustic waves is accompanied by a reincarnation of the heat radiated from a side of the thermoelectric device into the wave power which is removed away from the thermoelectric device by the originated acoustic waves propagating with the velocity of sound.

- In the matter of a thermoelectric device functioning as the highly-efficient detector and/or booster of acoustic waves, on the one hand, the controlled temperature difference between two opposite sides of the thermoelectric device, and, on the other hand, the controlled temperature distribution along a two-stage convergent-divergent phonendoscope, both allow for efficient detection and/or boosting of acoustic waves; and
- In the matter of the airfoil body: wing or capsule, supplied with built-in thermoelectric devices, the thermoelectric devices, aggregated into a surface matrix a side of which forms or at least is adjacently-aligned with a smoothly shaped surface of the airfoil body to control distributed temperature difference between opposite sides (for instance, upper and lower) of the airfoil body, provides for the desired distribution of static pressures in boundary layers adjacent the airfoil body thereby resulting in controllable lift-force and thrust.

Principal objects

Accordingly, it is a principal object of the present invention to overcome the limitations of existing methods and apparatuses for controlling the operation of aerodynamic devices such as wings and corpus of a flying vehicle, convergent-divergent nozzles, loudspeakers, and detectors of acoustic waves, all of a highly-efficient functionality.

BRIEF DESCRIPTION OF THE DRAWINGS

To understand the invention and to see how it may be carried out in practice, a preferred embodiment will now be described, by way of a non-limiting example only, referring to the accompanying drawings, in the drawings:

- **Of prior arts:**

  Fig. 1b is a schematic drawing of the convergent-divergent Venturi tube;

  Fig. 1c is a schematic view of the convergent-divergent de Laval nozzle;

  Fig. 1d is a schematic illustration graphics of gas velocity, static pressure, and temperature distributions within the de Laval convergent-divergent jet-nozzle;

Fig. 1f is a schematic drawing of a body blown by an airflow portion;

Fig. 1g is a schematic drawing of a classic prior art asymmetrical and mirror-symmetrical profiles of an airplane wing;

Fig. 1i is a schematic illustration of points of sail;

Fig. 1j is an illustration of a honeybee as an exemplary insect capable of flying;

Fig. 1k is a schematic illustration of a wind turbine, built-in into a cylinder;

Fig. 1n, composed of three parts: **Case (A)**, **Case (B)**, and **Case (C)**, comprises prior art schematic drawings of megaphones and a gramophone, each supplied by a horn;

Fig. 1L is a schematic drawing of a human ear profile in a sagittal plane;

Fig. 1o is a schematic drawing of a thermocouple;

Fig. 1p is a schematic drawing of a thermoelectric element;

Fig. 1q is a schematic drawing of a thermoelectric multi-module device;

Fig. 1r is an exemplary planar arrangement of thermoelectric elements;

Fig. 1t is a schematic drawing of a thermoelectric multi-module device;

and

- **Of embodiments, constructed according to the principles of the present invention:**

Fig. 5p is a schematic illustration of an elemental source and detector of sound;

Fig. 5q is a schematic illustration of a matrix of elemental sources and detectors of sound;

Fig. 5r is a schematic illustration of a multi-module thermoelectric device;

Fig. 5s is a schematic illustration of a two-stage sound amplifier;

Fig. 5t is a schematic illustration of a communication system;

Fig. 6a is a schematic illustration of an optimized convergent-divergent jet-nozzle;

Fig. 6b is a schematic illustration of an optimized inverse convergent-divergent nozzle;

Fig. 6c is a schematic illustration of a two-stage convergent-divergent jet-nozzle;

Fig. 7 shows comparative graphs of the dependencies of the nozzle extension ratio vs. the airflow M-velocity, calculated by the classical and suggested models;

Fig. 7a, composed of three parts: case **(A)**, case **(B)**, and case **(C)**, comprises schematic illustrations of sound boosters where: case **(A)** is a horn for a gramophone, case **(B)** is a phonendoscope, and case **(C)** is a hearing aid;

Fig. 7b is a schematic illustration of a compressor supplied by an optimized convergent-divergent jet-nozzle;

Fig. 7c is a schematic sectional view of a flying capsule;

Fig. 7d is a schematic sectional view of a flying capsule;

Fig. 8 is a schematic illustration of a symmetrical wing supplied with a TE device;

Fig. 8a is a schematic illustration of an actually-airfoil wing blown by the wind;

Fig. 8b is a schematic illustration of a flying airfoil body;

Fig. 8c is a schematic illustration of flying airfoil bodies;

Fig. 8d is a schematic illustration of two-stage airfoil wings;

Fig. 9a is a schematic illustration of a sequential cascade of airfoil bodies;

Fig. 9b is a schematic illustration of an in-line cascade of rings having airfoil walls;

Fig. 9c is a schematic illustration of two Archimedean screws having airfoil walls;

Fig. 9g is a schematic drawing of an improved wind-turbine;

Fig. 9h is a schematic side and front views of an improved wind-turbine;

Fig. 9j is a schematic illustration of a jet-ventilator;

Fig. 9k is a schematic illustration of a jet-propeller;

Fig. 9L is a schematic illustration of a multi-module jet-ventilator;

Fig. 9m is a schematic illustration of cascaded multi-module jet-propellers; and

Fig. 9n is a schematic illustration of a jet-transformer.

Fig. 9o is a schematic illustration of a levitating apparatus.

All the above and other characteristics and advantages of the invention will be further understood through the following illustrative and non-limitative description of preferred embodiments thereof.

DETAILED DESCRIPTION OF PREFERRED EMBODIMENTS

The principles and operation of a method and an apparatus according to the present invention may be better understood referring to the drawings and the accompanying description, it being understood that these drawings are given for illustrative purposes only and are not meant to be limiting.

Preface

The jet-effect occurring in moving fluid can be manifested as:

- the Venturi effect and the de Laval jet-effect resulting in either:
  - convective self-acceleration accompanied by self-cooling, or
  - self-retarding accompanying by self-warming,

  when a portion of the headway moving fluid is subjected to a reshaping;
- the Coanda-effect resulting in both:
  - lift-force acting on a profiled wing, and
  - thrust-force acting on a sail oriented as so-**called "B-Point of Sail"**;

  when a convexly-curved surface is tangentially blown by a headwind; and

- the waving jet-effect resulting in both:
  - acoustic wave (audible sound or ultrasound) origination, and
  - conveying of a tiny portion of fluid transmitting wave energy away along the direction of the acoustic wave propagation;

when a portion of the fluid is subjected to oscillating change in static pressure;

wherein these are manifestations of the jet-effect defined as an effect of transformation of the heat power into the kinetic power of fluid motion as a whole and, vice-versa, an effect of transformation of the kinetic power of fluid motion as a whole into the heat power. Further, the **DETAILED DESCRIPTION OF THE PREFERRED EMBODIMENTS** is divided between two paragraphs: **"Conceptual Idea" and "Embodiments", each having sub**-paragraphs.

Conceptual Idea

Prerequisites:

■ On the one hand, an inertialess controller is required; namely, in general, as a fluid flow acceleration is accompanied by varying thermodynamic parameters of portions of the fluid wherein the interrelation between the varying thermodynamic parameters is inertialess, control of the fluid flow should be if not inertialess then at least almost inertialess to provide the desired control of the thermodynamic parameters efficiently; and, in particular,

- as the Coanda-effect, that manifested by pulling-in the fluid portions forming a boundary layer and causing a lift-force, is accompanied by changes in thermodynamic parameters of the fluid portions wherein the interrelation between the changes is inertialess, a controller of the changes should be if not inertialess then at least almost inertialess to provide the desired boundary layer and lift-force;
- as the Venturi effect and the de Laval effect, both accompanied by **the fluid portions'** reshaping and inertialessly interrelated changes in thermodynamic parameters, again, a controller of the changes should be if not inertialess then at least almost inertialess to provide the desired thermodynamic parameters meeting the conditions of flow laminarity;
- as the upward-vectored lift-force is the property of the ambient-adjacent boundary layer, likewise, a controller of the changes in the thermodynamic properties of the ambient-adjacent boundary layer should be if not inertialess then at least almost inertialess to provide the desired property of the ambient-adjacent boundary layer; and
- as a sound propagating in the fluid is accompanied by oscillating changes: δP, $\delta \rho$, and δT, of thermodynamic parameters: the static pressure, mass density, and absolute temperature, correspondingly, of the fluid portions wherein the interrelation between the changes is inertialess,

alike, a controller of a source of the sound should be if not inertialess then at least almost inertialess to provide the desired frequency of oscillating changes; and

- On the other hand, an almost inertialess thermoelectric device having no moving parts can be used; namely, considering a thermoelectric (TE) device based on the Peltier effect, the almost inertialess interrelation between the current density $\boldsymbol{J}$ and the temperature difference $\boldsymbol{\Delta T}$, at least when removing the accumulated heat away is extra-fast and/or when the desired temperature difference $\boldsymbol{\Delta T}$ is extremely small, makes using the TE device (optionally made using Nano-technologies from a thermoelectric material of high quality) promising, in general, to control the changes of the thermodynamic parameters of the moving fluid, and, in particular, to:
  - create and control the lift-force; wherein, taking into attention that the TE device does not have moving parts, the using of the TE device allows to create and control the lift-force without the creation of undesired turbulence, and thereby, to create and control the lift-force much more efficiently than using wings supplied with moving flaps;
  - create and control laminarity of a flow within a convergent-divergent nozzle: either a Venturi pipe or a de Laval tube; wherein, taking into attention that the TE device does not have moving parts, the using of the TE device allows smoothing the distributed static pressure to suppress so-called Mach waves and thereby to control the laminarity; and
  - create, detect, and suppress the acoustic waves; wherein, as the TE device does not have moving parts, the using of the TE device allows creating the acoustic waves without the creation of undesired turbulence, and thereby, to launch and detect the acoustic waves (sound or ultrasound) much more efficiently than using classical speakers and microphones, correspondingly, which are supplied with a moving membrane.

Essence Of Concept

Thus, the conceptual idea of the present invention is in the use of a thermoelectric device to:

- control gradients of thermodynamic parameters of flow along a convergent-divergent nozzle: either a Venturi pipe or a de Laval tube;
- create a pressure difference between the upper and lower sides of an airfoil body (for instance, a wing) to originate and control lift-force;
- create a pressure difference between anterior and tail parts of an airfoil body to originate and control thrust;

- create the oscillating changes: δP, $\delta \rho$, and δT, of thermodynamic parameters: the static pressure, mass density, and absolute temperature, correspondingly, of a portion of the fluid, to pull-in and push-off the fluid portion, and, thereby, to create acoustic waves much more efficiently than using a standard speaker having a moving membrane; and, vice-versa,
- detect and/or suppress the oscillating changes: δP, $\delta \rho$, and δT, of thermodynamic parameters: the static pressure, mass density, and absolute temperature, correspondingly, of a portion of the fluid, and thereby to detect and/or suppress the acoustic waves much more efficiently than using a standard microphone having a moving membrane.

The conceptual idea, being one of the primary features of the present invention, lies in the basis of the disclosed method and aerodynamic apparatuses (fluid pushers-off and fluid motion-sensors) for the creation and controlling of lift-force and thrust and for the creation and detection of sound.

Embodiments

Elemental TE Device As Source Of Sound

Fig. 5p, composed of three parts: **Case (A) SOUND LAUNCHING MODE**, **Case (B) SOUND DETECTION MODE**, and **Case (C) GENERAL MODE**, is a schematic illustration of an elemental acoustic thermoelectric device **5P.0**, capable of functioning in three controllable modes: **"A"**, to originate temperature difference between two buses **5P.7A** and **5P.5A** using the Peltier effect and, **"B"**, vice versa, to detect the temperature difference between two buses **5P.7B** and **5P.5B** using the Seebeck effect, as well as **"C"** assuming simultaneous functioning of the modes **"A"** and **"B"**. Thus, in contrast to the standard use of a TE element, it is assumed to use the elemental acoustic thermoelectric device **5P.0** operating in the mode: **"C"**, which provides for improving in net-efficiency as described hereinbelow referring to **Fig. 5p Case (C) GENERAL MODE**. All the modes assume excluding the necessity of a normally-used ventilator.

The mode **"A"** is a case of forced controlling the temperature and thereby the static pressure of a portion of the ambient fluid, wherein the changes in temperature and static pressure are mutually-interrelated according to the equations $Eq.(1.1b)$ and $Eq.(1.3c)$. The mode of forced-varying temperature assumes that the varying of the temperature and thereby the static pressure of the portion of the ambient fluid is periodically alternating, i.e. increasing and decreasing the static pressure that, in turn, indicates to generating an elastic (acoustic) wave propagating in the ambient fluid. The mode **"A"** is concretized as **Case (A) SOUND LAUNCHING MODE**. The feature is that the acoustic wave permanently transmits the wave energy

away from the source in the direction of the Umov-vector collinear with the direction of the acoustic wave propagation. Thus, the elemental acoustic thermoelectric device **5P.0** operating in the mode **"A"** becomes interpreted as an aerodynamic apparatus – a fluid pusher-off, which is pulling-in and pushing-off a portion of the fluid and, thereby, is capable of triggering the conveying motion of a tiny portion of the ambient fluid (the conveying motion associated with the acoustic wave propagation), wherein the necessity of a powerful ventilator is excluded.

The mode **"B"** is a case of detecting the periodically alternating temperature changes of a portion of the ambient fluid. Again, the varying static pressure of the portion of the ambient fluid is interpreted as an indication of the presence of an elastic wave. So, the elemental acoustic thermoelectric device **5P.0** operating in the mode **"B"** becomes interpreted as an aerodynamic apparatus – a fluid motion-sensor, and the mode **"B"** is concretized as **Case (B) SOUND DETECTION MODE**.

Thus, the elemental acoustic thermoelectric device **5P.0**, called an **ELEMENTAL SOURCE AND DETECTOR OF SOUND**, constructed according to the principles of the present invention, is an aerodynamic apparatus: a fluid pusher-off and/or a fluid motion-sensor, capable of operation in the two modes: **Case (A) SOUND LAUNCHING MODE** and **Case (B) SOUND DETECTION MODE**, as either an **ELEMENTAL SOURCE OF SOUND 5P.0A** or an **ELEMENTAL DETECTOR OF SOUND 5P.0B**, correspondingly. Moreover, in **Case (C) GENERAL MODE**, the elemental acoustic thermoelectric device **5P.0** is capable of operation in both mentioned modes combined simultaneously.

From the point of view of construction, the two cases: **Case (A) SOUND LAUNCHING MODE** and **Case (B) SOUND DETECTION MODE**, differ as follows:

- In the **Case (A) SOUND LAUNCHING MODE**, an **ELEMENTAL SOURCE OF SOUND 5P.0A** comprises a TE element **5P.A** supplied with an individual controller **5P.8A** connected between the connection points **5P.61A** and **5P.62A** and comprising an integrated circuit (IC) **5P.81A** and a manipulatable source of **emf 5P.82A**, wherein two opposite sides of the TE element **5P.A** comprise, on the one side, an **ACTIVE COOLING AND HEATING BUS 5P.7A** and, on the other side, a **HEAT AND COLDNESS REJECTION BUS 5P.5A**, both merged in the ambient fluid and wherein the manipulations in the polarity of the source of **emf 5P.82A** are periodically oscillating such that the originated oscillating temperature differences between the two opposite sides interrelated with whereby originated oscillating pressure differences are regarded as indicators of the presence of an acoustic wave propagating and transmitting the heat energy away from the **ELEMENTAL SOURCE OF SOUND 5P.0A** as the wave energy, and hence preventing the heat accumulation near the **ELEMENTAL SOURCE OF SOUND 5P.0A**;

and

- In the **Case (B) SOUND DETECTION MODE,** an **ELEMENTAL DETECTOR OF SOUND 5P.0B** comprises a TE element **5P.B** supplied with an individual controller-sensor **IC DETECTOR 5P.8B** comprising an integrated circuit (IC) and a detector of an induced varying electric current [for instance, alternating current (AC)] originated by the TE element **5P.B** when a **HEAT AND COLDNESS SOURCE BUS 5P.7B** is exposed to ambient fluid and subjected to impacting acoustic wave characterized by varying heating and cooling of a tiny portion of the ambient fluid adjacent the **HEAT AND COLDNESS SOURCE BUS 5P.7B**, wherein the varying heating and cooling are manifested as periodically oscillating pressure and temperature, wherein, as the acoustic wave prevents the heat accumulation near the **ELEMENTAL DETECTOR OF SOUND 5P.0B**, one does not need in forcible thermostating the **ELEMENTAL DETECTOR OF SOUND 5P.0B**;

The inventor points out, again, that, the thermoelectric elements: **5P.A** and **5P.B**, as well as the thermoelectric elements **1.0** (**1.0A** and **1.0B**) described hereinabove in **THE BACKGROUND OF THE INVENTION** referring to **Fig. 1p**, are characterized by the time-invariant interrelation between the current density J and the temperature difference ΔT. On the other hand, the time-invariance allows implementing the elemental acoustic thermoelectric devices **5P.0**: an **ELEMENTAL SOURCE OF SOUND 5P.0A, ELEMENTAL DETECTOR OF SOUND 5P.0B**, and an elemental acoustic TE device **5P.0C** operating in general mode, such that:

- in the **Case (A) SOUND LAUNCHING MODE**, the **ELEMENTAL SOURCE OF SOUND 5P.0A** functioning in the **SOUND LAUNCHING MODE** differs from TE element **1.0A** (**Fig. 1p Case (A) REFRIGERATION MODE**) functioning in the **REFRIGERATION MODE** and normally supplied with the ventilator **1.9A** by that the source **1.6A** of DC **emf** and the ventilator **1.9A**, altogether are now replaced by an individual controller **5P.8A** having the integrated circuit **IC 5P.81A** and the manipulatable source of **emf 5P.82A** controlled by the integrated circuit **IC 5P.81A** such that the manipulatable source of **emf 5P.82A** is capable of generating an alternating **emf** of a frequency f in the range of frequencies of the audible sound and ultrasound, i.e. from 20 Hz and lower to 20 kHz and higher; wherein, optionally, the individual controller **5P.8A** can be implemented as a block **5P.80A** of an electric scheme supplied by a transformer which, exemplary and without loss of generality, is shown as as a tee bias **5P.86A** composed of a capacitor and inductive component, fitted to the alternating current and voltage. The transformer, in particular, implemented as tee bias **5P.86A**,
  - on the one hand, is connected to the metallic electrical contact pads **5P.41A** and **5P.42A** of an n-type (negative thermopower and electron carriers) semiconductor

material **5P.1A** and of a p-type (positive thermopower and hole carriers) semiconductor material **5P.2A**, correspondingly, and

- on the other hand, is connected to the generator of alternating current and voltage **5P.820A**, which is manipulatable by an individual integrated circuit **IC 5P.810A**,

to separate the AC generated by the generator **5P.820A** and the varying electric current, in general, AC+DC, induced in the circuit of the TE element **5P.A** (the DC component can become induced because of possibly-asymmetry of the elemental TE device **5P.0A**); wherein, referring to exemplary TE modules, made using Nano-technologies, characterized by the estimated local temperature rate is $1.25\ C/sec$ the estimated local temperature rate is $1.25\ C/sec$ as described hereinabove in **THE BACKGROUND OF THE INVENTION** referring to **Fig. 1p Case (A) TIME CHARACTERISTIC** and citing **D04**, the estimations of reachable SPL for audible sound are as follows:

- when 20 Hz sound is required, half of the time-period allowing for the temperature oscillation is $0.5 \times \tau_{20Hz} = 0.025\ sec$ and the reachable amplitude of the temperature difference is approximately $0.03K$ that corresponds to SPL=SDL=STL level of $155\ dB$;
- when 20 kHz sound is required, half of the time-period allowing for the temperature oscillation is $0.5 \times \tau_{20kHz} = 2.5 \times 10^{-5}\ sec$ and the reachable amplitude of the temperature difference is, approximately, $3 \times 10^{-5}\ K$ that corresponds to SPL=SDL=STL level of $95\ dB$;

The investor points out that the estimation is the worst-case estimation made with a spare reserve because the generated sound transmits the heat and coolness away with the velocity of sound in the ambient fluid, i.e., on the one hand, one does not need to use a ventilator for the heat removing (note, the gusty-choppy operating ventilator would not allow to generate so precise temperature differences), and, on the other hand, the not accumulated heat provides for desired inertialess of the thermoelectric element functioning. In other words, the SPL, much higher than the worst-case estimated $95\ dB$, is reachable. Thus, in any case, the reachable SPL is much higher than the usually used SPL between 0 to $80\ dB$, and so the **ELEMENTAL SOURCE OF SOUND 5P.0A** is capable to launch acoustic waves as audible sound **5P.91A** and **5P.92A**, launched from the **ACTIVE COOLING AND HEATING BUS 5P.A** and the **HEAT AND COLDNESS REJECTION BUS 5P.5A**, correspondingly, wherein the launched acoustic waves **5P.92A** differ from the launches acoustic waves **5P.91A** in phase on 180^0. It further will be evident for a commonly

educated person that the alternating current generated by the generator **5P.820A** results in the origination and radiation of an electromagnetic wave characterized by the frequency f of the current alternation;

- in the **Case (B) SOUND DETECTION MODE**, the **ELEMENTAL DETECTOR OF SOUND 5P.0B** functioning in the **SOUND DETECTION MODE** differs from TE element **1.0B** functioning in the **POWER GENERATION MODE** and normally supplied with the ventilator **1.9B** by that the load **1.6B** (**Fig. 1p Case (B) POWER GENERATION MODE**) and the ventilator **1.9B**, altogether are now replaced by an individual integrated circuit sensor-controller **IC DETECTOR 5P.8B** capable of detection AC originated by acoustic wave **5P.91B** impacting the **HEAT AND COLDNESS SOURCE BUS 5P.7B** which, as a result, becomes subjected to alternating heating and cooling accompanying by the origination of alternating electric current. Again, optionally, the connection of the individual integrated circuit **IC DETECTOR 5P.8B** to the TE element **5P.B** can be implemented using a transformer, which, exemplary and without loss of generality, is shown as a tee bias **5P.86B** fitted to the induced alternating electric current and voltage wherein the transformer (tee bias) **5P.86B**:
  - on the one hand, is connected to the metallic electrical contact pads **5P.41B** and **5P.42B** of an n-type (negative thermopower and electron carriers) semiconductor material **5P.1B** and a p-type (positive thermopower and hole carriers) semiconductor material **5P.2B**, correspondingly, and
  - on the other hand, is connected to the individual integrated circuit **IC DETECTOR 5P.810B**,

  to separate the AC+DC generated by the TE element **5P.B** and the AC induced in the individual integrated circuit **IC DETECTOR 5P.80B**. It further will be evident for a commonly educated person that the induced alternating electric current originated in the thermoelectric element **5P.B**, on the one hand, can be registered and/or recorded by any classic method, and on the other hand, results in the origination and radiation of an electromagnetic wave characterized by the frequency f of the induced current alternation that, in turn, can be detected using an RF receiving antenna; and
- in **Case (C) GENERAL MODE**, the elemental acoustic thermoelectric device **5P.0** having a TE element **5P.C**, now operating in the general mode as device **5P.0C**, is capable of operation in both mentioned modes: **SOUND LAUNCHING MODE** and **SOUND DETECTION MODE**, and control AC and DC simultaneously. For this purpose, the integrated circuit **5P.8C** comprises the transformer (tee bias) **5P.86C** separating AC and DC, such that the AC is generated or detected by the integrated circuit **IC 5P.82C** comprising both generator

and detector of alternating current, while DC is controlled by the integrated circuit **IC 5P.9C** such that

- the Peltier-DC current **5P.98C** is controllably generated by the **emf 5P.92C** manipulated by the integrated circuit **IC-PELTIER 5P.93C**, and
- the Seebeck-DC current **5P.94C** is controllably charging the chargeable **emf 5P.95C** (for example, a capacitor) controlled by the integrated circuit **IC-SEEBECK 5P.96C**;

wherein the Peltier-DC **5P.98C** and the Seebeck-DC current **5P.94C** are filtered using a set of diodes **5P.97C**. In practice, the fluid pusher-off has two opposite sides: face (first) **5P.7C** and back (second) **5P.5C**, which are not symmetrical from the point of view of the mechanic, temperature, and electric aspects. Normally, the accompanying Joule heating effect is not completely symmetrical heats the two opposite sides: face and back, because of different reasons, for instance, not identical electric impedance and not identical boundary conditions from the point of view of ambient temperature and heat removing. For the sake of concretization and without loss of generalization, consider the face side **5P.7C** being colder than the back side **5P.5C**. To compensate for the undesired asymmetry of the opposite sides of the elemental acoustic thermoelectric device **5P.0**, the Peltier effect is triggered in two styles: alternating and constant, wherein the constant Peltier-DC **5P.98C** allows compensating the asymmetry of the Joule heating and/or the undesired Joule heating effect at the face side. As well, in **Case (B) SOUND DETECTION MODE**, as the primarily-desired function of the **Case (C) GENERAL MODE**, the Seebeck effect may have two components: varying, manifested as an alternating current (AC), and direct, manifested as the Seebeck-DC **5P.94C**. The Seebeck-DC **5P.94C** can be used for charging a chargeable battery **5P.95C** or can be compensated by controllably-triggering the Peltier effect. Moreover, as the net-efficiency of the thermoelectric junctions (usually, about 15%) is partially determined by the undesired back thermoelectric effect which is either the Seebeck effect when the Peltier effect is primarily-desired or the Peltier effect when the Seebeck effect is primarily-desired, a sensor-controller including integrated circuits **5P.82C**, **5P.93C**, **5P.96C**, and the set of diodes **5P.97C** is used to make the back thermoelectric effect useful by separating the Peltier-DC and Seebeck-DC thereby providing for increasing the useful net-efficiency, as a charge acquired by the chargeable **emf 5P.95C** can be used. It will be evident for a commonly educated person that a capacitor and an inductive component of tee bias **5P.86C** can be controlled to vary proportion between the alternating and unidirectional components of the electric current. In

particular, when the tee bias is characterized by extremely small capacity and inductivity, both electric currents: the Peltier-DC and the Seebeck-DC, are not constant but varying, wherein each of the electric currents remains either positive or negative. As well, it will be evident for a commonly educated person that the directivity of diodes **5P.97C** can be controllably-manipulatable and the integrated circuits IC-Seebeck **5P.95C** and IC-Peltier **5P.952** can play the inversed role such that to redirect the Peltier-DC and Seebeck-DC.

As a consequence, from the point of view of functioning, the three cases: **(A)**, **(B)**, and **(C)**, differ as follows:

- In **Case (A) SOUND LAUNCHING MODE,** an **ELEMENTAL SOURCE OF SOUND 5P.0A** is capable of operation in a **SOUND LAUNCHING MODE** providing for audible sound and ultrasound launching; and, vice-versa,
- In **Case (B) SOUND DETECTION MODE,** an **ELEMENTAL DETECTOR OF SOUND 5P.0B** is capable of functioning in a **SOUND DETECTION MODE** providing for audible sound and ultrasound detection; and
- In **Case (C) GENERAL MODE,** the elemental acoustic thermoelectric device **5P.0C**, is capable of functioning in both the **SOUND LAUNCHING MODE** and the **SOUND DETECTION MODE** simultaneously, thereby, allowing for a style providing for a higher net-efficiency of the operation.

In view of the foregoing description referring to **Fig. 5p**, it will be evident for a commonly educated person that:

- In Relation To Accompanying Electro-Magnetic Waves,
  - When operating in the sound launching mode, the **ELEMENTAL SOURCE OF SOUND 5P.0A** radiates electromagnetic waves of the same frequency as the frequency of the launched acoustic waves; in other words, the metallic electrical contact pad **5P.3A** of the **ELEMENTAL SOURCE OF SOUND 5P.0A** operates as a transmitting antenna of electromagnetic waves,
  - If the **ELEMENTAL SOURCE AND DETECTOR OF SOUND 5P.0** is exposed to an electromagnetic wave of a certain frequency in the range between 20 Hz and 20 kHz (or higher), then the metallic electrical contact pad **5P.3A**, as a receiving antenna detecting the electromagnetic wave, plays the role of the generator of alternating electric current or voltage **5P.820A** providing the **emf** resulting in the generation of an acoustic wave (audible or ultrasound) of the same certain frequency; and

- If the **ELEMENTAL DETECTOR OF SOUND 5P.0B** is exposed to an acoustic wave of a certain frequency, the metallic electrical contact pad **5P.3B** radiates an electromagnetic wave of the same certain frequency and so plays the role of a transmitting antenna allowing to detect the presence of sound using a sensor of electromagnetic waves wirelessly;

■ In Relation To The Reversibility Of The **ELEMENTAL SOURCE AND DETECTOR OF SOUND,**

If the manipulatable source of **emf 5P.82A** is shunted and the integrated circuit **IC 5P.81A** provides for the functionality of the individual integrated circuit **IC DETECTOR 5P.8B**, the **ELEMENTAL SOURCE OF SOUND 5P.0A** can be adapted to function as the **ELEMENTAL DETECTOR OF SOUND 5P.0B** in the **Case (B) SOUND DETECTION MODE.** This allows using the TE element **5P.A** for operation as both:

- a source of sound when functioning in the sound launching mode, and
- a detector of sound when functioning in the sound detection mode;

and

■ In Relation To Phase-Inverter,

In the detection mode, the opposite sides **HEAT AND COLDNESS SOURCE BUS 5P.7B** and **HEAT AND COLD SINK BUS 5P.5B**, both become heated and cooled alternatingly with the frequency f equal to the frequency of the impacting sound, wherein the phase of the temperature changes adjacent to the **HEAT AND COLD SINK BUS 5P.5B** differs from the phase of the temperature changes adjacent the **HEAT AND COLDNESS SOURCE BUS 5P.7B** on 180^0. This, in particular, means that the TE element **5P.B** functions as a phase-inverter which receives the acoustic wave **5P.91B** impacting the **HEAT AND COLDNESS SOURCE BUS 5P.7B** and launches the acoustic wave **5P.92B** propagating away from the **HEAT AND COLD SINK BUS 5P.5B**, wherein the phase of the launched acoustic wave **5P.92B** differs from the phase of the received acoustic wave **5P.91B** on 180^0. It will be evident for a commonly educated person, that if now the individual integrated circuit **IC DETECTOR 5P.8B** is supplied by an amplifier providing for increasing an induced electric current, the TE element **5P.B** becomes capable of functioning as an amplifier of acoustic waves which receives the acoustic wave **5P.91B** impacting the **HEAT AND COLDNESS SOURCE BUS 5P.7B** and launches the amplified acoustic wave **5P.92B** propagating away from the **HEAT AND COLD SINK BUS 5P.5B**, wherein the phase of the launched acoustic wave **5P.92B** differs from the phase of the received acoustic wave **5P.91B** on 180^0.

Multi-Module Matrix Device

Fig. 5q, composed of two parts: **(A)** and **(B)**, is a schematic illustration of components of a multi-module thermoelectric device.

The inventor points out, that, taking into account the foregoing description of **THE BACKGROUND OF THE INVENTION** referring to **Figs. 1c** and **1d**, it will be evident for a commonly educated person that a **MULTI-MODULE SOURCE AND DETECTOR OF SOUND** is feasible by aggregating a multiplicity of the **ELEMENTAL SOURCES OF SOUND 5P.0A** and **ELEMENTAL DETECTORS OF SOUND 5P.0B** such that the **ELEMENTAL SOURCES OF SOUND 5P.0A** and **ELEMENTAL DETECTORS OF SOUND 5P.0B** are connected into a sequential electric scheme and arranged to create and detect, correspondingly, the changes of the thermodynamic parameters of the ambient fluid in unison.

In view of the foregoing description of the elemental acoustic thermoelectric devices **5P.0**, capable of functioning in two controllable modes: **"A"**, to originate temperature difference between two buses **5P.7A** and **5P.5A** using the Peltier effect and, **"B"**, vice versa, to detect the temperature difference between two buses **5P.7B** and **5P.5B** using the Seebeck effect, as well as **"C"** (**GENERAL MODE**) assuming a simultaneous use of the Peltier effect and the Seebeck effect, both as useful effects, it will be evident to a commonly educated person that the elemental acoustic thermoelectric device **5P.0** can be utilized as a combined both a microphone and speaker being placed at the same location and functioning simultaneously. This advantage over a prior art device for sound or ultrasound generation of **A05** provides additional degrees of freedom to implement useful, compact, and efficient devices.

Moreover, an arrangement of the **ELEMENTAL SOURCES OF SOUND 5P.0A** and **ELEMENTAL DETECTORS OF SOUND 5P.0B** as well as the devices **5P.0C** operating in **GENERAL MODE** can be more sophisticated.

Fig. 5q (A) is a schematic isometry illustration of a fragment of planar arrangement **5Q.MATRIX** of elemental thermoelectric elements **5Q.01**, arranged in a plane (X, Y) in a system of coordinates (X, Y, Z) **5Q.0** and electrically mutually isolated.

Fig. 5q (B) is a schematic illustration of a cross-sectional cut of a multi-module thermoelectric device **5Q.DEVICE**, called **MATRIX SOURCE AND/OR DETECTOR OF SOUND**, constructed according to the principles of the present invention.

The device **MATRIX SOURCE AND/OR DETECTOR OF SOUND 5Q.DEVICE** is composed of a multiplicity of $N = N_x \times N_y$ elemental TE devices **5Q.02**, where N_x and N_y are numbers of the TE devices **5Q.02** arranged along the axes X and Y, correspondingly. Each of the N elemental TE devices **5Q.02** is similar to the elemental TE device **5P.0** functioning as an

ELEMENTAL SOURCE AND/OR DETECTOR OF SOUND as described hereinabove in the subparagraph "In Relation To Phase-Inverter" **referring to Fig. 5p.** The $N_x \times N_y$ elemental TE devices **5Q.02** are arranged in a plane (X, Y) in a system of coordinates (X, Y, Z) **5Q.0**, electrically mutually isolated, and have individual thermo-conductive buses, i.e. each of the $N_x \times N_y$ elemental TE devices **5Q.02** has individual both controller **5Q.08** and thermo-conductive bus **5Q.05** to be controlled individually. Each of the controllers **5Q.08** comprises an individual integrated circuit **IC 5Q.81**, a manipulatable source of **emf** (for instance, a generator of alternating electric current and voltage) **5Q.82**, anda transformer (tee bias) which is built-in in **IC 5Q.81** and not shown here separately but described hereinabove referring to **Fig. 5p**. For the sake of simplicity of the schematic illustration:

- An arrangement along the axis X is shown only; and
- Points **5Q.03** symbolize that each of the numbers N_x and N_y can be much greater than shown.

Wherein:

- Each of the $N_x \times N_y$ elemental TE devices **5Q.02** is the **ELEMENTAL SOURCE OR DETECTOR OF SOUND 5P.0A** or **5P.0B** or **5P.0C** described hereinabove with the reference to **Fig. 5p Case (A) SOUND LAUNCHING MODE** or **Fig. 5p Case (B) SOUND DETECTION MODE** or **Fig. 5p Case (C) GENERAL MODE**, correspondingly; and
- Each of the $N_x \times N_y$ individual integrated circuits **IC 5Q.81**, is individually controlled by a common controller-dispatcher **5Q.04**.

In the launching mode, elemental acoustic waves, launched by the individually controlled $N_x \times N_y$ **ELEMENTAL SOURCES OF SOUND 5Q.02** of the device **MATRIX SOURCE AND/OR DETECTOR OF SOUND 5Q.DEVICE** can differ in amplitude, phase, frequency, and delay, all controlled by the common controller-dispatcher **5Q.04**. Thereby, the desired spatial interference map associated with the resulting acoustic wave composed of the elemental acoustic waves is feasible. Namely, a well-known technique "phased array" can be applied to the elemental acoustic waves when using the matrix of the multiplicity of $N_x \times N_y$ **ELEMENTAL SOURCES OF SOUND 5Q.02**. In contrast to the prior art device for sound or ultrasound generation of **A05**, the multi-module thermoelectric device **5Q.DEVICE**, each of the individual TE devices **5Q.02** of which is capable of functioning in three modes: launching elastic waves, detecting temperature changes, and in general mode allowing for creation and detection of temperature changes simultaneously, is characterized by a degree of freedom to apply the phased array principle

providing for additional specific properties of the multi-module thermoelectric device **5Q.DEVICE**, one of which is in control of spatial and temporal distributions of thermodynamic parameters of the ambient fluid portions adjacent to the individual thermo-conductive buses **5Q.05**. Another useful property of the device **MATRIX SOURCE AND/OR DETECTOR OF SOUND 5Q.DEVICE** is that the loudness of the resulting launched sound can be controlled by the quantity of operating **ELEMENTAL SOURCES OF SOUND 5Q.02**. In practice, the device **MATRIX SOURCE AND/OR DETECTORS OF SOUND 5Q.DEVICE** comprising the big number $N_x \times N_y$ of **ELEMENTAL SOURCES OF SOUND 5Q.02** provides for a big number of degrees of freedom for manipulation with characteristics of the elemental acoustic waves to create the desired waveform of the resulting launched acoustic wave. The big number of degrees of freedom allows for the coding, directing, and focusing of the resulting launched acoustic wave, wherein the device **MATRIX SOURCE AND/OR DETECTORS OF SOUND 5Q.DEVICE** remains relatively compact as not requiring big horns and is efficient comparing with classic speakers as not having moving components and so not originating concomitant turbulence.

In the detection mode, the $N_x \times N_y$ **ELEMENTAL DETECTORS OF SOUND 5Q.02** of the device **MATRIX SOURCE AND/OR DETECTOR OF SOUND 5Q.DEVICE** are capable to detect a reached beam of elemental acoustic waves and release $N_x \times N_y$ associated elemental electrical signals and the common controller-dispatcher **5Q.04** is capable to superpose the released $N_x \times N_y$ elemental electrical signals. If the beam brings coded information due to that the $N_x \times N_y$ elemental acoustic waves differ in amplitude and/or phase and/or frequency and/or delay, then the $N_x \times N_y$ **ELEMENTAL DETECTORS OF SOUND 5Q.02** release $N_x \times N_y$ different associated elemental electrical signals. Further, using the common controller-dispatcher **5Q.04** capable to superpose the released $N_x \times N_y$ elemental electrical signals using a decoding algorithm, a decoding of the coded information becomes feasible.

In view of the foregoing description referring to **Fig. 5p** and **Figs. 2b (A)** and **(B)** in combination with **Fig. 1d**, it will be evident for a commonly educated person that a three-dimensional matrix of a multiplicity of $N_x \times N_y \times N_z$ elemental TE devices **5Q.02**, where N_z is the number of the **ELEMENTAL SOURCES OF SOUND 5Q.01** arranged along the axis Z in a manner shown in **Fig. 1d**, can be implemented to increase the reachable amplitude of the oscillating temperature difference δT using a smaller amplitude of the oscillating current density J when the elemental TE devices **5Q.02** function to launch acoustic waves.

Diversity Of Uses For Multi-Module Matrix Devices

Thus, when the elemental acoustic thermoelectric devices **5P.0** are aggregated into a matrix thereby forming the matrix device **5Q.DEVICE**, it becomes possible a broad diversity of uses such as an acoustic wave phase inverter or optimal detector of sound, a sound amplifier, a phased array acoustic wireless charger, a suppressor of turbulence in a jet-nozzle, a suppressor of turbulence in a flow boundary layer, and a lift-and-thrust force booster, each of which will be described hereinbelow referring to **Figs. 5r**, **5s**, **5t**, **6a**, **7c**, and **8**, correspondingly.

Detector Of Sound

Fig. 5r is a schematic illustration of a multi-module thermoelectric device **5R.DEVICE**, comprising a matrix of a multiplicity of ***N*** **ELEMENTAL DETECTORS OF SOUND** **5R.02**, each of which comprises an individual integrated circuit controller as described hereinbefore referring to **Fig. 5p**, and a common controller-dispatcher **5R.04** capable to control the ***N*** **ELEMENTAL DETECTORS OF SOUND** **5R.02** individually by amplifying, and/or delays, and/or phase-shifting, and/or summing the associated induced individual electric currents. The multi-module thermoelectric device **5R.DEVICE** has an overall shape of a plate having two sides: **5R.71** and **5R.72**. When the side **5R.71** is exposed to an acoustic beam **5R.1.INPUT**, a secondary acoustic wave **5R.2.OUTPUT** is radiated from the side **5R.72** due to the Seebeck effect and the Peltier effect as a contribution to the resulting acoustic beam **5R.4.OUTPUT**, as described hereinabove in the **subparagraph** "In Relation To Phase-Inverter" **referring to Fig. 5p** considering an alone **ELEMENTAL SOURCE AND DETECTOR OF SOUND** **5P.0**. The two acoustic beams: **5R.1.INPUT** and the secondary acoustic wave **5R.2.OUTPUT, are marked by opposite signs: "+" and "−"**, correspondingly, symbolizing the 180^0 phase-difference between the fronts of the two acoustic beams: **5R.1.INPUT** and the secondary acoustic wave **5R.2.OUTPUT**, adjacent to the two sides: **5R.71** and **5R.72**, correspondingly.

It will be evident to a commonly educated person that the acoustic beam **5R.1.INPUT** acts on the side **5R.71** the thermoelectric device **5R.DEVICE** not only due to the oscillating changes in temperature but also mechanically impacting the side **5R.71** of the thermoelectric device **5R.DEVICE** due to the oscillating changes in static pressure. The mechanic impacts partially transmit the acoustic beam **5R.1.INPUT** through the thermoelectric device **5R.DEVICE** without the phase-inversion, thereby, resulting in the portion **5R.3.OUTPUT** of the acoustic beam **5R.1.INPUT**, which (the portion) is passed through the thermoelectric device **5R.DEVICE** as a contribution **5R.3.OUTPUT** to the resulting acoustic beam **5R.4.OUTPUT** and radiated from the

side **5R.72**. As soon as the front of the contribution **5R.3.OUTPUT** is not subjected to the phase-inversion and the velocity of acoustic waves in the solid material of the thermoelectric device **5R.DEVICE** is much higher than the velocity of the acoustic waves in the air, the phase of the contribution **5R.3.OUTPUT** radiated from the side **5R.72** is almost the same as the phase of the acoustic beam **5R.1.INPUT and so is reasonably indicated by sign "+"**. If the common controller-dispatcher **5R.04** of the thermoelectric device **5R.DEVICE** provides for amplifying the induced current to trigger the Peltier effect originated in unison with the triggered by the impacting acoustic beam **5R.1.INPUT** Seebeck effect, and, thereby, to amplify the secondary acoustic wave **5R.2.OUTPUT** exceeding the acoustic beam portion contribution **5R.3.OUTPUT**, the thermoelectric device **5R.DEVICE** is interpreted as a phase-inverter.

Optimized Detector Of Sound

If the common controller-dispatcher **5R.04** of the thermoelectric device **5R.DEVICE** comprises a so-called negative feedback loop to provide for that the two contributions:

- the secondary acoustic wave **5R.2.OUTPUT**, and
- the portion **5R.3.OUTPUT** of the acoustic beam **5R.1.INPUT** which (the portion) passed through the thermoelectric device **5R.DEVICE,**

having the mutually opposite phases are such that the resulting electric current in the thermoelectric devices **5R.02** is zero, in turn, providing that the resulting acoustic beam **5R.4.OUTPUT** has a zero amplitude, then the wave energy, brought by the acoustic beam **5R.1.INPUT**, and the electric energy, consumed by both a multiplicity of individual integrated circuit controllers and the common controller-dispatcher **5R.04**, altogether are transformed into the Joule heat and radiation of an electromagnetic wave which is accompanying the induced alternating current originated in the thermoelectric device **5R.DEVICE**. This also means that there are suppressed waves reflected from the side **5R.71**. Thus, the device **5R.DEVICE** is adapted to function as a detector of sound or a silencer, optimized to maximize the net-efficiency of sound detection.

Two-Stage Sound Amplifier

Fig. 5s is a schematic illustration of a two-stage sound amplifier **5S.DEVICE**, constructed according to the principles of the present invention as a multi-module thermoelectric device, representing a cascade of two mutually electrically-separated thermoelectric devices: **5S-1.DEVICE** and **5S-2.DEVICE**, each of which is similar to the thermoelectric device **5R.DEVICE** described hereinabove referring to **Fig. 5r**. The thermoelectric device **5S.DEVICE** comprises a multiplicity of $2N$ **ELEMENTAL DETECTORS OF SOUND 5S.02**, each of which comprises an

individual controller similar to the individual controller **5P.8A** described hereinbefore referring to **Fig. 5p**, and a common controller-dispatcher **5S.04** capable to control the $2N$ **ELEMENTAL DETECTORS OF SOUND** individually by amplifying, and/or delays, and/or phase-shifting, and/or summing the induced individual electric currents.

When the side **5S.71** is exposed to an impacting acoustic beam **5S.1.INPUT**, the inner side **5S.72** is cooled and heated in anti-phase relative to the heating and cooling side **5S.71**. Further, a secondary acoustic wave **5S.2.OUTPUT** is radiated from the side **5S.73** due to the Peltier effect as a contribution to the resulting acoustic beam **5S.4.OUTPUT**. The two acoustic beams: impacting **5S.1.INPUT** and the secondary acoustic wave **5S.2.OUTPUT**, are marked by **the same sign: "+", symbolizing the zero phase difference between the fronts of the two** acoustic beams: impacting **5S.1.INPUT** and the secondary acoustic wave **5S.2.OUTPUT**, adjacent to the two sides: **5S.71** and **5S.73**, correspondingly.

Again, it will be evident to a commonly educated person that the impacting acoustic beam **5S.1.INPUT** acts on the side **5S.71** of the thermoelectric device **5S.DEVICE** not only due to the oscillating changes in temperature but also mechanically impacting the side **5S.71** of the thermoelectric device **5S.DEVICE** due to the oscillating changes in static pressure. The mechanic impacts partially transmit the impacting acoustic beam **5S.1.INPUT** through the thermoelectric device **5S.DEVICE** without the phase-inversion, thereby, resulting in a contribution **5S.3.OUTPUT** to the resulting acoustic beam **5S.4.OUTPUT** radiated from the side **5S.73**. As soon as the front of the contribution **5S.3.OUTPUT** is not subjected to the phase-inversion and the wavelength of an acoustic wave in a solid material of the thermoelectric device **5S.DEVICE** is much greater than the thickness **5S.03** of the thermoelectric device **5S.DEVICE**, the phase of the contribution **5S.3.OUTPUT** radiated from the side **5S.73** is almost the same as the phase of the impacting acoustic beam **5S.1.INPUT** and so is reasonably **indicated by sign "+" as well. The two contributions: 5S.2.OUTPUT** and **5S.3.OUTPUT**, are in-phase, hence, in this case, the thermoelectric device **5S.DEVICE** is adapted to function as a two-stage sound amplifier, optimized to maximize the net-efficiency of sound boosting. As both the Seebeck effect and the Peltier effect are triggered in the thermoelectric device **5S.DEVICE**, the resulting sound-amplifying partially occurs at the expense of the ambient heat.

It will be evident for a commonly educated person that a phonendoscope and hearing aid, both can be supplied with the two-stage sound amplifier embodied as the thermoelectric device **5S.DEVICE**.

Acoustic Wireless Charger

Fig. 5t is a schematic illustration of a communication system **5T.SYSTEM**, constructed according to the present invention. The communication system **5T.SYSTEM** comprises:

- a multi-module thermoelectric device **5T.TX-ANTENNA**, having a matrix composed of a multiplicity of N **ELEMENTAL SOURCES OF SOUND 5T.02A** functioning in the **SOUND LAUNCHING MODE** and a common controller-dispatcher **5T.04A**, and
- a multi-module thermoelectric device **5T.RX-ANTENNA**, composed of a matrix composed of a multiplicity of N **ELEMENTAL DETECTORS OF SOUND 5T.02B** functioning in the **SOUND DETECTION MODE** and a common controller-dispatcher **5T.04B**.

While the common controller-dispatcher **5T.04A** provides for an implementation of the technique phased array applied to the matrix of the multiplicity of N **ELEMENTAL SOURCES OF SOUND 5T.02A** to form an acoustic beam **5T.1.INPUT** directed to the multi-module thermoelectric device **5T.RX-ANTENNA**, the common controller-dispatcher **5T.04B** provides for the operation of the sound detecting multi-module thermoelectric device **5T.RX-ANTENNA** similar to the operation of the multi-module thermoelectric device **5R.DEVICE** described hereinabove **in subparagraph "**Optimized Detector Of Sound**" referring to Fig. 5r**, namely, such that the two contributions **5T.2.OUTPUT** and **5T.3.OUTPUT** (both analogous to the aforementioned two contributions **5R.2.OUTPUT** and **5R.3.OUTPUT**) having the mutually opposite phases, such that the resulting acoustic beam **5T.4.OUTPUT** has zero amplitude (analogously to the aforementioned resulting acoustic beam **5R.4.OUTPUT**). The **IC DETECTOR 5T.8B** is similar to the **IC DETECTOR 5P.8B** (**Fig. 5p**) but is now specified as having a **DIODE BRIDGE 5T.81B** and a **RECHARGEABLE BATTERY 5T.81B**. An induced alternating electric current generated in the **IC DETECTOR 5T.8B** moves through the **DIODE BRIDGE 5T.81B** and charges the **RECHARGEABLE BATTERY 5T.81B**, thereby, cumulating the electric energy, which is acquired from the wave energy of the detected acoustic beam **5T.1.INPUT**. Thus, the communication system **5T.SYSTEM** represents an acoustic wireless charger.

To estimate the practical feasibility of the acoustic wireless charger, consider the multi-module thermoelectric device **5T.TX-ANTENNA** having a linear size of several times greater than $1\ mm$ and the acoustic beam **5S.1.INPUT** which is composed of acoustic waves at the ultrasound frequency of 340 kHz. In this case,

- the wavelength of the ultrasound is estimated as $1\ mm$; and
- half of the time-period allowing for the temperature oscillation is $0.5 \times \tau_{340kHz} \approx 1.5 \times 10^{-6}\ sec$ and the reachable amplitude of the temperature difference is, approximately, of $1.8 \times 10^{-6}\ K$ that corresponds to SPL=SDL=STL level of $70\ dB$.

The phased array technique is applicable to the wavelength of $1\ mm$, as the linear size of the multi-module thermoelectric device **5T.TX-ANTENNA** is assumed of several times greater than $1\ mm$. Normally, the net-efficiency of the electrical scheme of the **IC DETECTOR 5T.8B** is higher than 50%. Taking into account that the wave power is proportional to squired frequency; if the charging energy is further destined to generate a $2\ kHz$ sound, a reachable SPL of the $2\ kHz$ sound is about $109\ dB$. The estimation shows that the acoustic wireless charger can be sufficiently efficient when charging the multi-module thermoelectric device **5T.RX-ANTENNA** wirelessly from $1\ m$ distance using the 340 kHz ultrasound.

In view of the foregoing description referring to **Figs. 5q**, **5p**, **5r**, **5s**, and **5t**, it will be evident for a person skilled in the art that, if the multi-module thermoelectric device **5T.RX-ANTENNA** operates in a passive mode without the functioning of the dispatcher **5T.04B**, then the magnitudes of the contributions **5T.2.OUTPUT** and **5T.3.OUTPUT**, both are neither controlled nor optimized and so a non-zero resulting acoustic beam **5T.3.OUTPUT** determines a reduced net-efficiency of the acoustic wireless charger.

Convergent-Divergent Jet-Nozzle

Fig. 6a, composed of two parts: **(A) Shape** and **(B) Graph**, is a schematic illustration of a modified convergent-divergent jet-nozzle.

Fig. 6a (A) Shape shows schematically a sectional view of the modified convergent-divergent jet-nozzle **610** in a sagittal plane. The modified convergent-divergent jet-nozzle **610** having a shaped tunnel is applied to accelerate a laminarly flowing compressed and hot compressible-expandable fluid **611**. In contrast to the prior art convergent-divergent nozzles, which are passively adapted to only certainly-given velocity and thermodynamic parameters (and are not adapted to arbitrary velocity and thermodynamic parameters) of an incoming fluid flow to provide for a laminar flow **as described hereinabove in subparagraph "De Laval Effect"** referring to **Fig. 1c**, the modified convergent-divergent jet-nozzle **610**, constructed according to an exemplary embodiment of the present invention, allows for the implementation of either the enhanced Venturi effect or the enhanced de Laval jet-effect, each providing a laminar acceleration of fluid flow **611** for a wide range of velocities u_{in} and thermodynamic parameters: the static pressure P_{in}, absolute temperature T_{in}, and mass density ρ_{in}, of entering fluid flow **611** at an open inlet **617**. The shaped tunnel of the modified convergent-divergent jet-nozzle **610** has opposite walls **6A.WALLS**, which are either formed by or at least supplied with a surface matrix **6A.MATRIX** of densely-arranged elemental thermoelectric

devices **6A.TED**. The triplet of dots **6A.DOT** symbolizes that the elemental thermoelectric devices **6A.TED** are arranged unbrokenly. The surface matrix **6A.MATRIX** is analogous to the planar matrix **5Q.MATRIX** of elemental thermoelectric devices **5Q.02** described hereinabove referring to **Fig. 5q**, but now is aligned to the opposite walls **6A.WALLS's shape**. The opposite walls **6A.WALLS** are shaped, for the sake of concretization and without loss of generality, axis-symmetrically around an imaginary sagittal x-axis **615**, as a convergent funnel **612** comprising an open inlet **617** having a cross-sectional area A_{in} and diameter D_{in} , narrow throat **613** comprising point **618** of the narrowest cross-section cross-sectional area A_{th} and diameter D_{th}, and divergent exhaust tailpipe **614** having an open outlet **619** having a cross-sectional area A_{ou} and diameter D_{ou}. When moving through the smoothly shaped tunnel having controllably heated and/or cooled walls, the fluid stream **611** becomes subjected, on the one hand, to change in cross-sectional area and, on the other hand, to forcedly established temperature distributed due to controllably functioning densely-arranged elemental thermoelectric devices **6A.TED**. The linear sizes: D_{in}, D_{th} , D_{ou} may differ from associated linear sizes of the mentioned prior art passively adapted convergent-divergent nozzle, passively adapted to only certainly-given velocity and thermodynamic parameters of the incoming fluid flow **611**, on a thickness of a boundary layer nearby the opposite walls **6A.WALLS**. Thus, the thickness of the boundary layer near each of the walls **6A.WALLS** plays the role of a tolerance allowing for a degree of freedom to manipulate with the forcedly establishing of the temperature using the thermoelectric devices **6A.TED**. The surface matrix **6A.MATRIX** of the thermoelectric devices **6A.TED** provides for controllably distributed temperature along the sagittal axis **615** having a distance parameter x. The varying cross-sectional area of the smoothly shaped tunnel is characterized by a cross-sectional area profile function $A(x)$ of x interrelated with functions $u(x)$ and $T(x)$ of x representing profiles of the fluid flow's headway velocity and absolute temperature, correspondingly, along the tunnel length, wherein the thermoelectric devices **6A.TED** providing for a degree of freedom to interrelate the functions $A(x)$, $u(x)$, and $T(x)$ by a condition of flow continuity expressed as:

$$A(x) = \frac{A_* \sqrt{(\gamma-1)RT(x)}}{u(x)} \left(\frac{2RT(x)+u^2(x)}{(\gamma+1)RT(x)} \right)^{\frac{\gamma+1}{2(\gamma-1)}} \quad \text{Eq. (6.0),}$$

where A_* is a constant, γ is an adiabatic compressibility parameter of the flowing fluid, and R is a specific gas constant characterizing the fluid flow, wherein the functions $u(x)$ and $T(x)$ both are gradually-smoothed monotonic, wherein:

- the gradually-smoothed monotonic function of the absolute temperature $T(x)$ is determined by:
  - the absolute temperature T_{in} the fluid flow at the open inlet;
  - the temperature change $\delta T_0(x)$ interrelated with adiabatic compression-expansion occurred due to an adiabatic action of the Coanda-effect, in turn, determined by a curvature of the stationary geometrical configuration of the tunnel; and
  - forcedly established temperature contribution $\delta T_1(x)$ to the absolute temperature $T(x)$ along the boundary layers subjected to controllable heating and/or cooling action of the thermoelectric devices **6A.TED**,

  such that $T(x) = T_{in} + \delta T_0(x) + \delta T_1(x)$, and
- the gradually-smoothed monotonic function of the headway velocity $u(x)$ is determined by the certain headway velocity u_{in} of the fluid flow **611** at the open inlet, convective headway acceleration resulting in a velocity gradient along the tunnel length as the fluid flow **611** is subjected to the adiabatic Coanda-effect, and controllable headway acceleration occurred due to controllable heating and/or cooling action of the thermoelectric devices **6A.TED**.

The condition of flow continuity Eq. (6.0) is correct as for relatively slow motions corresponding to low M-velocities, lower than the specific M-velocity $M_* = \sqrt{(\gamma - 1)/\gamma}$ as well as for relatively fast motions corresponding to high M-velocities, higher than the specific M-velocity.

The constant A_* is a characteristic cross-sectional area defined for a certain fluid; the characteristic cross-sectional area A_* is a hypothetically-minimal reachable by a portion of the fluid when the portion of the fluid is convectively accelerated in an adiabatic process, according to the equation of continuity. Considering the case:

- when the minimal cross-sectional area A_{th} of the narrow throat is greater than the hypothetically-minimal reachable constant A_*, there are no critical condition points within the tunnel and the convergent-divergent nozzle **610** plays the role of a Venturi pipe providing for the Venturi effect; and
- when the minimal cross-sectional area A_{th} of the narrow throat is lesser than or equal to the hypothetically-minimal reachable constant A_* ($A_{th} \leq A_*$), the flowing fluid **611**, being subjected to a convective acceleration in an adiabatic process and crossing the minimal cross-sectional area A_{th} of the narrow throat **613**, is capable of reaching at most the specific M-velocity $M_* = \sqrt{(\gamma - 1)/\gamma}$ (which is a characteristic of the fluid as well) and so the convergent-divergent nozzle **610** plays the role of a de Laval jet-nozzle providing for the de

Laval jet-effect; wherein the condition $A_{th} < A_*$ contradicts the condition of flow continuity (6.0) and thereby the de Laval jet-effect is not optimized on the criterion of laminar motion of the fluid flow **611**.

Considering the case, when the modified convergent-divergent jet-nozzle **610** is destined to trigger the enhanced de Laval jet-effect recognized by a laminar motion of the fluid flow **611**, the narrow throat **613** should be narrow sufficient such that the minimal cross-sectional area A_{th} is the hypothetically-reachable minimal cross-sectional area A_* **providing the "critical condition" point 618** where the temperature-dependent M-velocity gradually reaches the value of the specific M-velocity $M_* = \sqrt{(\gamma - 1)/\gamma}$. In practice, to provide the strict condition $A_{th} = A_*$ using a passively adapted convergent-divergent nozzle is almost impossible. The surface matrix **6A.MATRIX** of the densely-arranged elemental thermoelectric devices **6A.TED** allows for such a control of the temperature contribution $\delta T_1(x)$ that the resulting gradually-smoothed monotonic function of the absolute temperature $T(x) = T_{in} + \delta T_0(x) + \delta T_1(x)$ satisfies the condition *Eq. (6.0)*.

The degree of freedom to manipulate with the function $T(x)$ via the function $\delta T_1(x)$ to satisfy the condition of flow continuity *Eq. (6.0)* provides for that the combined action on the fluid stream **611** provides for gradually-smoothed monotonic changes preventing jumps of the fluid stream headway velocity $u(x)$ and all of the thermodynamic parameters of the fluid: the static pressure $P(x)$, the absolute temperature $T(x)$, and the mass density $\rho(x)$, thereby, providing the following beneficial features:

- smoothing (or, preferred, linearizing) of the fluid stream headway velocity, providing suppression of the undesired flow turbulence;
- smoothing (or, preferred, linearizing) of the fluid stream static pressure, providing suppression of the undesired Mach waves and, thereby, suppression of nearby body vibrations;
- smoothing (or, preferred, linearizing) of the fluid stream mass density, providing suppression of the undesired flow disturbances accompanied by shock waves;
- smoothing of the flowing fluid absolute temperature, providing suppression of adjacent surface tensions; and
- smoothing (or, preferred, linearizing) of the flowing fluid M-velocity, providing a trade-off of suppressions of undesired all: the turbulence, vibrations, shock and Mach waves, and surface tensions.

The relatively fast fluid flow **611** provides for conditions allowing to exclude using a powerful ventilator, normally, accompanying thermoelectric devices.

Fig. 6a (B) Graph, in conjunction with **Fig. 6a (A) Shape**, is a schematic graphic illustration of the distribution of the flowing fluid **611's** four mutually-scaled parameters: headway velocity **620.u,** static pressure **630.P**, absolute temperature **640.T**, and M-velocity **650.M** along the length of nozzle **610,** constructed according to the principles of a preferred embodiment of the present invention to provide a linear function of M-velocity **650.M** of the flowing fluid. The narrowest cross-section of the narrow throat **613 provides the "critical condition" point 618**. Compressed and hot fluid **611** flows through the narrow throat **613**, where the velocity picks up **621** such that M-velocity **650.M** reaches the specific M-velocity $M_* = \sqrt{(\gamma - 1)/\gamma}$ at the critical condition point **618**. Ahead of the critical condition point **618**, the pressure and temperature fall, correspondingly **631** and **641**. Hot flowing fluid **611** crosses the critical condition point **618** and enters the widening stage of the narrow throat **613** and further divergent exhaust tailpipe **614** having an open outlet. Flowing fluid **611** expands there, and this expansion is optimized such that the extra-increase of velocity **622** is substantially smoothed; and the pressure and temperature extra-decrease, **632** and **642**, correspondingly, are substantially smoothed as well, in contrast to that at the critical condition point **180** associated with the classic prior art rocket nozzle **100** of **Figs. 1c**, **1d**. The smoothed change of static pressure **630.P** provides suppression of unwanted in general, acoustic waves, and, in particular, Mach waves. In practice, the suppression of Mach waves provides suppression of undesired vibrations that, in particular, especially important for fast accelerating vehicles.

It will be evident for a person skilled in the art that:

- If, in a particular case, the geometrical configuration of the shaped tunnel is such that, for a certain velocity u_{in} of a fluid stream **611** at the inlet **617** and certain thermodynamic parameters, the condition of flow continuity *Eq. (6.0)* is satisfied without the forcedly establishing temperature distribution, then the condition of flow continuity (6.0) reverts into the prior art equation *Eq. (1.a)* **described hereinabove in the subparagraph** "De Laval Effect" **referring to Fig. 1c**;
- If, in general, the geometrical configuration of the shaped tunnel is gradually-smoothed or, in a particular case, the geometrical configuration of the shaped tunnel is trivial cylindrical, wherein, in any case, the linear size of the narrow throat (for instance, the diameter D_{th}) is of the same order of value as the thickness of the boundary layer near each of the walls **6A.WALLS**, and if the fluid flow having the absolute temperature T_{in} corresponding to the

left point of the curve **640.T** enters the tunnel with velocity u_{in} corresponding to the left point of the curve **620.u**, then a forcedly established temperature profile along the shaped tunnel corresponding to the curve **640.T** provides for:

- the fluid stream static pressure decrease corresponding to the curve **630.P**,
- the fluid stream velocity increase corresponding to the curve **620.u**, and
- the fluid stream M-velocity linear increase corresponding to the curve **650.M**;

and

- In practice, if a substantial acceleration is desired, hardly, it is preferred to use the mentioned trivial cylindrical geometrical configuration assuming $\delta T_0(x) = 0$ and provide the desired temperature distribution $T(x)$ using the forcedly established temperature $\delta T_0(x)$ only, but it is preferred to use at least an almost adapted geometrical configuration already providing the temperature distribution $T_{in} + \delta T_0(x)$ and use the degree of freedom to compensate for a lack of temperature distribution $\delta T_1(x)$ using the densely-arranged elemental thermoelectric devices **6A.TED**.

A convergent-divergent jet-nozzle, constructed applying the condition of flow continuity *Eq. (6.0)* accompanied by the satisfying condition of the smoothed thermodynamic parameters of the flowing fluid **611** according to an exemplary embodiment of the present invention, allows the use of the enhanced de Laval jet-effect to accelerate incoming compressed and hot airstream **611** moving with low M-velocities to obtain outflowing accelerated and cooled jetstream **616**, reaching high M-velocities [i.e. M-velocities, higher than the specific M-velocity $M_* = \sqrt{(\gamma - 1)/\gamma}$], in particular, high-subsonic velocities.

In view of the foregoing description referring to **Fig. 6a**, it will be evident to a person skilled in the art that one can use different criteria of the gradualness of $u(x)$, $T(x)$, $P(x)$, $\rho(x)$, and $M(x)$, for different preferred optimizations of the convergent-divergent shape of a tunnel. Namely, the conditions, providing laminarity of the airstream motion, are:

- if suppression of disturbances, which are capable of growing into turbulence, is the most preferred, then $u(x)$ should be given as the linear function $u(x) = \overline{u}(x) = u_* + \alpha_u(x - x_*)$, where x is the x-coordinate at x-axis **615**, and α_M is a positive constant defining a scale factor and having a sense of constant gradient of velocity spatial distribution, i.e. $\alpha_u = \partial\overline{u}(x)/\partial x$, and the function $\delta T_1(x)$ should be established such that the function $T(x) = T_{in} + \delta T_0(x) + \delta T_1(x)$ would satisfy to the condition of flow continuity *Eq. (6.0)*; wherein because the higher the velocity of the moving stream **611** the

shorter the possible response time of the TE devices **6A.TED**: up to $2.5 \times 10^{-5}\ sec$ and shorter (as described hereinabove referring to **Fig. 5p**),

- the TE devices occupying a path of $5\ mm$ are capable of preventing a local temperature jump, and so preventing an origination of a turbulent vortex bigger than $5\ mm$ in a boundary layer moving with the velocity of $200\ m/sec$, and
- a hypersonic laminar flow (for instance, of $3500\ m/sec$) can be controlled in a long tunnel;

- if suppression of Mach waves and body vibrations are the most preferred, then the function $\delta T_1(x)$ should be established such that the temperature-dependent function $M(x) = u(x)/\sqrt{\gamma R \times [T_{in} + \delta T_0(x) + \delta T_1(x)]}$ becomes given as the function $M(x) = \sqrt{2\left\{[P_0/\overline{P}(x)]^{(\gamma-1)/\gamma} - 1\right\}/\gamma}$, where $\overline{P}(x)$ is a linear function of the static pressure vs. x-coordinate: $\overline{P}(x) = P_* + \alpha_P(x - x_*)$, P_* is the static pressure of the flowing fluid at the critical condition point x_*, and $\alpha_P = \partial\overline{P}(x)/\partial x$ is a constant gradient of the static pressure distributed along the x-axis within a specially shaped tunnel;
- if the suppression of temperature jumps is the most preferred, then the function $\delta T_1(x)$ should be established such that the function $[T_{in} + \delta T_0(x) + \delta T_1(x)]$ is a linear function $\overline{T}(x)$ of the fluid temperature vs. x-coordinate: $\overline{T}(x) = T_* + \alpha_T(x - x_*)$, T_* is the temperature of the flowing fluid at the critical condition point x_*, and $\alpha_T = \partial\overline{T}(x)/\partial x$ is a constant gradient of the fluid temperature distributed along the x-axis within a specially shaped tunnel;
- if suppression of shock waves is the most preferred, then the function $\delta T_1(x)$ should be established such that the temperature-dependent function $M(x) = u(x)/\sqrt{\gamma R \times [T_{in} + \delta T_0(x) + \delta T_1(x)]}$ becomes given as the function $M(x) = \sqrt{2\{[\rho_0/\overline{\rho}(x)]^{(\gamma-1)} - 1\}/\gamma}$, where $\overline{\rho}(x)$ is a linear function of the fluid mass density vs. x-coordinate: $\overline{\rho}(x) = \rho_* + \alpha_\rho(x - x_*)$, ρ_* is the mass density of said flowing fluid at the critical condition point x_*, and $\alpha_\rho = \partial\overline{\rho}(x)/\partial x$ is a constant gradient of the fluid mass density distributed along the x-axis within a specially shaped tunnel; and
- if a trade-off between all the mentioned suppressions is preferred; then the function $\delta T_1(x)$ should be established such that the temperature-dependent function $M(x) = u(x)/\sqrt{\gamma R \times [T_{in} + \delta T_0(x) + \delta T_1(x)]}$ becomes a linear function $M(x) = \overline{M}(x) = M_* + \alpha_M(x - x_*)$, where x is the x-coordinate at x-axis **615**, and α_M is a positive

constant defining a scale factor and having a sense of constant gradient of M-velocity spatial distribution, i.e. $\alpha_M = \partial\overline{M}(x)/\partial x$.

It will become further evident for a person, who has studied the present invention, that it is possible to compose a multi-stage nozzle composed of N nozzles each of which satisfies the condition of flow continuity *Eq. (6.0)*; wherein the N nozzles, enumerated from 1 to N, are united together to join the N tunnels associated with the N nozzles, correspondingly, such that each of the N tunnels is a fragment of a resulting unbroken tunnel formed thereby as a whole; an n-th fragment, where n is an integer between 1 and N: $1 \leq n \leq N$, has the varying cross-sectional area characterized by a cross-sectional area profile function $A_n(x)$ of x expressed as an individual condition of flow continuity:

$$A_n(x) = \frac{A_{*n}\sqrt{(\gamma-1)RT_n(x)}}{u_n(x)}\left(\frac{2RT_n(x)+u_n^2(x)}{(\gamma+1)RT_n(x)}\right)^{\frac{\gamma+1}{2(\gamma-1)}}$$

where A_{*n} is n-th constant, and the functions $u_n(x)$ and $T_n(x)$ are representing profiles of the fluid flow's headway velocity and absolute temperature, correspondingly, along the n-th fragment of the resulting unbroken tunnel length; the resulting unbroken tunnel as a whole is either converging, or divergent, or convergent-divergent, or two-stage convergent-divergent; or multi-stage convergent-divergent; wherein piecewise-monotonic profile functions $u(x)$, $P(x)$, $\rho(x)$, $T(x)$, and $M(x)$, composed of associated gradually-smoothed monotonic profile functions concatenated together, all remain gradually-smoothed along the resulting unbroken tunnel as a whole, thereby, the multi-stage nozzle is applicable to convey:

- in general, laminar flow to solve the problem of originated turbulence, and
- in particular, tiny portions of the fluid associated with an acoustic wave propagating within and along the tunnel to solve the problem of sound power dissipation.

Further, for the purposes of the present invention, the term "airfoil" or "actually-airfoil" should be understood as related to a wall shape and as specifying a convergent-divergent shape of a flow **portion's streamlines aligned to the airfoil wall, wherein, in contrast to a seemingly**-airfoil shape, the convergent-divergent shape calls for the condition of flow continuity *Eq. (6.0)* and at least one of the aforementioned conditions for the functions $u(x)$ and $T(x)$, thereby, providing laminarity of the flow portion motion.

In view of the foregoing description referring to **Fig. 6a**, it will be evident to a person skilled in the art that:

- In a more general case, when imaginary sagittal axis **615** is oriented at least partially in the **vertical direction in the Earth's gravitational field,** the condition of laminar flow should be

corrected becoming different from the condition of flow continuity *Eq. (6.0)* by a component depending on the gravitational acceleration g, namely:

$$\frac{A}{A_*} = \frac{M_*}{M}\left(\frac{1+\frac{\gamma}{2}M^2+\frac{g\Delta h}{RT}}{1+\frac{\gamma}{2}M_*^2}\right)^{\frac{\gamma+1}{2(\gamma-1)}} \qquad \text{Eq. (6.0a),}$$

where Δh is a change of the flow effective height with respect to the critical condition point. It will be further evident to a person skilled in the art that, when the considered temperatures and M-velocities are sufficiently high to provide for the conditions: $g\Delta h/RT \ll 1$ and $g\Delta h/RT \ll \gamma M^2/2$ to be satisfied, the use of the condition of flow continuity in the form of *Eq. (6.0)* becomes justified;

- Taking into account molecular interactions for flowing liquid or plasma, for which changes of the partial deep-stagnation pressure-a δP_a become at least noticeably distributed in space, the generalized adiabatic compressibility parameter γ in the condition of flow continuity *Eq. (6.0)* is not a constant but varies with the changes of the partial deep-stagnation pressure-a δP_a;
- If the flowing molecular fluid is an ionized gas, i.e. plasma, controlled by an external magnetic field, then the specifically shaped walls **6A.WALLS** of the tunnel can be imaginary, formed by streamlines of the flowing plasma subjected to and controlled by an action of the magnetic field;
- When the shape of the tunnel is not completely optimized on one of the mentioned criteria either:
    - smoothing of the flowing fluid velocity, or
    - smoothing of the flowing fluid M-velocity, or
    - smoothing of the flowing fluid static pressure, or
    - smoothing of the flowing fluid temperature, or
    - smoothing of the flowing fluid mass density,

at least because the tunnel shape must be adapted to the initial velocity and thermodynamic parameters of the laminarly flowing hot-and-compressed compressible-expandable fluid **611**, any of the desired optimizations is reachable by controlling the elemental TE devices **6A.TED** of the surface matrix **6A.MATRIX** while the densely-arranged elemental TE devices **6A.TED** are capable of providing for the desired temperature at the locations corresponding to the elemental TE devices **6A.TED** due to the Peltier effect. Moreover, the forcedly **established desired distributed temperature prevents the "separation-points" [like 1G.46** of

Fig. 1g Scheme (D)] of breaking or jumping of all: the headway velocity, the static pressure, the absolute temperature, and the mass density nearby the tunnel walls **6A.WALLS**. The feasibility of such a control is supported by the property of flowing fluid moving adjacent to an airfoil wall described hereinabove referring to **Fig. 1g Graph (D)**. Namely, on the one hand, a tiny portion of the flow, moving adjacent to a solid surface, can be heated or cooled by the solid surface when getting the temperature of the solid surface and, on the other hand, a big portion of the flow, moving farther from the solid surface, is capable of removing of excess heat or reverting the reduced portion of the heat, correspondingly; wherein, on the one hand, the faster flow the faster heat-transmitting, and, on the other hand, the tiny portion always has the temperature of the solid surface. In other words, it is possible to optimize the fluid stream within the shaped tunnel by changing the temperature of the fluid stream using the Peltier effect originated by the surface matrix **6A.MATRIX** of the elemental TE devices **6A.TED** built-in into the specifically shaped walls **6A.WALLS** of the tunnel;

- As the surface matrix **6A.MATRIX** of the elemental TE devices **6A.TED**, built-in into the specifically shaped walls **6A.WALLS** of the tunnel, is capable to transform the temperature differences between:
    - on the one hand, the inner side of the specifically shaped walls **6A.WALLS** which contacts with the fluid stream **611** within the tunnel, and
    - on the other hand, the outer side of the tunnel, which contacts with the ambient fluid,

  into electricity due to the Seebeck effect, it becomes possible to optimize the shape of the tunnel such that to take into account the change in temperature caused due to pumping out the heat energy of the fluid stream **611** to produce the controllably consumed electric power; wherein the optimization is such that to maintain the laminarity of the fluid stream **611** within the tunnel and, thereby, to provide efficient functionality of the elemental TE devices **6A.TED** use;

  and

- The parameter γ is varying when the chemical composition of the flowing fluid is changing.

De Laval Retarding-Effect

Fig. 6b, composed of two parts: **(A) Shape** and **(B) Graph**, is a schematic illustration of an inverse convergent-divergent jet-nozzle.

Fig. 6b (A) Shape illustrates a sectional view of the inverse convergent-divergent jet-nozzle **650** in a sagittal plane. Convergent-divergent jet-nozzle **650**, constructed according to the principles of a preferred embodiment of the present invention, as inverse de Laval nozzle,

applied to retard a fast fluid-flow **651**, streaming with a high M-velocity M_{651}, higher than the specific M-velocity $M_* = \sqrt{(\gamma-1)/\gamma}$. Convergent-divergent jet-nozzle **650** has the sectional shape mirror-symmetrically congruent to the sectional shape of the modified convergent-divergent jet-nozzle **610**, shown in **Fig. 6a (A) Shape**, and oriented to oncoming fluid-flow **651** in the back direction. Namely, the shaped tunnel of the inverse convergent-divergent jet-nozzle **650** has opposite walls **6B.WALLS**, which are either formed by or at least supplied with a surface matrix **6B.MATRIX** of densely-arranged elemental thermoelectric devices **6B.TED**. The triplet of dots **6B.DOT** symbolizes that the elemental thermoelectric devices **6B.TED** are arranged unbrokenly. A convergent funnel **652** having open inlet is as inverse divergent exhaust tailpipe **614 (Fig. 6a (A) Shape**), narrow throat **653** comprises point **658** of the narrowest cross-section, and divergent exhaust tailpipe **654** is as inverse convergent funnel **612**. Convergent funnel **652**, narrow throat **653**, and divergent exhaust tailpipe **654** have not real separation features between them. For the purpose of the present patent application narrow throat **653** is specified as a fragment of the inner tunnel having imaginary inlet **6531** and outlet **6532**, wherein the term "principal interval" of x-axis has a sense as corresponding to the interval occupied by the specifically shaped tunnel, i.e. at least comprising narrow throat **653**.

Fig. 6b (Graph), in conjunction with **Fig. 6b (A) Shape**, is a schematic graphic illustration of the distribution of the fluid **651's** three parameters: headway velocity **660.u,** static pressure **670.P**, and temperature **680.T** along the length of nozzle **650** calculated according to the condition of flow continuity *Eq. (6.0)* to provide a linear decrease in M-velocity of the flow. The linear function of M-velocity is not shown here.

The narrowest cross-section of the throat **653 provides the "critical condition" point 658**, triggering the inverse de Laval jet-effect, according to the condition of flow continuity Eq. (6.0), that is observed as an effect of flow slowing, when the flow moves along convergent funnel **652**, and further slowing, when the flow moves through the divergent stage of convergent-divergent jet-nozzle **650** downstream-behind the critical condition point **658**. For the purposes of the present patent application, the term "de Laval retarding-effect" is introduced as relating to the inverse de Laval jet-effect. Fast fluid-flow **651** moves along convergent funnel **652**, where, ahead of the critical condition point **658** of narrow throat **653**, the velocity falls **661**, and the pressure and temperature pick up, correspondingly **671** and **681**. The velocity falls **661** such that M-velocity M_{663}, corresponding to marker **663**, reaches the specific M-velocity $M_* = \sqrt{(\gamma-1)/\gamma}$ at the critical condition point **658**. Fluid-flow **651** exits throat **653** and enters the widening divergent exhaust tailpipe **654**, where fluid-flow **651** is subjected to an increase of

cross-sectional area, and this action is optimized such that the decrease of M-velocity **662** is accompanied by a substantially smoothed increase of the pressure and temperature, **672** and **682**, correspondingly. Slow hot-and-compressed fluid at position **656** outflows from wide exhaust tailpipe **654**. Again, the smoothed change of static pressure **670.P** provides suppression of unwanted Mach waves. In practice, the suppression of Mach waves provides suppression of undesired vibrations that, in particular, especially important for a fast decelerating flying vehicle.

In view of the foregoing description referring to **Fig. 6b**, it will be evident to a person skilled in the art that, on the one hand, to trigger the de Laval retarding-effect the high M-velocity M_{651} must be low sufficient to reach the specific M-velocity M_* while slowing in convergent funnel **652** and the convergent stage of throat **653**. On the other hand, taking into account that, in practice, for the case wherein fluid-flow **651** is an airflow, the M-velocity is distributed in the direction normal to an adjacent surface such that decreases almost down to zero at the surfaces of convergent-divergent jet-nozzle **650's walls 6B.WALLS**. Thus, a certain portion of fast fluid-flow **651** at the critical condition point **658** moves with the effective M-velocity equal to the specific M-velocity M_* and is subjected to a convergent-divergent reshaping and to forcedly established distributed temperature in throat **653**, thereby, the conditions for the de Laval retarding-effect triggering is satisfied for any high M-velocity M_{651}, higher than the specific M-velocity M_*.

In view of the foregoing description referring to **Figs. 6a** and **6b**, the de Laval jet-effect and the de Laval retarding-effect, both observed in the case of a converging flow, are specified as the following. The de Laval jet-effect is specified as an effect of a convergent flow portion convective acceleration, occurring, when the convergent flow portion moves with M-velocities lower than the specific M-velocity upstream-afore the critical condition point, reaches the specific M-velocity at the critical condition point, and moves with M-velocities higher than the specific M-velocity downstream-behind the critical condition point; and the de Laval retarding-effect is specified as an effect of a convergent flow portion warming and slowing, occurring, when the convergent flow portion moves with M-velocities higher than the specific M-velocity upstream-afore the critical condition point, reaches the specific M-velocity at the critical condition point, and moves with M-velocities lower than the specific M-velocity downstream-behind the critical condition point.

For the purposes of the present patent application, the terms "Venturi M-velocity", "de Laval M-velocity", "de Laval low M-velocity", and "de Laval high M-velocity" should be understood as the following:

- a Venturi M-velocity is defined as an M-velocity, lower than the specific M-velocity M_* and low sufficient to cross a narrow throat with said M-velocity, lower than the specific M-velocity M_*;
- a de Laval low M-velocity is defined as an M-velocity lower than the specific M-velocity M_* and high sufficient to reach the specific M-velocity M_* at the critical condition point x_*;
- a de Laval high M-velocity is defined as an M-velocity higher than the specific M-velocity M_* and low sufficient to reach the specific M-velocity M_* at the critical condition point x_*; and
- a de Laval M-velocity is at least one of the de Laval low M-velocity and the de Laval high M-velocity.

In view of the foregoing description referring to **Fig. 6b**, it will be evident to a person skilled in the art that one can optimize the specifically shaped tunnel of convergent-divergent jet-nozzle **650** providing such conformity of the cross-sectional area of the open inlet and the forcedly established temperature distribution with the de Laval high M-velocity of flowing fluid crossing the open inlet, that the flowing fluid M-velocity is substantially smooth at the entering the open inlet. Furthermore, one can control the cross-sectional area of the open inlet and the forcedly established temperature distribution, according to the condition of flow continuity Eq. (6.0), providing conformity of the thermodynamic conditions at the open inlet with the variable M-velocity of the entering flowing fluid. This may become important, for example, to suppress vibrations of a fast slowing vehicle.

Two-Stage Convergent-Divergent Jet-Nozzle

Fig. 6c is a schematic illustration of a two-stage convergent-divergent jet-nozzle **690** having an open inlet **6910** exposed to an incoming fast fluid flow **691**, streaming with a high M-velocity M_{691}, higher than the specific M-velocity $M_* = \sqrt{(\gamma-1)/\gamma}$, i.e. with a de Laval high M-velocity. Two-stage convergent-divergent jet-nozzle **690** comprises an inner tunnel, constructed according to the principles of a preferred embodiment of the present invention, having opposite walls **6C.WALLS**, which are either formed by or at least supplied with a surface matrix **6C.MATRIX** of densely-arranged elemental thermoelectric devices **6C.TED**. The triplet of dots **6C.DOT** symbolizes that the elemental thermoelectric devices **6C.TED** are arranged

unbrokenly. The inner tunnel comprises the first and second convergent-divergent stages, separated by a divergent-convergent (widened) reservoir (cavity) **694**. The first convergent-divergent stage performs the first-stage convergent inlet-funnel **692** gradually turning into the first-stage narrow convergent-divergent throat **693** having a local narrowest cross-section providing the first critical condition point **6981** and having an inverse-funnel shaped pipe leading to an open first-stage outlet **6930** adjacent to the widened reservoir **694**. The second convergent-divergent stage comprises the second-stage narrow throat **696**, having an open second-stage inlet **6960** adjacent to the widened reservoir **694**, a local narrowest cross-section providing the second critical condition point **6982**, the second-stage divergent exhaust tailpipe **697**, and an open outlet **6970**.

Incoming fast fluid-flow **691** is gradually slowing down, becoming warmer and more thickened and compressed as moving along the first convergent-divergent stage to the widened reservoir **694**. Then, slow hot-and-compressed fluid **695** further movies through the second convergent-divergent stage. The fluid flow is accelerating as moving through throat **696**, where exceeds the specific M-velocity $M_* = \sqrt{(\gamma-1)/\gamma}$ downstream-behind the second critical condition point **6982**.

The first and second convergent-divergent stages of the inner tunnel are characterized by cross-sectional area profile functions $A_1(x)$ and $A_2(x)$ of distance parameter x, correspondingly, such that:

$$A_1(x) = \frac{A_{*1}\sqrt{(\gamma-1)RT_1(x)}}{u_1(x)}\left(\frac{2RT_1(x)+u_1^2(x)}{(\gamma+1)RT_1(x)}\right)^{\frac{\gamma+1}{2(\gamma-1)}} \qquad \text{Eq. (6.1)}$$
$$x_{a,1} < x < x_{b,1}$$

$$A_2(x) = \frac{A_{*2}\sqrt{(\gamma-1)RT_2(x)}}{u_2(x)}\left(\frac{2RT_2(x)+u_2^2(x)}{(\gamma+1)RT_2(x)}\right)^{\frac{\gamma+1}{2(\gamma-1)}\frac{\gamma+1}{2(\gamma-1)}} \qquad \text{Eq. (6.2)}$$
$$x_{a,2} < x < x_{b,2}$$

where

$x_{a,1}$ and $x_{b,1}$ are x-coordinates of the open inlet **6910** and the open first-stage outlet **6930**, correspondingly, of the first convergent-divergent fragment,

$x_{a,2}$ and $x_{b,2}$ are x-coordinates of the open second-stage inlet **6960** and the open outlet **6970**, correspondingly, of the second convergent-divergent fragment,

A_{*1} and A_{*2} are the minimal cross-sectional areas of the first-stage narrow throat **693** and the second-stage narrow throat **696**, correspondingly, and the functions, on the one hand, $u_1(x)$ and $T_1(x)$ and, on the other hand, $u_2(x)$ and $T_2(x)$ $u_2(x)$ are representing profiles of the fluid flow headway velocities and absolute temperatures in the first and second convergent-divergent stages, correspondingly, along the inner tunnel length. The equations *Eq. (6.1)* and *Eq. (6.2)* are particular cases of the condition of flow continuity *Eq. (6.0)* described hereinbefore with references to **Figs. 6a** and **6b**, correspondingly. The cross-sectional area profile $A_{ca}(x)$ of the widened reservoir **694** is such that a function $A(x)$, which is composed of sequentially concatenated cross-sectional area profile functions $A_1(x)$, $A_{ca}(x)$, and $A_2(x)$, is smooth.

Jetstream **699**, outflowing through divergent exhaust tailpipe **697**, is faster and colder than slow hot-and-compressed fluid **695**, yet to be entered into the second convergent-divergent stage, as described hereinbefore tracing after incoming compressed and hot airstream **611** with reference to **Figs. 6a** and **6b**. Fast outflowing jetstream **699** has a cross-section wider than incoming fast fluid-flow **691** at the input of convergent inlet-funnel **692**. So, the M-velocity M_{699} of fast outflowing jetstream **699** is higher than the M-velocity M_{691} of fast fluid-flow **691**, according to the condition of flow continuity *Eqs. (6.1)* and *(6.2)*.

Thereby, two-stage convergent-divergent jet-nozzle **690** operates as a jet-booster based on the enhanced de Laval jet-effect launching outflowing jetstream **699**, which is faster than the fast fluid-flow **691** incoming with the de Laval high M-velocity M_{691}, i.e. higher than the specific M-velocity $M_* = \sqrt{(\gamma-1)/\gamma}$. This is one more teaching of the present invention.

In view of the foregoing description referring to **Figs. 6a, 6b,** and **6c** in combination with the foregoing description referring to **Figs. 5p** and **5q**, it will be evident to a person skilled in the art that, if a tunnel is preliminary optimized for a certain fluid, laminarly flowing within the tunnel with certain distributions of velocity and thermodynamic parameters, but, actually, the fluid is characterized by other thermodynamic parameters and enters the tunnel with another velocity, it remains possible to optimize the fluid stream within the shaped tunnel by forced establishing the temperature distribution of the fluid stream using the Peltier effect originated by a surface matrix of densely arranged elemental TE devices built-in into the walls of the tunnel.

Optimal Implementation of Convergent-Divergent Jet-Nozzle

Fig. 7 shows comparative graphs **700** for the dependencies of the nozzle tunnel extension ratio vs. the airflow M-velocity in an adiabatic process, calculated, on the one hand, using the classical model described, in particular, in **D11** and, on the other hand, suggested in prior arts

A01, A02, and A03 equation *Eq. (1.a)*, namely, curves **703** and **704** correspondingly; wherein the vertical axis **701** is the ratio A/A_*, and the horizontal axis **702** is the airflow M-velocity in an adiabatic process measured in temperature-dependent Mach numbers. The dashed curve **703** is the convergent-divergent cross-sectional area ratio A/A_* profile vs. the airflow M-velocity, calculated using classical equations derived from the Euler equations of fluid motion. The solid curve **704** is the convergent-divergent cross-sectional area ratio A/A_* profile vs. the airflow M-velocity of an adiabatic motion, calculated using the prior art equation Eq. (1.a) derived from the specified equations of fluid motion in an adiabatic process described in **A01**, **A02**, and **A03**. The critical condition point **708** corresponds to the specific M-velocity $M_* = \sqrt{(\gamma-1)/\gamma} \approx 0.5345$. Comparative graphs **700** show that one needs in a substantially extra-widened nozzle tunnel **704** to reach the airflow M-velocities substantially higher than 1 *Mach*.

One of the primary ideas of the present invention is that the desired improved dependence **704** is reachable using an arbitrary smoothly shaped tunnel if the temperature distribution along **the tunnel's walls is forcedly controlled to satisfy the** condition of flow continuity *Eq. (6.0)*.

Therefore, a convergent-divergent jet-nozzle, constructed according to an exemplary embodiment of the present invention, allows for a controllably-increased efficiency of the jet-effect for use at high-subsonic, transonic, supersonic, and hypersonic velocities that can be applied to rocket nozzle design.

Taking into account The Bernoulli Theorem written in the form via M-velocity:

$$\frac{T_0}{T} = \left(\frac{P_0}{P}\right)^{\frac{\gamma-1}{\gamma}} = \left(\frac{\rho_0}{\rho}\right)^{\gamma-1} = 1 + M^2\frac{\gamma}{2} \qquad \text{Eq. (7.1),}$$

where P_0, ρ_0, and T_0 are so-called stagnation thermodynamic parameters: the static pressure, the mass density, and the absolute temperature, and M is the M-velocity, one can derive conditions for the stagnation thermodynamic parameters and the thermodynamic parameters of the fluid flow: P_e, ρ_e, and T_e are so-called stagnation thermodynamic parameters: the static pressure, the mass density, and the absolute temperature, all at the exhaust-nozzle outlet to design an improved convergent-divergent nozzle to originate the enhanced de Laval effect. The exhaust-nozzle outlet M-velocity M_e is bonded with the ratios P_0/P_e and T_0/T_e as follows:

$$M_e = \sqrt{\frac{2}{\gamma}}\sqrt{\left(\frac{P_0}{P_e}\right)^{\frac{\gamma-1}{\gamma}} - 1} \qquad \text{Eq. (7.1a)}$$

$$\frac{P_0}{P_e} = \left(\frac{2+\gamma M_e^2}{2}\right)^{\frac{\gamma}{\gamma-1}} \qquad \text{Eq. (7.1b)}$$

$$\frac{T_0}{T_e} = \left(\frac{2+\gamma M_e^2}{2}\right) \qquad \text{Eq. (7.1c)}$$

$$\frac{\rho_0}{\rho_e} = \left(\frac{2+\gamma M_e^2}{2}\right)^{\frac{1}{\gamma-1}} \qquad \text{Eq. (7.1d)}$$

In contrast to a frequently used condition, saying that both: the de Laval jet-effect and the velocity of sound are reachable when the ratio P_0/P_e is of 1.893, equation *Eq. (7.1b)* shows that, on the one hand, to obtain the de Laval jet-effect [i.e. condition $M_e \geq M_*$] for air using a nozzle tunnel having an optimal convergent-divergent shape, one must provide the ratio P_0/P_* at least of 1.893, and, on the other hand, to accelerate an air portion up to the velocity of sound [i.e. $M_e = 1$], one must provide the ratio P_0/P_e at least of 6.406. Equation Eq. (7.1c) says that, on the one hand, to obtain the de Laval jet-effect for air utilizing a nozzle tunnel having an optimal convergent-divergent shape, one must provide the ratio T_0/T_* at least of 1.2; and, on the other hand, to accelerate an air portion up to the velocity of sound, one must provide the ratio T_0/T_e at least of 1.7. So, the principle condition either $1.893 < P_0/P_e < 6.406$ or/and $1.2 < T_0/T_e < 1.7$ can provide the de Laval jet-effect occurring without the phenomenon of shock sound-wave emission that is one of the primary principles of the present invention. Thus, a convergent-divergent jet-nozzle tunnel, constructed according to an exemplary embodiment of the present invention and exploited in accordance with the principle conditions, allows for an optimal implementation and efficient use of an enhanced jet-effect at de Laval M-velocities.

Use of Optimal Convergent-Divergent Jet-Nozzle

In view of the foregoing description referring to **Figs. 6a**, **6b**, and **6c** in combination with the description of sub-**paragraphs** "Horn as Sound-**Booster**" referring to prior art **Fig. 1n** and "External Ear as Sound Booster" **referring to prior art Fig. 1L**, it will be evident to a person skilled in the art that:

- an optimized at least one of converging, divergent, convergent-divergent, and two-stage convergent-divergent nozzle can play the role of an enhanced acoustic waveguide capable to:

- reduce a turbulent component of fluid motion accompanying acoustic waves and causing dissipation of a propagating sound; and
- amplify the intensity of acoustic waves at the expense of both the heat energy and the turbulence of fluid and so to boost the loudness of sound;

and

- the exponentially-divergent horn **n.C1** of gramophone **1n.C** (**Fig. 1n**) functions as the divergent exhaust tailpipe **614** of the convergent-divergent nozzle **610** (**Fig. 6a**), but not optimized according to the condition of flow continuity *Eq. (6.0)* yet.

Optimized Horn For Gramophone

Fig. 7a case (A) shows schematically a divergent horn **7a.A**, submerged in a molecular fluid (for the sake of concretization, the molecular fluid is air) and exposed to a portion of sound **7a.A0** entering an open inlet **7a.A1** and outflowing from the open outlet **7a.A2** of the divergent horn **7a.A**. The specific conveying motion of the air mass density is interpreted as composed of two complementary alternating movements of positive and negative changes of air mass density, wherein both alternating movements are in the same direction (that is the direction of sound propagation) and, when in open space or at the open inlet **7a.A1**, with the M-velocity of 1 Mach. The specific conveying motion of the air mass density is subjected to influence within the divergent horn **7a.A**. The cross-sectional area of the divergent horn **7a.A** varies along the divergent horn **7a.A** length, i.e. along a sagittal axis **7a.A5**, in accordance with the condition of flow continuity *Eq. (6.0)* such that to provide substantially laminar motion of the positive and negative changes of air mass density within the divergent horn **7a.A** due to the enhanced de Laval jet-effect applied to the moving positive and negative changes of air mass density, moving with the high M-velocity, higher than the specific M-velocity. In particular, when the open sound-inlet has a cross-sectional area A_{in}, the cross-sectional area profile $A(x)$ is a divergent cross-sectional area profile function $A_{horn}(x)$ expressed as:

$$A_{horn}(x) = \frac{A_{in}\sqrt{\gamma RT(x)}}{u(x)}\left(\frac{2RT(x)+u^2(x)}{(2+\gamma)RT(x)}\right)^{\frac{\gamma+1}{2(\gamma-1)}}, \qquad x_a < x < x_b$$

where γ is an adiabatic compressibility parameter of the fluid, x_a and x_b are x-coordinates of the open sound-inlet and open sound-outlet, correspondingly, and $u(x)$ is a monotonically-increasing gradually-smooth function of x representing a profile of the sound propagation velocity, i.e. a conveying velocity of the fluid tiny portion moving within and through the

divergent horn (the fluid tiny portion is the mentioned interpretation of the positive and negative changes of air mass density associated with the propagating sound).

The enhanced de Laval jet-effect, in particular, results in extra-acceleration of the laminar motion of the positive and negative changes of air mass density within the divergent horn **7a.A** at the expense of the air heat understood in the wide sense including the concomitant turbulence inherently accompanying the sound. Thus, the portion of sound **7a.A0** becomes boosted due to the enhanced de Laval jet-effect.

In practice, sometimes, not optimized functioning of the divergent horn **7a.A** occurs at least because of other portions **7a.A6** and **7a.A7** of ambient sound enter the divergent horn **7a.A** through the sidewalls of the divergent horn **7a.A**. To prevent the undesired reason, the divergent horn **7a.A** is further supplied with a matrix TE device **7a.A4** covering the surface of the divergent horn **7a.A.** The matrix TE device **7a.A4**, when functioning like the multi-module thermoelectric device **5R.DEVICE** comprising a matrix of a multiplicity of N **ELEMENTAL DETECTORS OF SOUND 5R.02** which results in the zero **5R.4.OUTPUT** as described hereinabove referring to **Fig. 5r**, is capable to isolate the entered portion **7a.A0** from the interfering portions **7a.A6** and **7a.A7**.

It will be evident for a person, who has studied the present invention, that the **ELEMENTAL SOURCE OF SOUND 5P.0A** described hereinabove referring to **Fig. 5P Case (A)**, can play the role of a source of the sound **7a.A0**, and so the **ELEMENTAL SOURCE OF SOUND 5P.0A** supplied with the divergent horn **7a.A** performs an efficiently functioning megaphone.

Phonendoscope and Sound Booster

Fig. 7a cases (B) and (C) are schematic illustrations of two-stage convergent-divergent nozzles **7a.B** and **7a.C**, destined for amplifying the intensity of an entering portion of sound **7a.B0** and **7a.C0**, correspondingly. The enhanced phonendoscope **7a.B** and sound booster **7a.C**, both constructed according to the principles of the present invention, comprise common configurational elaborated features, and while the two-stage convergent-divergent nozzle **7a.B** is configured to be used as an enhanced phonendoscope **7a.B**, the two-stage convergent-divergent nozzle **7a.C** is configured to have a corpus **7a.C1** ergonomically adapted to a **human's ear canal, thereby, allowing to** be used as a sound booster **7a.C** ergonomically **adapted to a human's ear 7a.EAR**. The mentioned common configurational elaborated features are related to optimized inner canals of the nozzles **7a.B** and **7a.C** which are the optimized two-stage convergent-divergent tunnels **7a.B2** and **7a.C2**, having:

- an open sound-inlet **7a.B5** and **7a.C5** of the cross-sectional area A_{IN} ,

- an open sound-outlet **7a.B6** and **7a.C6** of the cross-sectional area A_{OU}, and
- shaped portions of varying cross-sections as follows:
  - a convergent funnel **7a.B41** and **7a.C41**,
  - a first-stage narrow throat **7a.B42** and **7a.C42** having a local minimal cross-sectional area A_{th1} and a first-stage open sound-outlet **7a.B50** and **7a.C50**,
  - a divergent-convergent (widened) cavity **7a.B43** and **7a.C43** having a local maximal cross-sectional area A_{ca},
  - a second-stage narrow throat **7a.B44** and **7a.C44** having a second-stage open sound-inlet **7a.C60**, a local minimal cross-sectional area A_{th2}, wherein A_{th2} at most equal to A_{th1}, and
  - divergent funnel **7a.B45** and **7a.C45**, having an open sound-outlet **7a.B6** and **7a.C6**,

correspondingly.

Sound **7a.C0**, when entering the open inlet **7a.C5**, becomes subjected to the action of the optimized convergent-divergent tunnel **7a.C2** such that,

- first, when the sound **7a.C0** propagates through convergent funnel **7a.C41**, the sound intensity becomes,
  - on the one hand, decreased because the mass density change conveying with the velocity of sound becomes subjected to retarding due to the de Laval retarding effect applied to the mass density change moving with the high velocity, higher than the specific M-velocity, and
  - on the other hand, increased due to:
    - superposition of spatially distributed portions of sound becoming concentrated and joint in-phase, thereby, resulting in constructive interference,
    - transformation of the internal heat energy of fluid into the acquired power of sound, as a manifestation of the Venturi effect, applied to longitudinal oscillation motion with the particle velocity, and
    - suppression of concomitant turbulence, power of which, in the final analysis, becomes transformed into the acquired power of sound, as a phenomenon accompanying the Venturi effect applied to longitudinal oscillation motion with the particle velocity;

  and
- second, interrelations between the cross-sectional areas A_{in}, A_{th1}, A_{ca}, A_{th2} and A_{ou} satisfying conditions as follows:

(a) $\frac{A_{in}}{A_{th1}} \geq \sqrt{\left(\frac{\gamma-1}{\gamma}\right)\left(\frac{2+\gamma}{\gamma+1}\right)^{\frac{\gamma+1}{(\gamma-1)}}}$,

so, when the sound propagates through the first-stage narrow throat **7a.C42**, the sound intensity is predetermined by the conveying velocity u_{convey} and particle velocity $u_{particle}$, wherein the local conveying M-velocity is of $M_* = \sqrt{(\gamma-1)/\gamma}$ when crossing the narrowest cross-section within the first-stage narrow throat **7a.C42**;

(b) $A_{ca} > A_{th1}$,

so, when the sound propagates through widened cavity **7a.C43**, the local conveying M-velocity becomes lower than the specific M-velocity M_*, due to the de Laval retarding effect;

(c) $A_{ca} > A_{th2}$,

so, when the sound propagates through the second-stage narrow throat **7a.C44**, the local conveying M-velocity reaches the specific M-velocity M_*, due to the de Laval jet-effect;

(d) $A_{th1} \geq A_{th2}$, and

(e) $\frac{A_{ou}}{A_{th2}} > \sqrt{\left(\frac{\gamma-1}{\gamma}\right)\left(\frac{2+\gamma}{\gamma+1}\right)^{\frac{\gamma+1}{(\gamma-1)}}}$,

so, when the sound propagates further through divergent funnel **7a.C45**, the sound intensity becomes increased because the mass density change conveying with the varying velocity of sound becomes subjected to extra-acceleration due to the enhanced de Laval jet-effect, optimized to suppress turbulent component of the complicated movement of fluid when conveying the sound and applied to the mass density change moving with the high velocity, higher than the specific M-velocity; this effect of sound boosting is similar to that which occurs when using a classic gramophone supplied with an exponentially-divergent horn as described hereinabove in **THE BACKGROUND OF THE INVENTION** referring to prior art **Fig. 1n**, but now the divergent funnel configuration is optimized according to the condition of flow continuity *Eqs. (6.1) and (6.2)*, namely, the cross-sectional area profile smooth function $A(x)$ is composed of sequentially concatenated cross-sectional area profile functions $A_1(x)$, $A_{ca}(x)$, and $A_2(x)$, wherein:

- $A_1(x)$ is cross-sectional area profile function of the first convergent-divergent fragment, which provides for the enhanced de Laval retarding-effect resulting in deceleration of the fluid tiny portion moving laminarly,
- $A_2(x)$ is cross-sectional area profile function of the second convergent-divergent fragment, which provides for the enhanced de Laval jet-effect resulting in acceleration of the fluid tiny portion moving laminarly, and
- the cross-sectional area profile functions $A_1(x)$ and $A_2(x)$ are given by the equations expressed as:

$$\begin{cases} A_1(x) = \dfrac{A_{th1}\sqrt{(\gamma-1)RT_1(x)}}{u_1(x)}\left(\dfrac{2RT_1(x)+u_1^2(x)}{(\gamma+1)RT_1(x)}\right)^{\frac{\gamma+1}{2(\gamma-1)}}, & x_{a,1} < x < x_{b,1} \\ A_2(x) = \dfrac{A_{th2}\sqrt{(\gamma-1)RT_2(x)}}{u_2(x)}\left(\dfrac{2RT_2(x)+u_2^2(x)}{(\gamma+1)RT_2(x)}\right)^{\frac{\gamma+1}{2(\gamma-1)}}, & x_{a,2} < x < x_{b,2} \end{cases}$$

where:

$x_{a,1}$ and $x_{b,1}$ are x-coordinates of the open sound-inlet and the first-stage open sound-outlet, correspondingly, of the first convergent-divergent fragment,

$x_{a,2}$ and $x_{b,2}$ are x-coordinates of the second-stage open sound-inlet and open sound-outlet, correspondingly, of the second convergent-divergent fragment,

A_{th1} and A_{th2} are local minimal cross-sectional areas of narrow throats of the first and second convergent-divergent fragments, correspondingly;

$u_1(x)$ is a monotonically-decreasing gradually-smooth function of x, representing the conveying velocity u_{convey} within the first convergent-divergent fragment,

$T_1(x)$ is a monotonically-increasing gradually-smooth function of x, representing the temperature of the fluid within the first convergent-divergent fragment,

$u_2(x)$ is a monotonically-increasing gradually-smooth function of x, representing the conveying velocity u_{convey} within the second convergent-divergent fragment,

$T_1(x)$ is a monotonically-decreasing gradually-smooth function of x, representing the temperature of the fluid within the first convergent-divergent fragment,

$A_{ca}(x)$ is cross-sectional area profile function of the divergent-convergent cavity defined between $x_{b,1}$ and $x_{a,2}$ such that providing for the enhanced Venturi effect as a gradually-smooth function $u_{ca}(x)$ of x, representing a velocity profile of the tiny portion of the fluid moving in the divergent-convergent cavity between the first and second narrow throats, is such that an associated M-velocity function $M_{ca}(x)$, remains lower than the specific M-velocity $M_* = \sqrt{(\gamma-1)/\gamma}$; and

- $u_1(x)$, $u_{ca}(x)$, and $u_2(x)$ are such that, when sequentially-concatenated, as a whole form a gradually-smooth function $u(x)$ of x, representing a velocity profile of the fluid tiny portion moving within and through the two-stage convergent-**divergent nozzle's** through-hole tunnel-waveguide;

thereby, the conditions altogether providing for that, a portion of the propagating sound, entering the open sound-inlet, propagating through the two-stage convergent-divergent tunnel, and becoming launched from the open sound-outlet, becomes characterized by an increased Umov-vector and so has an amplified loudness.

In view of the foregoing description of the sub-**paragraphs** "Optimized Horn For Grammophone" referring to **Fig. 7a case (A) and** "Phonendoscope and Sound Booster" **referring to Fig. 7a cases (B) and (C)** in combination with the description of sub-**paragraphs:** "Sound as Complicated Movement in Molecular Fluid" **referring to prior art Fig. 1n and** "External Ear as Sound Booster" **referring to prior art Fig. 1L**, it becomes evident to a person who has studied the present patent application that, conceptually:

- The external ear **1L.0** (**Fig. 1L**) functions as the described passive sound booster **7a.C**, but not optimized for suppression of concomitant turbulences according to the condition *Eq. (6.0)* yet;
- An optimized two-stage convergent-divergent nozzle, optimized for suppression of concomitant turbulences according to the condition of flow continuity Eq. *(6.0)*, can be adapted to a diversity of applications as a wave-guiding and sound-amplifying nozzle for detectors or launchers of sound, for instance:

- the optimized two-stage convergent-divergent nozzle **7a.B** can be utilized as a phonendoscope; and
- the optimized two-stage convergent-divergent nozzle **7a.C** can be miniaturized to become adapted to the size of **a human's ear canal and play a role of a** passive sound booster utilized for amplifying the loudness of a portion of ambient sound;

and

- An optimized divergent horn, optimized for widening a front of sound accompanied by suppression of concomitant turbulences according to the condition of flow continuity *Eq. (6.0)*, can be scaled to play the role of an enhanced generalized gramophone utilized for boosting a sound launched by a source of acoustic waves.

It will be also evident for a person, who has studied the present invention, that each of the two-stage convergent-divergent nozzles **7a.B** and **7a.C**, when supplied with the two-stage sound amplifier **5S.DEVICE** described hereinabove referring to **Fig. 5s**, can play the role of an efficiently functioning hearing aid.

Compressor supplied by Convergent-Divergent Jet-Nozzle

Fig. 7b, having two parts: **Case (A)** and **Case (B)**, is a schematic illustration of a pressure-transformer **710.P** and a heat-transformer **710.H**, correspondingly, both constructed according to the principles of the present invention, to accelerate a compressed and heated air portion.

In pressure-transformer **710.P**, the optimized convergent-divergent jet-nozzle **710** with the critical condition point **718** comprises a reservoir **712** where an air portion **711** is compressed and thereby heated due to a piston **714**. As it was described hereinabove referring to **Fig. 7**, to trigger the enhanced de Laval jet-effect, one needs either to compress air portion **711** up to the static pressure $P_0 = 1.893 \times P_a$, where P_a is the ambient pressure (for instance, $P_a = 1\ bar$), or, alternatively, to heat the air portion **711** up to the absolute temperature $T_0 = 1.2 \times T_a$, where T_a is the ambient temperature (for instance, $T_a = 298\ K$), wherein the static pressure P_0 and increased temperature T_0 are interrelated. In this case, if the divergent portion **710** of the optimized de Laval nozzle has the outlet cross-sectional area wider than the cross-sectional area at the critical condition point **718** by the factor $1/M_* = \sqrt{\gamma/(\gamma-1)}$, the M-velocity of the outflowing stream **713** is about $1\ Mach$. To compress air portion **711** up to pressure $P_0 = 1.893\ bar$ one needs to consume the energy E_0 estimated as $(P_0 - P_a)V_0$, where V_0 is the volume of the gas reservoir **712**. For $V_0 = 1m^3$, the energy E_0 is estimated as $E_0 \approx 0.9 \times 10^5\ J = 90\ kJ$. The volume V_0 is composed of approximately $n \approx$

$(P_0/P_a) \times 1000/22.4 = 286$ moles of gas. When air portion **711** is accelerated and expanded in de Laval-like nozzle **710**, it acquires kinetic energy at the expense of thermodynamically related pressure and temperature decrease; wherein the pressure decreases from P_0 to P_a and the temperature decreases from T_0 to T_a. Again, consider the air portion **711** acceleration in hypothetically optimal convergent-divergent jet-nozzle **710** such that the velocity of the outflowing stream **713** is almost as the speed of sound, i.e. the exhaust M-velocity is of $M_e \approx 1$, i.e. such that $T_0/T_e = 1.7$ and $(T_0 - T_e) = T_0(1 - 1/1.7) = 0.412T_0$, where T_e is the absolute temperature of the cold outflowing stream **713** wherein the temperature difference $(T_0 - T_e) = 0.412T_0$ is estimated as $123\,C$. In this case, the acquired kinetic energy equals $K = n \times (T_0 - T_e)R$ that is estimated as:

$K = n \times 0.412T_0R \approx 286 \times 0.412 \times 298 \times 278 \approx 9{,}761{,}674\,J = 9{,}762\,kJ$.

This estimation shows that, taking into account a 15% net-efficiency of an engine pushing the piston **714**, the triggered acquired kinetic energy K may exceed the triggering consumed energy E_0 at least at subsonic velocities by the factor of about 16 times. The acquired kinetic energy can be applied to a vehicle motion or to an engine for electricity generation with positive net-efficiency. On the other hand, the acquiring of kinetic energy is accompanied by the air temperature decrease, therefore, such a convergent-divergent jet-nozzle can be applied to cooling of a vehicle engine as well as be used either for electricity harvesting by means of a Peltier element operating as a thermoelectric generator and/or as an effective condenser of vapor to water.

In heat-transformer **710.H**, the optimized convergent-divergent jet-nozzle **710.B**, optionally, unbrokenly covered with a multiplicity of thermoelectric devices **717.B** similar to the surface matrix **6A.MATRIX** of densely-arranged elemental thermoelectric devices **6A.TED** described hereinabove referring to **Fig. 6a**, has the outlet cross-sectional area wider than the cross-sectional area at the critical condition point **718.B** by the factor $1/M_* = \sqrt{\gamma/(\gamma - 1)}$ and supplied with a reservoir **712.B**, a wall of which is covered with another multiplicity of thermoelectric devices **714.B** and has a multiplicity of relatively long and narrow through-hole pipes **715.B**. Shape of the through-hole pipes **715.B** is not optimized for a laminar motion of flow neither if entering the reservoir **712.B** nor if outflowing back to ambient space.

Inner air portions **711.B** and outer air portions **716.B**, both are subjected to the functioning of the multiplicity of thermoelectric devices **714.B** such that, on the one hand, the inner air portions **711.B** are heated and thereby compressed and, on the other hand, the outer air portions **716.B** are cooled and thereby thickened. When the absolute temperature T_0 of the

inner portions **711.B** is kept equal $1.2 \times T_a$ [i.e. $T_0 = 357.6K$, i.e. $\Delta T = (T_0 - T_a) = 59.6\ C$ that, normally, is reachable by a thermoelectric device], the condition for triggering the enhanced de Laval jet-effect becomes satisfied. The optional covering with the multiplicity of thermoelectric devices **717.B** is for controlling the temperature distribution dependent on the velocity of the inner portions **711.B**, which (the velocity) in turn, is determined by the functioning of the multiplicity of thermoelectric devices **714.B**; the controlling is to provide laminarity of flow **719.B** within the optimized convergent-divergent jet-nozzle **710.B**. Points **718.B** symbolize that the thermoelectric devices **717.B** cover the optimized convergent-divergent jet-nozzle **710.B** unbrokenly. The asymmetry of conditions that, on the one hand, the temperature distribution along the relatively long pipes **715.B** is not optimized for a laminar motion of the flow, and on the other hand, the tunnel **710.B** is optimized for a laminar motion of the flow, causes a tendency of the inner air portions **711.B** to move directionally through the optimized convergent-divergent jet-nozzle **710.B**. As a result, the reservoir **712.B** is permanently filled with the fresh outer portions **716.B** via the through-hole pipes **715.B** such that the velocity of the outflowing stream **713.B** is almost as the speed of sound. Optionally, the pipes **715.B** can be fulfilled as valvular conduits (Tesla valves) to increase the efficacy of the jet-nozzle **710.B**.

Again, $T_0/T_e = 1.7$ and $(T_0 - T_e) = T_0(1 - 1/1.7) = 0.412T_0$, where T_e is the absolute temperature of the cold outflowing stream **713.B** wherein the temperature difference $(T_0 - T_e) = 0.412T_0$ is estimated as $123\ C$. In this case, the acquired kinetic energy equals $K = n \times (T_0 - T_e)R$ that is estimated as:

$$K = n \times 0.412T_0R \approx 286 \times 0.412 \times 298 \times 278 \approx 9{,}761{,}674\ J = 9{,}762\ kJ.$$

Taking into account a 15% net-efficiency of the multiplicity of the thermoelectric device, the triggered acquired kinetic energy K may exceed the triggering consumed energy E_0 at least at subsonic velocities by the factor of about **16** times. As the flow **719.B** within the optimized convergent-divergent jet-nozzle **710.B** becomes colder than the ambient fluid, the multiplicity of thermoelectric devices **717.B** can be also used for harvesting of electricity.

In view of the foregoing description referring to **Fig. 7b Case (B)**, it will be evident to a person skilled in the art that, instead of Peltier elements (thermoelectric devices **714.B**), any kind of electric heater (i.e. a thermoelectric device in the broad sense) can be used to increase the temperature of the inner air portions **711.B**, because the inertness of temperature difference controlling is not critical for a steady-established and relatively slow intake of air portions **711.B**.

Flying Capsule as Dragging-Jet Engine

Fig. 7c is a schematic sectional view of a flying capsule corpus **720** in a sagittal plane. Capsule corpus **720**, constructed according to the principles of the present invention, has an outer airfoil side **729** covered with a surface matrix thermoelectric device **729.TED** and inner walls, which are formed by another surface matrix thermoelectric device **722.TED**, in turn, forming a through-hole corridor having:

- an inner converging reservoir **721** as a dragging compressor having an open inlet **725** exposed to ambient wind **724**, and further
- a hypothetically optimal convergent-divergent tunnel **722** with a narrow throat comprising a critical condition point **728** and divergent exhaust tailpipe having an open outlet **726** of area A_e.

The velocity of ambient air **724** relative to capsule **720** is u_a which is substantially lower than the critical condition velocity u_* corresponding to the specific M-velocity $M_* = \sqrt{(\gamma - 1)/\gamma}$. The wind portion **727** enters the inner converging reservoir **721** with a velocity equal to u_{in}. The area A_{in} of inlet **725** is substantially wider than the area A_* **of the throat's cross**-section at the critical condition point **728** such that air portion **727** crosses the area A_* at the critical condition point **728** with the maximal reachable M-velocity equal to the specific M-velocity $M_* = \sqrt{(\gamma - 1)/\gamma}$, and so the enhanced de Laval jet-effect is expected in the divergent exhaust tailpipe having outlet **726**, where the velocity of outflowing jetstream **723** reaches a value u_{723} higher than the velocity u_* corresponding to the critical condition point **728**. In an exemplary embodiment of the present invention, an optimal shape of tunnel **722** and forcibly established temperature distribution along the inner walls using the surface matrix thermoelectric device **722.TED**, both provide that the value u_{723} is lower than the speed of sound u_{sound}. Outflowing jetstream **723** brings the kinetic power acquired at the expense of the flow's warmth. The acquired kinetic power of outflowing jetstream **723** may be high as or even become higher than the power consumed to compensate drag, defined by a drag coefficient corresponding to a concave shape of the inner converging reservoir **721**, and thereby to maintain the flying velocity u_a of capsule **720**. Capsule **720** is interpreted as a motionless dragging-jet engine.

Outer airfoil side **729** of capsule corpus **720** provides laminar-like flowing of wind outer sub-portions **731** and **732**, moving adjacent to outer airfoil side **729** and being subjected to both: forcibly established temperature distribution using the surface matrix thermoelectric device **729.TED** and the Coanda-effect operation and, thereby, attracted to the nearby surfaces of

outer airfoil side **729**. Outflowing jetstream **723** having the decreased static pressure sucks outer sub-portions **731** and **732**. The cumulative confluence of sub-portions **731**, **732**, and **723** constitutes the cumulative jetstream **734**, associated with the airfoil corpus of capsule **720**. In general, the formed cumulative jetstream **734**, composed of sub-portions **731**, **732**, and **723**, is turbulent; however, in an optimal case, the turbulence can be suppressed substantially. For simplicity, consider a case of a laminar-like cumulative jetstream **734**, **"bordered" by** streamlines **733**. On the one hand, the velocities of outer sub-portions **731** and **732**, being lower than the critical condition velocity u_*, are increasing as the attracted outer sub-portions enter the space of cumulative jetstream **734**, where the velocities increase is accompanied by a constriction of outer sub-portions **731** and **732**, in accordance with the condition of flow continuity *Eq. (6.0)*. On the other hand, at outlet **726**, the velocity of inner sub-portion **723** is of value u_{723} higher than the critical condition velocity u_*. According to the condition of flow continuity *Eq. (6.0)*, the velocity of inner sub-portion **723** is decreasing as the sub-portion enters the space of cumulative jetstream **734**, where inner sub-portion **723** is constricting as well. If the case is optimized such that both constrictions are identical, cumulative jetstream **734** is expected to be laminar-like indeed. Bordering streamlines **733** constitute an imaginary convergent-divergent jet-nozzle comprising a narrow throat having the minimal cross-sectional area at the outer critical condition point **738**, where the effective M-velocity of cumulative jetstream **734** reaches the specific value $M_* = \sqrt{(\gamma - 1)/\gamma}$. If, upstream-afore the outer critical condition point **738**, the effective M-velocity of cumulative jetstream **734** is lower than the specific M-velocity M_*, then the M-velocity of cumulative jetstream **734** is increasing as cumulative jetstream **734** moves such that outflowing divergent portion **735** has M-velocity higher than M_* downstream-behind the outer critical condition point **738**; and vice versa, if, upstream-afore the outer critical condition point **738**, the effective M-velocity of cumulative jetstream **734** is higher than the specific M-velocity M_*, then the M-velocity of cumulative jetstream **734** is decreasing as cumulative jetstream **734** moves such that outflowing divergent portion **735** has the M-velocity lower than the specific M-velocity M_* .

In view of the foregoing description referring to **Fig. 7c**, it will be evident to a person skilled in the art that:

- The shape of tunnel **722** and the forcibly established temperature distribution along the inner walls using the surface matrix thermoelectric device **722.TED**, both can be adapted to the velocity u_a of ambient air **724** and optimized to provide that the velocity value u_{723} of outflowing jetstream **723** becomes higher than the speed of sound u_{sound}. As

well, it will be evident to a person skilled in the art that the shape of tunnel **722** and outer airfoil side **729** of capsule **720** and forcibly established temperature distribution along the inner walls using the surface matrix thermoelectric device **729.TED**, both can be optimized to provide that outflowing divergent portion **735** has increasing M-velocity reaching values higher than the specific M-velocity M_*;

- Supplying a flying vehicle or helicopter's propeller blades by nozzles similar to capsule **720** operating as a jet-booster, one could save fuel consumption substantially and even provide a stable motion against a drag and skin-friction resistance entirely with no fuel burning at all. As well, it will be evident to a person skilled in the art that this is not a so-called "Perpetuum mobile", but the use of ambient fluid heat to produce useful motion, strongly according to the Energy Conservation Law. Furthermore, looking ahead referring to **Figs. 9d**, **9e**, and **9f** described hereinbelow, point out that an even number of such jet-boosters, attached to the even number of blades of a helicopter's propeller, result in stabilization of the effective velocities of incoming and outflowing jetstreams associated with the jet-boosters. The predictably equalized velocities enable easier controllable lift-forces when the helicopter is flying speedily;
- The described airfoil capsule can be stationarily exposed to oncoming wind (either natural or artificial) and thereby become applicable to efficient harvesting of electricity providing a positive net-efficiency; and
- One can further aggregate the open outlet of a specifically shaped convergent-divergent tunnel with an engine using the enhanced jet-effect providing an extra-accelerated and extra-cooled jetstream outflowing through the open outlet; wherein the engine is either a jet-engine, and/or a turbo-jet engine, and/or a motor applied to a vehicle, and/or a generator of electricity, and/or a cooler, and/or a Peltier element operating as a thermoelectric generator, and/or vapor-into-water condenser.

Fig. 7d is a schematic sectional view of a flying capsule **740**, constructed according to the principles of the present invention. Flying capsule **740's profile in a sagittal plane has an airfoil** outer contour and a contour of a specifically shaped two-stage inner tunnel. Similar to the flying capsule **720** illustrated hereinbefore referring to **Fig. 7c**, inner and outer walls **748** and **749** of capsule **740's tunnel and outer shell are supplied with forcedly controllable surface matrix** thermoelectric devices **748.TED** and **749.TED**, correspondingly. In contrast to flying capsule **720** illustrated hereinbefore referring to **Fig. 7c**, capsule **740** flies with a de Laval high M-velocity, i.e. higher than the specific M-velocity $M_* = \sqrt{(\gamma - 1)/\gamma}$, and the two-stage inner

tunnel is shaped similar to the tunnel of two-stage convergent-divergent jet-nozzle **690**, described above referring to **Fig. 6c**. Namely, the two-stage inner tunnel comprises two narrow throats providing for two associated critical condition points **741** and **742**. The oncoming fast flow **743** enters the open inlet **744** of the inner tunnel with a de Laval high M-velocity M_{743}, higher than the specific M-velocity M_*. Then flow **743** is gradually slowing down, becoming warmer and more compressed as moving to critical condition point **741** where reaching the specific M-velocity M_*, further, is gradually extra-slowing, extra-warming and extra-compressing as moving to reservoir **745**, according to the condition of flow continuity Eq. (6.0), further, is gradually accelerating, cooling, and becoming decompressed as moving to critical condition point **742** where again reaching the specific M-velocity M_*, and further, is gradually extra-accelerating, extra-cooling, and extra-decompressing as moving to outlet **746**, as described hereinbefore with references to **Figs. 6a, 6b,** and **6c**. The cross-section of outlet **746** is wider than the cross-section of inlet **744**, thereby providing for that capsule **740** operates as a jet-booster launching a widened and cooled outflowing jetstream **747** with a high M-velocity, higher than the de Laval high M-velocity of oncoming fast flow **743.**

In view of the foregoing description referring to **Figs. 7c** and **7d**, it will be evident for a person skilled in the art that one can use the surface matrix thermoelectric devices to provide for at least one of:

- Adapting to the de Laval high M-velocity M_{743} of the oncoming fast flow **743** and controlling the laminarity of both: the flow **473** moving within the specifically shaped two-stage inner tunnel and outer portions of the ambient-adjacent flow; and
- Harvesting electricity from originated temperature differences.

Modified Symmetrical Wing

Fig. 8, a schematic illustration of a symmetrical wing **8.00** supplied with a multi-layer TE device **8.20**, is composed of three sub-drawings:

- **Fig. 8 (A)** is a schematic drawing of a sectional profile of a modified symmetrical wing **8.00** in a sagittal plane (X, Z) in a system of coordinates (X, Y, Z);
- **Fig. 8 (B)** is a profile of temperature difference function $\Delta T(x)$ between two opposite surfaces: upper-side **8.01** and lower-side **8.02** along the X-axis in a system of coordinates $(X, \Delta T)$; and
- **Fig. 8 (C)** is a profile of temperature difference function $\Delta T(z)$ between two opposite butt-ends: anterior and tail, along the Z-axis in a system of coordinates $(\Delta T, Z)$.

The modified wing **8.00**, mirror-symmetrical relative to the horizontal plane (X, Y), having a cross-sectional thickness **8.ΔZ**, is oriented to meet the oncoming fluid flow **8.10** at the zero attack angle. The oncoming fluid flow **8.10**, when flowing around the modified symmetrical wing **8.00**, becomes divided into two portions:

- upper-side **8.11**, forming the upper-side boundary layer **8.31** moving nearby the upper-side surface **8.01** and having thickness **8.41**; and
- lower-side **8.12**, forming the upper-side boundary layer **8.32** moving nearby the lower-side surface **8.02** and having thickness **8.42**;

each of which is subjected to the action of the Coanda-effect. If the upper-side **8.01** and lower-side **8.02** surfaces of the modified symmetrical wing **8.00** are made from the same material and have the same temperature, the two portions: upper-side **8.11** and lower-side **8.12**, of fluid flow, both are subjected to the mirror-symmetrically acting Coanda-effect such that the lift-force is zero and only the **Archimedes' upward**-vectored force **8.LIFT** acts on the modified symmetrical wing **800** against the downward attracting gravitational force. Normally, the effective mass density of the modified symmetrical wing **800** is much greater than the mass density of the natural air, and if the ambient fluid is the natural air, then the **Archimedes' upward**-vectored force is much weaker than the downward attracting gravitational force. Speaking strictly, the two boundary layers **8.31** and **8.32** differ in thermodynamic parameters: the static pressure, mass density, and absolute temperature, as the boundary layers **8.31** and **8.32**, both characterized by the mass density and subjected to gravitational downward attraction, occupy spaces differing in height above the world Oceanus level. The seemingly-insignificant difference in the static pressures is a reason for **Archimedes' upward**-vectored force.

The modified symmetrical wing **800** is modified by that the upper-side **8.01** and lower-side **8.02** surfaces are mutually-contacted through the multi-layer TE device **8.20**, which is similar to the multi-layer TE multi-module device **1t.0** comprising a matrix of TE elements aggregated in layers one above another multi-stage repeatedly as described hereinabove referring to prior art **Fig. 1t**. The multi-layer TE device **8.20** comprises:

- the upper-side layer composed of unbrokenly arranged anterior TE devices **8.21**, withers TE devices **8.23**, and tail TE devices **8.25**, all having an upper side forming the upper-side surface **8.01** of the modified symmetrical wing **8.00**, and
- the lower-side layer composed of unbrokenly arranged anterior TE devices **8.22**, withers TE devices **8.24**, and tail TE devices **8.26**, all having a lower side forming the lower-side surface **8.02** of the modified symmetrical wing **8.00**,

wherein points **8.27** and **8.28** symbolize that TE devices are arranged unbrokenly.

The multi-layer TE device **8.20**, when controlled by a controller, provides for an additional temperature difference **8.ΔT(x)** (additional to the seemingly-insignificant temperature difference) between the upper-side **8.01** and lower-side **8.02** surfaces along the X-axis.

The profile of the modified symmetrical wing **8.00** is airfoil in a certain sense only. When the ambient velocity is in a certain range of velocities, the stalling effect, accompanied by broken or jumping all: the headway velocity, the static pressure, the absolute temperature, and the mass density, occurs nearby the separation point **1G.46** resulting in reducing lift-force drastically, as **described hereinabove in the subparagraph**: "Broken Boundary Layer" **referring to Fig. 1g Scheme (E)**.

The inventor points out that all parameters: the headway velocity, the static pressure, the absolute temperature, and the mass density, are interrelated according to laws of gas state and laws of aerodynamics, and so controlling of at least one of the parameters allows to control all the other parameters. In particular, to suppress the uncontrolled stalling effect, the use of the multi-layer TE device **8.20** controlled by a controller allows for providing a forcibly established specific temperature distribution along the upper-side **8.01** and lower-side **8.02** contours of the modified symmetrical wing **8.00** profile. The forcibly established specific temperature distribution along the upper-side **8.01** and lower-side **8.02** contours is such to provide the mentioned thermodynamic conditions for laminar flowing in the boundary layers **8.31** and **8.32**, correspondingly, each of which becomes an optimized convergent-divergent nozzle, completely optimized on one of the mentioned criteria either:

- smoothing of the flowing fluid M-velocity, or
- smoothing of the flowing fluid static pressure, or
- smoothing of the flowing fluid absolute temperature, or
- smoothing of the flowing fluid mass density,

as described hereinabove in the subparagraph "Convergent-Divergent Jet-Nozzle" **referring to Fig. 6a**. Thus, it is preferred to use a specifically distributed additional temperature difference **8.ΔT(x)**, distributed along the contours **8.01** and **8.02**. An exemplary distribution of the additional temperature difference **8.ΔT(x)** is optimized to provide laminar motions of portions **8.11** and **8.12** accompanied by gradual changes in M-velocities dependent on the cross-sectional area of the boundary layers **8.31** and **8.32**, correspondingly, according to the condition of flow continuity *Eq. (6.0)*, adapted to the M-velocity of oncoming flow **8.10** equal to $0.35\ Mach$ and effective thicknesses **8.41** and **8.42**, both equal to $3.7\ cm$. The specifically distributed additional temperature difference **8.ΔT(x)**, having a zone downstream behind the TE

devices **8.25** and **8.26** where the temperature differences **8.T2** are reversed in sign, is such that, downstream behind the sharp butt-end **8.03** of the modified symmetrical wing **8.00**, the velocities of the upper-side **8.11** and lower-side **8.12** portions gradually become the same and the temperatures of both upper-side **8.11** and lower-side **8.12** portions become gradually reverted to the temperature of the ambient fluid. This condition is necessary to prevent or at least to suppress turbulence downstream behind the sharp butt-end **8.03** thereby making the modified symmetrical wing **8.00** actually-airfoil.

Considering an action of the multi-layer TE device **8.20** making the upper-side surface **8.01** colder than the lower-side surface **8.02**, when fresh portions of fluid are suddenly transformed into the upper-side and lower-side boundary layers, the additional effective temperature difference **8.ΔT(eff)** equal to $\overline{\Delta T}$ causes suddenly originated effective temperature differences between fluid portions, i.e.:

- $\overline{\Delta T_1}$ between the upper-side portion of the ambient fluid and a tiny portion within the refreshed upper-side boundary layer **8.31**,
- $\overline{\Delta T_2}$ between a tiny portion within the refreshed upper-side boundary layer **8.31** and a tiny portion within the refreshed lower-side boundary layer **8.32**,
- $\overline{\Delta T_3}$ between a tiny portion within the refreshed lower-side boundary layer **8.32** and the refreshed lower-side portion of the ambient fluid,

wherein the condition: $\overline{\Delta T_2} = -(\overline{\Delta T_1} + \overline{\Delta T_3})$ says that the ambient fluid outside the boundary layers remains in normal thermodynamic conditions. There are extremely low velocities of airflow in close proximity above the upper-side solid surface **8.01** and under the lower-side solid surface **8.02 as described hereinabove in the subparagraph:** "Boundary-layer" referring to **Fig. 1g Graph (D)**. Hence, the condition $\overline{\Delta T_2} \lesssim \overline{\Delta T}$ (again, $\overline{\Delta T}$ is the additional effective temperature difference **8.ΔT(eff)** between the upper-side and lower-side surfaces: **8.01** and **8.02**) is satisfied also when the wing **8.00** moves. When the refreshed boundary layers are relatively thin and well-aligned with the airfoil surfaces, the approximation $\overline{\Delta T_2} \cong \overline{\Delta T}$ becomes justified. The higher the ambient velocity, the thinner the refreshed boundary layers, and the more appropriate the interrelation $\overline{\Delta T_2} \cong \overline{\Delta T}$. Further, for concretization, the relatively thin and well-aligned boundary layers flowing with high-subsonic velocities are assumed. Considering fresh incoming portions of the boundary layers, the suddenly originated additional effective temperature differences $\overline{\Delta T_1}$, $\overline{\Delta T_2}$, and $\overline{\Delta T_3}$ are interrelated with the suddenly originated additional effective static pressure differences, additional to the seemingly-

insignificant static pressure difference **associated with Archimedes' upward**-vectored force. Namely, the suddenly originated $\overline{\Delta T_1}$, $\overline{\Delta T_2}$, and $\overline{\Delta T_3}$ are interrelated with the suddenly originated additional effective static pressure differences of:

- $\overline{\Delta P_1}$ between the upper-side portion of the ambient fluid and a tiny portion within the refreshed upper-side boundary layer **8.31**,
- $\overline{\Delta P_2}$ between a tiny portion within the refreshed upper-side boundary layer **8.31** and a tiny portion within the refreshed lower-side boundary layer **8.32**,
- $\overline{\Delta P_3}$ between a tiny portion within the refreshed lower-side boundary layer **8.32** and the refreshed lower-side portion of the ambient fluid,

correspondingly. The resulting suddenly originated negative additional effective pressure difference $\overline{\Delta P_2}$ interrelates with the suddenly originated positive additional effective pressure differences: $\overline{\Delta P_1}$ and $\overline{\Delta P_3}$, wherein:

- the suddenly originated positive additional effective pressure difference $\overline{\Delta P_1}$ results in downward pulling-in the upper-side portion of the ambient fluid and upward pulling-in the modified symmetrical wing **8.00** into the refreshed upper-side boundary layer **8.31**, and
- the suddenly originated positive additional effective pressure difference $\overline{\Delta P_3}$ results in downward pushing-off the lower-side portion of the ambient fluid and upward pushing-off the modified wing symmetrical **8.00** away from the refreshed lower-side boundary layer **8.32**,

thereby, both contributing to the upward-vectored force **8.LIFT** applied to the modified symmetrical wing **8.00** in unison, wherein the condition: $\overline{\Delta P_2} = -(\overline{\Delta P_1} + \overline{\Delta P_3})$ says that the ambient fluid outside the boundary layers remains in normal thermodynamic conditions. Thus, the suddenly originated additional positive effective pressure difference $(-\overline{\Delta P_2}) = (\overline{\Delta P_1} + \overline{\Delta P_3})$ works for both:

- downward shifting the upper-side and lower-side portions of the ambient fluid, and
- a positive contribution ΔF_{LIFT} to the upward-vectored force **8.LIFT**,

in the same extent, i.e. not more than half the sum $(\overline{\Delta P_1} + \overline{\Delta P_3})$ contributes to the lift. Moreover, as the contribution to the lift works if the additional effective static pressure differences are originated between two fresh portions of air just suddenly, a velocity-dependent suddenness factor C_S determines the value of the positive contribution ΔF_{LIFT} to the upward-vectored force **8.LIFT**. Namely, as the interaction between, on the one hand, the wing and, on the other hand, the refreshed and suddenly heated or cooled boundary layers is relevant only, then, when the relatively thin boundary layers (the thickness of which is velocity-dependent) are

strictly-aligned to the relatively big airfoil surfaces of the modified symmetrical wing **8.00**, the velocity-dependent suddenness factor C_S tends to 1 ($C_S \to 1$), and, the slower-refreshed and so thicker the boundary layer and the weaker the alignment, the smaller the velocity-dependent suddenness factor C_S. Assuming an airfoil corpus, a simplified approximation for the velocity-dependent suddenness factor C_S defined hereinabove by the equitation Eq. (1.1j) is further specified for higher M-velocities by the expression:

$$C_S = \begin{cases} M/M_* \ , & M \leq M_* \\ \exp\left(1 - M/M_*\right) \ , & M > M_* \end{cases} \ , \quad \text{Eq. (8.0a)}$$

where M is M-velocity and M_* is the specific M-velocity. The approximation Eq. (8.0a) makes physical sense: the greater the difference $|1 - M/M_*|$, the lower the suddenness factor, which is manifested as a thicker boundary layer. Thus, the positive contribution ΔF_{LIFT} is defined as:

$$\Delta F_{LIFT} = \frac{1}{2} \times C_S \times A_{(X,Y)} \times (-\overline{\Delta P_2}), \quad \text{Eq. (8.0b)}$$

where $A_{(X,Y)}$ is the area of a projection of the upper-side surface **8.01** (or the lower-side surface **8.02**) of the modified symmetrical wing **8.00** in a horizontal plane (X, Y). As the high-subsonic velocity range is assumed, the approximation $C_S = 1$ is used for the estimation of the concept's practicality for industrial use [For comparison, in the case of wings waving by a pigeon to result in the effect of the bird taking-off dominantly-vertically (the case is highlighted **hereinabove in the subparagraph "Flying Bird" referring to Fig. 1i**), the suddenness factor C_S is estimated as about 0.01 that gives ΔF_{LIFT} of approximately $3.5N$ obtained by the waving that explains the effect of the bird taking off dominantly-vertically so efficiently]. To evaluate the concept's practicality for industrial use, an exemplary positive contribution ΔF_{LIFT} to the upward-vectored force **8.LIFT** is estimated referring to the specifically distributed additional temperature difference **8.ΔT(x)** considering:

- the normal ambient air conditions: $T \approx 300K$, $P \approx 100{,}000Pa$, and $\gamma = 7/5$;
- the wing **8.00** having a chord of $2\ m$ and a span of $10\ m$; i.e. $A_{(X,Y)} = 20\ m^2$; and
- the normally reachable value of the additional temperature difference **8.T1** using TE devices is $-75C$, and taking into account that it is preferred to use the specifically distributed additional temperature difference **8.ΔT(x)**, distributed on the upper-side **8.01** and lower-side **8.02** surfaces along the X-axis, the suddenly originated effective difference of $\overline{\Delta T_2} = \overline{\Delta T} = -30C$ is taken for the estimation, noting that $\overline{\Delta T_2}$ is interrelated with the suddenly originated effective additional static pressure difference $\overline{\Delta P_2}$ according to

equation $Eq.\ (1.1b)$ **described hereinabove in the subparagraph** "Lift-Force Mechanism" referring to **Fig. 1g**.

Thereby, the values are quantified as follows: $C_S = 1$, the ratio $(-\overline{\Delta T_2})/T \approx 0.1$, the ratio $(-\overline{\Delta P_2})/P \approx 0.1 \times (7/5)/(2/5) = 0.35$, the suddenly originated additional static pressure difference is $(-\overline{\Delta P_2}) = (\overline{\Delta P_1} + \overline{\Delta P_3}) \approx 0.35 \times 10^5 Pa$, and the contribution ΔF_{LIFT} **8.LIFT** to the upward-vectored force is

$$\Delta F_{LIFT} = \frac{1}{2} \times C_S \times A_{(X,Y)} \times (-\overline{\Delta P_2}) \approx 0.35 \times 10^6 N \qquad \text{Eq. (8.0c)}$$

that is sufficient to support a mass of $35\ ton$ fast-moving horizontally in the air.

In view of the foregoing description referring to **Fig. 8 (A) and (B)**, it will evident for a person skilled in the art that the modified symmetrical wing **8.00** has advantages as follows:

- it becomes relevant to use an increased upward-vectored force, increased by the contribution ΔF_{LIFT}, to contribute to the lift-force;
- it is possible to use the zero attack angle only or at least dominantly but not to use flaps to control lift-force;
- it becomes possible to control flow laminarity within the upper-side and lower-side boundary layers;
- it becomes solved the problem of arising a negative lift-force at M-velocities higher than the specific M-velocity; and
- it becomes possible to imitate an actually-airfoil wing by suppression turbulence downstream behind the modified symmetrical wing.

Further, the controlled multi-layer TE device **8.20** allows for the controllable creation of an additionally distributed temperature difference **8.ΔT(z)** between the anterior and tail butt-ends of the modified symmetrical wing **800**. For the sake of concretization, the shown additional distributed temperature difference **8.ΔT(z)** is negative such that the additionally distributed temperature difference **8.ΔT(z)** providing the negative effective temperature difference $\Delta T_{FORE-TAIL}$ between the anterior and tail butt-ends. Analogously and in contrast to the origination of the positive contribution to the lift-force **8.LIFT** by the added upward-vectored force ΔF_{LIFT}, a contribution to the thrust **8.THRUST** by the added positive thrust ΔF_{THRUST} is provided due to the added negative effective temperature difference $\Delta T_{HEAD-TAIL}$ interrelated with the added negative effective static pressure difference $\Delta P_{HEAD-TAIL}$. Namely, analogously to the specification of the force ΔF_{LIFT}, the force ΔF_{THRUST} is specified as:

$$\Delta F_{THRUST} = -\frac{1}{2} \times C_u \times \Delta P_{HEAD-TAIL} \times A_{(Y,Z)} \qquad \text{Eq. (8.0d),}$$

where $A_{(Y,Z)}$ is the cross-sectional area in a frontal plane (Y, Z). To estimate the practicality of the concept, an exemplary positive contribution ΔF_{THRUST} to thrust **8.THRUST** is estimated referring to the added negative effective temperature difference $\Delta T_{FORE-TAIL}$ considering:

- the value of cross-sectional thickness **8.ΔZ** of the modified symmetrical wing **8.00** equal to $0.2\ m$ and a span of $10\ m$; i.e. $A_{(Y,Z)} = 2\ m^2$; and
- the value of the negative effective temperature difference $\Delta T_{HEAD-TAIL}$ using TE devices of $-60C$, i.e. the ratio $(-\Delta T_{HEAD-TAIL})/T \approx 0.2$; so, referring to the equation $Eq.\ (1.1b)$ **described hereinabove in the subparagraph** "Sound as Complicated Movement in Molecular Fluid" **prefacing the reference to Fig. 1n**, the ratio $(-\Delta P_{HEAD-TAIL})/P \approx 0.7$, and $(-\Delta P_{HEAD-TAIL}) \approx 0.7 \times 10^5\ Pa$.

Thereby, the force ΔF_{THRUST} is estimated as $(1/2) \times (0.7 \times 10^5 Pa) \times (2\ m^2) = 0.7 \times 10^5 N$ that is sufficient to overcome a velocity-dependent drag in the air when moving with the headway velocity u_0 of the high-subsonic velocity range, that can be confirmed referring to the condition derived from the well-known drag and skin-friction equation as follows:

$$u_0 = \{|\Delta F_{THRUST}|/[0.5 \times \rho_{AIR} \times (C_d \times A_{(Y,Z)} + C_f \times A_{(X,Y)})]\}^{1/2} \quad \text{Eq. (8.0e),}$$

where: $A_{(Y,Z)} = 2\ m^2$, $A_{(X,Y)} = 20\ m^2$,

C_f is the skin-friction coefficient, normally, given as about **0.045** for an airfoil wing,

C_d is the drag coefficient, normally, given as about **0.5** for a frontal convexly-rounded configuration of an actually-airfoil wing, and

ρ_{AIR} is the mass density of the air, normally, given as about $1.18\ kg/m^3$,

i.e. $u_0 \approx 250\ m/sec$.

In view of the foregoing description of the subparagraph "Modified Symmetrical Wing" referring to **Fig. 8**, it becomes evident for a commonly educated person that, using the surface matrix thermoelectric devices as an enhanced distributor of static pressure, a spatial function of temperature differences $\Delta T(x, z)$ within boundary layers can be enforced to provide for temperature asymmetry of a geometrically symmetrical wing to control lift-force and thrust, and, in particular, flying capsules **720** and **740 described hereinabove in the subparagraph** "Flying Capsule as Dragging-Jet Engine" **referring to Figs. 7c** and **7d**, both can have an optimized thrust and controlled lift-force.

Shaped Wing as a Convergent-Divergent Jet-Nozzle

Fig. 8a is a schematic visualization **800** of an oncoming wind portion **820**, without loss of generality, moving horizontally and flowing around actually-airfoil biconvex wing **810**, supplied

with a multi-layer TE device **8a.TED**. Oncoming wind portion **820** comprises airflow sub-portions **821**, **822**, **823**, and **824** flowing around actually-airfoil biconvex wing **810**, having a side-view sectional profile, constructed according to the principles of the present invention. The side-view sectional profile determines a sagittal axis **820.0**. The upper side of actually-airfoil biconvex wing **810** comprises:

(a) a forward part meeting upper-side sub-portion **822** having imaginary cross-section **831**;

(b) a withers **810a** defined as the highest point on the upper side of the airfoil profile convexity, where sliding sub-portion **822** has imaginary narrowed cross-section **832**; and

(c) a rearward part, attracting and, thereby, redirecting the mass-center of the upper-side sliding sub-portion **822** backward-downward, where sliding sub-portion **822** has imaginary widened cross-section **833**.

The upper and lower sides of the actually-airfoil biconvex wing **810**, each having a convexity: **810a** and **810b**, correspondingly, join together forming a sharp trailing end **810c**.

When airflow sub-portions **821**, **822**, **823**, and **824** are flowing around actually-airfoil wing **810**, the streamlines [not shown here] of sub-portions **822** and **823**, flowing near actually-airfoil biconvex wing **810**, are curving in alignment with the airfoil-profile, the streamlines [not shown here] of portions **821** and **824**, flowing farther from actually-airfoil biconvex wing **810**, keep substantially straight trajectories aligned with imaginary horizontal lines **811** and **812** (collinear with the sagittal axis **820.0**) correspondingly above and under actually-airfoil wing **810**. Actually-airfoil biconvex wing **810's sur**face material properties, porosity, and structure are elaborated according to the principles of the present invention such that air sub-portions **822** and **823** are subjected to the Coanda-effect, defined by the partial pressure-c δP_c, rather than to the skin-friction resistance, occurring in an imaginary boundary layer and being quantified by the difference $(a_w - a - \delta a)$, where a and a_w are the van der Waals parameters characterizing the fluid and attraction between the fluid and an adjacent wall, correspondingly, and δa is the van der Waals parameter characterizing the partial deep-stagnation pressure-a δP_a. Imaginary lines **811** and **812** can be considered as imaginary walls, thereby, together with the airfoil-profile forming imaginary nozzles. The upper-side imaginary nozzle comprises imaginary cross-sections **831**, **832**, and **833**, and the lower-side imaginary nozzle comprises imaginary cross-sections **834** and **835**. Cross-section **831** is wider than cross-section **832** and cross-section **832** is narrower than cross-section **833**, thereby, the upper-side imaginary nozzle has a convergent-divergent shape, and sliding sub-portion **822** represents a convergent-

divergent jetstream while flowing through cross-sections **831**, **832**, and **833**. Cross-section **834** is wider than cross-section **835**, so the lower-side imaginary nozzle has a converging shape.

The orientation of the sharp trailing end **810c** collinear with the sagittal axis **820.0** predetermines the direction of motion tendency of the outflowing sub-portions **822** and **823**, which are going off from the sharp trailing end and joining downstream behind the cross-sections **833** and **835**, correspondingly. For the purposes of the present invention, an angle between the sagittal axis **820.0** collinear with the direction of motion tendency of the lower-side outflowing sub-portion **823** and the horizontal direction defines an angle of attack (called also an attack angle). The definition of the attack angle is in conformance with the definition of the attack angle specified hereinabove in **the subparagraph "**Airfoil Wing (definition of attack angle)**" of THE BACKGROUND OF THE INVENTION** for a classic wing associated with a fuselage of airplane. Here is the zero attack angle in the shown schematic visualization **800**. The zero attack angle provides for minimized impact by the oncoming flow and a generation of the lift-force due to the Coanda-effect only or at least dominantly.

Consider a case, when actually-airfoil biconvex wing **810** flies with a certain de Laval low M-velocity M_{810} that is lower than the specific M-velocity $M_* \approx 0.5345\, Mach \approx 664\, km/h$, but such that sliding sub-portion **822**, moving through the upper-side imaginary nozzle, reaches the specific M-velocity M_* when passes through the narrowest cross-section **832**. So, the de Laval-like jet-effect arising is expected above actually-airfoil wing **810**, i.e. within the upper-side imaginary convergent-divergent jet-nozzle. This is accompanied by the static pressure decrease and extra-decrease, as described hereinabove with the reference to **Fig. 6a (B) Graph**, and thereby results in the lift-effect, becoming stronger. The narrowest cross-section **832** linear size, i.e. thickness δ of a boundary layer, dependent on both a so-called **"characteristic size"** L_* and the so-called Reynolds Number Re, can be estimated using, for example, approximation by Prandtl: $\delta = 0.37 \times L_*/Re^{0.2}$, where L_* has the sense of a chord of an airfoil wing. As well, the thickness δ of the boundary layer can be specified experimentally for a kind of body corpus. In view of the foregoing description referring to **Fig. 6a** and **Fig. 8a**, it will be evident to a person skilled in the art that, interpreting the narrowest cross-section **832's** linear size as the thickness of the boundary layer, one can apply the condition of flow continuity *Eq. (6.0)* to design an improved profile of the wing.

In view of the foregoing description referring to **Fig. 8a**, it will be evident to a person skilled in the art that the described de Laval-like jet-effect is similar to the classical de Laval jet-effect, but arising in an optimized convergent-divergent tunnel having imaginary walls formed by

streamlines of a flow. Namely, the specifically shaped convergent-divergent tunnel comprises two opposite walls; wherein one of the two opposite walls is constructed from a solid material and another of the two opposite walls is imaginary and formed by streamlines of the flowing fluid subjected to the Coanda-effect operation.

Further, it will be evident to a person skilled in the art that considering the case, when actually-airfoil biconvex wing **810** flying with a certain Venturi M-velocity $\boldsymbol{M_{810}}$,

which (the Venturi M-velocity $\boldsymbol{M_{810}}$) is lower than the specific M-velocity $\boldsymbol{M_*} = \sqrt{(\gamma-1)/\gamma} \approx 0.5345\, Mach \approx 664\, km/h$ and such that, when sliding sub-portion **822** moves through the upper-side imaginary nozzle and passes through the narrowest cross-section **832**, the maximally accelerated M-velocity remains lower than the specific M-velocity $\boldsymbol{M_*}$,

the condition of flow continuity *Eq. (6.0)* allows designing an improved profile of the wing optimized to meet flow, oncoming with the Venturi M-velocity $\boldsymbol{M_{810}}$. While a gradual change in static pressure within boundary layers adjacent to the upper-side and lower-side surfaces of the actually-airfoil biconvex wing **810** is the primary condition for the suppression of undesired turbulences nearby the wing surfaces, one of the primary criteria of the optimization is also to provide minimized differences between velocity-vectors and static pressures of the outflowing sub-portions **822** and **823**, as the primary condition for suppression of undesired turbulences downstream behind the sharp trailing end **810c**. While the curvatures of the upper-side and lower-side surfaces should provide gradual changes of the static pressures and M-velocities, the sharpness of the sharp trailing end **810c** should provide the dominantly horizontal direction of motion tendency of both outflowing sub-portions **822** and **823**.

Thus, a method for a wing profile design, based on the condition of flow continuity *Eq. (6.0)* according to an exemplary embodiment of the present invention, allows optimizing the wing airfoil shape to reach the best efficiency of the lift-effect as a result of the Coanda-jet-effect accompanied by enhanced at least one of the Venturi effect and de Laval jet-effect occurring above and under the wing. The inventor notes that the profile of the actually-airfoil biconvex wing **810**, designed and optimized using the condition of flow continuity *Eq. (6.0)*, has a shape similar to a shape of a birdwing rather than to the shape of the classic wing of the airplane.

The actually-airfoil biconvex wing **810**, while designed and optimized using the condition of flow continuity *Eq. (6.0)* applied to the overall geometrical configuration only, is actually-airfoil in a certain sense when considering the mentioned certain M-velocity $\boldsymbol{M_{810}}$. To provide optimized conditions for a wide range of velocities, the actually-airfoil biconvex wing **810**, is

further supplied with the multi-layer TE device **8a.TED** built-in between the upper-side and lower-side surfaces of the actually-airfoil biconvex wing **810**. The multi-layer TE device **8a.TED** comprises:

- an upper side forming the upper-side surface of the actually-airfoil biconvex wing **810**, and
- a lower side forming the lower-side surface of the actually-airfoil biconvex wing **810**.

The multi-layer TE device **8a.TED**, when controlled by a controller, provides for additional forcibly established temperature difference, additional to the temperature difference between the upper-side and lower-side surfaces along the sagittal axis **820.0** determined by the Coanda-effect accompanied by at least one of the Venturi effect and the de Laval effect. The forcibly established temperature difference $\left(\Delta T_0(x) + \Delta T(x)\right)$ distributed along the sagittal axis **820.0**, where:

- $\Delta T_0(x)$ is the distributed original temperature difference between the upper-side and lower-side boundary layers specified when designing the overall geometrical configuration of the actually-airfoil biconvex wing **810** considering the mentioned certain M-velocity M_{810} and the derivative distribution $M_{810}(x)$ along the sagittal axis **820.0**, and
- $\Delta T(x)$ is the additional forcibly established distribution of the temperature difference,

provides for adaptation of the overall shape of the actually-airfoil biconvex wing **810** to an arbitrary velocity u_{8a} of the oncoming wind portion **820**. For this purpose, the forcibly established distribution of the temperature difference $\left(\Delta T_0(x) + \Delta T(x)\right)$ is defined as:

$$\left(\Delta T_0(x) + \Delta T(x)\right) = \frac{1}{\gamma R} \times \left[\frac{u_{8a}}{M_{810}(x)}\right]^2.$$

The Coanda-Effect Operation Providing An Imaginary Convergent-Divergent Nozzle

Fig. 8b is a schematic illustration of a flying airfoil body **840** having the shape of an elongated drop. For simplicity and without loss of reasoning, the shape is axis-symmetrical around the longitudinal axis **841**. The airfoil body **840** comprises:

- a forward part meeting oncoming flow portion **851**;
- **a "withers", defined as the highest point on the upper side of the airfoil profile,** where sliding sub-portion **853** has an imaginary narrowed cross-section **868**, and
- a rearward part.

When an oncoming air portion **851**, originally having a cross-sectional area **861**, is running at the forward part of flying body **840**, it is subjected to the Coanda-effect operation resulting in air portion **851** reshaping, and thereby forming an ambient-adjoining convergent-divergent jetstream, comprising sliding sub-portions: **852** being convergent, **853** being narrow and having

imaginary narrowed cross-section **868** of the minimal cross-sectional area, **854** being divergent, and **855** becoming convergent due to the Coanda-effect attraction. Body **840's** surface material properties, porosity, and structure are implemented according to the principles of the present invention, thereby providing that air portion **851** is subjected to the Coanda-effect, defined by the partial pressure-c δP_c, rather than to the skin-friction resistance, occurring in an imaginary boundary layer and being quantified by the difference $(a_w - a - \delta a)$. Furthermore, sliding sub-portions **855**, join together, forming the resulting cumulative air portion **856**. Oncoming air portion **851** and all the mentioned derivative sub-portions move within space **"bordered" by imaginary walls marked by dashed contours 842**. The imaginary walls **842** together with the airfoil surface of body **840** constitute an imaginary tunnel. The **tunnel's cross**-section gradually constricts from the inlet cross-section **862** to the narrowest cross-section **868** and then gradually widens up to the outlet cross-section **863**. I.e. sliding sub-portions **852** are shrinking while reaching the withers of airfoil body **840**, where the cross-sections **868** of sub-portions **853** become minimal. Then, behind the withers, the cross-sections of sub-portions **854** and **855** are widening as moving.

Sliding sub-portions **855**, being under the subjection of the Coanda-effect operation, turn aside in alignment with the slippery surfaces of airfoil body **840's rearward part and** join together, forming the resulting air portion **856**. It results in a convergence of resulting air portion **856**, i.e. in that, cross-section **864**, located farther downstream, becomes narrower than cross-section **863** located immediately behind airfoil body **840**, and opposite streamline-fragments **843** form an imaginary convergent funnel. Furthermore, opposite streamline-fragments **844**, which are bordering flow portion **857**, constitute an imaginary divergent stage of a tunnel downstream-behind the narrowest cross-section **864**. The converging opposite streamline-fragments **843** and divergent opposite streamline-fragments **844** together constitute the imaginary convergent-divergent tunnel, and, correspondingly, portions **856** and **857** together constitute an outflowing convergent-divergent jetstream.

As the shape of the imaginary convergent-divergent tunnel comprising streamlines **843 – 844** and cross-sections **863**, **864**, and **865** is a derivation of the Coanda-effect operation nearby the solid surfaces of the airfoil body **840**, the airfoil body **840** is supplied with a matrix TE device (which is not shown here), built-in within the airfoil body **840's** corpus and in close proximity under the solid surfaces to control the surface temperature and thereby to control the Coanda-effect and laminarity of the streamlines **842 – 843 – 844**.

Jet-Booster based on the Venturi Effect

First, consider a case, when airfoil body **840** flies with a Venturi M-velocity, i.e. with a low M-velocity, lower than the specific M-velocity $M_* = \sqrt{(\gamma-1)/\gamma} \approx 0.5345\ Mach$, and low sufficient to provide that M-velocity M_{868} of accelerated sliding sub-portions **853**, passing cross-sections **868** over the withers, and M-velocity M_{864} of accelerated sub-portions **856**, passing through the narrowest cross-section **864**, both remain lower than the specific M-velocity M_*, i.e. $M_{868} < M_*$ and $M_{864} < M_*$. In this case, the narrowest cross-section **864** of outflowing air portion **856** is narrower than the original cross-section **861** of oncoming air portion **851**, and the M-velocities M_{861}, M_{863}, M_{864}, M_{865}, and M_{868}, where the indices correspond to markers of associated cross-sections, satisfy the following conditions:

- $M_{861} < M_{868} < M_*$,
- $M_{863} < M_{868} < M_*$,
- $M_{863} < M_{864} < M_*$,
- $M_{861} < M_{864} < M_*$, and
- $M_{865} < M_{864} < M_*$.

Thus, body **840** operates as a jet-booster basing on the Venturi effect occurring in the imaginary tunnel adjacent to body **840's** surfaces.

A practical application of the phenomenon that, under certain conditions, outflowing portion **856**, moving through the narrowest cross-section **864**, has a velocity higher than the velocity of oncoming portion **851** is one of the primary teachings of the present invention.

Jet-Boosters based on the de Laval-like Jet-Effect

Secondly, consider a case, when airfoil body **840** flies relatively slowly, such that sliding sub-portions **853** passes cross-sectional areas **868** with an M-velocity that remains lower than the specific M-velocity, i.e. $M_{853} < M_*$, but high sufficient to provide that the increased M-velocity of portion **856** is higher than the M-velocity of sub-portions **853** and reaches the specific M-velocity $M_* = \sqrt{(\gamma-1)/\gamma}$ at the critical condition point **864**. In this case, M-velocity M_{863} is the de Laval low velocity and the de Laval-like jet-effect is triggered, resulting in that the M-velocity of the divergent flow portion **857** exceeds the specific M-velocity M_*. In this case, the M-velocities M_{861}, M_{863}, M_{864}, M_{865}, and M_{868} satisfy the following conditions:

- $M_{861} < M_{868} < M_*$,

- $M_{863} < M_{868} < M_*$,
- $M_{863} < M_{864} = M_*$,
- $M_{861} < M_{864} = M_*$, and
- $M_{865} > M_{864} = M_*$.

So, body **840** operates as a jet-booster basing on the de Laval-like jet-effect occurring in the imaginary tunnel downstream-behind airfoil body **840**. Thereby, the Coanda-jet-effect operation forcedly forms convergent-divergent laminar-like streamlines downstream-behind airfoil body **840**, wherein the static pressure is distributed gradually along the convergent-divergent laminar-like streamlines that provides an optimized extension of air portion **857** resulting in the enhanced de Laval-like jet-effect accompanied by extra-cooling and extra-acceleration of air portion **857**. This is one more teaching of the present invention.

A practical application of the phenomenon that, under certain conditions, outflowing portion **857** has an M-velocity higher than the specific M-velocity is one of the primary teachings of the present invention.

It will be evident to a person skilled in the art that the enhanced jet-effect results in an optimized reactive thrust-force applied to airfoil body **840**.

Thirdly, consider a case, when airfoil body **840's shape is optimized using** the condition of flow continuity Eq. (6.0) basing on an estimated linear size of cross-section **868**, and when airfoil body **840** flies with a de Laval low M-velocity M_{851}, i.e. lower than the specific M-velocity $M_* = \sqrt{(\gamma - 1)/\gamma} \approx 0.5345\ Mach$, but high sufficient to provide that M-velocity of sliding sub-portions **853** reaches the value of the specific M-velocity, i.e. $M_{868} = M_*$ at the critical condition point **868**. Thereby, the enhanced de Laval-like jet-effect occurs downstream-behind the withers, providing that $M_* < M_{854} < M_{855}$, where the indexes correspond to associated sliding air sub-portions. In this case, according to the condition of flow continuity Eq. (6.0), shrinking portion **856**, moving with a de Laval high M-velocity, is slowing down, becoming warmer and more compressed, as moving on the way to the critical condition point associated with cross-section **864**. The de Laval-like retarding-effect occurs downstream-behind cross-section **864** resulting in portion **857** expanding and further slowing down, warming, and compressing while reaching cross-section **865**. The M-velocities M_{861}, M_{863}, M_{864}, M_{865}, and M_{868} satisfy the following conditions:

- $M_{861} < M_{868} = M_*$,
- $M_{863} > M_{868} = M_*$,
- $M_{863} > M_{864} = M_*$,

- $M_{861} < M_{864} = M_*$, and
- $M_{865} < M_{864} = M_*$.

So, in the final analysis, body **840** operates as a jet-booster, triggering both the de Laval-like jet-effect and the de Laval-like retarding-effect.

Fourthly, consider a case, when airfoil body **840's shape is optimized using** the condition of flow continuity Eq. (6.0) basing on an estimated linear size of cross-section **868**, and when airfoil body **840** flies with a de Laval high M-velocity, i.e. higher than the specific M-velocity $M_* = \sqrt{(\gamma - 1)/\gamma} \approx 0.5345\ Mach$. According to the condition of flow continuity Eq. (6.0), the de Laval-like retarding-effect occurs in the imaginary convergent-divergent tunnel formed by streamlines **842**. Namely, shrinking air potions **852** are slowing down, becoming warmer and more compressed, as moving on the way to withers such that the M-velocity of the narrowest sliding sub-portions **853** reaches the specific M-velocity, i.e. $M_{868} = M_*$ at the critical condition point **868**; and further, portions **854** continue to slow down while expanding downstream-behind the withers. Relatively slowly moving sliding sub-portions **855**, now having a de Laval low M-velocity, join downstream-behind cross-section **863**, thereby, providing for resulting shrinking portion **856** acceleration, accompanied by a decrease of temperature and static pressure, while reaching again the specific M-velocity M_* at the narrowest cross-section **864**. The de Laval-like jet-effect occurs downstream-behind cross-section **864** resulting in expanding portion **857** further acceleration accompanied by a deeper decrease of temperature and static pressure on the way to cross-section **865**. So, the M-velocities M_{861}, M_{863}, M_{864}, M_{865}, and M_{868} satisfy the following conditions:

- $M_{861} > M_{868} = M_*$,
- $M_{863} < M_{868} = M_*$,
- $M_{863} < M_{864} = M_*$,
- $M_{861} > M_{864} = M_*$, and
- $M_{865} > M_{864} = M_*$.

Again, in the final analysis, body **840** operates as a jet-booster, triggering both the de Laval-like retarding-effect and the de Laval-like jet-effect.

In view of the foregoing description referring to **Figs 6a**, **7a**, **7b**, **7c**, **8a**, and **8b**, it will be evident to a person skilled in the art that:

- a method for an airfoil body shape design, based on the condition of flow continuity *Eq. (6.0)* according to an exemplary embodiment of the present invention, allows, modifying the

overall geometry of the body, to optimize the efficiency of the enhanced jet-effect occurring outside of the body;

- the described convergent-divergent jet-nozzles can be applicable to many apparatuses using mechanical and heat energy provided by either a flowing gas or liquid;
- triggering and controlling the desired de Laval-like jet-effect can be provided by manipulating by the oncoming wind de Laval M-velocity. As the M-velocity is temperature-dependent, one can heat or cool air portions flowing within a specifically shaped tunnel, in particular, in an imaginary tunnel around a flying body;
- reaching and controlling the desired de Laval-like jet-effect can be provided by manipulating by the value of specific M-velocity, depending on the generalized adiabatic compressibility parameter γ. For example, one can inject a gas composed of multi-atomic particles into a tunnel, in particular, into an imaginary tunnel around a flying body. As well, it will be evident to a person skilled in the art that, for example, micro-flakes-of-snow could play the role of such multi-atomic particles. Another technique to change the generalized adiabatic compressibility parameter γ and thereby to control the specific M-velocity is to ionize the flow, moving through the tunnel; and
- the described convergent-divergent jet-nozzles can be applicable to many apparatuses using mechanical and heat energy, provided by flowing gas or liquid.

Two-stage operation of the Coanda-jet-effect

Fig. 8c is divided into two parts: **Case (A)** and **Case (B)**.

Fig. 8c Case (A) is a schematic illustration of flying airfoil bodies **850** and **860**, arranged such that the withers of airfoil bodies **860** follow downstream-behind the withers of body **850**. For simplicity and without loss of reasoning, each airfoil body **850** and **860** has the shape of an elongated drop **840** described above referring to **Fig. 8b**. All reference numerals **841**, **861**, **851**, **862**, **852**, **868**, **853**, **842**, and **854** are the same as described referring to **Fig. 8b**.

Consider a case, when flying airfoil bodies **850** and **860** meet oncoming portion **851** with a de Laval high M-velocity M_{851}, higher than the specific M-velocity $M_* = \sqrt{(\gamma-1)/\gamma} \approx 0.5345\, Mach$. According to the condition of flow continuity Eq. (6.0), sub-portions **852** of flowing fluid (for instance and without loss of generality, the flowing fluid is airflow) are slowing down as constricting on the way to the withers of body **850**, such that M-velocity of the narrowest sliding sub-portions **853** reach the specific M-velocity, i.e. $M_{853} = M_*$ at the critical condition point **868.** The de Laval-like retarding-effect occurs downstream-behind the withers. It provides the condition $M_* > M_{854}$, where index "854" corresponds to air sub-portions **854**. So,

airfoil bodies **860** meet oncoming sub-portions **854** flowing slower than with the specific M-velocity $M_* = \sqrt{(\gamma - 1)/\gamma}$, but high sufficient to provide the critical condition near their [bodies **860**'s] withers. Again, according to the condition of flow continuity Eq. (6.0), air sub-portions **859** have an M-velocity M_{859} higher than the specific M-velocity M_*. Thus, flying airfoil bodies **850** and **860** meet the upstream air portions, and leave the downstream air portions, flowing faster than with the specific M-velocity $M_* = \sqrt{(\gamma - 1)/\gamma}$. Furthermore, a cumulative cross-section of air sub-portions **859**, wider than cross-section **861** of oncoming portion **851**, means that the M-velocity M_{859} is higher than the high M-velocity M_{851} of oncoming portion **851**. In this case, the Coanda-jet-effect two-stage operation accelerates a portion of ambient airflow that originally moves faster than with the specific M-velocity M_*. Thus, in contrast to the case when a body, having a not-optimized shape, flies in an air-environment with transonic, and/or supersonic, and/or hypersonic velocities, flying airfoil body **850**, operating in tandem with each flying airfoil body **860**, moving downstream behind the withers of airfoil body **850**, results in a specific effect of acceleration and cooling air portion **851**, oncoming faster than with the specific M-velocity M_*. This is one other primary teaching of the present invention.

Fig. 8c Case (B) is a schematic illustration of a sectional cut of flying actually-airfoil wings **850.B** and **860.B** in a sagittal plane. The flying actually-airfoil wings **850.B** and **860.B** are arranged to meet and act on an oncoming portion **851.B** of flowing fluid sequentially (for instance and without loss of generality, the flowing fluid is airflow). In view of the foregoing description referring to **Fig. 8c Case (A)**, it becomes evident that, in particular, considering a tandem **880.B** of two airfoil bodies consolidated as a whole embodied in the form of actually-airfoil wings **850.B** and **860.B** (for instance, each of which similar to that described hereinabove referring to **Fig. 8a**) will provide the described specific effect of acceleration and cooling of the airflow portion **851.B** originally oncoming faster than with the specific M-velocity M_*. The tandem **880.B** comprises all the features of the flying airfoil bodies **850** and **860** of **Case (A)**, and, in contrast to **Case (A)**, the two airfoil bodies, namely, the two actually-airfoil wings **850.B** and **860.B**, have an asymmetry relative to the horizontal plane **841.B**.

The reference numerals are as follows:

- **851.B** is an oncoming flow portion yet to be subjected to an action of the tandem **880.B** of two actually-airfoil wings **850.B** and **860.B** consolidated as a whole;

- **852.B1** and **852.B2** are sub-portions of the oncoming flow portion **851.B** in positions where, when running on the first met local convexity **869.B1** and **869.B2**, correspondingly, subjected to convergence above and under the tandem **880.B**;
- **868.B1** and **868.B2** are narrowed cross-sections of the locally-minimal cross-sectional areas, correspondingly, above and under the first met local convexity: **869.B1** and **869.B2**, of the tandem **880.B**;
- **853.B1** and **853.B2** are sub-portions of the oncoming flow portion **851.B** in positions where, when flowing adjacent to the first met local convexity: **869.B1** and **869.B2**, correspondingly, subjected to narrowing to have narrowed cross-sections **868.B1** and **868.B2** of the locally-minimal cross-sectional areas, correspondingly, above and under the first met local convexity: **869.B1** and **869.B2**, of the tandem **880.B**;
- **854.B1** and **854.B2** are sub-portions of the oncoming flow portion **851.B** in positions where, when passing the first met local convexity: **869.B1** and **869.B2**, correspondingly, subjected to divergence above and under the tandem **880.B**;
- **852.B3** and **852.B4** are sub-portions of the oncoming flow portion **851.B** in positions where, when running on the second met local convexity: **869.B3** and **869.B4**, correspondingly, subjected to convergence above and under the tandem **880.B**;
- **868.B3** and **868.B4** are narrowed cross-sections of the locally-minimal cross-sectional areas, correspondingly, above and under the second met local convexity: **869.B3** and **869.B4**, of the tandem **880.B**;

  and
- **854.B3** and **854.B4** are sub-portions of the oncoming flow portion **851.B** in positions where, when passing the second met local convexity: **869.B3** and **869.B4**, correspondingly, subjected to divergence above and under the tandem **880.B**.

The profiles of the two actually-airfoil wings **850.B** and **860.B** are elaborated to meet the oncoming flow portion **851.B** originally oncoming faster than with the specific M-velocity M_* such that the two boundary layers composed of the sub-portions, flowing above and under the tandem **880.B**, correspondingly, both, when subjected to action by the tandem **880.B**, become subjected to a two-stage convergence-divergence accompanying first, by the triggered de Laval retarding-effect and then by the triggered de Laval jet-effect. Borders of the two boundary layers are schematically marked by double-dot dashed lines **842.B1** and **842.B2** symbolizing imaginary, in general, curved surfaces formed by streamlines bordering the portion **581.B** above and under the tandem **880.B**, correspondingly; without loss of generality, the surfaces

are indicated as being almost plane and separating, on the one hand, the two two-stage convergent-divergent boundary layers composed of sub-portions of the portion **581.B**, which are substantially deforming as moving along the tandem **880.B**, and, on the other hand, portions of the ambient flowing fluid which remain relatively weakly deformed. The triggering of the de Laval retarding-effects occurs when the retarding of sub-portions **852.B1** and **852.B2** are such that the sub-portions **853.B1** and **853.B2** cross the narrowed cross-sections **868.B1** and **868.B2** of the locally-minimal cross-sectional areas, correspondingly, with the specific M-velocity M_*; and the triggering of the de Laval jet-effects occurs when the acceleration of sub-portions **852.B3** and **852.B4** are such that the sub-portions **853.B3** and **853.B4** cross the narrowed cross-sections **868.B3** and **868.B4** of the locally-minimal cross-sectional areas, correspondingly, again, with the specific M-velocity M_*.

The asymmetry of the tandem **880.B** relative to the horizontal plane **841.B** causes that:

- on the one hand, as soon as the upper-side outlet sub-portion **854.B3** is wider than the upper-side inlet sub-portion **852.B1**, integrally, the upper-side sub-portion becomes accelerated, as it is described hereinabove in the sub-**paragraph** "Two-Stage Convergent-Divergent Jet-Nozzle" **referring to Fig. 6c**; and
- on the other hand, since the lower-side outlet sub-portion **854.B4** is narrower than the lower-side inlet sub-portion **852.B2**, integrally, the lower-side sub-portion remains retarded.

Such an action of the tandem **880.B** on the sub-portions of the relatively fast oncoming flow portion **851.B**, which (the action) is imbalanced relative to the horizontal plane **841.B**, originates a resulting upwardly-vectored lift-force cumulatively acting on the tandem **880.B**, that is also one of the primary teachings of the present invention.

Fig. 8d is a schematic illustration of two-stage airfoil wings, constructed according to the principles of the present invention: **(A)** a two-stage wing **870** having a side-view sectional double-humped airfoil profile **871**, and **(B)** a two-stage wing **8d** having a side-view sectional classical airfoil profile and modified by supplying with the multi-layer TE device **8d.TED**.

In **Fig. 8d (A)**, the orientation of the double-humped airfoil profile **871** determines a sagittal axis **871.0**, in turn, oriented horizontally. The two-stage double-humped airfoil wing **870** comprises two withers: forward **872** and rear **873**, separated by concavity **874**. The lift-force force originated by the profile is analyzed, considering the flying M-velocity which is higher than the specific M-velocity $M_* = \sqrt{(\gamma - 1)/\gamma} \approx 0.5345\, Mach$, i.e. when the lift-force, originated by a classical wing **10.A described hereinabove the subparagraph** "Airfoil Wing (definition of attack angle)" **referring to Fig. 1g Case (A)**, is negative.

An oncoming flow portion **875** runs at the double-humped airfoil wing **870**, becomes a boundary layer moving adjacent to the upper-side surface of the double-humped airfoil wing **870** under an imaginary surface, which, in a sagittal sectional plane, is indicated by a double-dot dashed line **871.1** symbolizing an imaginary, in general, the curved surface formed by streamlines bordering the portion **875** above the double-humped airfoil wing **870**, and passes positions: **801**, **802**, **803**, **804**, **805**, **806**, **807**, **808**, and **809** sequentially with associated M-velocities: M_{801}, M_{802}, M_{803}, M_{804}, M_{805}, M_{806}, M_{807}, M_{808}, and M_{809}, correspondingly. The double-humped airfoil profile **871** provides for the Coanda-jet-effect two-stage operation: upstream-afore and downstream-after concavity **874**. At position **801**, flow portion **875**, having the de Laval high M-velocity M_{801}, is yet to be subjected to the Coanda-jet-effect operation over wing **870's profiled surfaces**. The double-humped airfoil profile **871** causes that the cross-sectional area of portion **875** is varying as portion **875** moves over wing **870** as the boundary layer under the imaginary surface **871.1**. So, portion **875** shrinks at position **802** while upping over the forward part, has the first local minimum of cross-section area at position **803** above the forward withers **872**, expands at position **804** while downing into concavity **874**, reaches the local maximum of cross-section area at position **805** when passing concavity **874**, shrinks again at position **806** on the way to the rear withers **873**, gets the second local minimal value of cross-section area at position **807** above the rear withers, and expands at positions **808** and **809**. Thus, there are two convergent-divergent portions of the boundary layer moving adjacent to the upper-side surface of the double-humped airfoil wing **870**:

- first, upstream relative to concavity **874**, comprising positions **802**, **803**, **804**, and **805** when flowing over the forward withers **872,** and
- second, downstream relative to concavity **874**, comprising positions **805**, **806**, **807**, **808**, and **809** when flowing over the rear withers **873.**

Each of the two convergent-divergent portions of the boundary layer is elaborated according to the condition of flow continuity *Eq. (6.0)* providing for gradually smooth changes of M-velocity to suppress undesired turbulences.

According to the condition of flow continuity *Eq. (6.0)*, portion **875**, as the boundary layer moving under the imaginary surface **871.1**, is subjected to the de Laval-like jet-effect and the de Laval-like retarding-effect such that:

- at position **802**, the flow convergence is accompanied by the de Laval-like retarding-effect resulting in compressing and warming of flow portion **875** and a decrease of M-velocity, i.e. $M_{801} > M_{802}$;

- at position **803**, the first critical condition point, where the varying value of flow portion **875's** cross-sectional area has the first local minimum, provides for that the M-velocity of flow portion **875** reaches the specific M-velocity M_*, so, $M_{801} > M_{802} > M_{803} = M_*$, i.e. the critical condition of the de Laval-like retarding-effect triggering is satisfied;
- at position **804**, the flow divergence is accompanied by further compressing and warming of flow portion **875** and a decrease of M-velocity lower than the specific M-velocity M_*, i.e. $M_* > M_{804}$;
- at position **805** above concavity **874**, the M-velocity M_{805} is minimal, thereby, providing the condition: $M_{801} > M_{802} > M_{803} = M_* > M_{804} > M_{805}$;
- at position **806**, the flow convergence is accompanied by cooling of flow portion **875**, a decrease of static pressure, and an increase of M-velocity, i.e. $M_{805} < M_{806}$;
- at position **807**, the second critical condition point, where the varying value of the flow portion **875's cross**-sectional area has the second local minimum, is designed to provide for that the M-velocity of flow portion **875** reaches the specific M-velocity M_*, i.e. the condition $M_{805} < M_{806} < M_{807} = M_*$ triggering the de Laval-like jet-effect is satisfied; and so,
- at positions **808** and **809**, the flow divergence is accompanied by further cooling of flow portion **875**, a decrease of static pressure, and an increase of M-velocity, i.e. $M_{805} < M_{806} < M_{807} = M_* < M_{808} < M_{809}$.

Depending on profile **871**, the M-velocity M_{809} of flow portion **875** at downstream position **809**, may exceed the high M-velocity M_{801} of flow portion **875** at upstream position **801**, so, wing **870** can be used as a jet-booster based on the de Laval-like jet-effect, operating at high velocities. In general, the use of a double-humped airfoil profile of a wing flying with the de Laval high M-velocities, in order to provide for the desired jet-effect, is yet one of the teachings of the present invention.

In view of the foregoing description referring to **Fig. 8d (A)**, it will be evident to a person skilled in the art that the effect of high M-velocity acceleration by the Coanda-jet-effect two-stage operation is applicable, for example, to high-speed aircraft design. One of the primary advantages of a double-humped airfoil wing is that, in contrast to a classic wing, the double-humped airfoil wing **870** being stationary (not-variably) configured-and-oriented has a positive lift-force as for low M-velocities and for high M-velocities.

In view of the foregoing descriptions referring to **Figs. 8a**, **8c**, and **8d (A)**, it will be also evident to a person skilled in the art that a pair of actually-airfoil wings (i.e. having sharp trailing ends adapted to provide laminarity of air sub-portions outflowing downstream behind the sharp

trailing ends), being arranged in-line along a sagittal axis one downstream behind the other and combined as a whole being stationary (not-variably) configured-and-oriented, can function similar to a double-humped airfoil wing **870** to provide a positive lift-force as for low M-velocities as well as for high M-velocities. Thus, the tandem **880.B** of two airfoil bodies embodied in the form of actually-airfoil wings **850.B** and **860.B** consolidated as a whole (**Fig. 8c Case (B)**) can be interpreted as a broken double-humped airfoil wing.

In view of the foregoing descriptions referring to **Figs. 6c**, **7d**, **8c**, and **8d (A)**, it will be evident to a person skilled in the art that, considering a body, flying in air-environment with transonic, and/or supersonic, and/or hypersonic velocities, i.e. with high M-velocities higher than the specific M-velocity $M_* = \sqrt{(\gamma - 1)/\gamma}$,

- in contrast to a case, wherein a body having an arbitrary shape is decelerating when air-fluxes, which flow nearby around the body, become warmer and extra-warmed,
- a specifically-shaped body, having a double-humped airfoil profile providing for the two-stage operation of the Coanda-jet-effect, is accelerating, and air-fluxes, which flow nearby around the accelerating specifically-shaped body, become cooled and extra-cooled.

In **Fig. 8d (B)**, it is shown a schematic drawing of a modified airfoil wing **8d**, supplied with the multi-layer TE device **8d.TED** built-in between the upper-side and lower-side surfaces of the modified airfoil wing **8d**. The modified airfoil wing **8d** has a side-view sectional classical airfoil profile, the orientation of which determines a sagittal axis **8d.0** oriented horizontally. For the purpose of the comparison between two wings: the double-humped airfoil wing **810** and the modified airfoil wing **8d**,

when the flying M-velocity is higher than the specific M-velocity $M_* = \sqrt{(\gamma - 1)/\gamma} \approx 0.5345\ Mach$;

an oncoming flow portion **8d.5** runs at the modified airfoil wing **8d**, becomes a boundary layer moving adjacent to the upper-side surface of the airfoil wing **870** under an imaginary surface, which, in a sagittal sectional plane, is indicated by a double-dot dashed line **8d.1** symbolizing an imaginary, in general, the curved surface formed by streamlines bordering the portion **8d.5** above the airfoil wing **8d**, and passes positions: **8d.1**, **8d.2**, **8d.3**, **8d.4**, **8d.5**, **8d.6**, **8d.7**, **8d.8**, and **8d.9** sequentially with associated M-velocities: M_{D1}, M_{D2}, M_{D3}, M_{D4}, M_{D5}, M_{D6}, M_{D7}, M_{D8}, and M_{D9}, correspondingly. The temperature distribution along the upper-side surface is forcibly controlled by the multi-layer TE device **8d.TED** such that as the flow moves nearby above the modified airfoil wing **8d:**

- when crossing the positions **8d.02**, **8d.03**, and **8d.04**, the temperature is gradually increasing thereby imitating the flow convergence and divergence when moving within a de Laval tube similar to the case when the flow moves nearby above the double-humped airfoil wing **870** crossing the positions **802**, **803**, and **804**, correspondingly; and
- after reaching the position **8d.05** and further, when crossing the positions **8d.06**, **8d.07**, **8d.08**, and **8d.09**, the temperature is gradually decreasing thereby imitating the flow convergence and divergence when moving within a de Laval tube similar to the case when the flow moves nearby above the double-humped airfoil wing **870** crossing the positions **806**, **807**, **808**, and **809**, correspondingly.

An advantage of the modified airfoil wing **8d** over the double-humped airfoil wing **870** is that the modified airfoil wing **8d** provides for all the useful properties of the double-humped airfoil wing **870** in a wide range of velocities, wherein all the useful properties are controllably improved using degrees of freedom of the multi-layer TE device **8d.TED.** While the overall geometry of the double-humped airfoil wing **870** is optimized to be adapted to the certain M-velocity M_{875} of oncoming flow **875**, the modified airfoil wing **8d** is capable to be optimally adapted to an arbitrary M-velocity $M_{8d.5}$ of oncoming flow portion **8d.5**. For this purpose, the forcibly established distribution of the temperature difference $\Delta T_{8d}(x)$ between the upper-side and lower-side boundary layers around the modified airfoil wing **8d** is defined as:

$$\Delta T_{8d}(x) = \Delta T_{870}(x) \times \left[\frac{M_{8d.5}}{M_{875}}\right]^2,$$

where $\Delta T_{870}(x)$ is the distributed original temperature difference between the upper-side and lower-side boundary layers specified when designing the overall geometrical configuration of the double-humped airfoil wing **870** considering the mentioned certain M-velocity M_{875} of oncoming flow **875**.

Cascaded Jet-Boosters

Fig. 9a is a schematic illustration of a sequential cascade of in-line arranged airfoil bodies **9011**, **9013**, **9014**, **9015**, and **9016**, each in the shape of an elongated drop, exposed to oncoming wind **900** having the ambient M-velocity substantially lower than the specific M-velocity $M_* = \sqrt{(\gamma - 1)/\gamma}$. The shape and forcedly distributed temperature of the elongated drops is optimized using the condition of flow continuity Eq. (6.0) basing on a specified thickness of a boundary layer over convex withers, as described hereinabove referring to **Figs. 8a** and **8b**. Points **9012** symbolize that the sequence of airfoil bodies may be

much longer than shown. For simplicity, oncoming wind **900** is laminar. Trace a moving-small-portion **910** of ambient oncoming wind **900** passing positions **911**, **9110**, **912**, **913**, **9130**, **914**, **9140**, **915**, **9150**, **916**, **9160**, and **917**, considering a case when moving-small-portion **910** is subjected to the Coanda-jet-effect in an adiabatic process, defined by the partial pressure-c δP_c, rather than affected by the skin-friction resistance, quantified by the difference $(a_w - a - \delta a)$. Moving-small-portion **910** at position **911** is yet to be subjected to the Coanda-jet-effect operation. I.e. at least the forward airfoil body **9011** meets moving-small-portion **910** with M-velocity, lower than the specific M-velocity $M_* = \sqrt{(\gamma - 1)/\gamma}$, and so body **9011** operates as a jet-booster based on the Venturi effect occurring in the adiabatic process in an imaginary tunnel adjacent to body **9011**, as described above referring to **Fig. 8b**. Further, moving-small-portion **910** is subjected to a cascaded operation of the Coanda-jet-effect in the adiabatic process by in-line arranged airfoil bodies **9011**, **9013**, **9014**, **9015**, and **9016**, each of which operates as an elemental jet-booster, while meeting moving-small-portion **910** with M-velocity, lower than the specific M-velocity $M_* = \sqrt{(\gamma - 1)/\gamma}$. The cascaded operation of the Coanda-jet-effect results in aligning of the Brownian random motion of moving-small-portion **910's** molecules with the surfaces of in-line arranged airfoil bodies **9011**, **9013**, **9014**, **9015**, and **9016**, that is observed as an increase of the effective velocity of moving-small-portion **910**, accompanied by moving-small-portion **910** temperature decrease, as moving-small-portion **910** sequentially passes positions **9110**, **9130**, **9140**, **9150**, and **9160**, where flowing as ambient-adjoining convergent-divergent jetstreams. Thus, this results in an increase of moving-small-portion **910's kinetic energy at the expense of moving**-small-portion **910's internal heat energy**. Consider certain identical cross-sectional areas at positions **911**, **912**, **913**, **914**, **915**, **916**, and **917**, marked by dashed ellipses, such that the Coanda-jet-effect operation influence is still perceptible within the marked areas. Considering flow velocities much lower than the specific M-velocity $M_* = \sqrt{(\gamma - 1)/\gamma}$, the effective velocity of flow crossing the marked areas at positions **911**, **912**, **913**, **914**, **915**, **916**, and **917** increases exponentially as the flow moves along the sequential cascade of in-line arranged airfoil bodies **9011** - **9016**. For example, if the Coanda-jet-effect operation of each of airfoil bodies **9011** - **9016** in the adiabatic process provides an increase of the effective velocity of a flow portion, crossing the associated marked area, on 2%, then after 35 airfoil bodies **9011** - **9016** the effective velocity of the wind portion, crossing the marked area, is twice as high as the velocity of oncoming wind **900** yet to be subjected to the Coanda-jet-effect multi-stage cascaded operation. Consider a case, when the M-velocity M_{9130} of moving-small-portion **910**, flowing as an ambient-adjoining convergent-

divergent jetstream nearby the withers of airfoil body **9013**, reaches the specific M-velocity $M_* = \sqrt{(\gamma - 1)/\gamma}$ at position **9130**. Triggering of the de Laval-like jet-effect causes the M-velocity M_{914} at position **914** to become higher than the specific M-velocity M_*. The moving-small-portion **910** becomes cooled between positions **913** and **9130** and becomes extra-cooled between positions **9130** and **914**. Running at airfoil body **9014**, moving-small-portion **910** is subjected to the de Laval-like retarding-effect, **such that the portion's** M-velocity decreases down to the specific M-velocity $M_* = \sqrt{(\gamma - 1)/\gamma}$ at position **9140** nearby the withers of airfoil body **9014**, and becomes lower than the specific M-velocity M_* at position **915**. The moving-small-portion **910** becomes warmer between positions **914** and **9140** and becomes extra-warmed between positions **9140** and **915**. Then moving-small-portion **910** is subjected to the de Laval-like jet-effect and the M-velocity increases again. Thus, when the sequence of airfoil bodies **9011 – 9016** is sufficiently long, the effective M-velocity of moving-small-portion **910** reaches the value of the specific M-velocity $M_* = \sqrt{(\gamma - 1)/\gamma}$ nearby the withers of airfoil bodies and varies around the value between the airfoil bodies. This is yet one more of the teachings of the present invention.

In view of the foregoing description referring to **Fig. 9a**, it will be evident to a person skilled in the art that:

- in a more general case, when oncoming wind **900** is turbulent, such that moving-small-portion **910** comprises whirling groups of molecules, the Coanda-jet-effect multi-stage cascaded operation results in aligning also of the turbulent motion of the whirling groups of molecules with the surfaces of in-line arranged airfoil bodies **9011**, **9013**, **9014**, **9015**, and **9016**, that is observed as an increase of the effective velocity of moving-small-portion **910**, accompanied by moving-small-portion **910's inner** turbulence decrease, as moving-small-portion **910**, flowing as ambient-adjoining convergent-divergent jetstreams nearby around the withers of airfoil bodies **9011**, **9013**, **9014**, **9015**, and **9016**, sequentially passes positions **9110**, **9130**, **9140**, **9150**, and **9160**, correspondingly. Thus, this results in an increase of moving-small-portion **910's kinetic energy also at the** expense of moving-small-portion **910's inner turbulent energy;**
- the effect of M-velocity acceleration and stabilization by a multi-stage cascaded operation of the Coanda-jet-effect thereby reinforced multi-repeatedly is applicable, for example, to a high-speed long-train design;
- the effect of M-velocity stabilization is applicable, for example, to a flying train-like object, in particular, supplied with wings, which are not shown here, providing for a lift-force;

- an arrangement of airfoil bodies **9011**, **9013**, **9014**, **9015**, and **9016** along a smoothly curved locus, instead of the in-line arrangement, can be implemented; and
- the stabilized temperature difference between the extra-cooled airflow portions subjected to the triggered de Laval-like jet-effect and the extra-warmed airflow portions subjected to the triggered de Laval-like retarding-effect can be used to power a Peltier-element operating as a thermoelectric generator producing electricity.

Reference is now made again to **Fig. 9a**, wherein now, all the in-line arranged airfoil bodies **9011**, **9013**, **9014**, **9015**, and **9016** are made from a conductive material, for simplicity, from a hypothetic super-conductor, wherein the sequence is exposed to electric flux **900**. In view of the foregoing description referring to prior art **Fig. 1f**, the inventor points out that the effective electric flux crossing the marked areas at positions **911**, **912**, **913**, **914**, **915**, **916**, and **917** is self-increasing exponentially as flowing along the sequential cascade of in-line arranged airfoil conductive bodies **9011** to **9016** due to the electromagnetic jet-effect.

Fig. 9b is a schematic illustration of a sequential multi-stage cascade of outer and nested airfoil rings **920**, exposed to oncoming wind **921**. Outer and nested airfoil rings **920** are formed by coiled-up walls having an actually-airfoil wing profile and forcedly distributed temperature, similar, for example, to that of actually-airfoil wing **810**, shown schematically in **Fig. 8a**. Thereby, outer and nested airfoil rings **920** have shapes of streamlined converging nozzles. The actually-airfoil wing profiles and forcedly distributed temperature are optimized using the condition of flow continuity *Eq. (6.0)* basing on the specified thickness of a boundary layer over convex withers, as described hereinabove with the references to **Fig. 8a**. Points **929** symbolize that the sequence of outer and nested airfoil rings **920** may be much longer than shown. Airflow portions **922**, flowing as ambient-adjoining convergent-divergent jetstreams, sliding outside of the sequential multi-stage cascade of outer rings **920**, as well as wind portions **923**, flowing and impacting inside of outer and nested airfoil rings **920**, are subjected to the Coanda-jet-effect operation. Again, consider a case when airflow portions **922** and **923** are subjected to the Coanda-effect operation rather than to skin-friction resistance, thereby providing that each pair of outer and nested airfoil rings **920** operates as an elemental jet-booster. Airflow portions **922** and **923** join a cumulative outflow **924**, wherein the Coanda-effect provides streamlines **925** forming an imaginary convergent-divergent nozzle downstream-behind the sequential multi-stage cascade of outer and nested airfoil rings **920**. A sufficiently long multi-stage cascade of outer and nested airfoil rings **920** provides that the M-velocity of resulting cumulative outflow **924** reaches the specific M-velocity $M_* = \sqrt{(\gamma - 1)/\gamma}$ at the minimal cross-section **926** of

the imaginary convergent-divergent nozzle and the de Laval-like jet-effect is triggered downstream-behind the minimal cross-section **926**. Airflow portion **927** is expanded adiabatically; therefore, it is extra-cooled and extra-accelerated. A prolonged multi-stage cascade of outer and nested airfoil rings **920** may enable the M-velocity of airflow portions **922** to reach the specific M-velocity M_* nearby the withers of airfoil outer rings **920**. In this case, airflow portions **922** become subjected to the de Laval-like jet-effect, such that the effective M-velocity of airflow portions **922** is stabilized, as described hereinbefore referring to **Fig. 9a**, considering a sequential multi-stage cascade of in-line arranged airfoil bodies, each having the shape of an elongated drop.

Fig. 9c is a schematic illustration of a modified sequential multi-stage cascade of the outer and nested airfoil rings **920** of **Fig. 9b** into a pair of unbroken spirals shaped as the Archimedean screws **931** and **932** by helical coiling-up walls having airfoil profile **937** and forcedly distributed temperature, for example, similar to described above referring to **Fig. 8a**. Airfoil profile **937**, also shown separately above and to the left in an enlarged scale, and forcedly distributed temperature, both are optimized using the condition of flow continuity Eq. (6.0) basing on the specified thickness of a boundary layer over convex withers, as described hereinabove with the reference to **Fig. 8a**, and taking into account an M-velocity range used for the spirals **931** and **932**. Oncoming airflow portion **933** is yet to be subjected to the Coanda-jet-effect operation. Both: the sliding outside air sub-portions **934** flowing around and the inside impacting air sub-portions **935** flowing through the pair of spirals **931** and **932**, are subjected to the Coanda-jet-effect operation, resulting in a converging flow when convergent flow sub-portions **934** and **935** laminarly join a resulting cumulative outflow **936**. I.e. a fragment [for instance, one coil] of the pair of spirals **931** and **932** operates as an elemental jet-booster, and a longer fragment of converging spirals **931** and **932** provides higher acceleration of the airflow. Again, the Coanda-jet-effect provides streamlines **930** forming an imaginary convergent-divergent jet-nozzle downstream-behind the airfoil construction.

Moreover, the two spirals **931** and **932** have counter helical screwing rotations, namely: clockwise and inverse-clockwise, thereby providing a spatially varying cross-sectional area of gaps between the walls of the two spirals **931** and **932**. The spatially varying cross-sectional area of the gaps provides a Venturi effect for velocities lower than the specific M-velocity $M_* = \sqrt{(\gamma-1)/\gamma}$ and the de Laval-like jet-effect for velocities providing for reaching the specific M-velocity $M_* = \sqrt{(\gamma-1)/\gamma}$ at the critical condition point where the variable cross-sectional area of gaps becomes minimal. Sufficiently long converging spirals **931** and **932** provide

acceleration of the airflow and stabilization of the effective velocity at the value of the specific M-velocity $M_* = \sqrt{(\gamma - 1)/\gamma}$ analogous to the cases described above with references to **Figs. 9a** and **9b**.

In view of the foregoing description of **Figs. 9a, 9b,** and **9c**, it will be evident to a person skilled in the art that:

- One can implement many alterations, re-combinations, and modifications of elemental jet-boosters, taught herein, without departing from the spirit of the disclosure that can be generalized as the following. A sufficiently long aggregation of elemental jet-boosters provides acceleration of an airflow portion, reaching the specific M-velocity $M_* = \sqrt{(\gamma - 1)/\gamma}$, thereby triggering alternating the de Laval-like jet-effect and the de Laval-like retarding-effect, resulting in a stable alternation of the airflow portion effective M-velocity above and below the specific M-velocity $M_* = \sqrt{(\gamma - 1)/\gamma}$ between the elemental jet-boosters; and
- The cumulative useful kinetic-power, including both: the originally brought kinetic-power and the acquired kinetic-power, provided by a multiplicity of elemental jet-boosters, aggregated into an adiabatic converging system, depends on the quality and quantity of the elemental jet-boosters and how the elemental jet-boosters are arranged and exploited. Moreover, it will be evident to a person skilled in the art that a sequential in-line multi-stage cascading of the elemental jet-boosters has a special sense.

For example, consider an aggregation comprising N elemental jet-boosters exposed to an ambient flow and oriented such that each elemental jet-booster provides an increase of the effective velocity of the flow portion moving through a certain effective cross-sectional area, by a factor F, wherein $F > 1$, and for simplicity and without loss of the explanation generality, consider a case of sufficiently low velocity of the ambient flow and assume that it is the same factor, independently of the elemental jet-boosters arrangement and exploitation. As well, for simplicity, consider the case, when the M-velocities of accelerated flow remain lower than the specific M-velocity $M_* = \sqrt{(\gamma - 1)/\gamma}$, thereby, justifying neglecting the flow's mass density change in further approximate estimations. As the kinetic-power of a flow portion moving through a certain cross-sectional area is directly proportional to the cross-sectional area and proportional to the third power of the flow portion velocity, each elemental jet-booster, when operating separately, launches a jetstream having the solitary useful kinetic-power, indicated by W_1, proportional to the third power of the factor F, expressed by $W_1 = W_0 \times F^3$, where W_0

is the originally brought ambient useful kinetic-power associated with the effective cross-sectional area of one elemental jet-booster.

The solitary acquired kinetic-power ΔW_1 is defined by the difference between the solitary useful kinetic-power W_1 and the originally brought ambient useful kinetic-power W_0, namely, $\Delta W_1 = W_0 \times (F^3 - 1)$; and so the aggregation, comprising N such elemental jet-boosters and thereby accelerating the flow portions, moving through N effective cross-sectional areas, results in the cumulative useful kinetic-power:

- indicated by $W_{parallel}$, equal to $W_{parallel} = N \times W_1 = N \times W_0 \times F^3$, wherein the cumulatively acquired kinetic-power $\Delta W_{parallel}$ is defined as:

$$\Delta W_{parallel} = N \times \Delta W_1 = N \times W_0 \times (F^3 - 1),$$

in the case, when the elemental jet-boosters operate independently, that occurs,

  - if the elemental jet-boosters are arranged in parallel, or
  - if the elemental jet-boosters are arranged sequentially, but operating in a not adiabatic process, allowing for the solitary useful kinetic-power W_1 to be consumed in parallel within or behind each elemental jet-booster and restored afore each next elemental jet-booster;

or, alternatively,

- indicated by $W_{sequential}$, equal to $W_{sequential} = W_0 \times (F^3)^N$, wherein the cumulatively acquired kinetic-power $\Delta W_{sequential}$ is defined as:

$$\Delta W_{sequential} = W_0 \times [(F^3)^N - N],$$

in the case, when the elemental jet-boosters are arranged sequentially operating in the adiabatic process, and the consumption of the cumulative useful kinetic-power is allowed behind the downstream-end of the last elemental jet-booster only.

In an exemplary practical case, the effective velocity increase factor equals $F = 1.097$. Then the following conditions become satisfied:

- the condition $W_{sequential} < W_{parallel}$ is satisfied for $N \leq 8$;
- the condition $W_{sequential} > W_{parallel}$ is satisfied for $N \geq 9$;
- the condition $W_{sequential} > 2W_{parallel}$ is satisfied for $N \geq 13$;
- the condition $W_{sequential} > 3W_{parallel}$ is satisfied for $N \geq 15$; and
- the condition $W_{sequential} > 4W_{parallel}$ is satisfied for $N \geq 16$.

In view of the foregoing description of **Figs. 9a**, **9b**, and **9c**, one of the primary teachings is that an artificial wind can be used for the profitable harvesting of electricity. For example, one can:

- use a big-front ventilator [or group of ventilators], having 50%-net-efficiency, i.e. consuming electric-power $W_{consumed}$ and creating an originally incoming artificial airflow, bringing kinetic-power $W_{income} = 0.5 \times W_{consumed}$, wherein the originally incoming artificial airflow has the front area A_{income} of 4 times bigger than the effective cross-sectional area of an elemental jet-booster and has the effective velocity u_{income};
- implement a sequential multi-stage cascade, comprising $N = 15$ elemental jet-boosters, each of which is characterized by the effective velocity increase factor $F = 1.097$, such that altogether making an outflowing artificial jetstream, having the velocity $u_{jetsrteam} = u_{income} \times F^N$ [$F^N = 1.097^{15} \approx 4$] and having the resulting effective frontal cross-sectional area $A_{jetsrteam}$, decreased approximately 4 times relative to the area A_{income} of originally incoming airflow [$A_{income}/A_{jetsrteam} = F^N \approx 4$]. Thus, the outflowing artificial jetstream brings the resulting useful kinetic-power $W_{jetsrteam}$, estimated as:

$W_{jetsrteam} = \left[\left(u_{jetsrteam}/u_{income}\right)^3 \times \left(A_{jetsrteam}/A_{income}\right)\right] \times W_{income}$, i.e.

$W_{jetsrteam} = [4^3/4] \times W_{income} = [16] \times 0.5 \times W_{consumed} = 8 \times W_{consumed}$;

and

- use a wind-turbine, producing electricity with 50%-net-efficiency, thereby, harvesting the useful electric-power W_{useful} of 4 times higher than the consumed electric-power $W_{consumed}$, namely,

$$W_{useful} = 0.5 \times W_{jetstream} = 0.5 \times (8 \times W_{consumed}) = 4 \times W_{consumed} .$$

Wherein, the profit becomes greater than estimated, when the de Laval-like jet-effect is triggered. Thereby, in view of the foregoing description referring to **Figs. 9a**, **9b**, and **9c**, it will be evident to a person skilled in the art that profitable harvesting of electricity, using a jet-effect created by a multi-stage cascaded operation of the Coanda-jet-effect thereby reinforced multi-repeatedly, is feasible, for example, attaching sequentially arranged elemental jet-boosters to a sufficiently-long moving vehicle and using a wind-turbine, arranged behind the downstream-end of the last elemental jet-booster.

In view of the foregoing description referring to **Figs. 9a**, **9b**, and **9c**, the inventor points out that, when reaching the stabilized effective velocity equal to the value of the specific M-velocity $M_* = \sqrt{(\gamma - 1)/\gamma}$, the periodical local extra-acceleration and extra-retarding generate a forced extra-intensive elemental acoustic wave, wherein the distance between each

two neighbor withers equals half of the wavelength of the forced extra-intensive elemental acoustic wave. Furthermore, the forced extra-intensive elemental acoustic waves are superposed in-phase thereby constituting the resulting extra-intensive acoustic wave as constructive interference. It will be evident to a person skilled in the art that the arrangement of airfoil bodies, either:

- **9011**, **9013**, **9014**, **9015**, and **9016** as shown in **Fig. 9a**; or
- a multi-stage cascade of outer and nested airfoil rings **920** as shown in **Fig. 9b**; or
- a pair of unbroken spirals shaped as the Archimedean screws **931** and **932** by helical coiling-up walls having airfoil profile **937**, as shown in **Fig. 9c**,

subjected to the generalized jet-effect (namely, the Coanda-jet-effect, the de Laval-like jet-effect, the de Laval-like retarding effect, and the enhanced waving jet-effect) and supplied by an acoustic detector capable of detection of the resulting extra-intensive acoustic wave power, can play a role of an electricity generator that, in the final analysis, produces the electric power at the expense of the warmth of the air.

Jet-Turbine as Improved Wind-Turbine

Fig. 9g is a schematic drawing of a jet-rotor of modified improved wind-turbine, called also a jet-turbine, **9.0**, constructed according to the principles of the present invention to operate under relatively fast airflow **9.1** for producing the electric power at the expense of the warmth of relatively fast airflow **9.1**.

Modified improved wind-turbine or jet-turbine **9.0** comprises:

- axle **9.2** oriented along sagittal axis **9.21** codirected with fast airflow **9.1**,
- identical asymmetrical biconvex actually-airfoil blades **9.3**, attached to axle **9.2**; and
- an engine, which is not shown here, having a stator and rotatable shaft; the engine is capable of transforming the power of the forced mechanic rotational motion **9.4** of axle **9.2** into electric power.

The primary feature, making the jet-turbine **9.0** practically implementable and extremely efficient, is the specifically configured and so specifically functioning biconvex actually-airfoil blades **9.3**. Namely, in contrast to standard wind-turbines having standardly shaped blades configured to be subjected to impacting by an incoming airflow that, in particular, results in the airflow turbulence, retarding, and warming, the jet-turbine **9.0** has asymmetrical biconvex wing-like actually-airfoil blades **9.3**:

- having opposite convex sides **9.31** and **9.32** with withers differing in convexity, and

- being oriented along and so adapted to the incoming fast airflow jetstream **9.11** headway motion.

Thereby configured and oriented blades provide the zero attack angle:

- to exclude or at least to minimize the impact by the incoming fast airflow jetstream **9.11**, but
- to provide an interaction with the fast airflow jetstream **9.11** by the Coanda-jet-effect only, thereby resulting in acceleration and cooling of outflowing jetstream **9.6** and resulting in lift-forces, acting on identical biconvex actually-airfoil blades **9.3** and being imbalanced because of the aligned asymmetry of the identical biconvex airfoil blades.

In this case, the axle **9.2** rotational motion, shown by the curved arrow having numeral **9.4**, is caused by the cumulative resulting lift-force. Take note again, that the Coanda-jet-effect is triggered by the airflow kinetic-power and is actually powered at the expense of the airflow warmth but not at the expense of the incoming fast airflow jetstream **9.11** kinetic-power; contrariwise, the kinetic-power of outflowing jetstream **9.6** is increased or at least not decreased with respect to the oncoming fast airflow **9.1**. Thus, in contrast to the standard wind-turbines, the proposed improved wind-turbine **9.0** is specifically characterized:

- by the mechanism of operation, that is the Coanda-jet-effect but not the impact; and
- by the power source of an operation, that is the warmth but not the kinetic power of airflow.

Also, in contrast to a kind of the standard wind-turbines having wing-like blades moving around a vertical axis, the proposed jet-turbine **9.0** is specifically characterized by the excluding of varying poorly-streamlined positions of the wing-like blades. As well, in contrast to the standard wind-turbines, the productivity of the proposed jet-turbine **9.0** is defined by the area of the biconvex airfoil blades rather than by a so-**called "swept area", namely, the produced electric** power due to the Coanda-effect is specified as proportional to the biconvex airfoil blades area, i.e. the productivity can be increased substantially for a given swept area.

In view of the foregoing description referring to **Fig. 9g**, it will be evident to a person skilled in the art that jet-turbine **9.0** comprising:

- the biconvex airfoil blades, having a wing-like sectional contour with a longer so-called chord of wing, and/or
- an increased quantity of the biconvex airfoil blades,

both circumstances provide for enforcing of the desired Coanda-jet-effect. As well, it is self-suggested a sequential in-line arrangement of a multiplicity of jet-turbines **9.0** one downstream after another (optionally, alternatingly differing in asymmetry to become forcedly rotated

alternatingly clockwise and inverse-clockwise, correspondingly), each separately and all together efficiently operating within the given swept area.

Moreover, at least one of the profiles **9.31** and **9.32** is implemented to provide the enhanced de Laval jet-effect, when the incoming fast airflow jetstream **9.11** is flowing with a de Laval M-velocity and so a portion of jetstream **9.11** is reaching the specific M-velocity nearby the withers of the asymmetrical biconvex actually-airfoil blades **9.3**. In this case, the extra-efficiency of the modified improved wind-turbine is expected.

Furthermore, optionally, sides **9.31** and **9.32** differ in shape such that one of the sides has one convex withers and the opposite side has a double-humped airfoil profile providing for the two-stage operation of the Coanda-jet-effect as described hereinabove with the reference to **Fig. 8d**. Such asymmetrical blades, when exposed to oncoming fast airflow **9.1** moving with a high M-velocity, higher than the specific M-velocity, become subjected, on the one hand, to the de Laval retarding effect, and on the other hand, to the enhanced de Laval jet-effect. This provides for extra-increased lift-forces acting in unison and in the same direction of rotation and so rotating axle **9.2**. In this case, the extra-efficiency of the modified improved wind-turbine is expected in a wide range of velocities.

Fig. 9h is a schematic drawing comprising the side-view and front view of a jet-rotor of jet-turbine **9.7**, constructed according to the principles of the present invention to operate under relatively fast airflow **9.70** for producing the electric power at the expense of the warmth of relatively fast airflow **9.70**. An engine of the jet-turbine, which (the engine) having a stator and rotatable shaft, is not shown here. Axle **9.73**, collinear with sagittal axis **9.74**, is oriented to be codirected with the headway motion of the relatively fast airflow **9.70.** In relation to all the principal features, the jet-turbine **9.7** is similar to the jet-turbine **9.0**, described hereinabove referring to **Fig. 9g**, but now, referring to the aforementioned optional diversity of the implementation of the principal features, the biconvex actually-airfoil blades, which have opposite at least partially convex sides **9.71** and **9.72** with withers differing in convexity, are further curved and screwed to optimize a suppression of turbulence as well as are cascaded one downstream after another to provide a multi-stage repeated operation of the Coanda-jet-effect thereby contributing to the desired cumulative lift-force to rotate axle **9.73**.

In view of the foregoing description referring to **Figs. 9g** and **9h**, it will be evident to a person skilled in the art that jet-turbine **9.0** or **9.7**, when attached to a flying aircraft, is capable of efficient harvesting of the electric power from the ambient air warmth.

Furthermore, in view of the description expound hereinabove with references to **Figs. 5i**, **5j**, **5k**, **9a**, **9b**, **9c**, **9d**, **9e**, and **9f**, the inventor points out that the mentioned multiplicity of jet-turbines **9.0** or **9.7**, arranged sequentially one downstream after another [**not shown here**], results in the generation of acoustic waves accompanied by extraction of the internal heat energy of ambient air in favor for the wave power due to the enhanced waving jet-effect. Thus, a system, comprising the arrangement and a detector of the acquired wave power, has an additional degree of freedom to increase the efficacy of the production of electricity.

In view of the foregoing description referring to **Figs. 9g** and **9h** in combination with the **foregoing description of subparagraphs "**Point of Sail**" and "**Flying Bird**", both with the reference** to prior art **Fig. 1i**, it will be evident to a person skilled in the art that the construction of jet-turbine **9.7**, when having a controllable speed of the axle **9.73** rotation adapted to the velocity of oncoming airflow **9.70** to keep the airflow remaining laminar, provides a controllable net jet-thrust against the oncoming airflow **9.70** and so becomes applicable as a kind of jet-engine for a controllable and substantially noiseless flying.

Furthermore, in view of the foregoing description referring to **Figs. 9g** and **9h**, it will be evident to a person skilled in the art that jet-rotor **9.7** having relatively massive actually-airfoil wings,

> when being attached to a body moving in a fluid and being capable of free rotation around the sagittal axis **9.74** due to the self-originated lift-forces acting on all the massive wings in unison and in the same direction of rotation,

creates the gyroscopic effect that is defined as a tendency of the moving body to maintain a steady direction collinear with the sagittal axis **9.74** being the axis of the massive wings rotation and is manifested as a resistance to gusty fluctuations of motion of the ambient fluid, wherein the energy to generate the desired gyroscopic effect improving ballistic properties of the moving body is harvested from the ambient fluid warmth due to the Coanda-jet-effect.

Jet-Ventilator and Jet-Propeller

Fig. 9j is a schematic drawing of a modified improved ventilator, called also a jet-ventilator, **9J.0**, constructed according to the principles of the present invention to create a headway laminarly moving flow. The jet-ventilator **9J.0** comprises a jet-rotor, which also is marked by numeral **9J.0**, and a motor, which is not shown here, having a stator and rotatable shaft. The motor, being powered by either a burned fuel or electrical power, forcedly rotates the rotatable shaft and, thereby, the jet-rotor **9J.0**.

One of the specifics of the jet-ventilator **9J.0** is that blades **9J.1**, having a profile **9J.2** similar to the profile of actually-airfoil biconvex wing **810** described hereinabove referring to **Fig. 8a**, are configured to be actually-airfoil and, when rotating, oriented to run over air portions **9J.6** (yet to be subjected to a motion) under the zero attack angle and to act on the air portions **9J.6** due to the Coanda-effect only. As the air portions **9J.6**, when subjected to the Coanda-effect, originate lift-force **9J.3** acting on the blades **9J.1**, the blades **9J.1** push-off the air portions **9J.6** in the opposite direction collinear to sagittal axis **9J.7 according to Newton's Third Law**. Thereby, headway-forwarding air portions become a headway-forwarding laminar no-whirling outflow **9J.5** created by the jet-ventilator **9J.0**. As the used blades **9J.1** are actually-airfoil, relatively low power consumption can provide a relatively fast rotation **9J.9** of the blades **9J.1**, wherein the velocity of the fast rotation **9J.9** is in conformance with an optimal configuration **9J.2** of the actually-airfoil blades **9J.1.** Since the desired acceleration of the outflow occurs due to the Coanda-effect only, the method of accelerating the outflow allows for significantly reducing energy consumption compared with the classical technique based on the impact of the blades. It will be evident for a commonly educated person, that the concept of jet-ventilator **9J.0** is applicable to any fluid either gas or liquid. A disadvantage of the technique to create the laminar no-whirling flow **9J.5** is that the relatively fast rotation **9J.9** of the blades **9J.1** produces relatively slow laminar no-whirling flow **9J.5**.

Fig. 9k is a schematic drawing of jet-propeller **9K.0**, constructed according to the principles of the present invention. The jet-propeller **9K.0** comprises a jet-rotor, which also is marked by numeral **9K.0**, and a motor, which is not shown here, having a stator and rotatable shaft. The motor, being powered by either a burned fuel or electrical power, forcedly rotates the rotatable shaft and, thereby, the jet-rotor **9K.0**. As the function difference between jet-propeller **9K.0** and jet-ventilator **9J.0** is that, while the jet-rotor of jet-ventilator **9J.0** acts to initially motionless air portions **9J.6**, the jet-rotor of jet-propeller **9K.0** acts to airflow **9K.6** oncoming to blades with a certain velocity; so, the primary constructive difference between jet-propeller **9K.0** and jet-ventilator **9J.0** is in the orientation of blades. Namely, blades **9K.1** of jet-propeller **9K.0** are turned on a certain angle **9K.8**, called also pitch, such that, when rotating with a certain rate **9K.9**, to run over oncoming airflow **9K.6** under the zero attack angle and to act on oncoming airflow **9K.6** due to the Coanda-effect only. As the lift-force **9K.3** acting on wings **9K.1** has a component directed collinearly to sagittal axis **9K.7** against the direction of the oncoming airflow **9K.6**, the oncoming airflow **9K.6** becomes subjected to acceleration according to **Newton's Third Law, thereby forming, resulting hea**dway-forwarding outflow **9K.5**. As the

certain velocity of oncoming airflow **9K.6**, the certain rate of blades **9K.1** rotation **9K.9**, and the certain angle **9K.8** of blades **9K.1** orientation, all are interrelated, one can adapt the blades **9K.1** rotation rate **9K.9** and angle of orientation **9K.8** to the oncoming flow velocity **9K.6** to provide the zero attack angle to act on oncoming airflow **9K.6** due to the Coanda-effect only. When all the parameters are matched, the resulting headway-forwarding outflow **9K.5** accelerated by jet-propeller **9K.0** is laminar and no-whirling.

In view of the foregoing description referring to **Figs. 9j** and **9k**, it becomes evident, that:

- jet-propeller **9K.0** can comprise a variable pitch being capable of being adapted to the velocity of oncoming flow and rotation rate;
- jet-ventilator **9J.0** can be interpreted as a particular case of jet-propeller **9K.0**, the pitch of which is adapted to initially stationary fluid;
- jet-ventilator **9J.0**, pitch **9J.8** of which providing the zero attack angle of meeting stationary portions of air, and jet-propeller **9K.0**, pitch **9K.8** of which being adapted to the velocity of airflow **9J.5** created by jet-ventilator **9J.0**, can be arranged in-line: the jet-propeller after the jet-ventilator, thereby forming a system that as a whole performs an improved jet-ventilator providing for boosted outflow; and
- since the blades of jet-propeller **9K.0**, when moving, meet the ambient fluid at the zero attack angle and so, on the one hand, consume power to overcome a minimized drag and, on the other hand, produce the useful-beneficial power of accelerated outflow at the expense of ambient warmth due to the Coanda-jet-effect, a net-efficiency higher than 100% becomes reachable.

Reference is now made to **Fig. 9L**. **Fig. 9L** is a schematic illustration of a multi-module jet-ventilator **9L.0**, constructed according to the principles of the present invention to create a boosted headway-forwarding laminar no-whirling **9L.5**. The multi-module jet-ventilator **9L.0** comprises a tuple of modules **9L.01** to **9L.07** attached to a common shaft. Each of the modules **9L.01** to **9L.07** is characterized by an individual pitch, wherein:

- **The "zero" pitch of the first module 9L.01** provides for that, when the rotating blades of the first module **9L.01** run over the originally stationary portion of air **9L.6** at the zero attack angle, the first module **9L.01** functions as jet-ventilator **9J.0** described hereinabove referring to **Fig. 9j**;
- A relatively small pitch of the second module **9L.02** provides for that, when the rotating blades of the first module **9L.02** run over portions of a relatively slow flow originated by the first module **9L.01** at the zero attack angle, i.e. the second module **9L.02** functions as jet-ventilator **9K.0** adapted to a certain oncoming flow as described hereinabove referring to **Fig. 9k**;

- The individual pitch of each next module: **9L.03 to 9L.07**, provides for that, when the rotating blades of the next module: **9L.03 to 9L.07** run over portions of a flow originated the previous module: **9L.02 to 9L.06**, correspondingly, at the zero attack angle, i.e. all each of the modules **9L.03 to 9L.07** functions as jet-ventilator **9K.0** adapted to an associated oncoming flow as described hereinabove referring to **Fig. 9k**.

As a result of all the modules **9L.01** to **9L.07** operation as a whole, the resulting headway-forwarding laminar no-whirling outflow **9L.5** becomes accelerated reaching a relatively high velocity vectored collinearly to sagittal axis **9L.7.**

Fig. 9m is a schematic illustration of a cascade **9M.0** of multi-module jet-ventilator **9M.01** and two multi-module propellers **9M.02** and **9M.03** aggregated along the common sagittal axis **9M.7**. The cascade **9M.0** is constructed according to the principles of the present invention, wherein the multi-module jet-ventilator **9L.0** and multi-module propellers **9M.02** and **9M.03**, each comprises a tuple of modules attached to a common shaft. The multi-module jet-ventilator **9M.01** acts on an initially stationary portion of fluid **9M.6** and creates outflow **9M.51**, which, in turn, becomes oncoming flow **9M.51** blowing the multi-module jet-propeller **9M.02.** The multi-module jet-propeller **9M.02** acts on the oncoming flow **9M.51** and creates outflow **9M.52**, which, in turn, becomes oncoming flow **9M.52** blowing the multi-module jet-propeller **9M.03.** The multi-module jet-propeller **9M.03** acts on the oncoming flow **9M.52** and creates the resulting outflow **9M.53.** Without loss of generality, the tuple of the multi-module jet-ventilator **9M.01** is a triplet of modules attached to a common shaft. As well, again, without loss of generality, a tuple of each of jet-propellers **9M.02** and **9M.03** is a triplet of modules attached to a common shaft. Each of the mentioned modules comprises three sets of blades, wherein each of the sets is characterized by an individual pitch. The pitches of modules and rates of rotations **9M.91**, **9M.92**, and **9M.93** are chosen such that all the blades run over portions of oncoming flow at the zero attack angle. Optionally, blades of jet-propeller **9M.02** are configured for rotations **9M.91** and **9M.92** in mutually-opposite directions: clockwise and contrary-clockwise, correspondingly. The alternating directions of the rotations of in-line arranged jet-rotors are preferred to compensate for the unwanted whirling of flow. Although the unwanted whirling is purposely suppressed by excluding or at least minimizing the impact by blades, it (the unwanted whirling) can be originated due to other effects such as skin-friction between the flow and blades as well as jet-**thrust described hereinabove in subparagraphs "**Point of Sail**" and "**Flying Bird**", both with** the reference to prior art **Fig. 1i**.

Heat-Turbine and Jet-Transformer

Fig. 9n is a schematic illustration of a concept to transform ambient warmth into electricity. The concept is embodied as a heat-turbine **9n.H** and jet-transformer **9n.J** comprising:

- a laminar flow maker **9n.2**, in turn, comprising at least one of:
  - a shaped heater **9n.21**, conceptually, having a geometry of convex-concave corpus having airfoil outer walls **9n.211** and paraboloidal inner wall **9n.213** and being supplied by a point heater **9n.212** located in the focus of the paraboloidal inner wall **9n.213**;
  - a shaped jet-ventilator **9n.22**, conceptually, embodied as a multi-module jet-ventilator described hereinabove in the subparagraph Jet-Ventilator and Jet-Propeller referring to **Figs. 9j, 9k, 9L,** and **9m** [here, for simplicity of the drawing, a one-module jet-ventilator **9n.22** is shown];
- a specifically shaped pipe **9n.1** having the optimized convergent-divergent inner tunnel, described hereinabove in sub-**paragraph** "Convergent-Divergent Jet-Nozzle" **with** reference to **Fig. 6a**; namely, the convergent-divergent inner tunnel, elevated above the ground to allow for the ambient air **9n.41** entering the optimized convergent-divergent inner tunnel, comprises forcedly controllable thermoelectric devices **9n.TED** built-in into walls **9n.WALLS** such that the geometry of the tunnel, temperature distribution along the tunnel, and velocity of the upward laminar flow become interrelated according to the condition of flow continuity Eq. (6.0); and
- at least one jet-turbine **9n.3**, designed as the jet-turbine **9.7** described hereinabove referring to **Fig. 9h**;

all, constructed according to the principles of the present invention.

The Case When The Shaped Heater **9n.21** Is Used In The Heat-Turbine **9n.H**

The specifically shaped pipe **9n.1** is upward-oriented. The point heater **9n.212** supplies the heat energy to a fluid portion adjacent to the focus of the parabolically-concave surface **9n.213** of the shaped heater **9n.21's** convex-concave corpus, thereby, on the one hand, to trigger the **Archimedes' upward**-vectored force lifting the heated fluid portion and, on the other hand, to align the airflow **9n.42** upward along the vertical axis **9n.51** which is a sagittal axis, for the case. The upward airflow **9n.42** is relatively slow and substantially-laminar. The optimized convergent-divergent inner tunnel of the specifically shaped pipe **9n.1**, supplied with forcedly controllable thermoelectric devices **9n.TED** built-in into walls **9n.WALLS**, is designed according to the condition of flow continuity Eq. (6.0) to provide for substantial suppression of jumps of the air thermodynamic parameters and, thereby, to provide for the substantial acceleration of the airflow **9n.42**, laminarly and so noseless streaming upward. So, the heating triggers the

upward motion of air, and, in turn, the fluid motion itself triggers the convective acceleration as the airflow moves through the narrowing cross-section of the optimized convergent-divergent inner tunnel. Considering:

- the temperature above the exhaust **9n.54** equal T_e that is lower than the temperature T_a of the ambient air; the condition $T_e = T_a$ is for the worst-case estimation;
- the temperature near the level **9n.52** equal T_0, and
- the temperature near the narrow throat **9n.53** equal T_*,

equation (7.1c), described hereinabove referring to **Fig. 7a**, says that:

- to obtain the enhanced de Laval jet-effect for air utilizing the optimized convergent-divergent inner, one must provide the ratio T_0/T_* at least of **1.2**; and
- to provide that the temperature T_e of outflowing stream **9n.44** above the exhaust **9n.54** become equal to the temperature of ambient air, to accelerate an air portion up to the velocity of sound, one must provide the ratio T_0/T_e at least of **1.7**.

Hence, providing the heating of air near the level **9n.52** up to about the temperature 234^0C only, the condition of the enhanced de Laval jet-effect becomes satisfied, in turn, providing that the relatively low heat power, supplied by point heaters **9n.212**, triggers the enhanced de Laval jet-effect transforming the warmth of the moving airflow into the acquired kinetic power of the airflow. The energy E_0, necessary for warming 1 cube meter of air from the temperature 25^0C up to the temperature 234^0C, is estimated as $E_0 = \rho V C_V (T_0 - T_a)$, where V is the volume of 1 cube meter, ρ is the air mass density, $\rho \approx 1.2\ kg/m^3$, C_V is the air heat capacity, $C_V \approx 0.72\ kJ/(kg \cdot K)$, thereby, $E_0 \approx 1.2 \times 1 \times 0.72 \times (234 - 25) \approx 180\ kJ$.

As the mentioned assumed condition allows to accelerate the airflow portion **9n.54** up to the specific M-velocity $M_* = \sqrt{(\gamma - 1)/\gamma}$ near the narrow throat **9n.53** and to accelerate the airflow portion **9n.54** up to almost the speed of sound (i.e. the exhaust M-velocity is of $M_e \approx 1$), then, an exemplary estimation is as follows:

- the acquired kinetic energy, $\mathrm{K_e}$, of the outflowing airflow portion **9n.54**, which (the acquired kinetic energy $\mathrm{K_e}$) is specified as the difference between bringing heat energies, equals $K_e \approx n \times (T_0 - T_e) \times R$, where n is number of moles in the considered 1 cube meter of air, $n \approx 44.64$, and R is the specific gas constant, approximated for the air by $R = 287\ J/(kg \cdot K)$, i.e. $K_e \approx 44.64 \times 209 \times 287 \approx 2{,}677\ kJ$, that, in turn, says that the acquired kinetic energy $\mathrm{K_e}$ may exceed the consumed energy E_0 at least at subsonic velocities by the factor of 15; and

- the acquired kinetic energy, K_*, of the airflow portion **9n.54**, when crossing the narrow throat, equals $K_* \approx n \times (T_0 - T_*) \times R \approx 764\ kJ$, thereby showing that the acquired kinetic energy K_* may exceed the consumed energy E_0 by the factor of 4.24.

It will be evident to a commonly educated person that, if not to use the optimized convergent-divergent inner tunnel, designed according to the condition of flow continuity Eq. (6.0), the mentioned effective conversion of the airflow heat energy into the airflow kinetic energy is impossible because of originated turbulences and Mach waves, both accompanied by noise and energy dissipation back to the air warmth.

The jet-turbine **9n.3** meets the upping laminar airflow and provides for the production of electricity neither retarding the upward airflow and nor distorting the upward airflow laminarity as described hereinabove referring to **Figs. 9g** and **9h**. The inventor points out again that the improved wind-turbine **9n.3** harvests electric power at the expense of the airflow warmth but not from the airflow kinetic power, wherein the increased kinetic power of the airflow plays the role of a boosted trigger of the lift-force rotating the improved wind-turbine. Moreover, optionally, in-line arranged several jet-turbines **9n.3** provide for a multi-stage repeatedly harvesting of electricity from the same airflow portion.

It will be evident to a person who has studied the present invention that both the outer convex wall **9n.211** and the inner wall **9n.213** can be supplied with built-in matrix thermoelectric devices to control the laminarity of the entering heated flow **9n.42**.

The Case When The Shaped Jet-Ventilator **9n.22** Is Used In Jet-Transformer **9n.J**

The substantially-laminar airflow **9n.42** enters the specifically shaped pipe **9n.1** with a certain velocity u_{in}. The optimized convergent-divergent inner tunnel of the specifically shaped pipe **9n.1**, supplied with forcedly controllable thermoelectric devices **9n.TED** built-in into walls **9n.WALLS**, is designed according to the condition of flow continuity *Eq. (6.0)* such to be adapted to the velocity u_{in} to result in the substantial acceleration of the airflow **9n.42**, laminarly and so noseless streaming along the optimized convergent-divergent inner tunnel; wherein, in this case, the orientation of the sagittal axis **9n.51** is not obligatory upward.

Levitating Apparatus Imitating Effects Of Taking-off of Bird and Insect

Fig. 9o is a schematic illustration of a levitating apparatus **9o.0** comprising:

- a shaped propeller **9o.1**, conceptually, embodied as a multi-module jet-ventilator [here, for simplicity of the drawing, a pair of counter-rotating one-module jet-ventilators is shown; the rotations are indicated by the circle arrows **9o.13** and **9o.14**] described hereinabove in the subparagraph Jet-Ventilator and Jet-Propeller referring to **Figs. 9j, 9k, 9L,** and **9m**; and

- a capsule **9o.2** having a dominantly-airfoil overall shape and being optionally scaled to fit a person [a sculpture **9o.3** is shown instead of the person].

The wings **9o.11** and **9o.12** of the shaped propeller **9o.1** are supplied with thermoelectric **devices as described hereinabove in subparagraphs** "Modified Symmetrical Wing" **and** "Shaped Wing as a Convergent-Divergent Jet-Nozzle" **referring to Figs. 8** and **8a** such that providing the effective temperature difference ΔT_{WING} between the upper and lower sides of the wings **9o.11** and **9o.12**. Shell **9o.SHELL** of the capsule **9o.2** is supplied with a matrix thermoelectric device **9o.TED** such that the temperature of the shell **9o.SHELL**'s outer side is forcedly controlled to be gradually distributed along the axis **Z** providing the integral temperature difference $\Delta T_{Z,CAPSULE}$ around the ambient temperature $T_{AMBIENT}$. The gradually smoothed curve **9o.4** is in coordinates **(T, Z)**, where the axis-**T** indicates the temperature. When the wings **9o.11** and **9o.12** are rotating around the vertical axis **9o.AXIS**:

- while the wings **9o.11** and **9o.12** are subjected to:
  - the lift-force F_{LIFT}, that is a measure of the lift-**effect of a "cold-blooded" wing**, i.e. is provided by the airfoil geometry of the wings **9o.11** and **9o.12**, and
  - the positive contribution ΔF_{BIRD} to the upward-vectored force, wherein the originated effect of the contribution ΔF_{BIRD} imitates the effect of taking-off of a bird;
- the capsule **9o.2** is subjected to blowing by fresh portions of air triggering the positive contribution ΔF_{INSECT} to the upward-vectored force, wherein the originated effect of the contribution ΔF_{INSECT} imitates the effect of taking-off of an insect.

To evaluate the practicality of the flying apparatus **9o.0** for industrial use, exemplary positive contributions ΔF_{BIRD} and ΔF_{INSECT} to the upward-vectored force are estimated considering:

- the normal ambient air conditions: $T = T_{AMBIENT} \approx 300K$, $P = P_{AMBIENT} \approx 100{,}000Pa$, $\rho = \rho_{AMBIENT} \approx 1.2\ kg/m^3$, and $\gamma = 7/5$;
- an exemplary version of the shaped propeller **9o.1** performing a two-module ventilator having two triplets of wings **9o.11** (i.e. **6** wings);
- each of the wings **9o.11** has a chord of $0.25\ m$ and a span of $0.5\ m$; i.e. the total area of the wings is $A_{WINGS} = 6 \times 0.25 \times 0.5 = 0.75\ m^2$;
- the effective temperature difference between the upper and lower sides of the wings is $\Delta T_{WING} = -30C$;
- the refreshed air portions on the upper and lower sides of the wings are subjected to suddenly originated effective difference in static pressures along the axis **Z**, indicated by ΔP_{WING}, interrelated with ΔT_{WING} according to equation $Eq.\ (1.1b)$ described

hereinabove in the subparagraph "Sound as Complicated Movement in Molecular Fluid" prefacing the reference to **Fig. 1n**, namely, the ratio $(-\Delta T_{WING})/T \approx 0.1$, the ratio $(-\Delta P_{WING})/P \approx 0.1 \times (7/5)/(2/5) = 0.35$, and so the suddenly originated effective additional static pressure difference is $(-\Delta P_{WING}) \approx 0.35 \times 10^5 Pa$;

- the velocity-dependent suddenness factor, indicated by C_{WING}, for calculation of the ΔF_{BIRD} is given by **0.1** as corresponding to the effective velocity u_{WING} of the wings rotation **9o.12** as fast as $20\ m/sec$;
- the cross-sectional area **9o.21** of a projection of the capsule **9o.2**, $A_{(X,Y),CAPSULE}$, in a horizontal plane is given by $0.8\ m^2$;
- the integral temperature difference, $\Delta T_{Z,CAPSULE}$, is given by $-30C$;
- the refreshed air portions, when flowing around the capsule **9o.2**, are subjected to suddenly originated effective difference in static pressures along the axis **Z**, indicated by $\Delta P_{Z,CAPSULE}$, interrelated with $\Delta T_{Z,CAPSULE}$ as follows: the ratio $\left(-\Delta T_{Z,CAPSULE}\right)/T \approx 0.1$, the ratio $\left(-\Delta P_{Z,CAPSULE}\right)/P \approx 0.1 \times (7/5)/(2/5) = 0.35$, and so the suddenly originated additional static pressure difference is $\left(-\Delta P_{Z,CAPSULE}\right) \approx 0.35 \times 10^5 Pa$; and
- the velocity-dependent suddenness factor, indicated by $C_{CAPSULE}$, for calculation of the ΔF_{INSECT} is given by **0.027** as corresponding to the velocity u_{BLOW} of a flow **9o.15** when blowing the capsule **9o.2** given by $5\ m/sec$.

Thus, the originated forces are estimated as follows:

- the lift-force F_{LIFT} provided by the geometry of the six wings **9o.11**, wherein the geometry is characterized by the coefficient of lift C_L exemplary given by **0.5**, is estimated as:

$$F_{LIFT} = 0.5 \times \rho \times A_{WINGS} \times C_L \times u_{WING}^2 \approx 90N;$$

- the contribution ΔF_{BIRD} to the upward-vectored force, which (ΔF_{BIRD}) is a measure of the imitated effect of taking-off of a bird, is:

$$\Delta F_{BIRD} = (1/2) \times C_{WING} \times A_{WINGS} \times (-\Delta P_{WING}) \approx 1{,}427N;$$

- the contribution ΔF_{INSECT} to the upward-vectored force, which (ΔF_{INSECT}) is a measure of the imitated effect of taking-off of an insect, is:

$$\Delta F_{INSECT} = (1/2) \times C_{CAPSULE} \times A_{(X,Y),CAPSULE} \times (-\Delta P_{Z,CAPSULE}) \approx 385N;$$

and, thereby,

- the accumulated contribution to the upward-vectored force is estimated as $(F_{LIFT} + \Delta F_{BIRD} + \Delta F_{INSECT}) \approx 1{,}839\ N$ that is sufficient to raise a mass of $184\ kg$.

Wherein, concerning power consumption:

- to rotate the shaped propeller **9o.1** having wings **9o.11** and **9o.12** oriented to meet the ambient air portions at the zero attack angle dominantly, minimal power consumption is required for overcoming the minimal drag of wings only; and
- to support the required temperature differences, ΔT_{WING} and $\Delta T_{CAPSULE}$, a 15% net-efficiency of standard Peltier elements determines the required power consumption.

Further, the matrix thermoelectric device **9o.TED** is capable of providing for controlled distribution of the shell **9o.SHELL's temperature along the axis X**. The gradually smoothed curve **9o.5** is in coordinates **(X, T)**, where:

- axis **X** indicates the horizontal direction;
- the maximal frontal cross-sectional area of the capsule **9o.2**, indicated by $A_{(Y,Z),CAPSULE}$, is given by $2\ m^2$;
- the integral temperature difference between the coordinates X_{LEFT} and X_{RIGHT} of the capsule **9o.2** location, indicated by $\Delta T_{X,CAPSULE}$, is given by $30C$; and
- the refreshed air portions, when flowing around the capsule **90.2**, are subjected to suddenly originated effective difference in static pressures along the axis **X**, indicated by $\Delta P_{X,CAPSULE}$, interrelated with $\Delta T_{X,CAPSULE}$ as follows: the ratio $(\Delta T_{X,CAPSULE})/T \approx 0.1$, the ratio $(\Delta P_{X,CAPSULE})/P \approx 0.1 \times (7/5)/(2/5) = 0.35$, and so the suddenly originated additional static pressure difference is $\Delta P_{X,CAPSULE} \approx 0.35 \times 10^5 Pa$.

Thus, the possible thrust **9o.THRUST** for a sideward motion is:

$$\Delta F_{X,THRUST} = (1/2) \times C_{CAPSULE} \times A_{(Y,Z),CAPSULE} \times (-\Delta P_{Z,CAPSULE}) \approx 950N$$

that allows moving the mentioned mass of $184\ kg$ with an acceleration of about $5\ m/sec^2$ in a horizontal direction. The controllable difference between the speeds of counter rotations **9o.13** and **9o.14** provides a controlled rotation of the capsule **9o.2** around the axis **9o.AXIS**.

In view of the foregoing description referring to **Figs. 9n** and **9o**, it will be evident to a person skilled in the art that:

- the levitating apparatus **9o.0** can be further supplied with at least one of the heat-transformer **710.H** and the jet-transformer **9n.J** having the shaped jet-ventilator **9n.22** and oriented such that the sagittal axis **9n.51** is directed downward and/or sideward;
- Instead of Peltier elements (thermoelectric devices **9o.TED**), any kind of electric heater and/or cooler (i.e. a thermoelectric device in the broad sense) can be used to control the temperature distribution over the shell **9o.SHELL's,** because the inertness of

temperature difference controlling is not critical for the steady-established and relatively slow blowing flow **9o.15**; and

- In general, when allowed tolerances to the temperature difference controlling are relatively big, an electric heater consuming electric power and radiating Jole heat which is interpreted as a trivial thermoelectric device can be used.

In The Claims

In the claims, reference signs are used to refer to examples in the drawings for the purpose of easier understanding and are not intended to be limiting on the monopoly claimed.

CLAIMS

1. **A nozzle [610, 650]** having a corpus having a shaped tunnel within the corpus; the shaped tunnel having solid inner walls forming:
   - an open inlet;
   - an open outlet; and
   - a varying cross-sectional area, varying along the shaped tunnel length having a distance parameter x such that a stationary geometry of the shaped tunnel is either converging, or divergent, or convergent-divergent;

   the solid inner walls are supplied with an **acoustic thermoelectric device** built-in into the solid walls; the **acoustic thermoelectric device** comprising:
   - a multiplicity of elemental acoustic thermoelectric devices **[5P.0]** aggregated as a whole in a matrix of a phased array; and
   - a controller-dispatcher;

   the acoustic thermoelectric device is further specified as follows:
   - the multiplicity of the elemental acoustic thermoelectric devices aggregated as a whole in a surface matrix arrangement having two opposite sides: first and second, wherein the first side having a thermoconductive bus being thermally in contact with the solid inner walls and the second side having a thermoconductive bus being thermally in contact with a solid outer surface of the corpus contacting with ambient fluid;
   - each of the thermoelectric elements is supplied with the integrated circuit representing an individual sensor-controller comprising the controllably manipulatable source of **emf**; and
   - the controller-dispatcher capable of controlling each of the elemental acoustic thermoelectric devices as well as the acoustic thermoelectric device as a whole;

   the built-in acoustic thermoelectric device is capable of at least one of:
   - consuming electric power to trigger at least one of the Joule heating effect and the Peltier effect to provide a temperature difference between at least one of:
     - the solid inner wall of the shaped tunnel and the solid outer surface of the corpus contacting with the ambient fluid, and
     - different points of the solid inner wall,

     and

- triggering the Seebeck effect to harvest electric power induced from a temperature difference between at least one of:
  - the solid walls of the shaped tunnel and solid surfaces of the corpus contacting with ambient fluid, and
  - different points of the solid walls;

wherein, when the nozzle is exposed to fluid flow:

- entering the open inlet with a headway velocity u_{in},
- forming boundary layers adjacent to the solid inner walls, and
- outflow from the open outlet with a headway velocity u_{ou},

the controller-dispatcher providing that the acoustic thermoelectric device causes forcedly distributed temperature along the solid inner walls, wherein the varying cross-sectional area of the shaped tunnel is characterized by a cross-sectional area profile function $A(x)$ of x interrelated with functions $u(x)$ and $T(x)$ of x representing profiles of the fluid flow's headway velocity and absolute temperature, correspondingly, along the shaped tunnel length, wherein the thermoelectric device providing for a degree of freedom to interrelate the functions $A(x)$, $u(x)$, and $T(x)$ by a condition of flow continuity expressed as:

$$A(x) = \frac{A_* \sqrt{(\gamma-1)RT(x)}}{u(x)} \left(\frac{2RT(x)+u^2(x)}{(\gamma+1)RT(x)} \right)^{\frac{\gamma+1}{2(\gamma-1)}}$$

where A_* is a constant, γ is an adiabatic compressibility parameter of the flowing fluid, and R is a specific gas constant characterizing the fluid flow, wherein the functions $u(x)$ and $T(x)$ both are gradually-smoothed monotonic, wherein:

- the gradually-smoothed monotonic function of the absolute temperature $T(x)$ is determined by:
  - an absolute temperature T_{in} of the fluid flow at the open inlet;
  - temperature change $\delta T_0(x)$ interrelated with adiabatic compression-expansion occurred due to an adiabatic action of the Coanda-effect, in turn, determined by a curvature of the stationary geometry of the shaped tunnel, and
  - forcedly established temperature contribution $\delta T_1(x)$ to the absolute temperature $T(x)$ along the boundary layers subjected to controllable at least one of heating and cooling action of the thermoelectric device, such that $T(x) = T_{in} + \delta T_0(x) + \delta T_1(x)$,

and

- the gradually-smoothed monotonic function of the fluid flow's headway velocity $u(x)$ is determined by the headway velocity u_{in} of the fluid flow at the open inlet, convective headway acceleration resulting in a velocity gradient along the shaped tunnel length as the fluid flow is subjected to the adiabatic Coanda-effect, and controllable headway acceleration occurred due to controllable heating and/or cooling action of the thermoelectric device;

thereby, providing for conditions for a laminar motion of the fluid flow and beneficial features as follows:

- smoothing of the fluid flow's headway velocity profile function $u(x)$, providing suppression of undesired turbulence;
- smoothing of the fluid flow's static pressure profile function $P(x)$, providing suppression of undesired Mach waves and, thereby, suppression of vibrations of the nozzle corpus;
- smoothing of the fluid flow mass density profile function $\rho(x)$, providing suppression of undesired disturbances of the fluid flow accompanied by shock waves;
- smoothing of the fluid flow absolute temperature profile function $T(x)$, providing suppression of adjacent surface tensions; and
- smoothing of the fluid flow temperature-dependent M-velocity profile function $M(x)$, providing a trade-off of suppressions of undesired all: the turbulence, vibrations, shock and Mach waves, and surface tensions.

2. **A multi-stage nozzle** composed of N nozzles of **claim 1** consolidated as a whole; wherein the N **nozzles**, enumerated from 1 to N, are united together to join the N shaped tunnels associated with the N nozzles, correspondingly, such that each of the N shaped tunnels is a fragment of a resulting unbroken shaped tunnel formed thereby as a whole; an n-th fragment, where n is an integer between 1 and N: $1 \leq n \leq N$, has the varying cross-sectional area characterized by a cross-sectional area profile function $A_n(x)$ of x expressed as an individual condition of flow continuity:

$$A_n(x) = \frac{A_{*n}\sqrt{(\gamma-1)RT_n(x)}}{u_n(x)}\left(\frac{2RT_n(x)+u_n^2(x)}{(\gamma+1)RT_n(x)}\right)^{\frac{\gamma+1}{2(\gamma-1)}}$$

where A_{*n} is n-th constant, and the functions $u_n(x)$ and $T_n(x)$ are representing profiles of the fluid flow's headway velocity and absolute temperature, correspondingly, along the n-th fragment of the resulting unbroken shaped tunnel length; the resulting unbroken

shaped tunnel as a whole is either converging, or divergent, or convergent-divergent, or two-stage convergent-divergent; or multi-stage convergent-divergent; wherein piecewise-monotonic profile functions $u(x)$, $P(x)$, $\rho(x)$, $T(x)$, and $M(x)$, composed of associated gradually-smoothed monotonic profile functions concatenated together, all remain gradually-smoothed along the resulting unbroken shaped tunnel as a whole,

thereby, the multi-stage nozzle is applicable to convey:

- in general, laminar flow to solve the problem of originated turbulence, and
- in particular, tiny portions of the fluid, associated with an acoustic wave incoming the open inlet and propagating within and along the resulting unbroken shaped tunnel, to solve the problem of sound power dissipation.

3. **A sound amplifier comprising the multi-stage nozzle** of **claim 2** and an inlet acoustic thermoelectric device, wherein the inlet acoustic thermoelectric device is arranged nearby the open inlet and controlled by the controller-dispatcher to provide frequent changes in temperature of a nearby portion of the fluid to at least one of originate an acoustic wave and boost an incoming acoustic wave, to provide that when further the acoustic wave entering the open inlet of the shaped tunnel such that the fluid flow entering the open inlet with the headway velocity u_{in} is a tiny portion of the fluid subjected to conveying motion inherently accompanying the acoustic wave entering the open inlet and propagating along the shaped tunnel; wherein the sound amplifier is either:

- **a megaphone [7a.A]**, wherein:
    - the resulting unbroken shaped tunnel is configured as a divergent funnel,
    - an M-velocity of the conveying motion at the open inlet is higher than $\sqrt{(\gamma-1)/\gamma}$, and
    - the parameter x is a coordinate increasing along the divergent tunnel from the inlet to the outlet such that the profile function $A(x)$ takes the value A_* out of the divergent horn on the side of the open inlet; or
- **a phonendoscope [7a.B]**, wherein the resulting unbroken shaped tunnel is two-stage convergent-divergent, further specified as comprising sequentially joint elements as follows:
    - the open inlet characterized by an inlet cross-sectional area, indicated by A_{in} ,
    - a convergent funnel characterized by a monotonically varying cross-sectional area;

- a first narrow throat characterized by a local minimal cross-sectional area, indicated by A_{th1} ;
- a widened cavity characterized by a local maximal cross-sectional area, indicated by A_{ca} ;
- a second narrow throat characterized by a local minimal cross-sectional area, indicated by A_{th2} ;
- a divergent funnel characterized by a monotonically varying cross-sectional area; and
- the open outlet characterized by an outlet cross-sectional area, indicated by A_{ou};

wherein conditions:

- $\frac{A_{in}}{A_{th1}} \geq \sqrt{\left(\frac{\gamma-1}{\gamma}\right)\left(\frac{2+\gamma}{\gamma+1}\right)^{\frac{\gamma+1}{(\gamma-1)}}}$,
- $A_{ca}/A_{th1} > 1$,
- $A_{ca}/A_{th2} \geq 1$,
- $A_{th2}/A_{th1} \leq 1$, and
- $\frac{A_{ou}}{A_{th2}} > \sqrt{\left(\frac{\gamma-1}{\gamma}\right)\left(\frac{2+\gamma}{\gamma+1}\right)^{\frac{\gamma+1}{(\gamma-1)}}}$,

are satisfied to provide that the phonendoscope becomes capable of amplifying a loudness of an incoming sound yet to become subjected to an action of the phonendoscope; or

- **a hearing aid [7a.C]** embodied as the phonendoscope, wherein said corpus has an outer geometrical **configuration ergonomically adapted to a human's ear canal, such that the open outlet is faced to an eardrum within the human's ear canal**.

4. **An airfoil capsule [720, 740]** comprising an airfoil outer overall shape and at least one of the nozzle of **claim 1** and the multi-stage nozzle of **claim 2**.

5. **An airfoil wing [8.00, 800]** comprising at least one of the nozzle of **claim 1** and the multi-stage nozzle of **claim 2 [8.31, 8.32]**, wherein the shaped tunnel further having an imaginary wall formed by streamlines of the fluid flow;

wherein the corpus of the multi-stage nozzle is further specified as having an airfoil geometrical configuration recognizable by a sectional elongated profile, comprising two opposite curved sides: an upper side and a lower side, and two opposite butt-ends: forward being rounded and rearward being sharp, such that when the airfoil wing is exposed to an oncoming portion of the fluid flow, the oncoming portion flowing around the airfoil wing becomes divided into two sub-portions: an upper-side sub-portion of the oncoming portion of the fluid flow forming an upper-side boundary layer and a lower-side sub-portion of the oncoming portion of the fluid flow forming a lower-side boundary layer;

wherein the upper side comprising:

- a forward part meeting the upper-side boundary layer;
- an upper-side convexity, where the upper-side boundary layer, when sliding upon the upper-side convexity, has an imaginary narrowed cross-section;
- a rearward part, attracting and, thereby, redirecting mass-center of the sliding upper-side boundary layer backward-downward due to the Coanda-effect, thereby causing an imaginary widened cross-section of the sliding upper-side boundary layer neaby the rearward part; and
- the built-in acoustic thermoelectric device along the upper side for distributed heating or cooling the upper-side boundary layer;

and wherein the lower side is curved to form a lower-side convexity; said lower-side meeting the lower-side boundary layer,

wherein:

- a sagittal axis **[820.0]** is defined as an axis codirected with a motion of the oncoming portion of the fluid flow yet to be subjected to an action of the airfoil wing;
- an attack angle is defined as an angle between a sagittal axis and a direction of motion tendency of said lower-side boundary layer when the lower-side boundary layer outflowing nearby and stalling from the sharp rearward butt-end of the airfoil wing; and
- a zero attack angle is specified as said attack angle equal to zero;

wherein the airfoil geometrical configuration is further specified such that, when the airfoil wing is exposed to the oncoming portion of the fluid flow at the zero attack angle:

- the sectional elongated profile of the airfoil wing is either mirror-symmetrical **[8.00]** or asymmetrical **[800]** relative to a sagittal axis; and

- each of the two boundary layers: upper-side and lower-side, representing said shaped tunnel: upper-side or lower-side, correspondingly, further having an imaginary wall formed by streamlines bordering associated said boundary layer: upper-side or lower-side, correspondingly;

thereby, providing for:

- improved laminarity of the portion of the fluid flowing around the airfoil wing;
- that, when stalling from the sharp rearward butt-end of the airfoil wing, the upper-side and lower-side boundary layers, both have the same headway velocity u_{ou}, and the same thermodynamic parameters: the static pressure, mass density, and absolute temperature, such that the two boundary layers: upper-side and lower-side, when joining together to move as a whole downstream behind the airfoil wing, form a uniform resulting outflowing portion of the fluid flow remaining laminar;
- improving wing properties manifested as: decreased drag, increased lift-force due to improved laminarity of the fluid flow, and, when the upper side of the airfoil wing is colder than the lower side of the airfoil wing, further increased lift-force due to imitating an effect of taking-off of a bird;
- overcoming a problem of efficient use of another airfoil wing arranged downstream behind the airfoil wing; and
- a benefit of in-line cascading a next said airfoil wing after a previous said airfoil wing resulting in increased cumulative lift-force.

6. **A tandem** of two airfoil wings of **claim 5** consolidated as a whole **[880.B]**;
the tandem is exposed to an oncoming portion of fluid flow;
the two airfoil wings: first and second, are arranged to meet the oncoming portion **[851.B]** of the fluid flow, divide the oncoming portion of the fluid flow into two sub-portions: an upper-side sub-portion of the oncoming portion of the fluid flow forming an upper-side boundary layer **[852.B1, 853.B1, 854.B1, 852.B3, 853.B3, 854.B3]** and a lower-side sub-portion of the oncoming portion of the fluid flow forming a lower-side boundary layer **[852.B2, 853.B2, 854.B2, 852.B4, 853.B4, 854.B4]**, and act on at least one of the boundary layers: upper-side and lower-side, sequentially in two stages: first and second, namely:

- at the first stage, the first airfoil wing, meeting the oncoming portion of the fluid flow yet to be subjected to the Coanda-effect and acting on the oncoming portion of the fluid flow by the Coanda-effect, and
- at the second stage, the second airfoil wing, meeting the oncoming portion of the fluid flow already subjected to the action by the first airfoil wing at the first stage;

wherein:

- a specific M-velocity is defined as $\sqrt{(\gamma-1)/\gamma}$;
- a first convexity is defined as at least one of the upper-side and lower-side convexity **[869.B1 or 869.B2]** of the first airfoil wing; and
- a second convexity is defined as at least one of the upper-side and lower-side convexity **[869.B3 or 869.B4]** of the second airfoil wing;

such that at least one of the two boundary layers: upper-side and lower-side, each of which originated adjacent to the upper or lower side of the tandem of two airfoil wings, correspondingly, is composed of two parts: first, flowing nearby the first convexity, and second, flowing nearby the second convexity; each of the two boundary layers: upper-side or lower-side, is subjected to at least one of:

- the Venturi effect, when an M-velocity of the upper-side or lower-side boundary layer, correspondingly, remains lower than the specific M-velocity;
- the de Laval effect of flow acceleration nearby the first convexity and to de Laval effect of flow retarding nearby the second convexity, when an M-velocity of the oncoming portion of fluid flow **[851.B]** is lower than the specific M-velocity and sufficiently high to reach the specific M-velocity nearby the first convexity; or
- the de Laval effect of flow retarding nearby the first convexity and to de Laval effect of flow acceleration nearby the second convexity, when an M-velocity of the oncoming portion of fluid flow **[851.B]** is higher than the specific M-velocity;

such that the varying cross-sectional areas of the parts of the boundary layer: first, flowing nearby the first convexity, and second, flowing nearby the second convexity, are characterized by cross-sectional area profile functions $A_1(x_1)$ and $A_2(x_2)$ of distance parameters x_1 or x_2, correspondingly; each of the cross-sectional area profile functions $A_1(x_1)$ and $A_2(x_2)$ is given by the individual condition of flow continuity wherein the distance parameter x is x_1 or x_2 associated with the parts of the boundary layer: first, flowing nearby the first convexity, and second, flowing nearby the second convexity, correspondingly,

thereby, providing for that the tandem of two airfoil wings consolidated as a whole has a positive lift-force for low M-velocities, lower than the specific M-velocity, and for high M-velocities, higher than the specific M-velocity.

7. **A double-humped wing [870]** comprising the tandem of two airfoil wings of **claim 6** wherein the two airfoil wings are merged as a whole to form an unbroken double-humped corpus such that to act on the upper-side boundary layer sequentially in two stages: first and second, thereby, providing for that the double-humped airfoil wing has a positive lift-force for low M-velocities, lower than the specific M-velocity, and for high M-velocities, higher than the specific M-velocity.

8. **A jet-rotor [9.7]** comprising an axle **[9.73]** oriented along a sagittal axis and supplied with a set of blades, wherein the set of blades is a set of at least one of:
    - the airfoil wings of **claim 5**;
    - the tandems of two airfoil wings consolidated as a whole of **claim 6**; and
    - the double-humped wings of **claim 7**;

    the blades are oriented to:
    - be exposed to the oncoming portion of the fluid flow at the zero attack angle and thereby subjected to an action of lift-forces originated due to the Coanda-effect dominantly, wherein the Coanda-effect is accompanied by at least one of:
        - the Venturi effect; and
        - the de Laval jet-effect;

      and
    - vector the originated lift-forces in a frontal plane perpendicular to the sagittal axis to rotate the axle around the sagittal axis in unison,

    thereby, providing for:
    - improved laminarity of the oncoming portion of the fluid flow when flowing around the jet-rotor;
    - suppression of turbulence of the oncoming portion of the fluid flow when moving downstream behind the jet-rotor, and
    - increased lift-forces acting in unison and in the same direction of rotation and so rotating the axle, when the de Laval jet-effect is triggered.

9. **A jet-turbine [9.7]** comprising:

- an engine, having a stator and rotatable shaft, and
- the jet-rotor of **claim 8**;

wherein the axle **[9.73]** is attached to the rotatable shaft to provide for the rotatable shaft to be rotated in unison with the axle rotation around the sagittal axis,

thereby, providing for:

- increased efficiency of the jet-turbine in a wide range of wind velocities;
- overcoming the problem to efficient use a wind turbine adjacently arranged downstream behind another wind turbine, and
- a benefit of in-line cascading a next said jet-turbine immediately after a previous said jet-turbine resulting in increased cumulative efficiency of producing electricity.

10. A tuple of the jet-turbines of **claim 9**, wherein the jet-turbines are arranged in-line along a common sagittal axis one downstream behind another.

11. An enhanced jet-propeller [9K.0] comprising:

- a motor, having a stator and rotatable shaft, and
- a jet-rotor **[9K.0]** having an axle supplied with a tuple of sets of blades **[9K.1, 9L.01, 9L.02]** in-line arranged sequentially one after another along a sagittal axis, wherein:
  - the axle is attached to the rotatable shaft to provide for the rotatable shaft to be rotated in unison with the axle rotation around the sagittal axis; and
  - each of the sets **[9K.1, 9L.01, 9L.02]** of blades is composed of at least one of:
    - the airfoil wings of **claim 5**,
    - the tandem of two airfoil wings consolidated as a whole of **claim 6**, and
    - the double-humped wings of claim **7**;

wherein:

- a pitch, as a measure of a blade orientation, is defined as an angle between the sagittal axis and an angle of view defined for the blade of the jet-rotor being stationary;

each of the sets of blades comprises blades assembled with an individual pitch, adapted to a rate of a forced rotation of the rotatable shaft and axle, such that each of the blades runs over portions of the fluid flow **[9K.6,9L.6,9M.6]** at the zero attack angle and, thereby, is:

- subjected to an action of lift-force **[9K.3]** originated due to the Coanda-effect dominantly, wherein the Coanda-effect is accompanied by at least one of:
    - the Venturi effect; and
    - the de Laval jet-effect;

  and
- vectored to have a dominant component of headway motion collinear to the sagittal axis;

thereby, due to the Coanda-effect dominantly, each of the blades acts on the portions of the fluid flow by a pushing force vectored against the component of lift-force according to **Newton's third law and so to accelerate the portions of the fluid flow in conformance with** the vectored pushing force thereby resulting in a dominantly-laminarly headway-forwarding fluid flow directed along the sagittal axis.

12. A tuple of the enhanced jet-propellers of **claim 11**, wherein the enhanced jet-propellers **[9L.0, 9M.01, 9M.02]** are arranged in-line along the sagittal axis **[9M.7]** one downstream behind another.

13. A heat-transformer [710.H] comprising:

- the **nozzle** of **claim 1**; and
- a reservoir [**712.B**] having walls supplied with:
    - pipes [**715.B**], each of which having a through-hole tunnel allowing for an ambient fluid portion to enter the reservoir and become an inner fluid portion; the through-hole tunnel having a sectional profile being either symmetric relative to a cross-sectional plane or asymmetric with a property of a valvular conduit (Tesla valve); and
    - a multiplicity of thermoelectric devices [**714.B**] capable of heating the inner fluid portion to trigger a motion of the heated inner fluid portion [**711.B**] toward the shaped tunnel of the nozzle [**710.B**].

14. A heat-turbine [9n.H] comprising:

- the **nozzle** of **claim 1** wherein the shaped tunnel **[9n.1]** is oriented along a **vertical** sagittal axis **[9n.51]**;

- a heater capable of heating a portion of the ambient fluid to trigger the **Archimedes'** upward-vectored force lifting the heated fluid portion and thereby to create an upward-moving dominantly-laminarly headway-forwarding fluid flow; and
- the jet-turbine **[9.n3]** of **claim 9** capable of transforming the kinetic power of the jet-rotor rotation into electric power;

wherein:

- said heater is capable to increase an absolute temperature of the portion of the ambient fluid entering the shaped tunnel up to a value T_{in} being higher than the absolute temperature T_a of the ambient fluid outside the nozzle such that ratio T_{in}/T_a is at least **1.2** to provide a condition that when the upward-moving dominantly-laminarly headway-forwarding fluid flow moves within the converging funnel and becomes subjected to the Venturi effect, the upward-moving dominantly-laminarly headway-forwarding fluid flow reaches the specific M-velocity within the narrow throat and so triggering the de Laval jet-effect; and
- the jet-rotor of the jet-turbine is arranged either:
  - within the shaped tunnel near or downstream behind the narrow throat, where the M-velocity is determined by the specific M-velocity, or
  - immediately beyond the open outlet, where the M-velocity is determined by a cross-sectional area of the open outlet according to the condition of flow continuity;

  the jet-rotor of the jet-turbine is arranged to be exposed to said upward-moving dominantly-laminarly headway-forwarding fluid flow moving through and outflowing from the shaped tunnel such that all the blades of the jet-rotor are oriented to meet portions of said dominantly-laminarly headway-forwarding fluid flow at the zero attack angle; wherein an overall shape of the blades is adapted to the M-velocity dependent on the x coordinate along the sagittal axis to satisfy conditions of said upward-moving dominantly-laminarly headway-forwarding fluid flow;

thereby, providing for:

- creation of the upward-moving dominantly-laminarly headway-forwarding fluid flow due to triggering the **Archimedes' upward**-vectored force lifting the heated portion of the ambient fluid;
- an acceleration of the upward-moving dominantly-laminarly headway-forwarding fluid flow within the shaped tunnel due to the Venturi effect

- triggering the de Laval jet-effect for further acceleration of the upward-moving dominantly-laminarly headway-forwarding fluid flow within the shaped tunnel;
- powering the jet-turbine exposed to the accelerated upward-moving dominantly-laminarly headway-forwarding fluid flow;
- overcoming a problem of efficient producing electricity from the heated portion of the ambient fluid; and
- a benefit of triggering the **Archimedes' upward**-vectored force lifting the heated portion of the ambient fluid and triggering the de Laval jet-effect for producing electricity.

15. A jet-transformer [9n.J] comprising:

- the nozzle of **claim 1**;
- the enhanced jet-propeller of **claim 11**, the enhanced jet-propeller capable of creating said dominantly-laminarly headway-forwarding fluid flow directed along the sagittal axis; and
- the jet-turbine of **claim 9** capable of transforming the kinetic power of the jet-rotor rotation into electric power;

wherein:

- the enhanced jet-propeller providing for that the dominantly-laminarly headway-forwarding fluid flow, when entering the open inlet having the distance parameter indicated by x_{in}, has an M-velocity equal to $M(x_{in})$ estimated according to the condition of flow continuity such that the dominantly-laminarly headway-forwarding fluid flow, when moving along the converging funnel and becoming subjected to the Venturi effect, reaches the specific M-velocity within the narrow throat and so triggering the de Laval jet-effect wherein distribution of M-velocities along the sagittal axis is determined by the value $M(x_{in})$ of the M-velocity at the open inlet having the cross-sectional area $A(x_{in})$; and
- the jet-rotor of the jet-turbine is arranged either:
  - within the shaped tunnel near or downstream behind the narrow throat, where the M-velocity is determined by the specific M-velocity, or
  - immediately beyond the open outlet, where the M-velocity is determined by a cross-sectional area of the open outlet according to the condition of flow continuity;

the jet-rotor of the jet-turbine is arranged to be exposed to said dominantly-laminarly headway-forwarding fluid flow moving through and outflowing from the shaped tunnel

such that all the blades of the jet-rotor are oriented to meet portions of said dominantly-laminarly headway-forwarding fluid flow at the zero attack angle; wherein an overall shape of the blades is adapted to the M-velocity dependent on the x coordinate along the sagittal axis to satisfy conditions of said dominantly-laminarly headway-forwarding fluid flow;

thereby, providing for:

- creation of the upward-moving dominantly-laminarly headway-forwarding fluid flow due to triggering the Coanda-effect using the jet-ventilator;
- an acceleration of the upward-moving dominantly-laminarly headway-forwarding fluid flow within the **shaped tunnel** due to the Venturi effect;
- triggering the de Laval jet-effect for further acceleration of the upward-moving dominantly-laminarly headway-forwarding fluid flow within the shaped tunnel;
- powering the jet-turbine exposed to the accelerated upward-moving dominantly-laminarly headway-forwarding fluid flow; and
- overcoming a problem of a benefiting use of the de Laval jet-effect for producing electricity.

16. A levitating apparatus [9o.0] comprising:

- the enhanced jet-propeller **[9o.1]** of **claim 11**, the enhanced jet-propeller capable of creating said dominantly-laminarly headway-forwarding fluid flow; and
- a capsule **[9o.2]** having a shell composed of two parts: upper and lower;

wherein said shell has a dominantly-airfoil overall shape and is supplied with built-in thermoelectric elements capable of supporting gradually distributed temperature, distributed along the shell;

wherein the jet-rotor is located above the capsule such that to be capable of blowing the shell of the capsule from above by the dominantly-laminarly headway-forwarding fluid flow;

thereby, providing for that,

- when the upper sides of the jet-rotor blades are colder than the lower sides of the enhanced jet-rotor wings, an effect of taking-off of the levitating apparatus due to an imitated effect of taking-off of a bird is originated; and
- when the upper part of the shell is colder than the lower part of the shell, an effect of taking-off of the levitating apparatus due to an imitated effect of taking-off of an insect is originated.

17. **The levitating apparatus** of **claim 16** further comprising at least one of: the airfoil capsule of **claim 4,** the heat-transformer of **claim 13,** and the jet-transformer of **claim 15**.

2020281012 11 Mar 2021

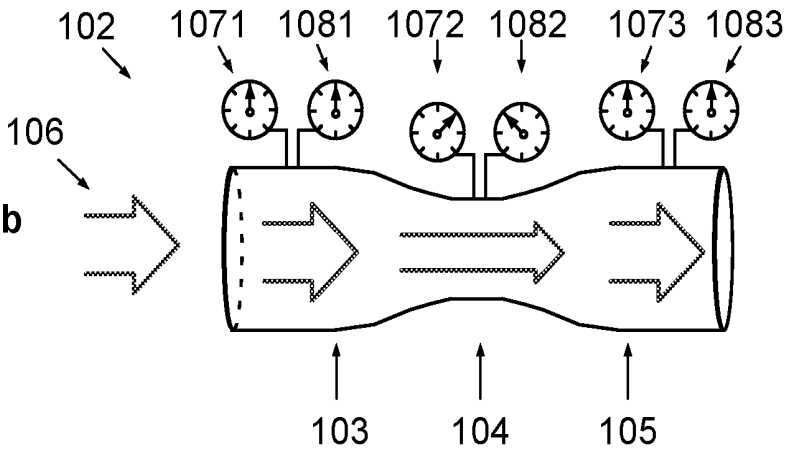

Prior Art Fig. 1b

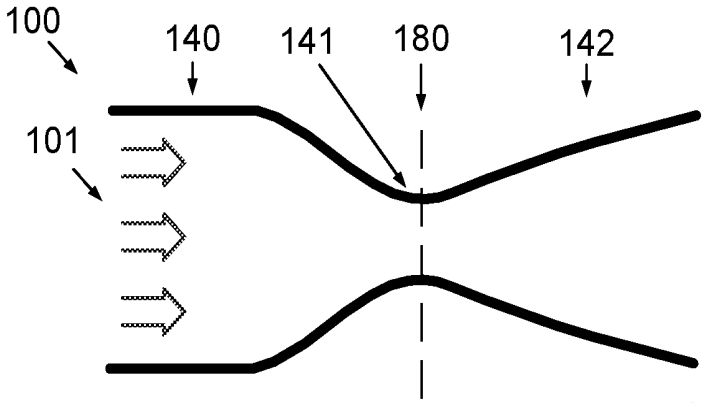

Prior Art Fig. 1c

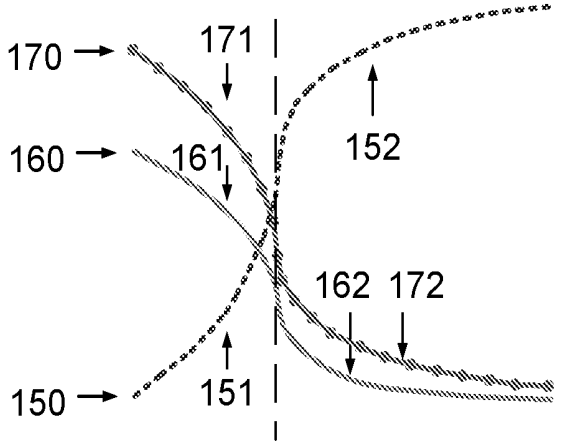

Prior Art Fig. 1d

11 Mar 2021
20202810 12

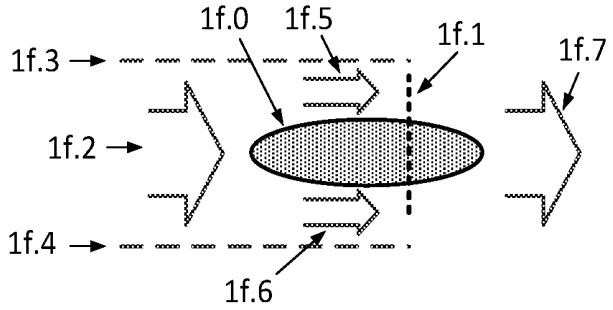

Prior Art Fig. 1f

Prior Art Fig. 1g

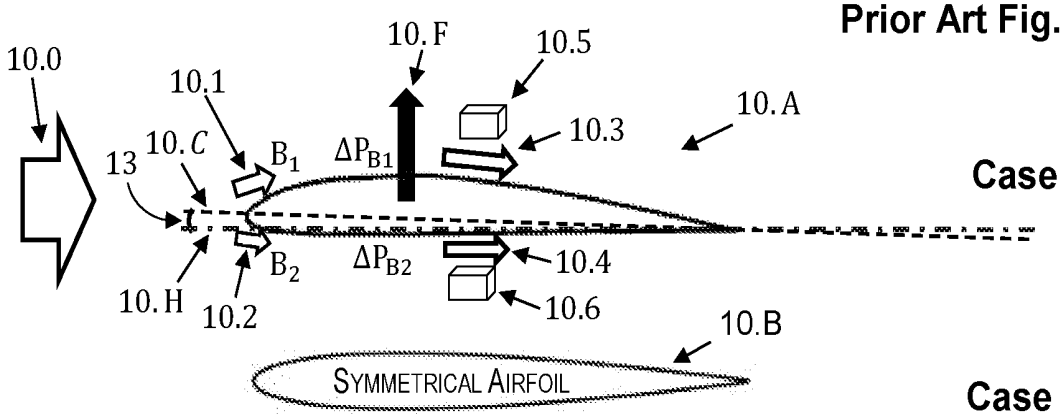

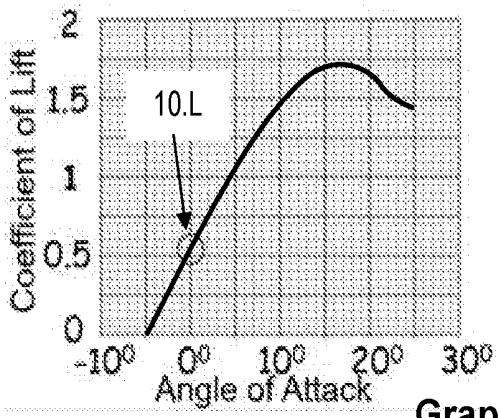

Graph (C)

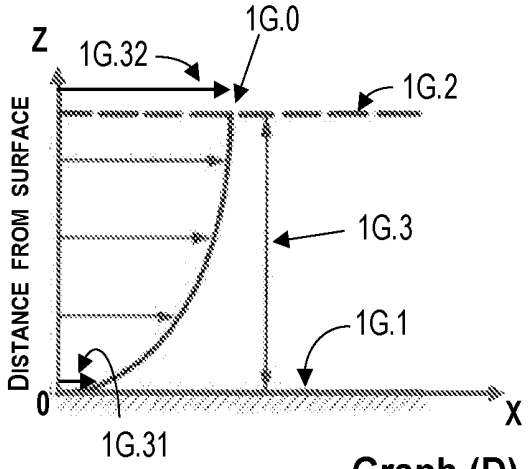

Graph (D)

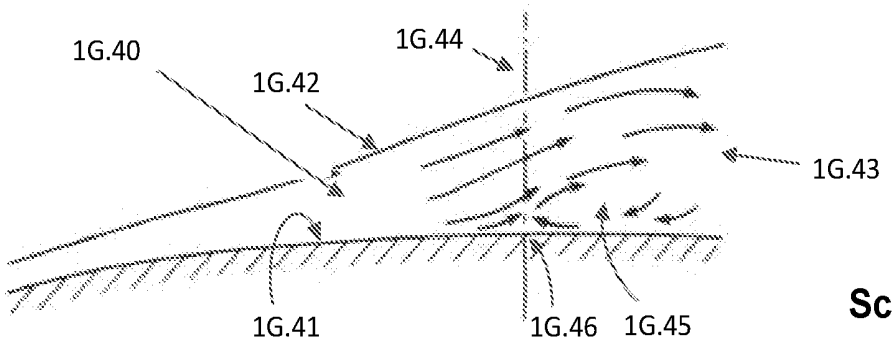

Scheme (E)

2020281012 11 Mar 2021

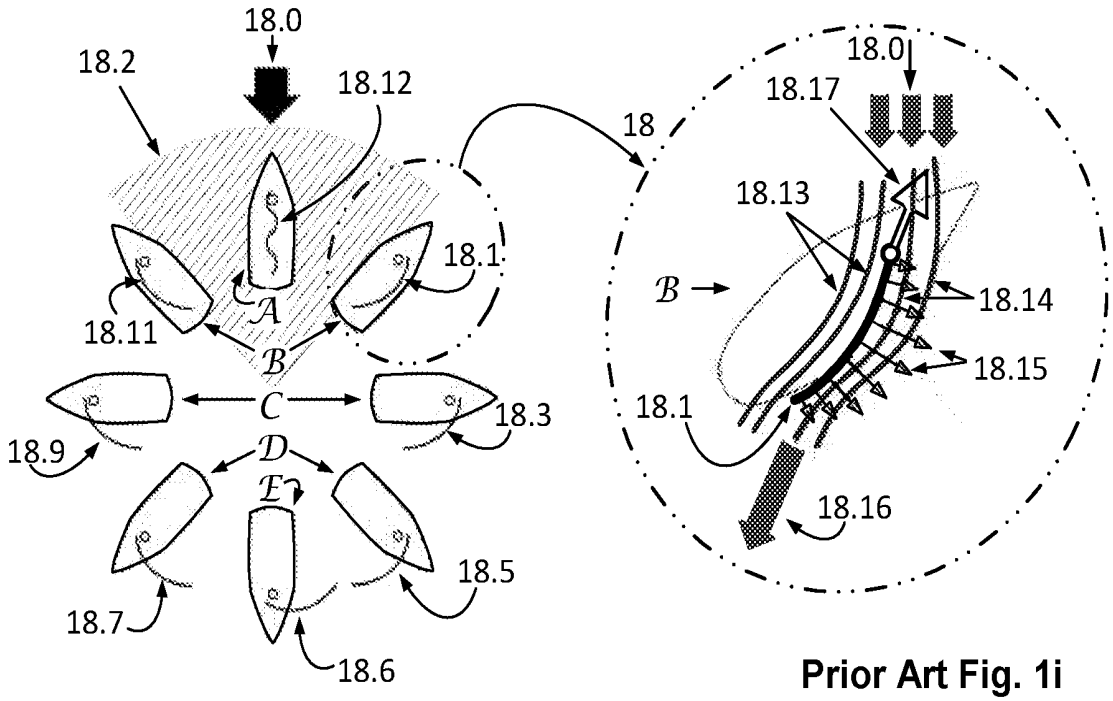

Prior Art Fig. 1i

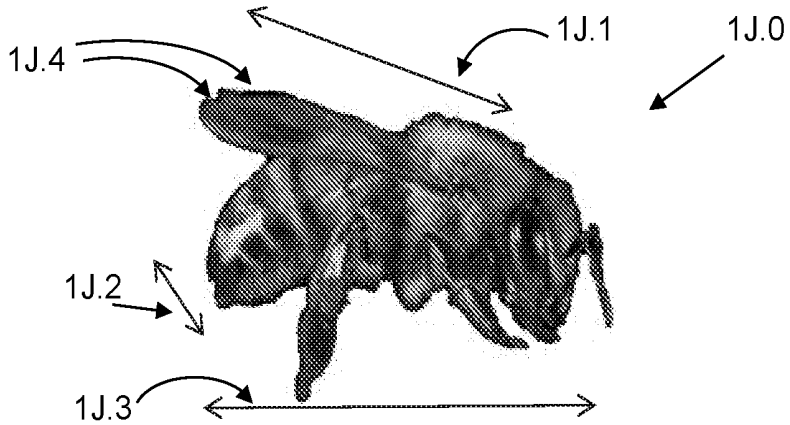

Prior Art Fig. 1j

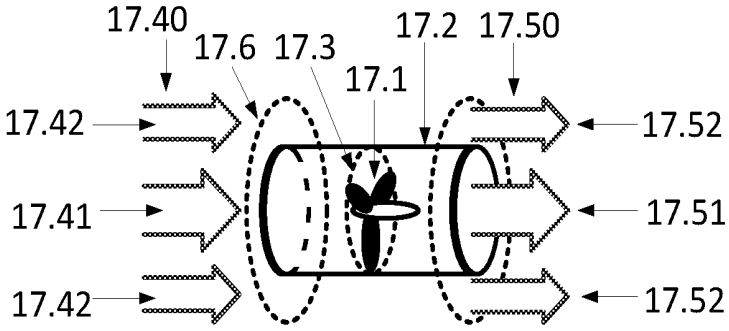

Prior Art Fig. 1k

Prior Art Fig. 1n

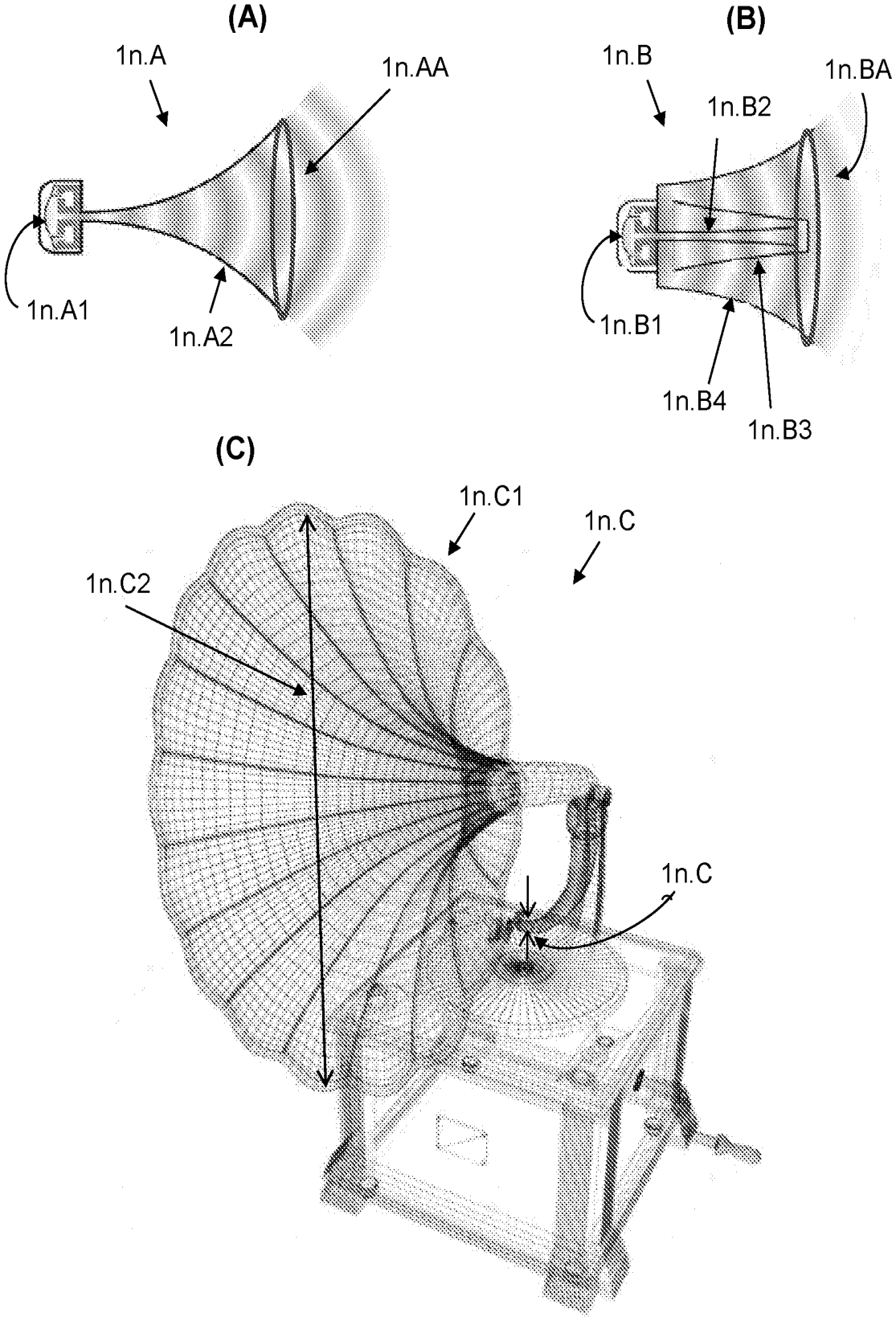

Prior Art Fig. 1L

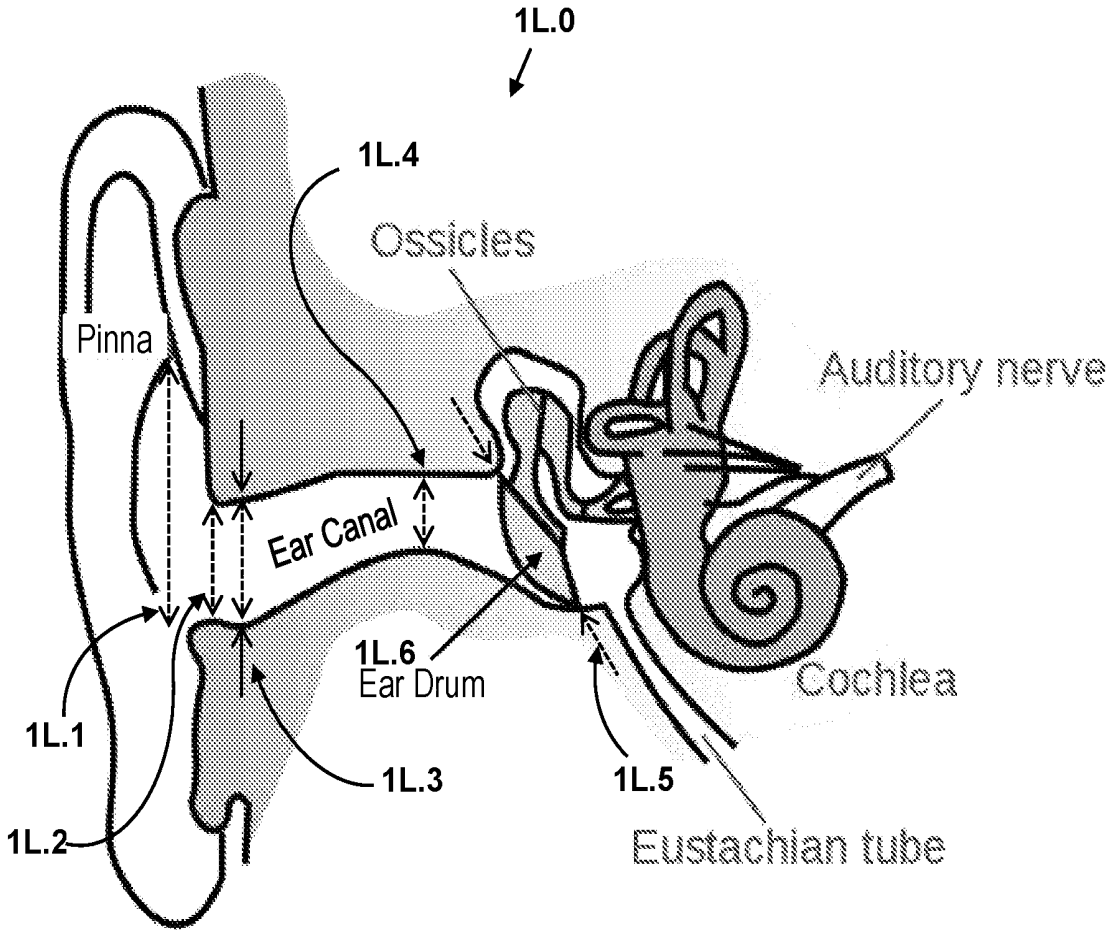

Prior Art Fig. 1o

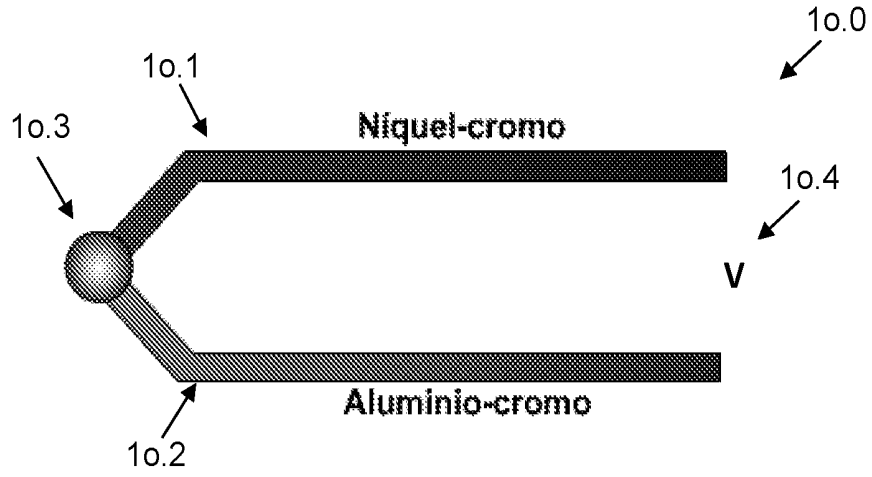

20202810 12 11 Mar 2021

Prior Art Fig. 1p

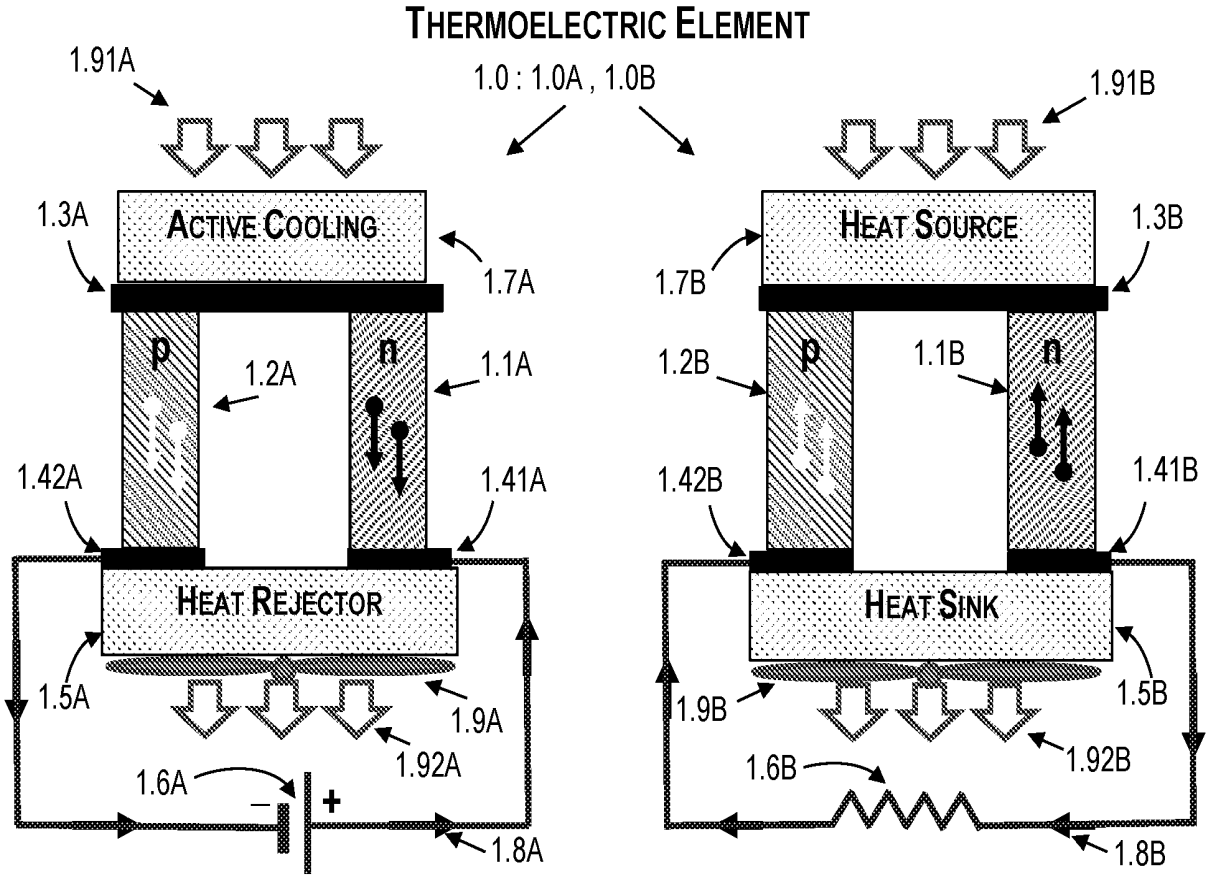

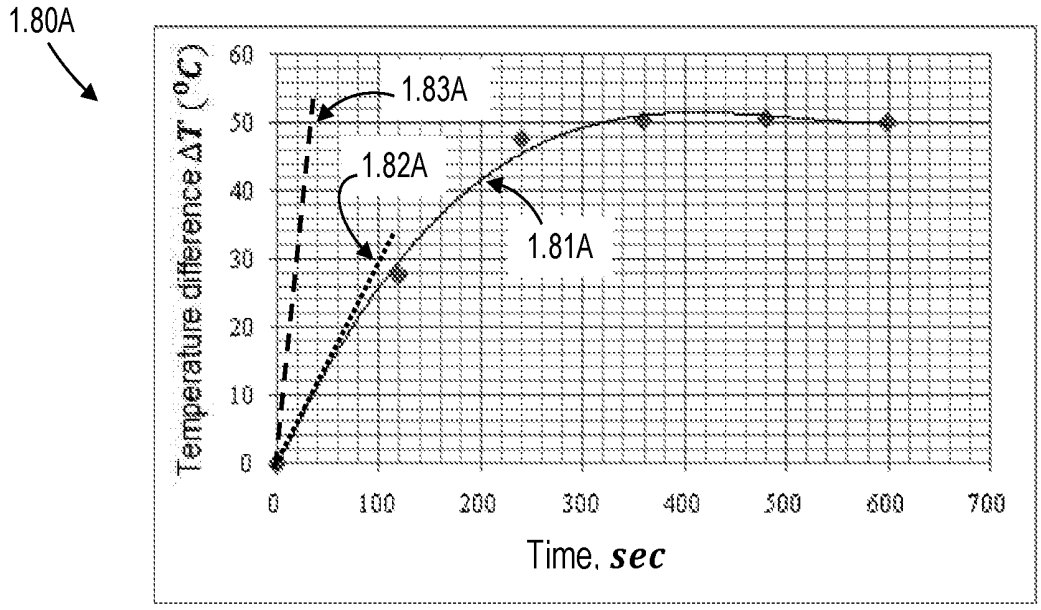

Case (A) TIME CHARACTERISTIC

20202810 12 11 Mar 2021

Prior Art Fig. 1q

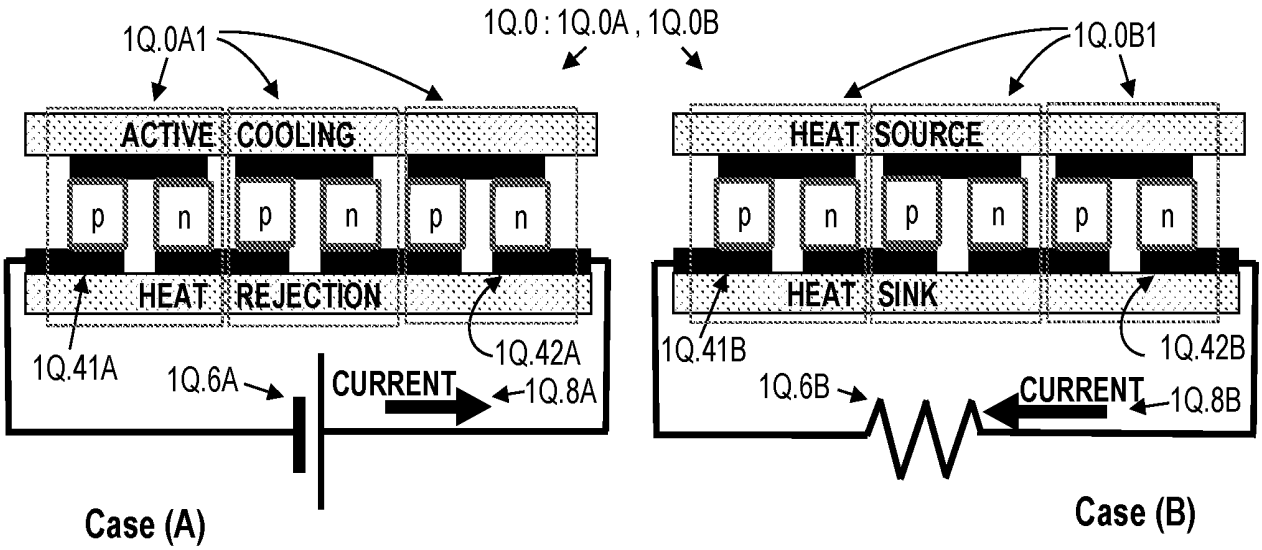

Prior Art Fig. 1r

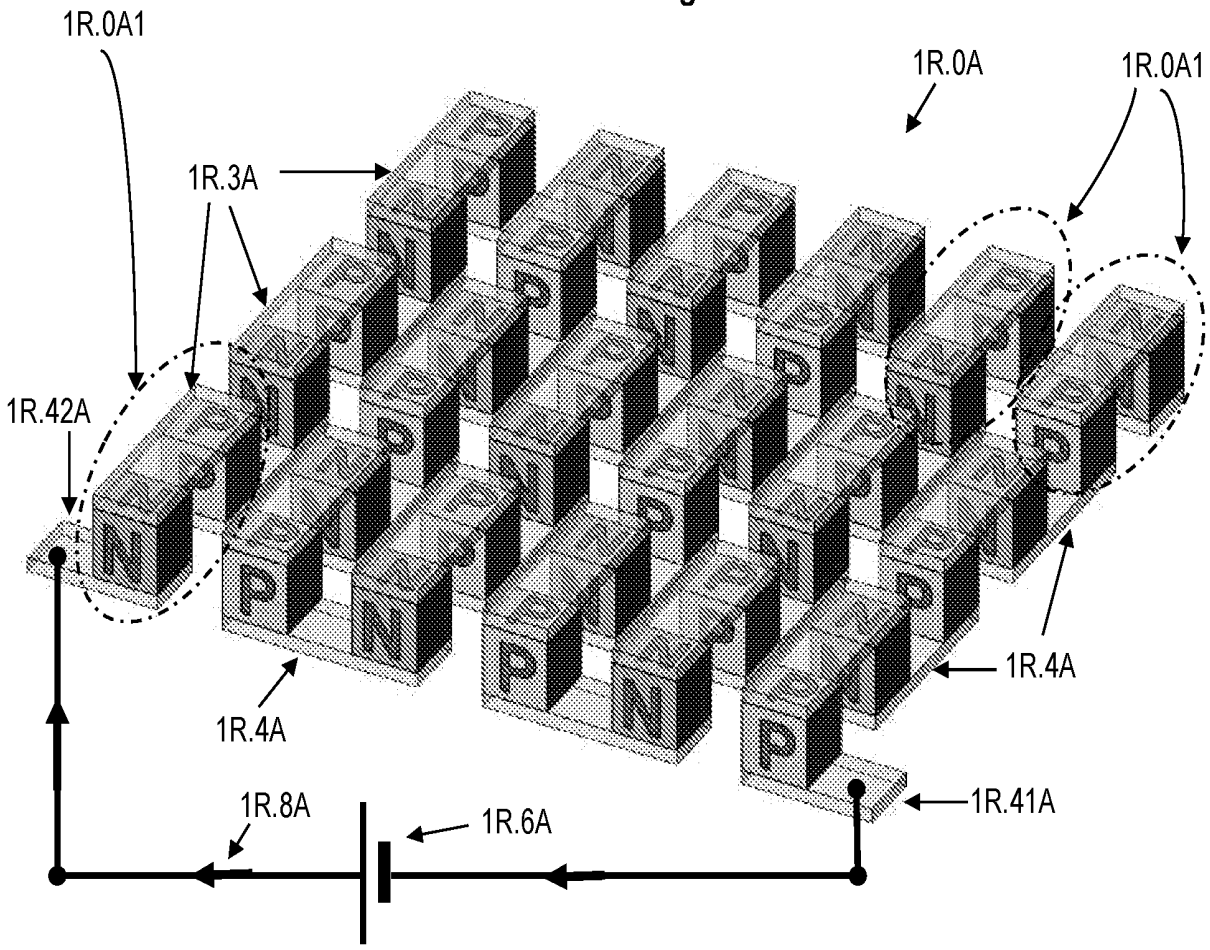

20202810 12 11 Mar 2021

Prior Art Fig. 1t

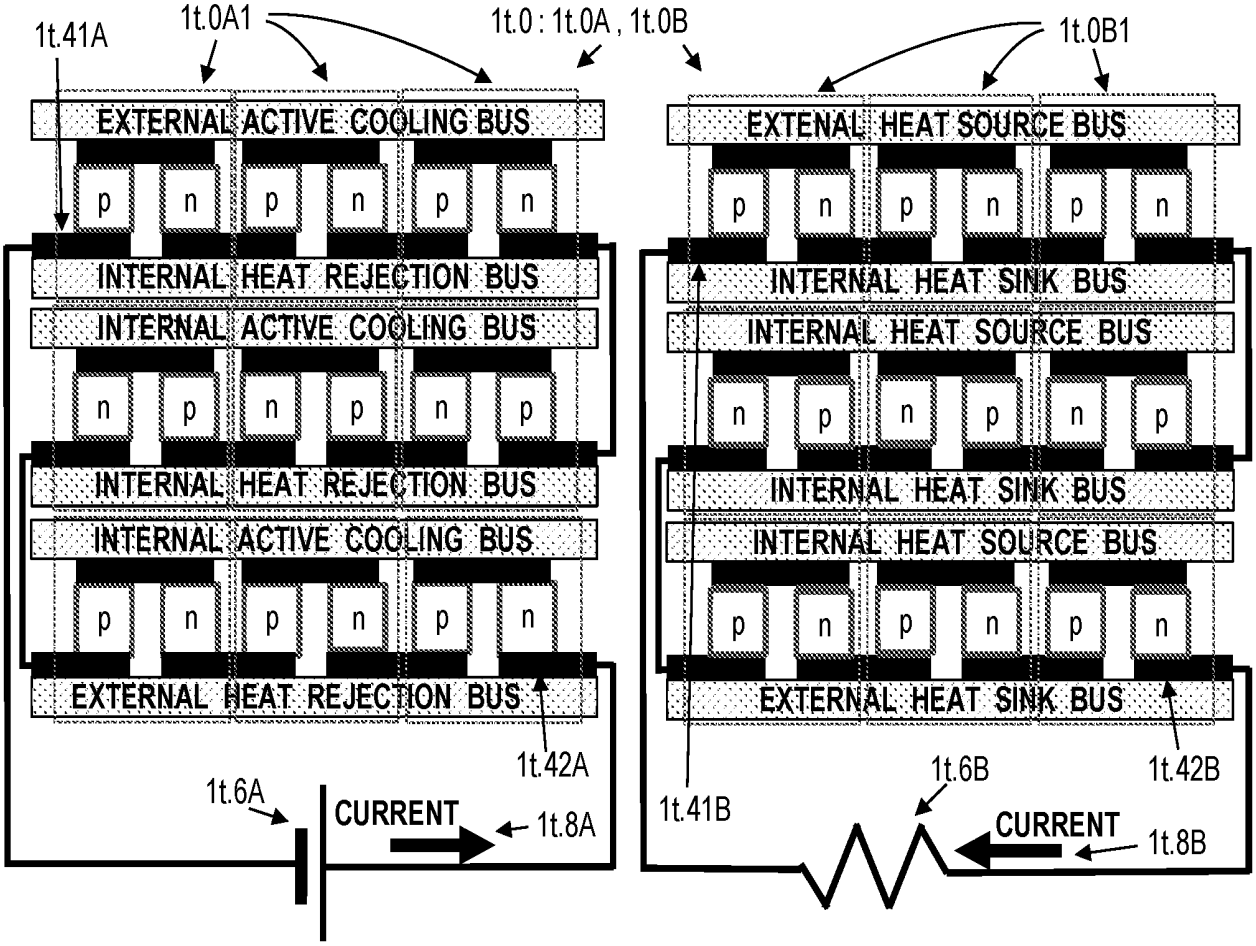

Case (A)

Case (B)

20202810 12 11 Mar 2021

Fig. 5p

ELEMENTAL SOURCE AND DETECTOR OF SOUND

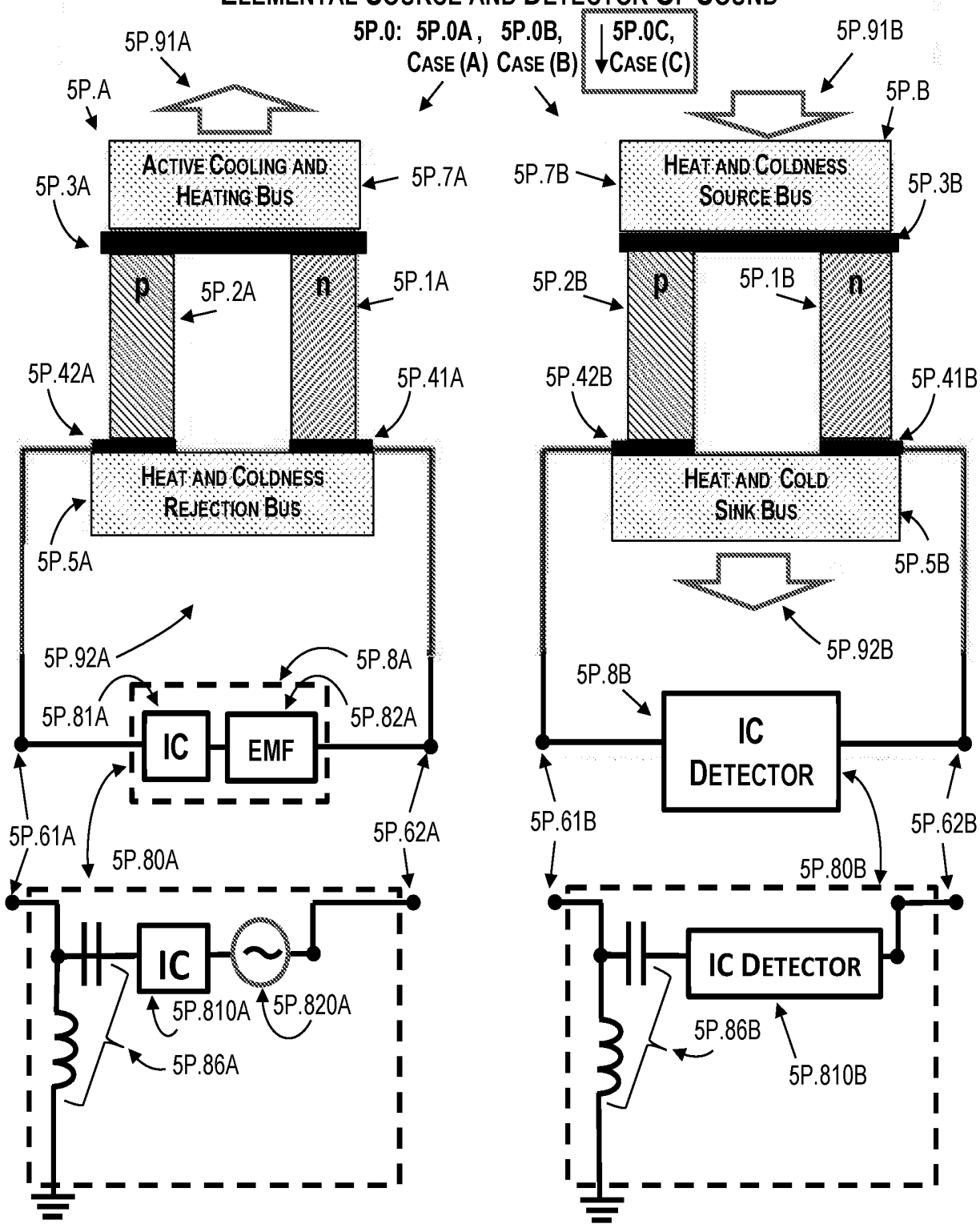

Case (A) SOUND LAUNCHING MODE

Case (B) SOUND DETECTION MODE

20202810 12 11 Mar 2021

Fig. 5p Case (C) General Mode

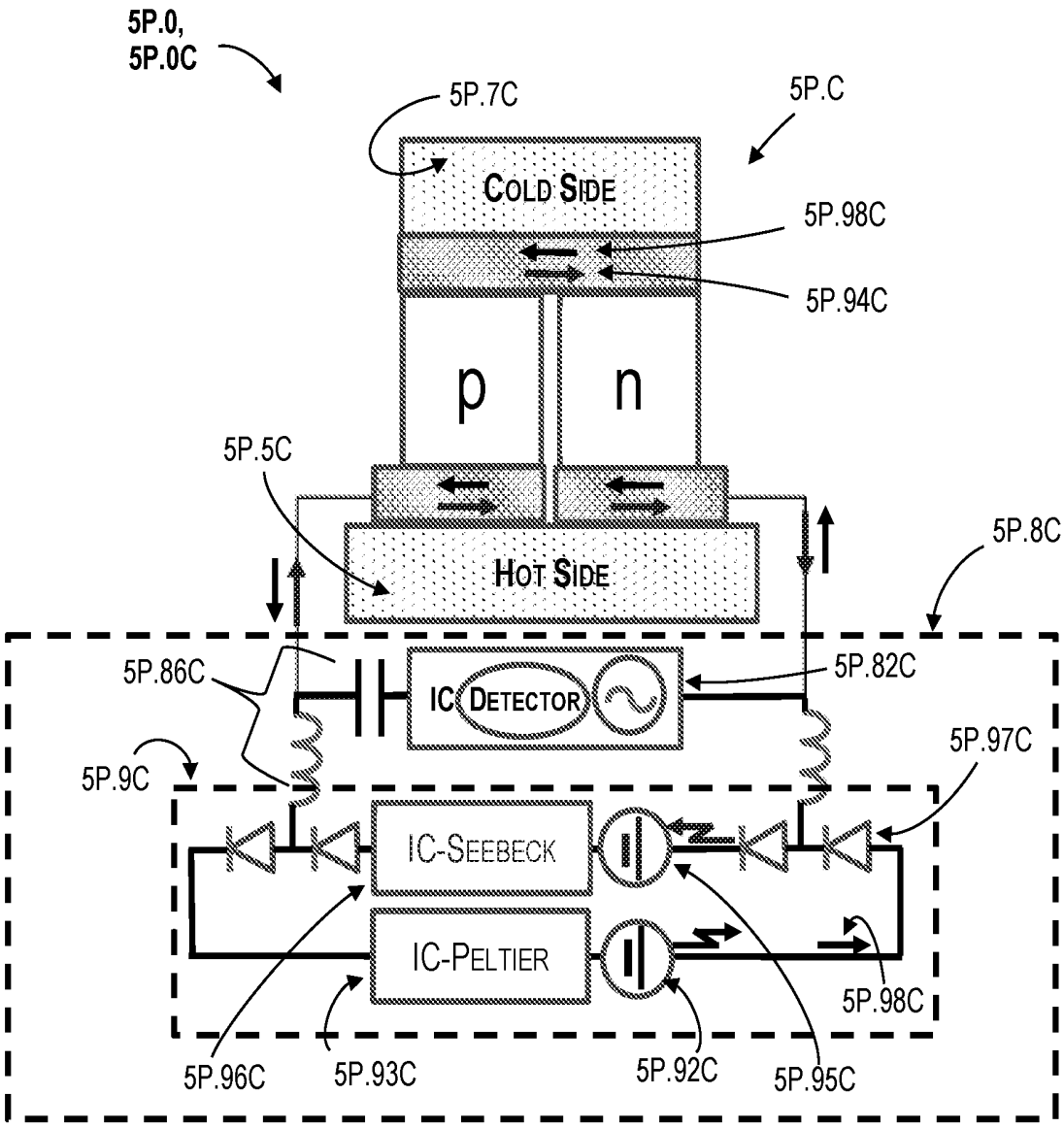

20202810 12 11 Mar 2021

Fig. 5q

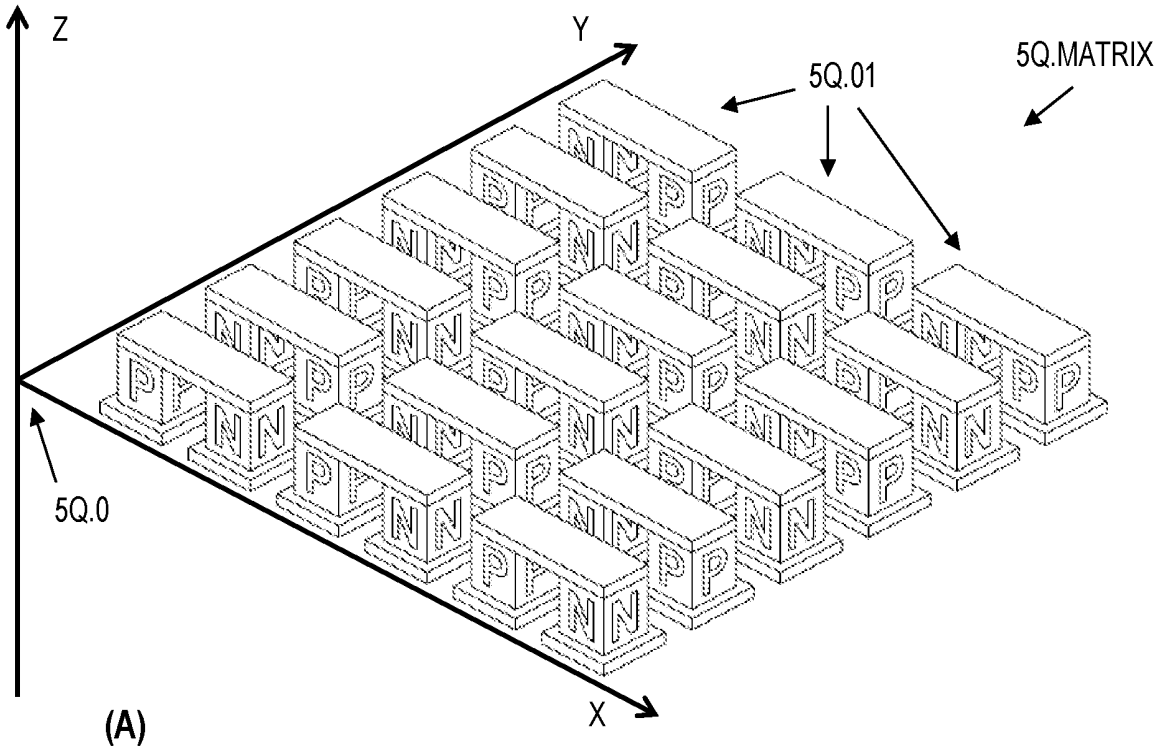

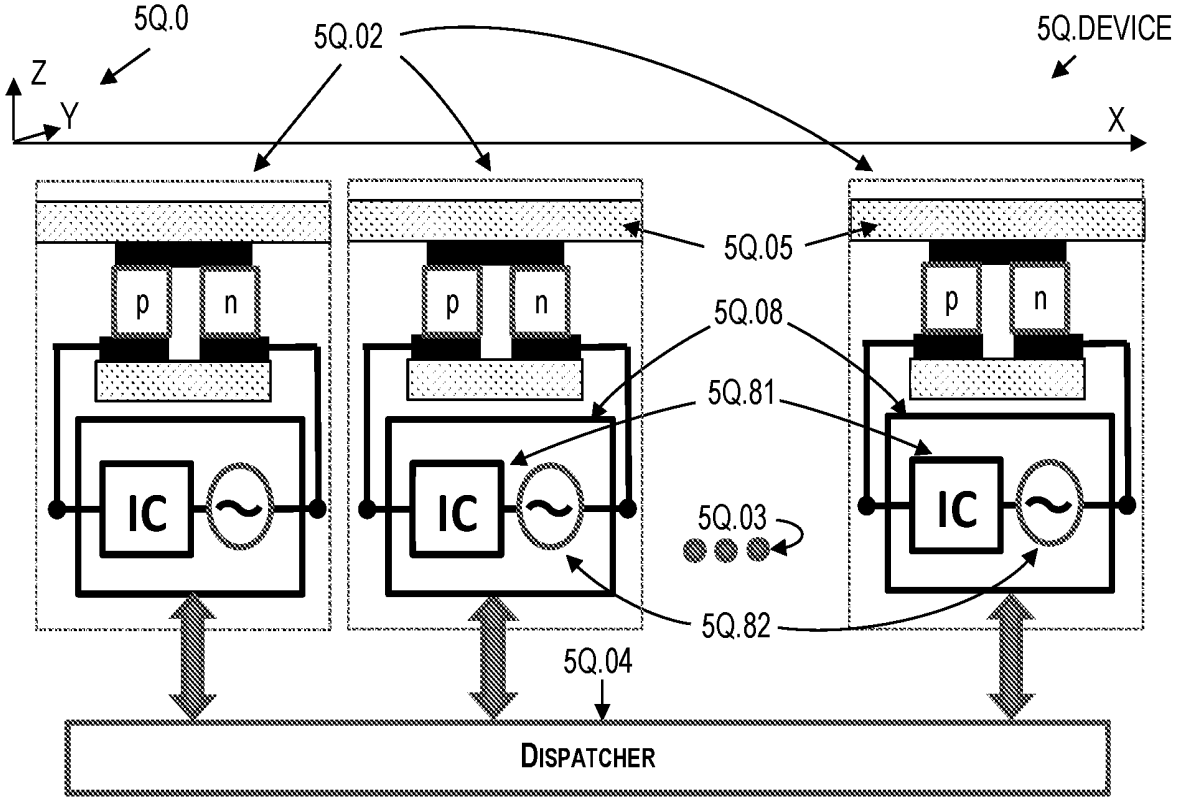

2020281012 11 Mar 2021

Fig. 5r

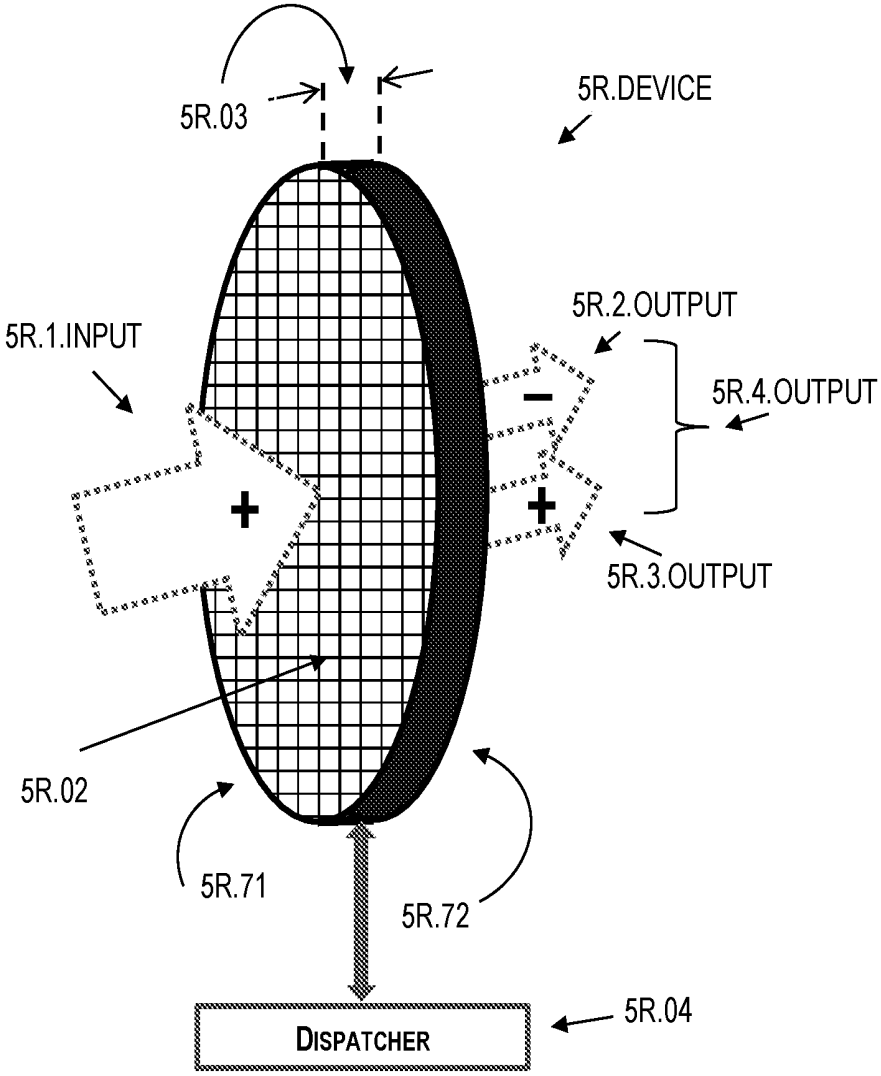

2020281012 11 Mar 2021

Fig. 5s

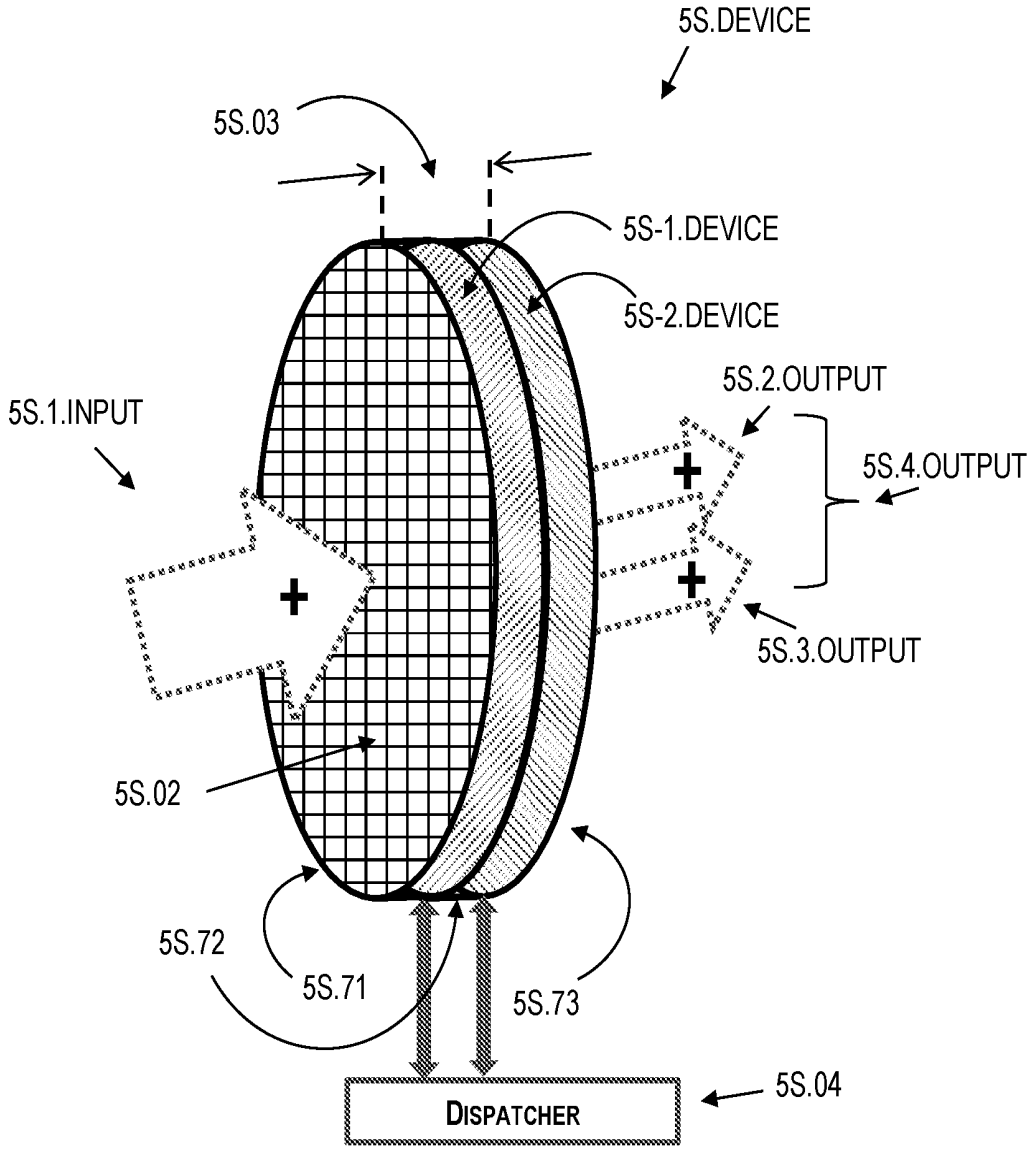

20202810 12 11 Mar 2021

Fig. 5t

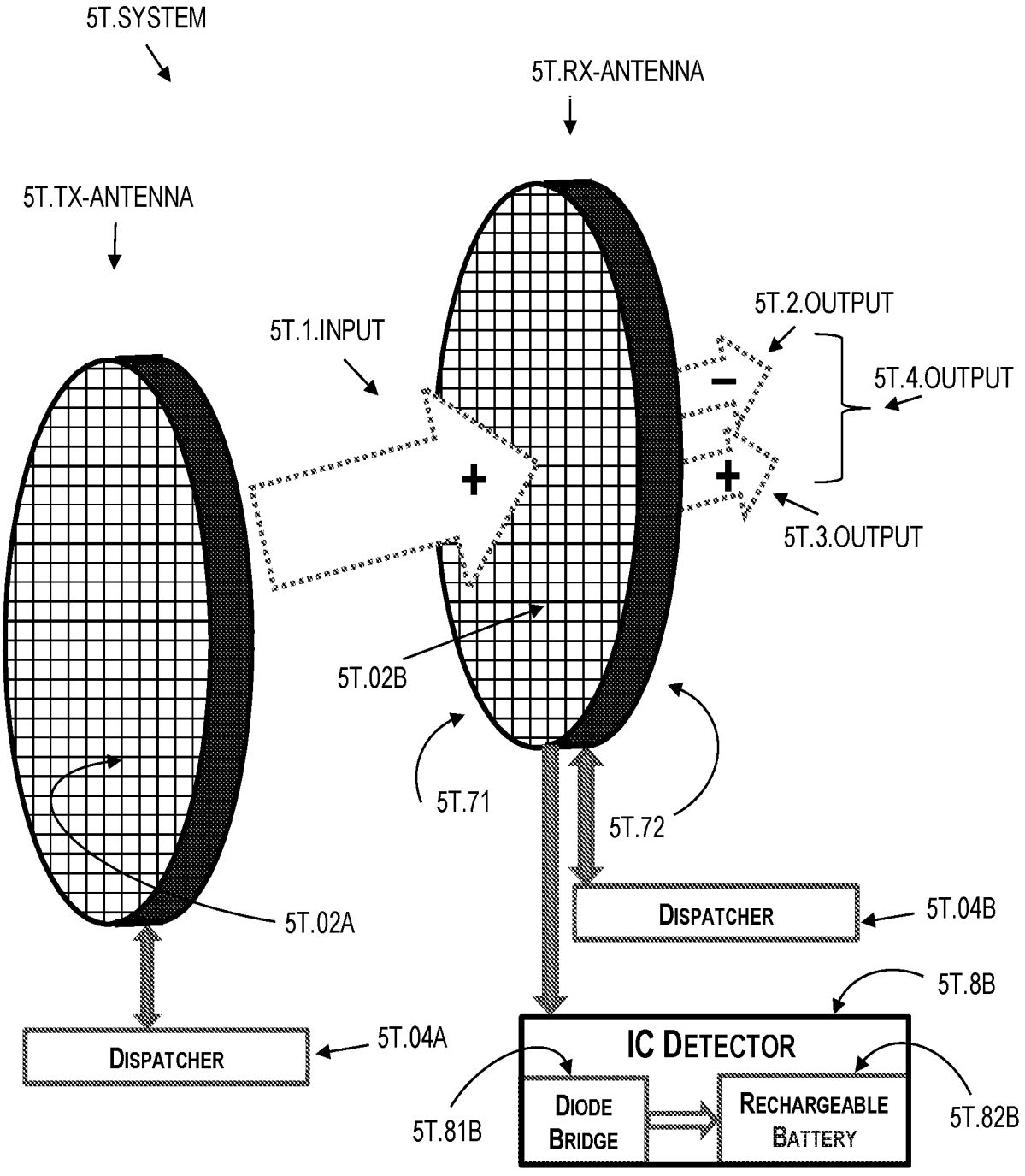

2020281012 11 Mar 2021

Fig. 6a

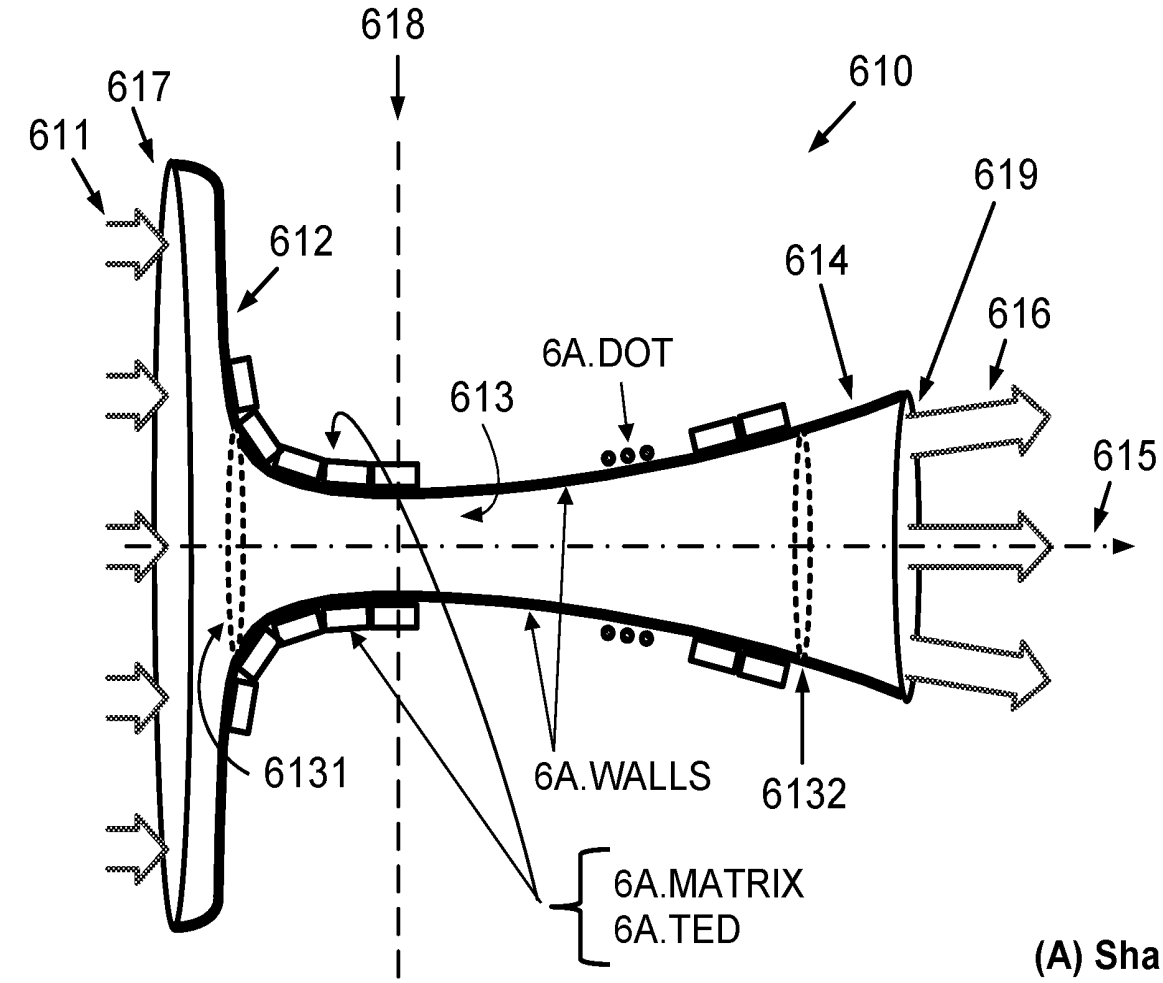

(A) Shape

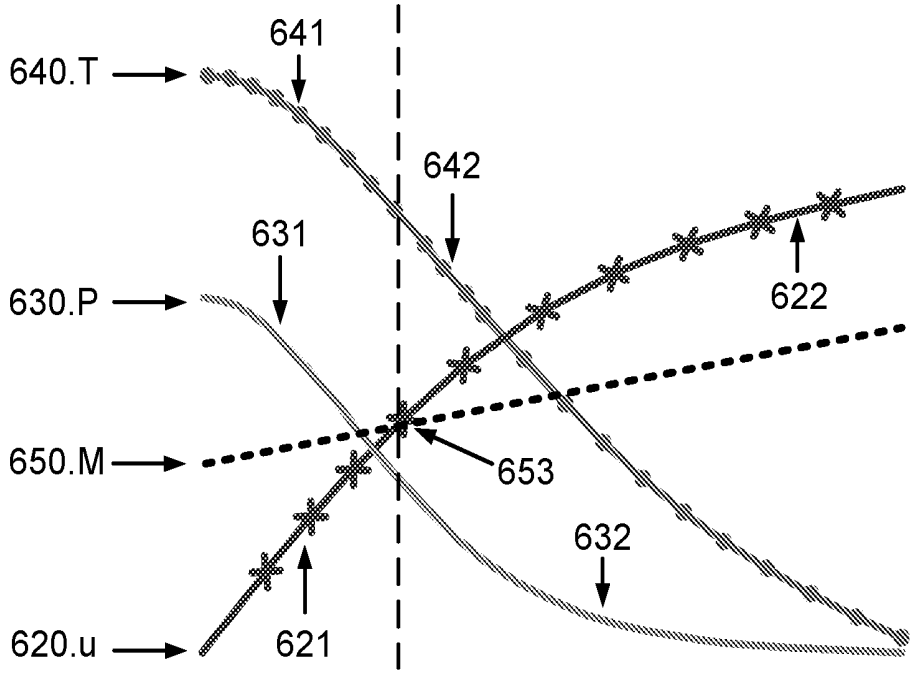

(B) Graph

20202810 12 11 Mar 2021

Fig. 6b

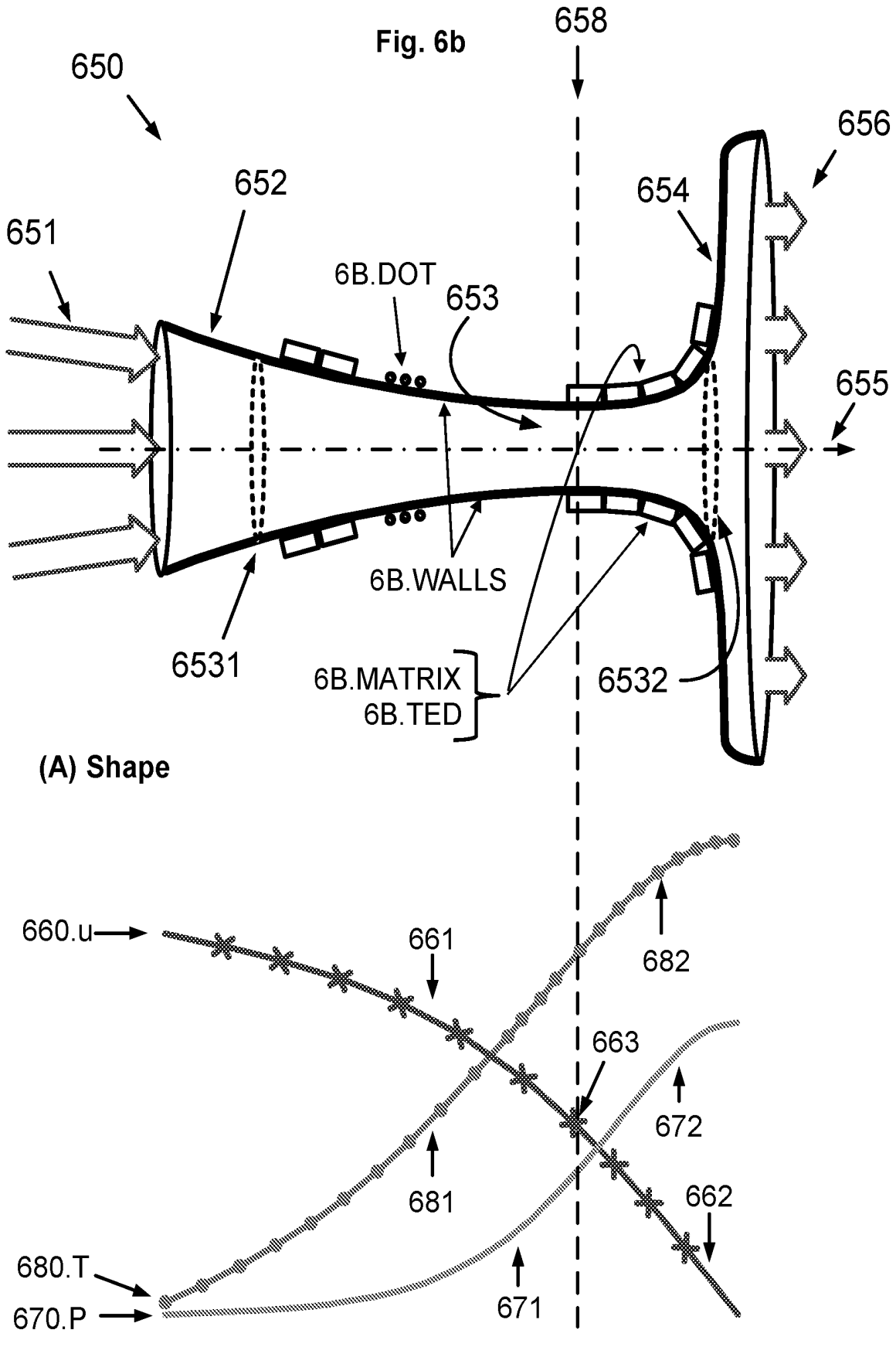

Fig. 6c

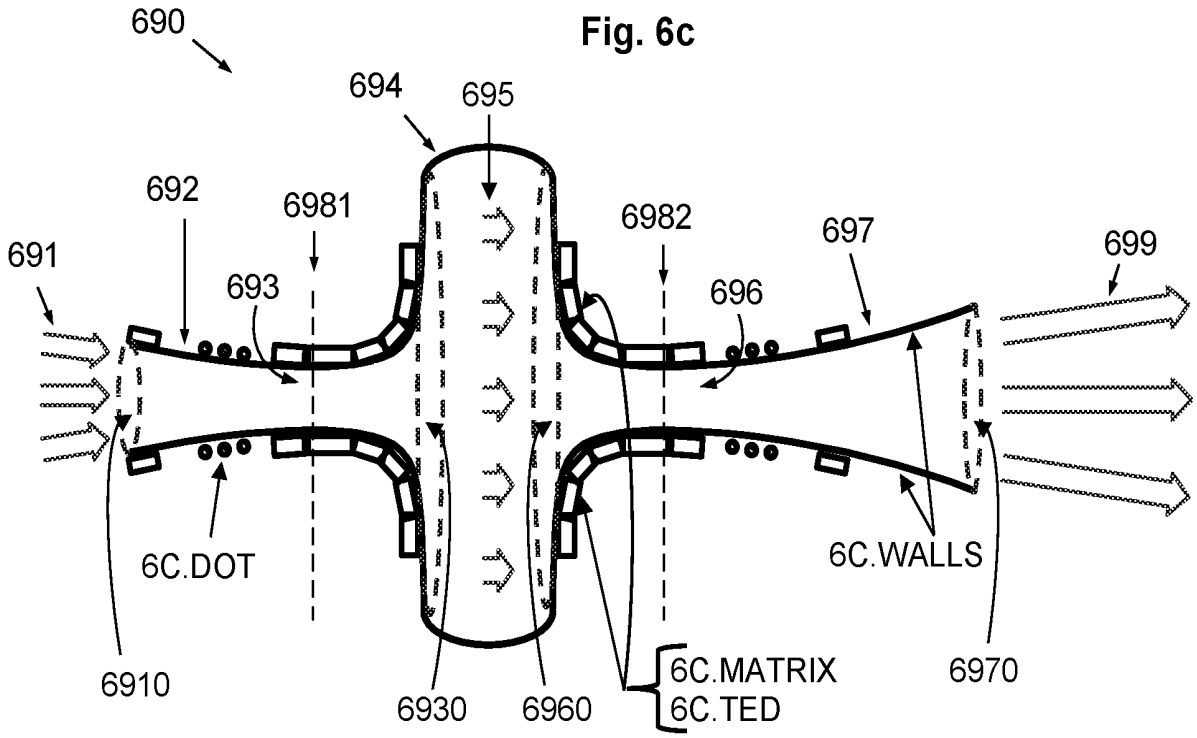

Fig. 7

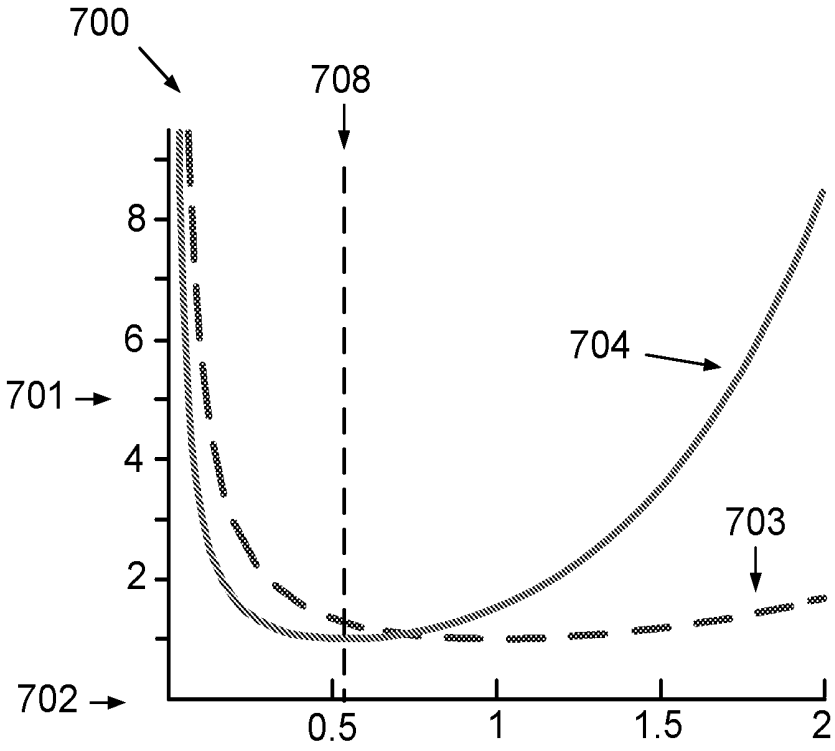

20202810 12 11 Mar 2021

Fig. 7a case (A)

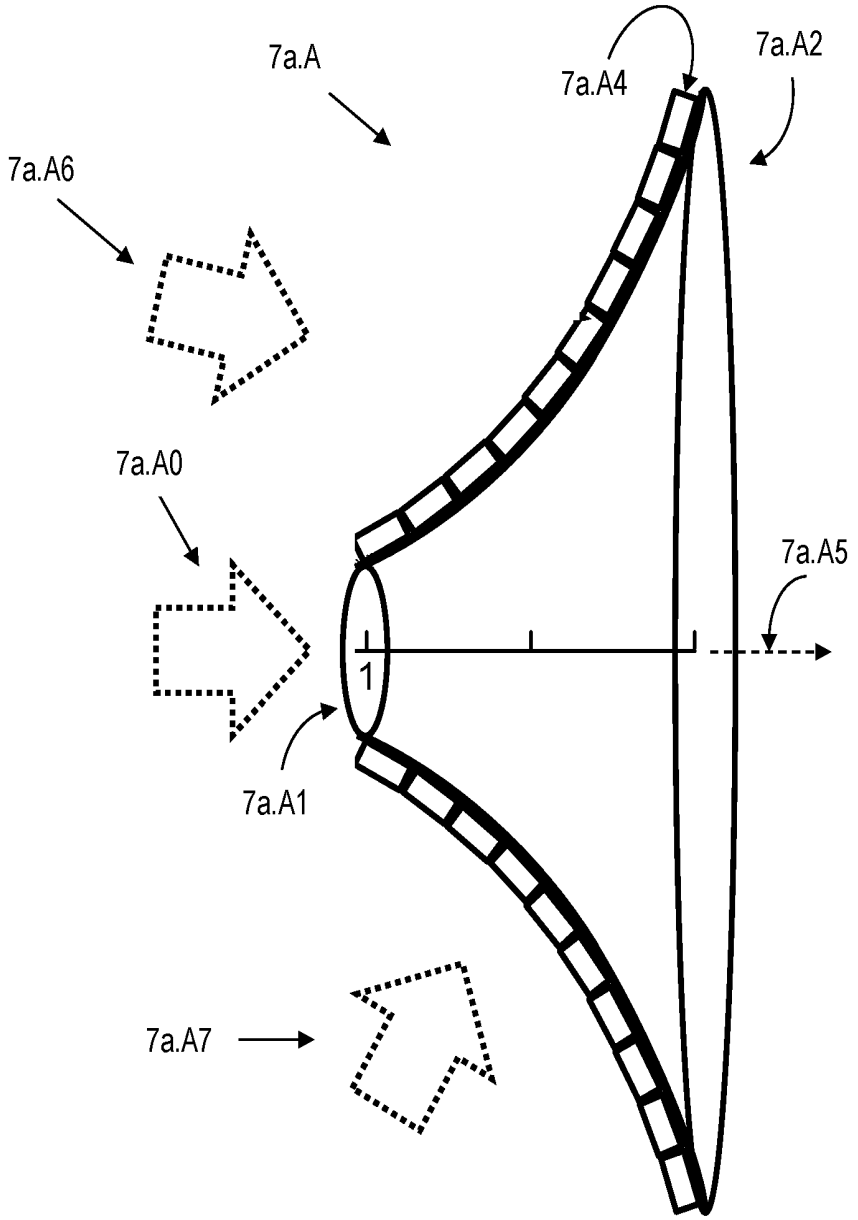

20202810 12 11 Mar 2021

Fig. 7a case (B)

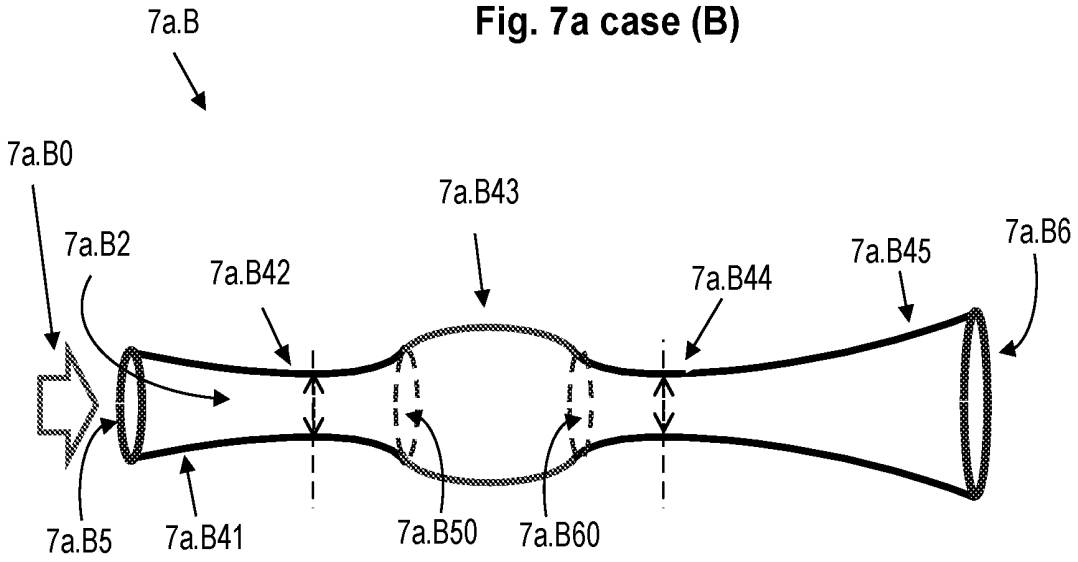

Fig. 7a case (C)

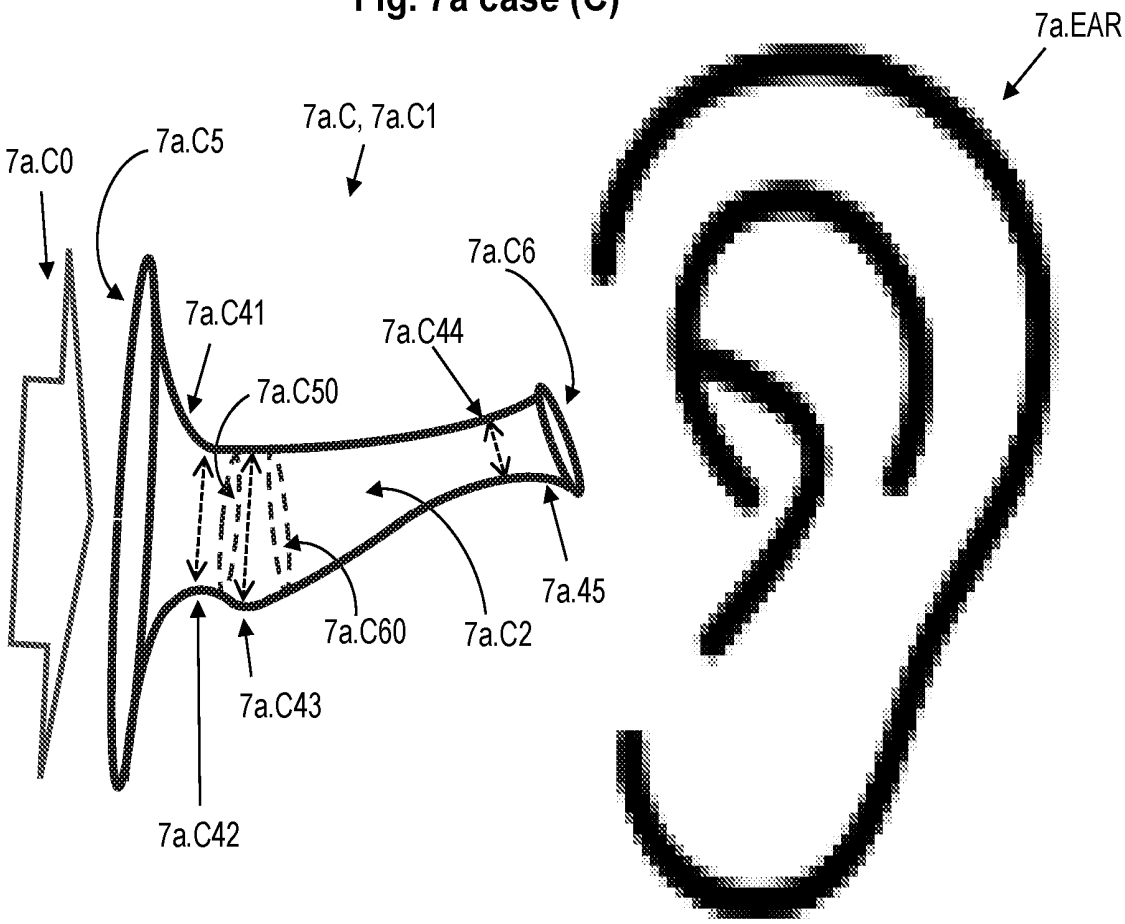

2020281012 11 Mar 2021

Fig. 7b

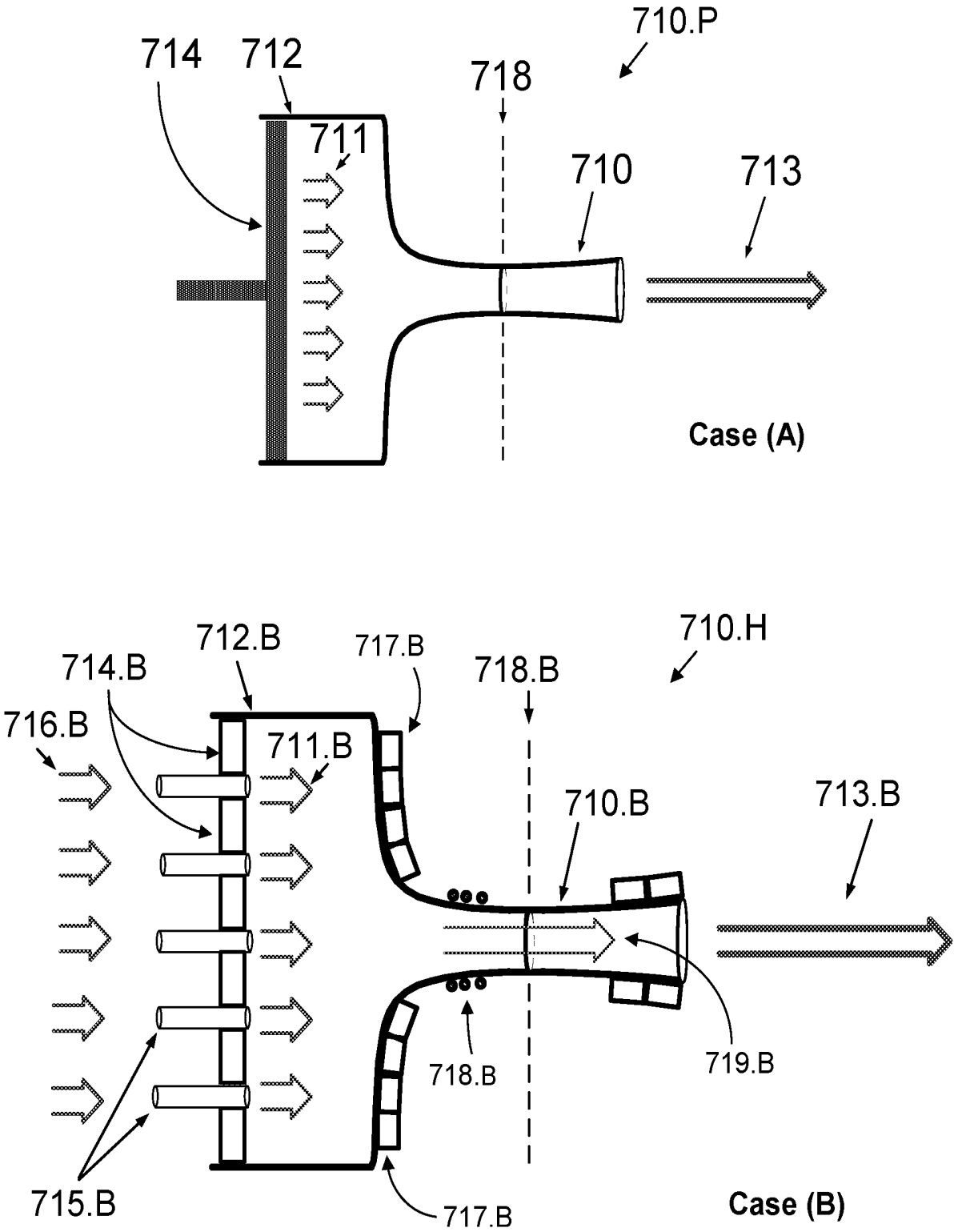

Fig. 7c

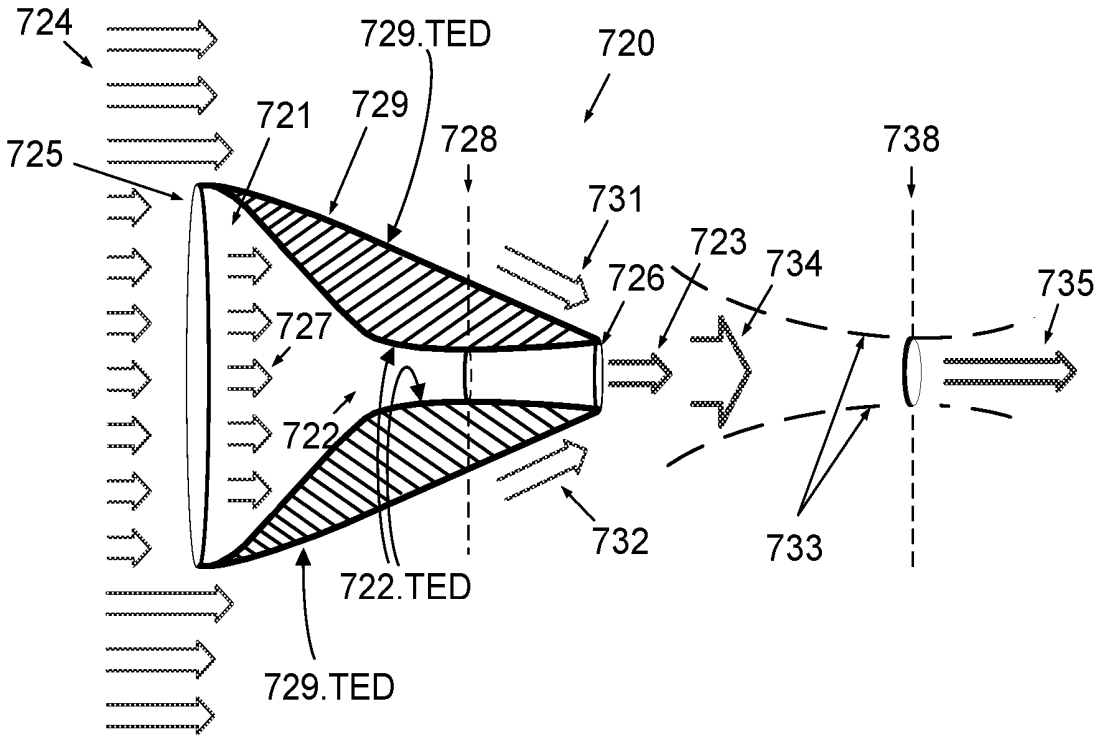

Fig. 7d

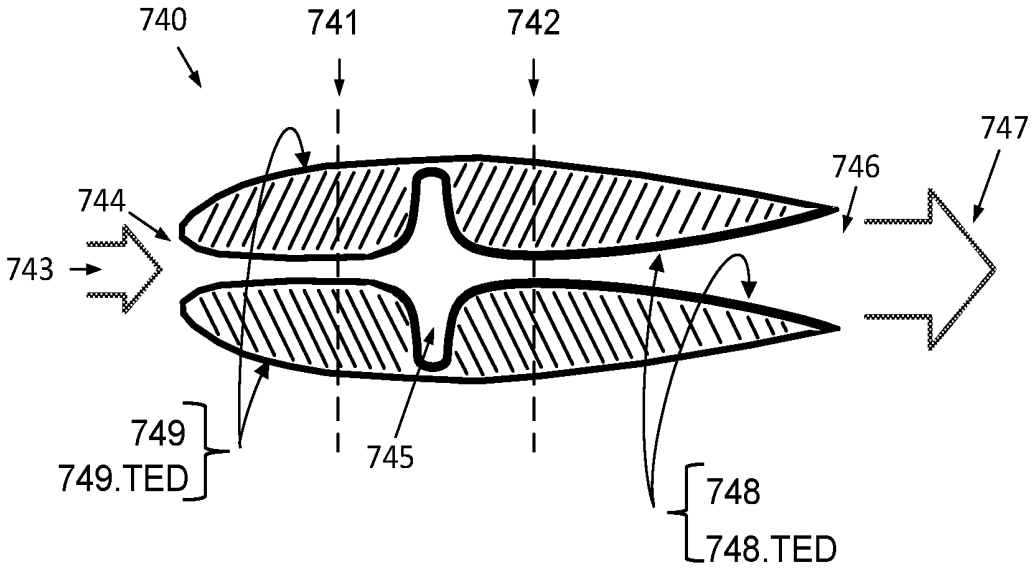

Fig. 8

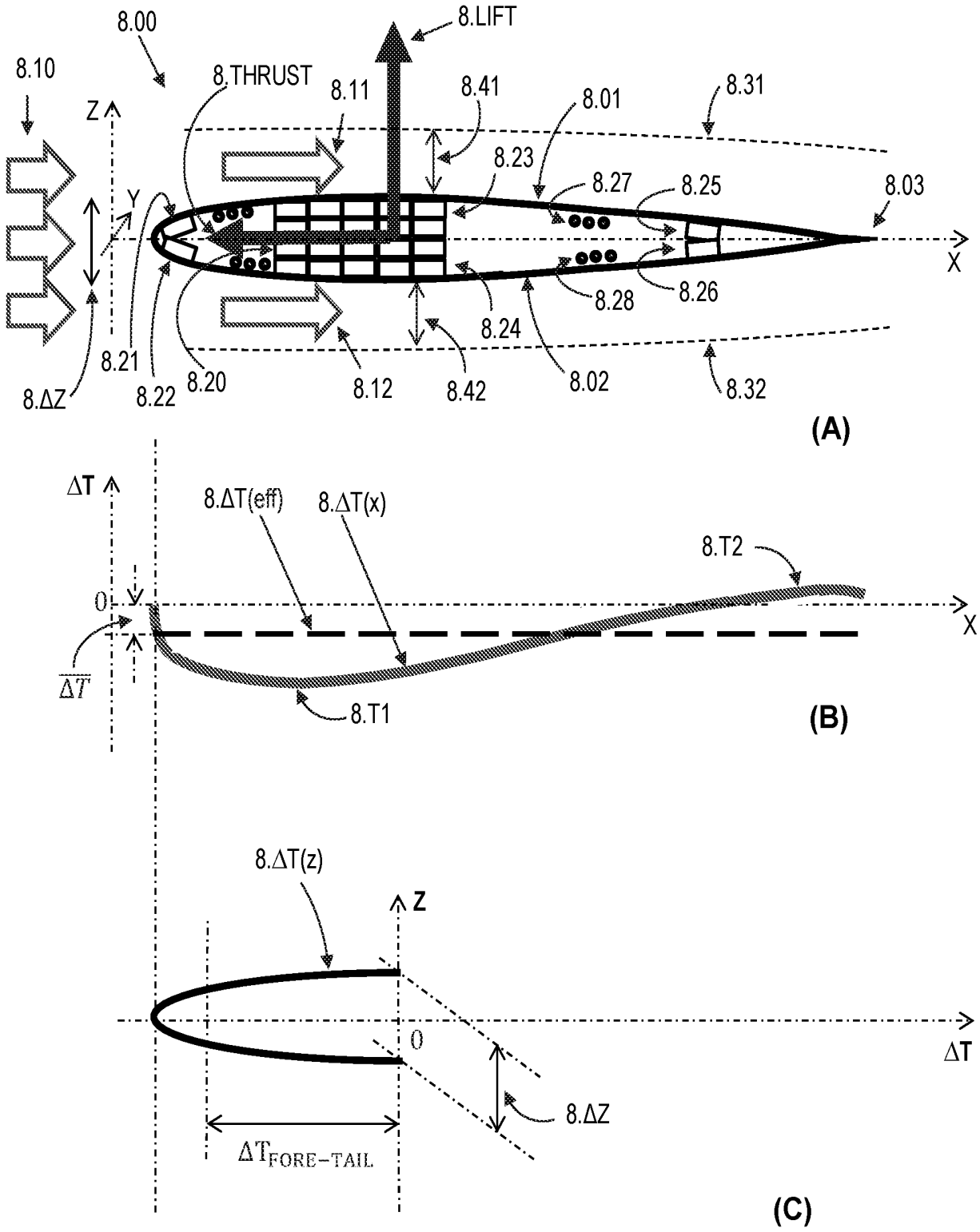

2020281012 11 Mar 2021

Fig. 8a

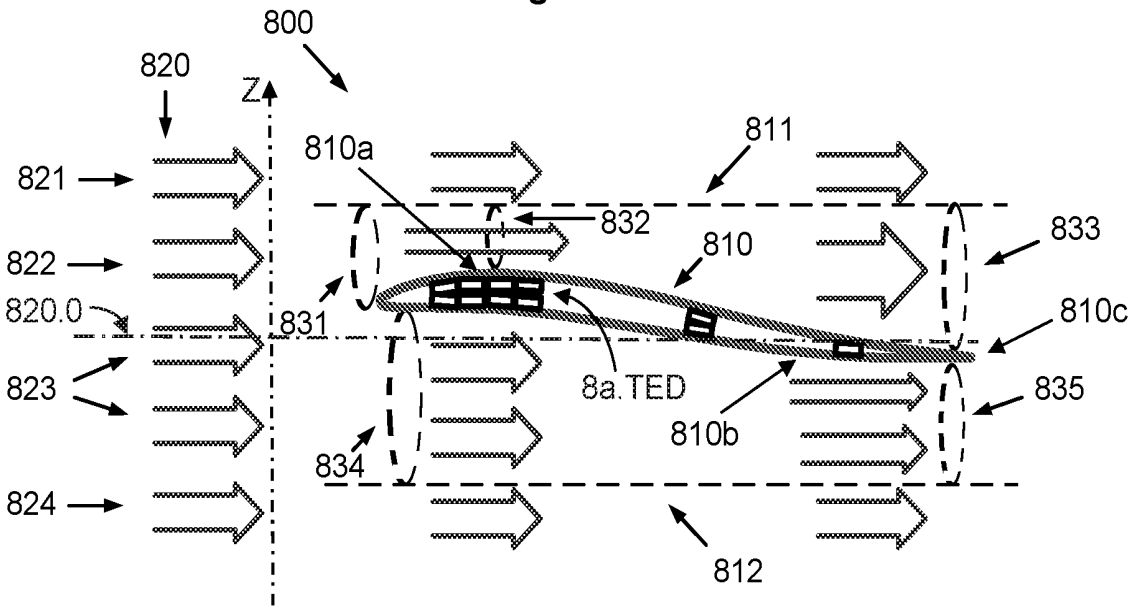

Fig. 8b

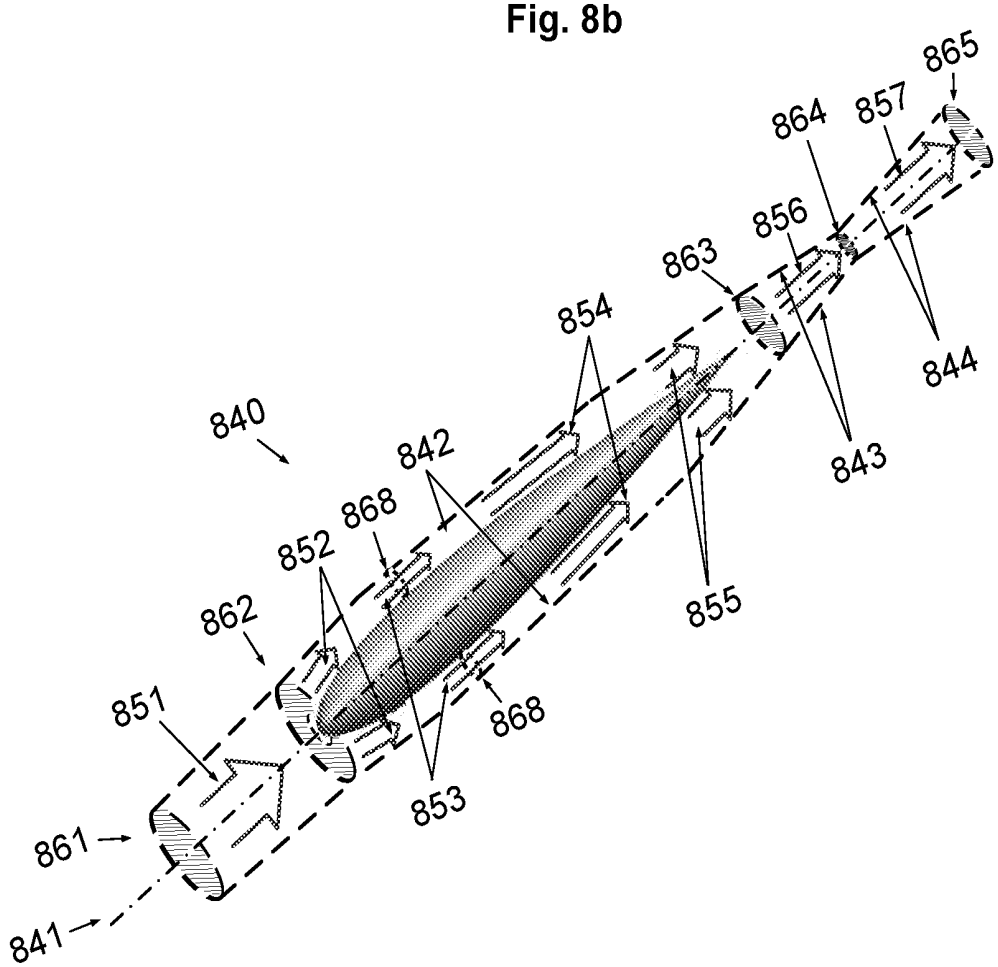

2020281012 11 Mar 2021

Fig. 8c

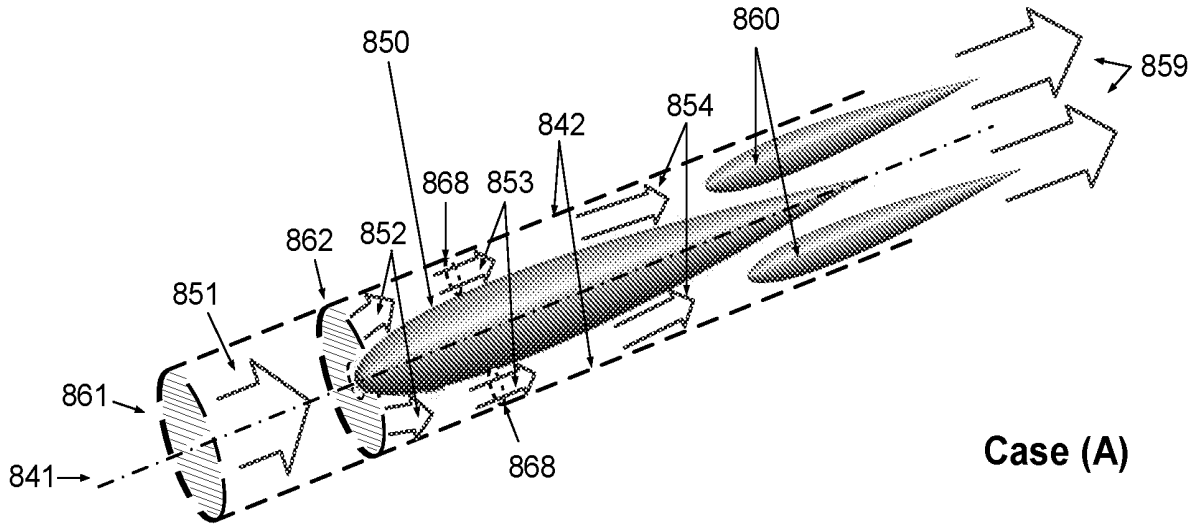

Case (A)

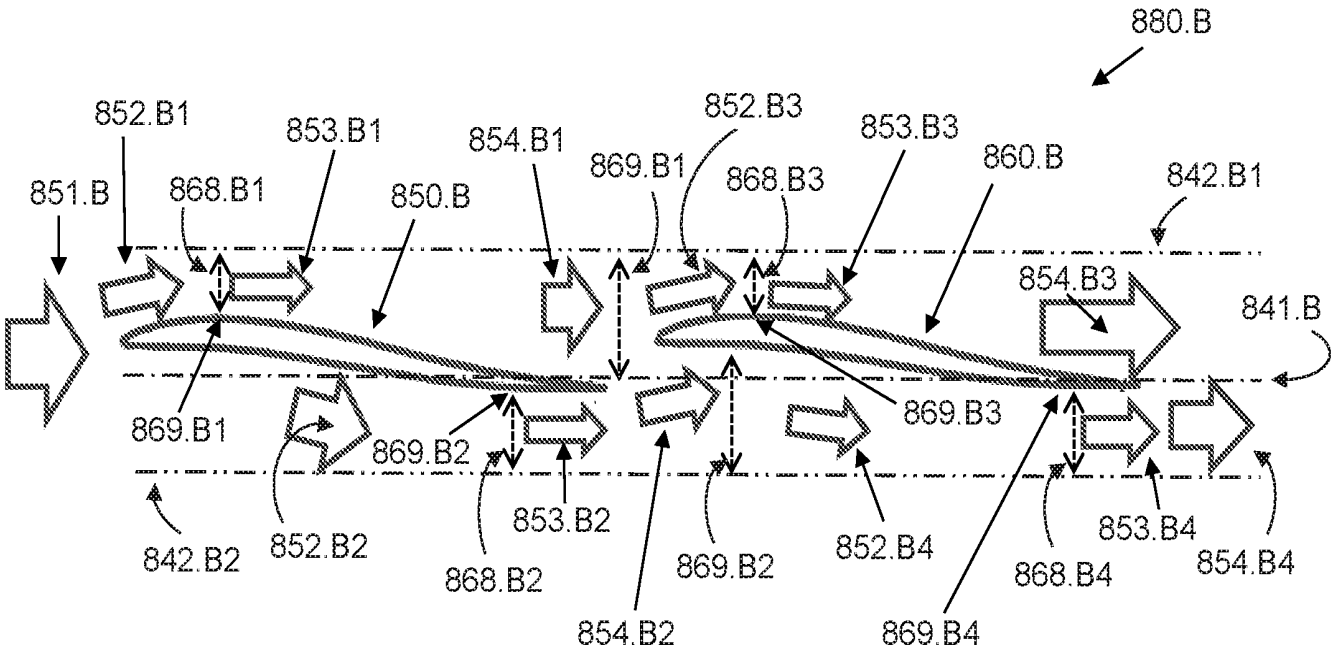

Case (B)

Fig. 8d

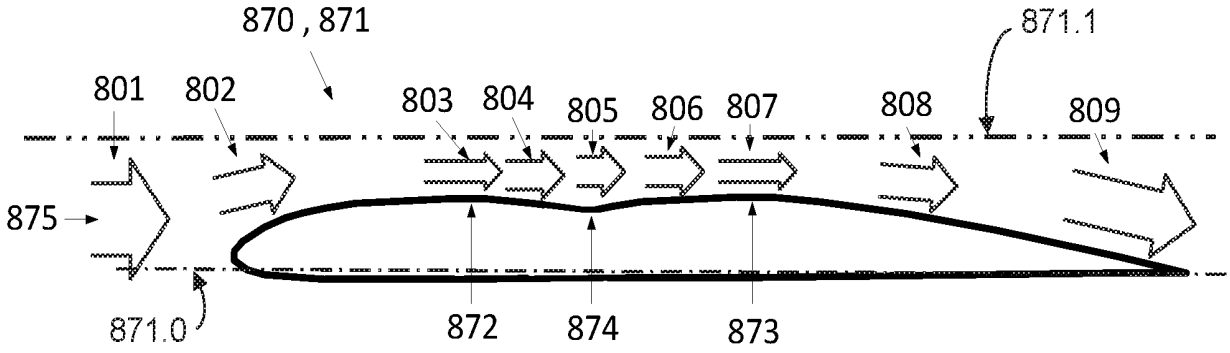

(A)

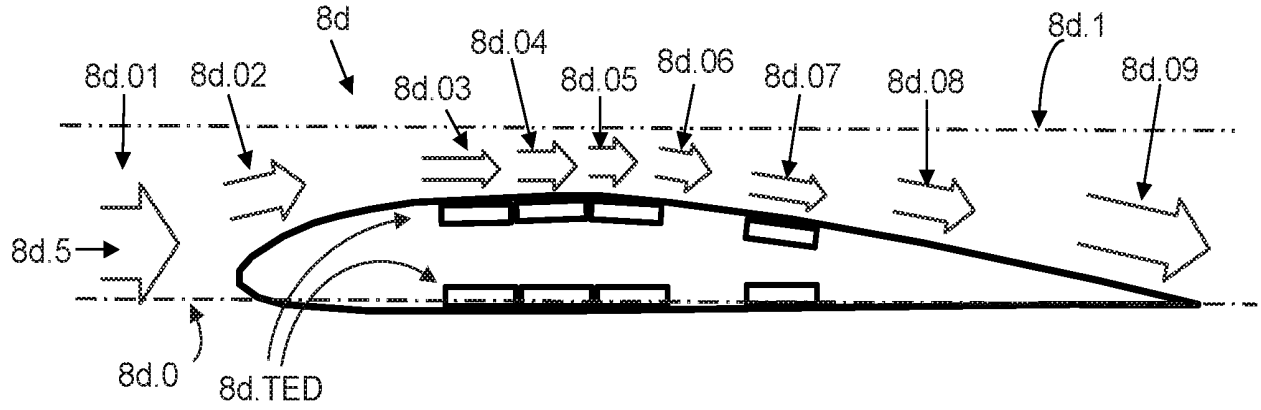

(B)

Fig. 9a

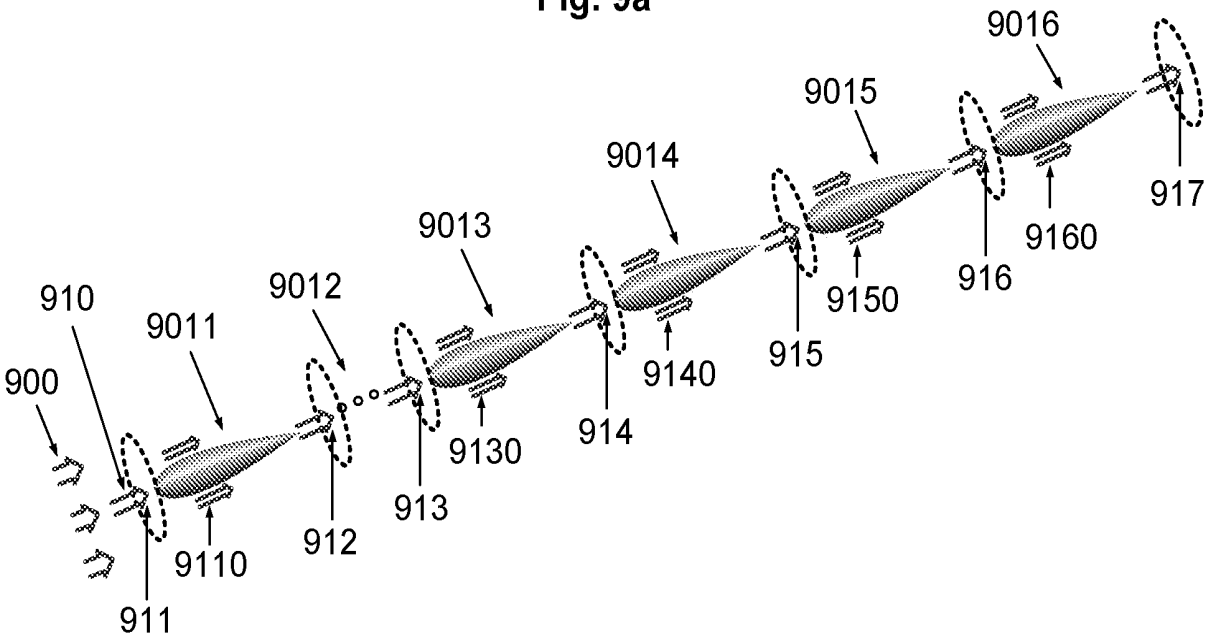

Fig. 9b

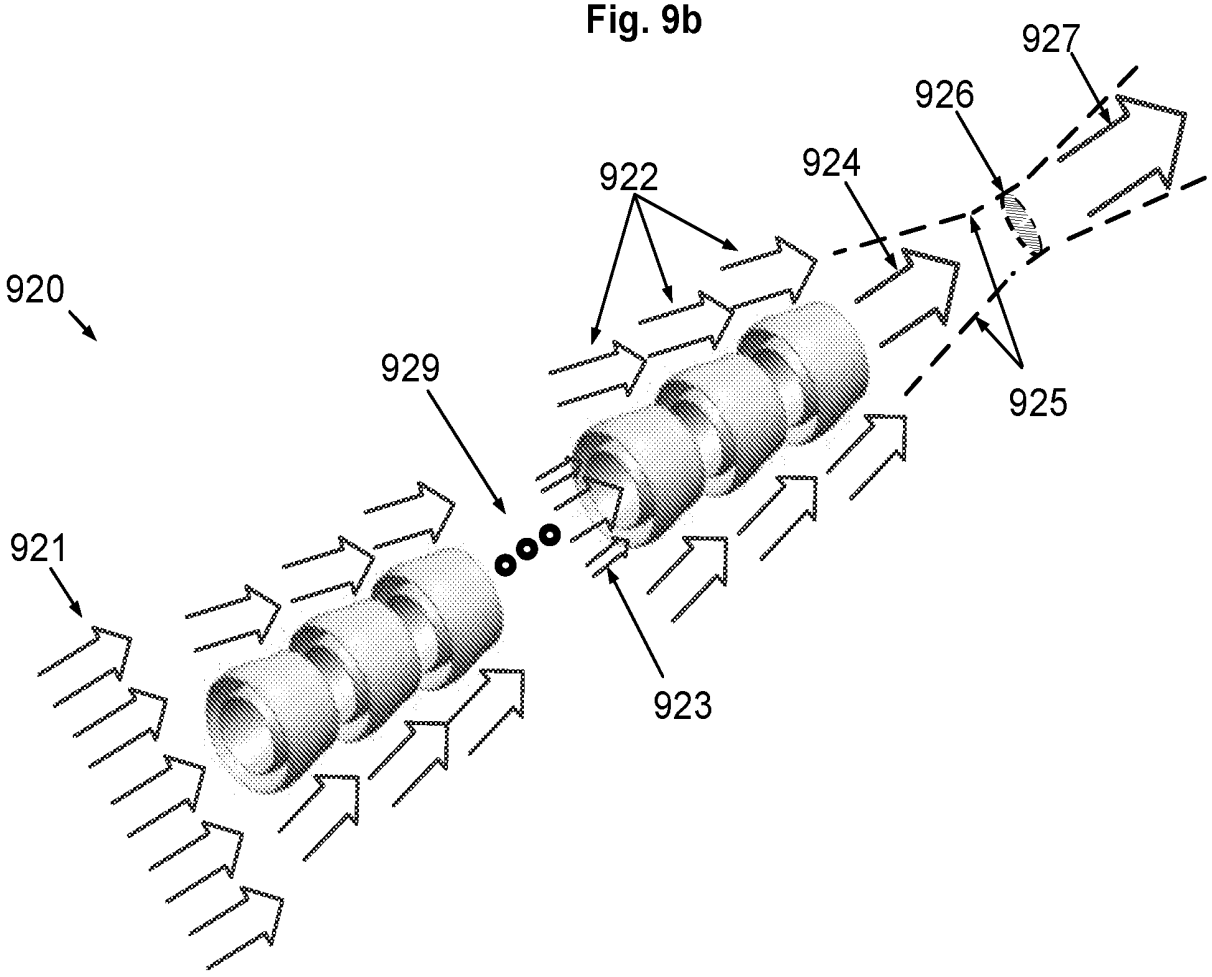

Fig. 9c

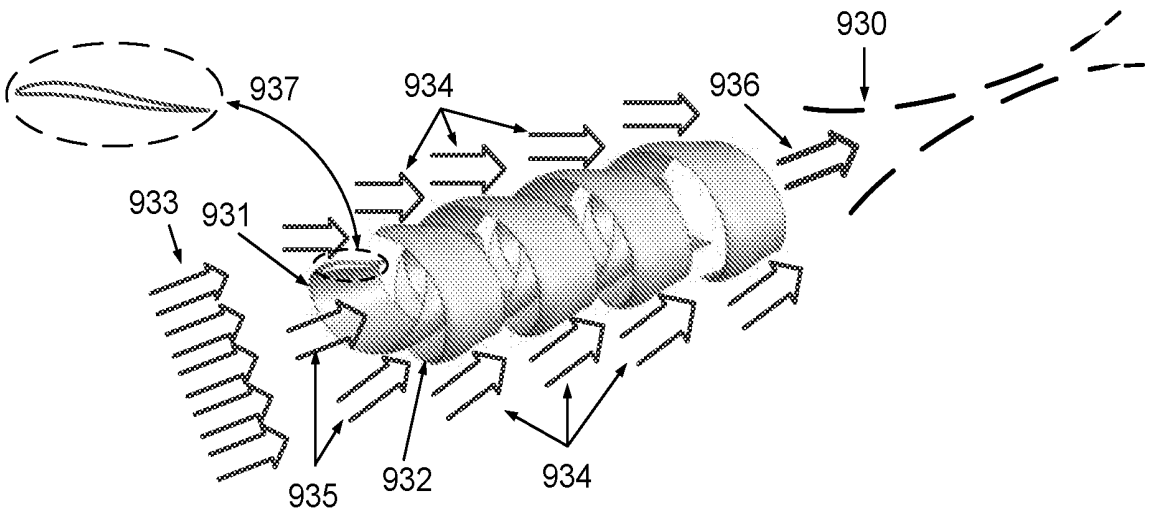

Fig. 9g

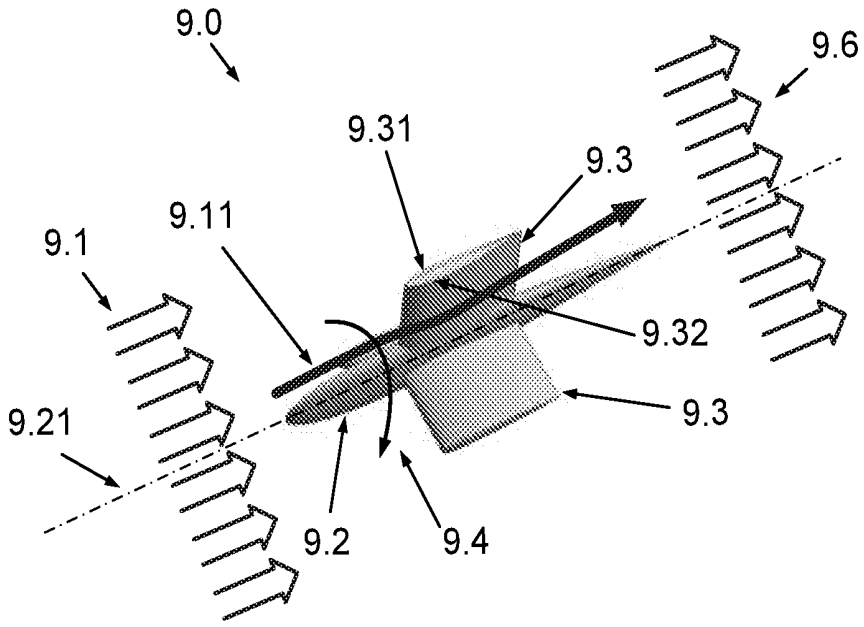

11 Mar 2021
2020281012

Fig. 9h

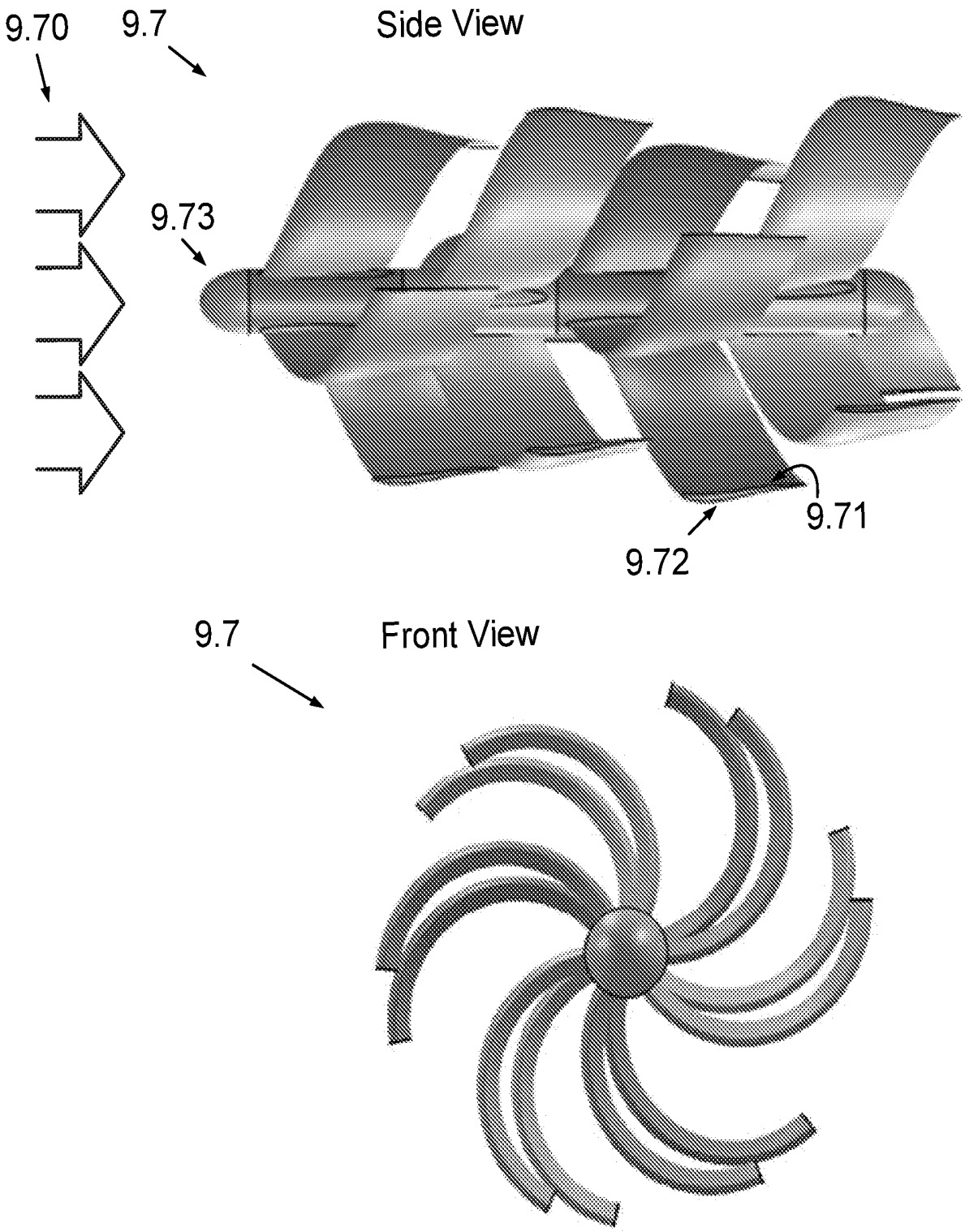

2020281012 11 Mar 2021

Fig. 9j

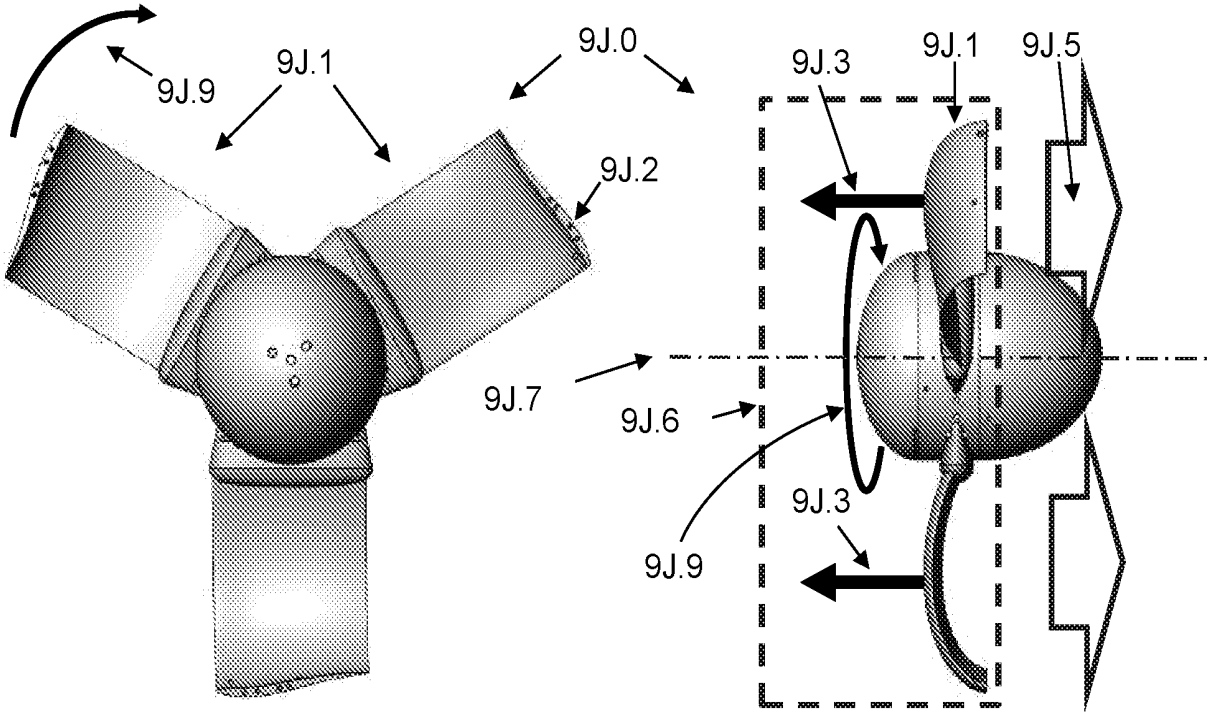

Front View

Side View

Fig. 9k

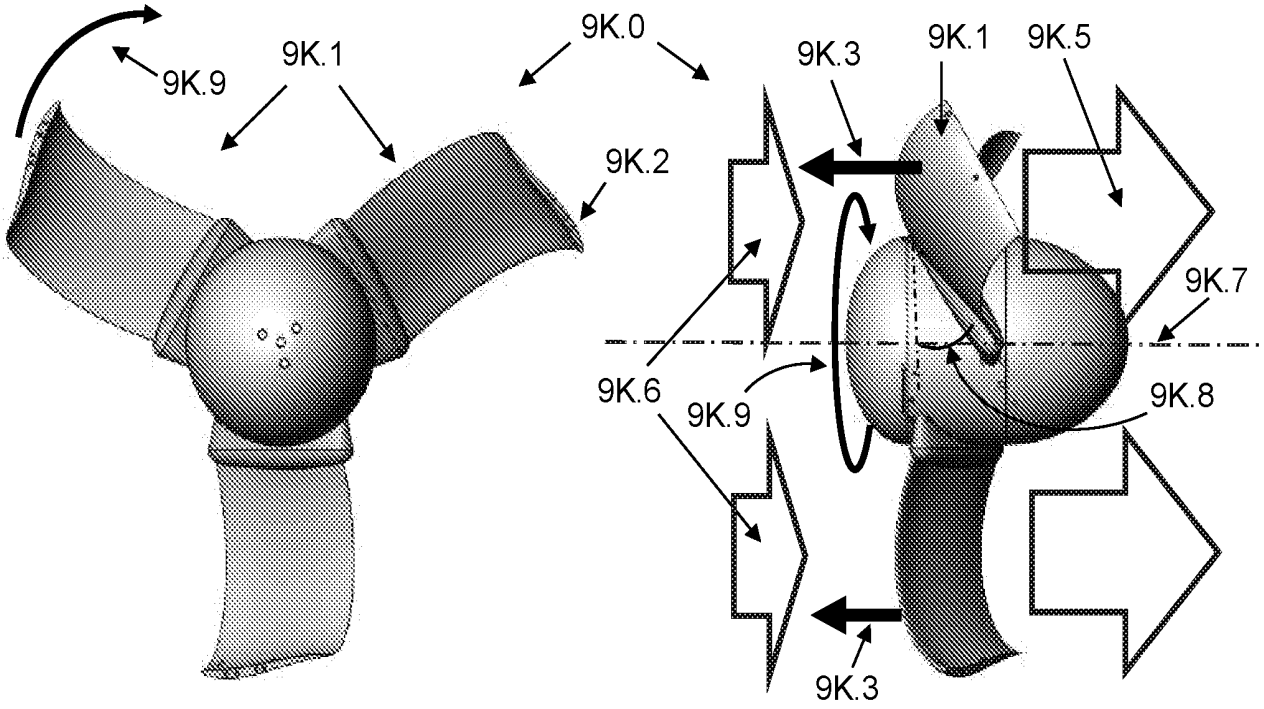

Front View

Side View

20202810 12 11 Mar 2021

Fig. 9L

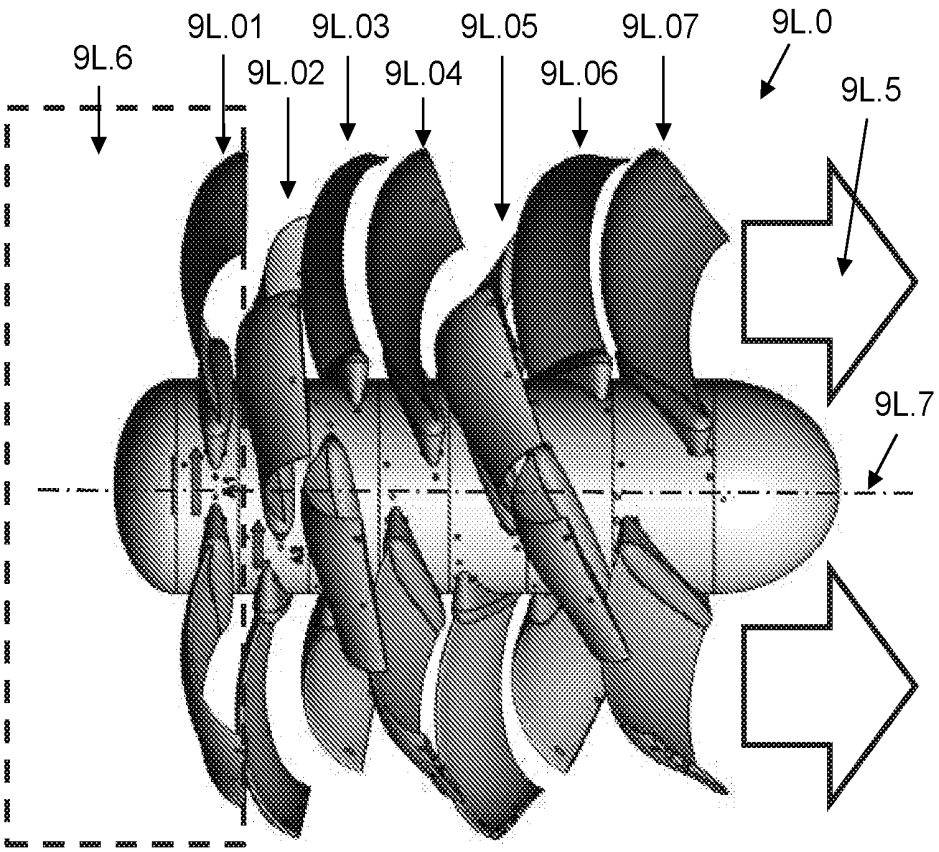

Fig. 9m

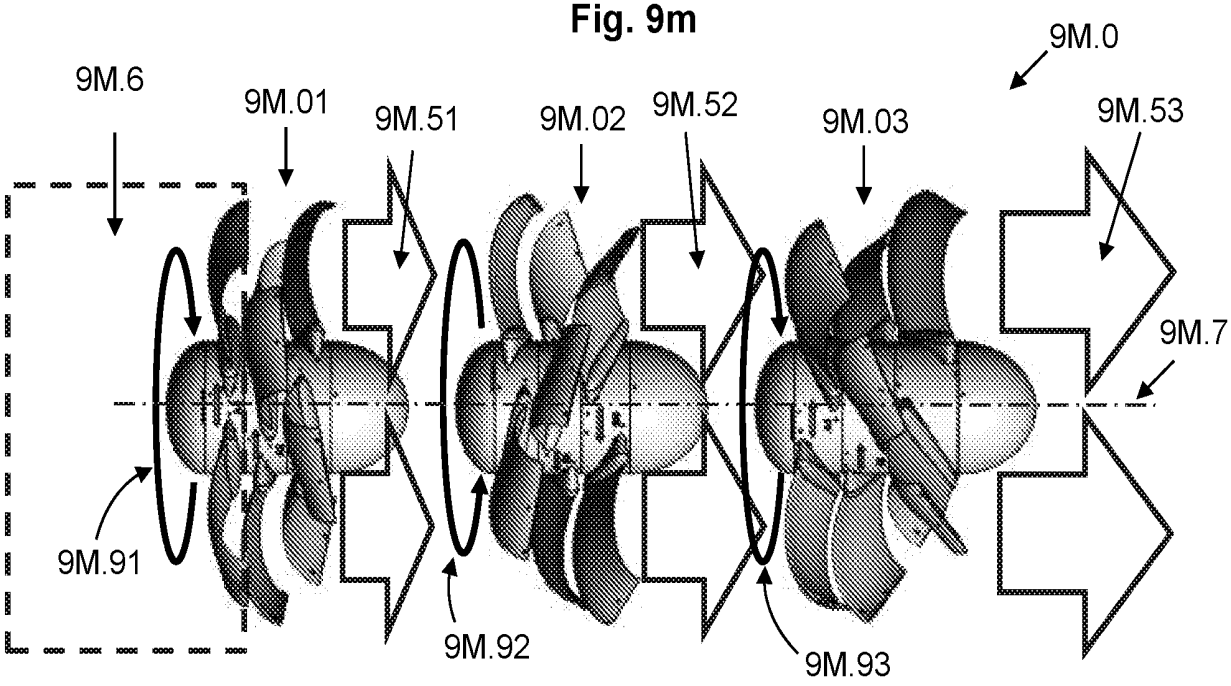

20202810 12 11 Mar 2021

Fig. 9n

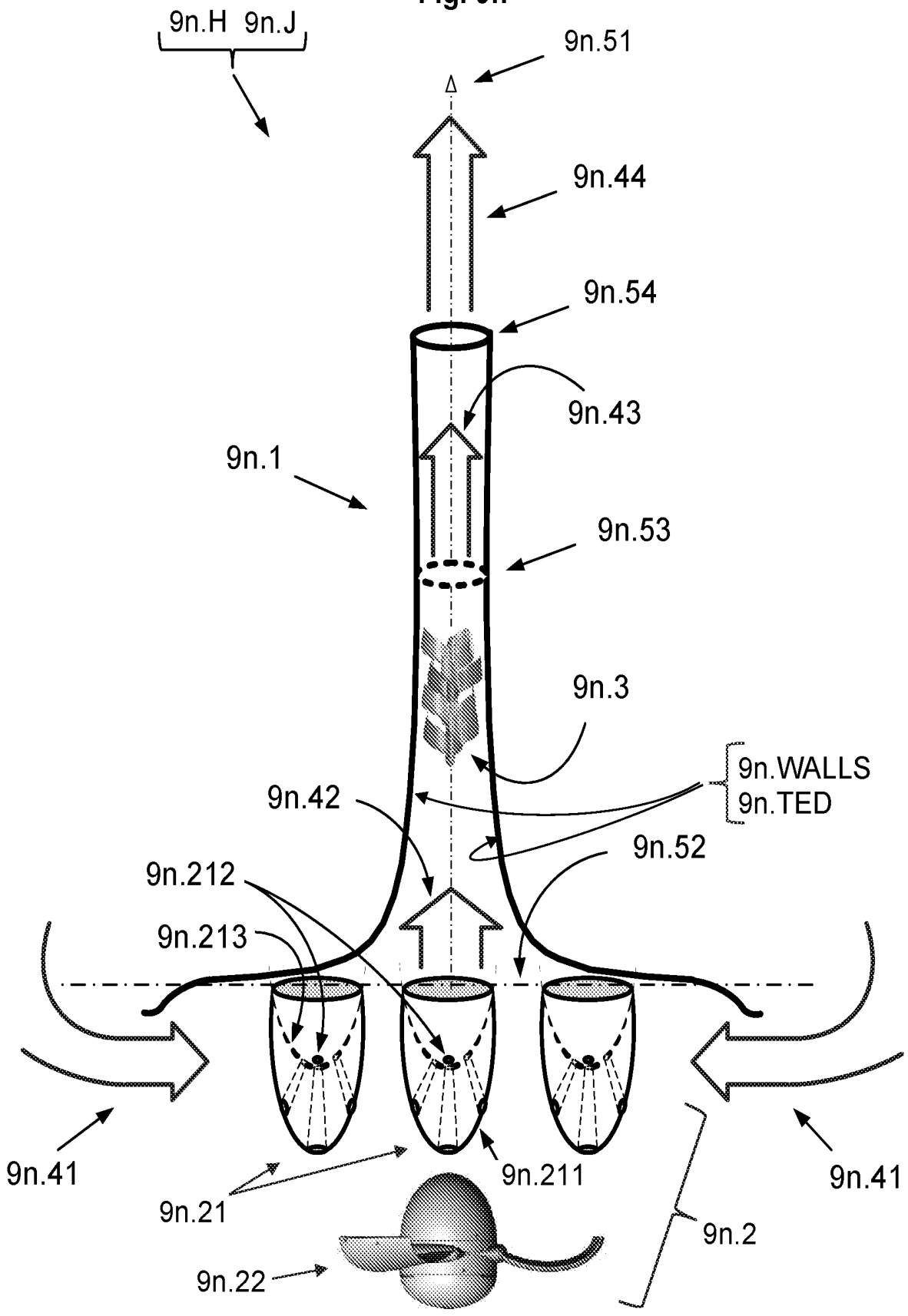

Fig. 9o